

1970

The Morphology Of The Opisthonephric Kidney Of The Great Lakes Lamprey, Petronyzon Marinus L

John Harold Youson

Follow this and additional works at: <https://ir.lib.uwo.ca/digitizedtheses>

Recommended Citation

Youson, John Harold, "The Morphology Of The Opisthonephric Kidney Of The Great Lakes Lamprey, Petronyzon Marinus L" (1970).
Digitized Theses. 437.
<https://ir.lib.uwo.ca/digitizedtheses/437>

This Dissertation is brought to you for free and open access by the Digitized Special Collections at Scholarship@Western. It has been accepted for inclusion in Digitized Theses by an authorized administrator of Scholarship@Western. For more information, please contact tadam@uwo.ca, wlsadmin@uwo.ca.

The author of this thesis has granted The University of Western Ontario a non-exclusive license to reproduce and distribute copies of this thesis to users of Western Libraries. Copyright remains with the author.

Electronic theses and dissertations available in The University of Western Ontario's institutional repository (Scholarship@Western) are solely for the purpose of private study and research. They may not be copied or reproduced, except as permitted by copyright laws, without written authority of the copyright owner. Any commercial use or publication is strictly prohibited.

The original copyright license attesting to these terms and signed by the author of this thesis may be found in the original print version of the thesis, held by Western Libraries.

The thesis approval page signed by the examining committee may also be found in the original print version of the thesis held in Western Libraries.

Please contact Western Libraries for further information:

E-mail: libadmin@uwo.ca

Telephone: (519) 661-2111 Ext. 84796

Web site: <http://www.lib.uwo.ca/>

THE MORPHOLOGY OF THE OPISTHONEPHRIC KIDNEY OF THE GREAT
LAKES LAMPREY, Petromyzon marinus (L.)

by

John Harold Youson

Department of Zoology

PART I: Text

Submitted in partial fulfillment
of the requirements for the degree of
Doctor of Philosophy

Faculty of Graduate Studies
The University of Western Ontario
London, Canada.

August, 1969

ABSTRACT

The structure of the opisthonephric kidney of the Great Lakes lamprey, Petromyzon marinus L., was studied throughout life using the light and electron microscopes. Three-dimensional reconstructions of the circulation were made from kidneys perfused with India ink or photographic emulsion.

Growth of the kidney is accompanied by degeneration. The kidney of ammocoetes grows by a posterior proliferation of nephrogenic tissue as degeneration proceeds at the anterior end. The adult kidney forms during transformation while the ammocoetes kidney degenerates. In the adult, degeneration is seen at the anterior tip of the kidney and throughout the kidney during the post-spawning migration.

The kidney consists of glomera and a segmented tubular nephron. A single long glomus extends almost the entire length of the adult kidney. Several glomera are placed end to end in ammocoetes and an increase in number and length occurs with increasing age.

The glomera consist of looped glomeruli which anastomose with one another. In ammocoetes each loop is surrounded by a Bowman's capsule while in the adult no Bowman's capsules are seen but instead the dilated end of a nephron is interposed between the loops. In both ammocoetes and adults the capillary endothelium is

thick and surrounded by a layer of podocytes; elsewhere a simple squamous epithelium is found.

The tubular nephron is divisible into five regions: neck, proximal, intermediate, distal, and collecting segments which drain into an archinephric duct. The straight intermediate, distal, and collecting segments parallel sinusoids in the adult kidney suggesting the operation of a counter-current mechanism.

The cells of the tubules, particularly the distal segment, contain large quantities of smooth endoplasmic reticulum and mitochondria which likely reflect their role in ion transport. Basal infoldings of the plasma membrane are not seen but instead intercellular spaces are well developed and likely indicate the ability for water transport.

The cells of the tubules in ammocoetes contain large amounts of glycogen in varying degrees and this may reflect variations in the degree of differentiation or metabolic activity between the cells.

Prismatic cristae in cells of undifferentiated tubules of ammocoetes enclose mitochondrial granules in complex, hexagonal tubes which are star-shaped in transverse section.

The archinephric duct of ammocoetes appears to be involved in urine formation while the duct in adult secretes mucus and is able to contract^{to} aid in the expulsion of urine.

A renal portal system is lacking. The circulation is characterized by the presence of a medial artery supplying the glomera and a system of capillaries and sinusoids supplying the

tubules. Sinuses draining the kidney are more complex in the adult.

The kidney of the lamprey is not primitive but appears as highly evolved from the archinephric type as the kidneys of higher vertebrates; it is probably able to perform most of the functions attributed to them.

ACKNOWLEDGEMENTS

I would like to extend my appreciation to Dr. A.W.A. Brown former Head of the Department of Zoology, for making laboratory facilities available. I am especially indebted to Dr. D.B. McMillan for his support and encouragement while directing my research.

I am grateful for the technical assistance provided by Miss Barbara H.E. Durnford, and Messrs. Robert W.F. Garnett, John A. Sholdice, and Dale H. Larson.

I would like to thank Dr. R.R. Shivers for his helpful suggestions during the preparation of this manuscript.

Finally, I would like to thank my wife, Betty, for her encouragement, understanding, patience, and valuable technical assistance.

This investigation was made possible through a grant from the National Research Council of Canada to Dr. D.B. McMillan. The writer wishes to express his appreciation for this assistance.

TABLE OF CONTENTS

ABSTRACT	iii
ACKNOWLEDGEMENTS	vi
INTRODUCTION	1
MATERIALS AND METHODS	6
OBSERVATIONS	10
GROSS MORPHOLOGY	10
CIRCULATION	11
Blood Supply to the Glomus	11
Blood Supply to the Tubules and the Drainage ..	13
Ammocoetes	13
Adult	14
RENAL CORPUSCLE	15
TUBULAR NEPHRON	22
Neck Segment	23
Proximal Segment	25
Proximal Pars Convoluta	26
Proximal Pars Recta	30
Intermediate Segment	32
Ammocoetes	32
Adult	35

Distal Segment	37
Ammocoetes	37
Adult	42
Distal Pars Recta	43
Distal Pars Convoluta	44
Collecting Segment	46
Ammocoetes	46
Adult	47
ARCHINEPHRIC OR URETERIC DUCT	49
Ammocoetes	49
Adult	51
GROWTH AND DEGENERATION	55
Growth	55
Degeneration	58
Ammocoetes and Newly-Transformed Adult	58
Adult	59
Migrating Adult	59
CELLS OF THE INTERTUBULAR AREA	61
Pigment Cells	61
Intertubular Cells	61
DISCUSSION	63
Renal Corpuscle	64
The Tubule	68
Neck Segment	70
Proximal Segment	70

	ix
Intermediate Segment	73
Distal Segment	75
Collecting Segment	78
Archinephric Duct	79
Cell Coat	82
Cytoplasmic Fibrils	82
Golgi Apparatus	83
Renal Glycogen	84
Smooth and Rough Endoplasmic Reticulum	85
Intercellular Spaces	87
Mitochondria	88
Circulation	90
Growth and Degeneration	92
Intertubular Tissue	94
Epilogue	96
SUMMARY	97
LITERATURE CITED	100
VITA	x

INTRODUCTION

The appearance of the sea lamprey, Petromyzon marinus L., a cyclostome, in the Great Lakes has become a matter of concern to those concerned with the fishing industry. During the present century these lampreys have been blamed for an almost complete collapse of commercial fishing in the Great Lakes watersheds (Applegate, '50). Because of an interest in eradicating this problem, the life cycle of this animal (Applegate, '50) and methods for its control have been vigorously investigated (Tibbles, '61).

The filter-feeding larvae of the lamprey, the ammocoetes, dwell in the mud of stream bottoms for $5 \frac{1}{2} \pm 2$ years (Thomas, '62) and then undergo transformation in their sixth year to emerge as adults (Gage, '28; McDonald, '59) which migrate to the lake and feed on the body fluids of bony fish. After 10 to 20 months the adults return to the stream where they spawn once and immediately die (Applegate, '50).

The kidney of the lamprey is of interest for several reasons: the lamprey is taxonomically one of the lowest vertebrates available; the lampreys of the Great Lakes are a landlocked group of a marine species; the lamprey undergoes a change from the vegetable diet of the ammocoetes to the high-protein diet of the adult; and the kidney presents an unusual opportunity to study degenerative changes, not only in the ammocoetes but also in the migrating and

spawning adults.

Of prime interest is the ability of this species to live in both a marine and freshwater environment, a feature which requires a highly developed mechanism for osmoregulation. Because the lamprey is able to tolerate a wide range of salinities, early investigators were led to group marine cyclostomes with elasmobranchs, which cope with the problems of osmoregulation by varying the content of urea in their blood (Marshall and Smith, '30). Recent studies have shown that little or no urea is found in the plasma of the anadromous river lamprey, Lampetra fluviatilis, in fresh water (Robertson, '54; Urist and Van de Putte, '67) or after transference to sea water for a short time (Urist and Van de Putte, '67). In addition, Entospherus tridentatus, a fresh water-adapted form of the Pacific lamprey, lacks a complete ornithine-urea cycle; this cycle is present in many aquatic animals which produce urea for temporary nitrogen storage or for osmoregulation (Read, '68). E. tridentatus secretes most of its nitrogen in the form of ammonia from the gills (Read, '68). It seems then that the mechanism for osmoregulation is not the same as is found in elasmobranchs. Because the skin of the lamprey is relatively impermeable to electrolytes and water (Bentley, '62) and the gills have been shown to be permeable to ions (Morris, '56) it may be that the gills are the site of active uptake of ions (Morris, '60). On the other hand, L. fluviatilis elaborates a single neurohypophyseal hormone, 8-arginine-oxytocin or vasotocin, which increases sodium loss, and an adrenocortical hormone, aldosterone, which decreases sodium loss, (Bentley and Follett, '62) and there is some evidence to suggest that the

renal tubules have some control over sodium (Bentley and Follett, '63). L. fluviatilis in fresh water takes up large quantities of water osmotically and excretes it as a hypotonic solution (Bentley and Follett, '63). This evidence has led to the suggestion that the lamprey possesses a mechanism for osmoregulation and excretion of nitrogenous wastes similar to that of freshwater teleosts rather than elasmobranchs (Wikgren, '53; Hardisty, '56; Morris, '56, '60; Bentley and Follett, '63; Read, '68), that is, the kidney is principally an organ for water excretion and electrolyte conservation (Smith, '59).

The present investigation has been prompted by this comparison and by recent electron microscopic studies attempting to correlate the structure of kidneys of various teleosts (Gritzka, '63); Bulger, '65; Bulger and Trump, '65a, '65b, '68; Olsen and Ericsson, '68; Bulger and Trump, '69) and a cyclostome, the hagfish (Parks and McFarland, '66; Ericsson, '67; Ericsson and Seljelid, '68), with known function in these species and with kidney structure and function in higher vertebrates. These studies have shown similarities and differences among vertebrate nephrons and have added to the knowledge of evolutionary development and function in the vertebrate kidney. A study of the kidney of the lamprey would aid in explaining the evolution of the kidney and its function in osmoregulation and nitrogen excretion.

Several nineteenth century biologists studied the kidney of the lamprey; notable among these was Rathke in 1827 (cited by Wheeler, 1899). Wheeler's (1899) study is among the most thorough and describes the development of a pronephros and an opisthonephros

in ammocoetes and a opisthonephros in adults. A few investigators ^{Requard and Policard,} appearing later deal with the pronephros (Hatta, '00; '02a, '02b, '02c; Torrey, '38; Gerard, '54). These investigators were limited by their inability to identify species of ammocoetes. This problem has been solved for P. marinus by the work of Vladykov ('50, '60) who provided a taxonomic key for the ammocoetes, and Thomas ('62) who showed their age-length relationships. More recent studies of the autumn migrating L. fluviatilis (Bentley and Follett, '63; Vinnichenko, '66) have provided little structural evidence to suggest similarities with kidneys of higher vertebrates. The study of Vinnichenko ('66) appears to be the only electron microscopic study of the lamprey kidney and deals with the animal in its autumn migration to the spawning grounds when changes are said to occur in the kidney due to the accumulation of biliverdin (Lanzing, '59). It is felt that a description of the kidney of P. marinus during all stages of the life cycle will provide a more suitable basis to relate to structure and function.

Since there is confusion in the terminology regarding kidneys, some of the terms used in this study should be defined. The major kidney of the lamprey will be referred to as an opisthonephros; this is the term coined by Kerr ('19) and described by Hyman ('49) as a "kidney which extends the length of the coelom behind the pronephros and hence has used up the mesomere tissue from which in amniotes, both mesonephros and metanephros come". In this usage, a mesonephros is the temporary embryonic kidney of an amniote. A glomerulus is a capillary tuft or plexus supplied by a single afferent arteriole and drained by a single efferent

arteriole and may be surrounded by a Bowman's capsule to constitute a renal corpuscle. In the pronephros of many animals the glomeruli unite to form a massive knot of capillaries, the glomus (Fraser, '50). This term has been restricted, until now, to the pronephros because few anatomists appear to be aware of the fact that the opisthonephric kidney of the lamprey contains a union of glomeruli. The term glomus will be used in this present work to designate this compound glomerulus of the opisthonephros of the lamprey. A renal corpuscle and its draining tubule constitute a nephron, the fundamental unit of the kidney.

The present investigation involves an examination of the kidneys of P. marinus from the first half-year of larval life, through transformation to the parasitic adult stage and the spawning migration. Five main features of the kidney will be examined:

1. A comparison of the structure of the renal corpuscle and tubular nephron during the life cycle.
2. The circulation of blood through the kidney in both ammocoetes and adults.
3. A comparison of the structure of the lamprey kidney to that of higher vertebrates.
4. The processes of degeneration and growth throughout the life cycle.
5. The function of some structures common to all vertebrate kidneys and those which appear to be unique to the lamprey.

MATERIALS AND METHODS

Ammocoetes, ranging in length from 16 to 148 mm, were obtained at various times throughout a period extending from September 1967 to March 1969 by means of an electro-shocker (Tibbles, '61; Thomas, '62) from Stoney, Venison, and Young's Creeks which flow into Lake Erie along its northern shore. Newly-transformed adults, 162 to 173 mm in length, were obtained in the same fashion in September 1967 and 1968. Tooth development was noted to confirm the identification of newly-transformed adults (Vladykov, personal communication). Parasitic adults, 49.0 to 52.5 cm in length, were taken in the winter of 1967 and fall of 1968 by fishermen gill-netting in Lake Erie near Port Dover, Ontario. Migrating adults, 49.0 to 53.0 cm in length, were taken in the spring of 1968 near their spawning grounds at Delhi, Ontario. All animals were anaesthetized in a 0.05% solution of tricaine methanesulphonate (MS222, Kent Chemicals Limited) according to the method of Thorson ('59) before dissection. While under the anaesthetic, ammocoetes were identified as to species (Vladykov, '50, '60) and classified into groups according to age (Thomas, '62).

Kidneys were fixed for light microscopy in Bouin's fluid (Gray, '54, p. 224) for 24 hours, dehydrated in ethanol, cleared in

terpineol, and embedded in Tissuemat (m.p. 56.5° C., Fisher Scientific Company). All kidneys were sectioned serially at 9 μ , mounted on glass slides, and stained with the periodic acid leucofuchsin method of Lillie ('54) followed by Mayer's haemalum (Lillie's modification, '42) and 1% orange G. In addition, several ammocoetes and adults were perfused before fixation with a 1:1 mixture of India ink in distilled water or with Kodak NTB2 nuclear track emulsion. Excess blood and perfusion fluid were permitted to leak out through an incision in the head or tail. Mounted sections containing the perfused emulsion were treated before staining with a 5% solution of hydroquinone, made basic with Microdol-X developer, until they appeared black. The sections were then placed in Kodak Acid Fixer for 10 minutes and rinsed.

For electron microscopy, some kidneys were fixed for 1 1/2 hours in ice-cold 1% osmium tetroxide buffered to a pH of 7.2 with veronal acetate (Zetterqvist, '56) either by immersion of 1-mm slices or by dropping the fixative directing onto the tissue in situ for 5 to 10 minutes followed by immersion of 1-mm slices for 1 1/2 hours. Others were flooded in situ with 3% ice-cold glutaraldehyde buffered to a pH of 7.4 with 0.3M sodium phosphate (Sabatini et al., '63), removed and fixed in toto for 2 hours by immersion in the solution, washed in several changes of distilled water buffered as with the primary fixative, and cut into 1-mm slices. The slices were postfixed in ice-cold 1% osmium tetroxide buffered to a pH of 7.4 with 0.1 M sodium phosphate (Millonig, '62) for 2 hours. Tissues were rinsed in distilled water, dehydrated in a

series of chilled ethanol to propylene oxide, and embedded in Epon 812 (Luft, '61). Silver and gold sections were cut with glass knives on a Porter-Blum MT-1 or a Reichert Om-U2 ultramicrotome, mounted on uncoated copper grids, and stained with aqueous uranyl acetate (Watson, '58) and lead citrate (Reynolds, '63). Some sections were mounted on tantalum or nickel grids, oxidized with 2% periodic acid for 30 minutes, and stained with lead citrate for positive identification of glycogen (Perry and Waddington, '66). In addition, 0.5- to 1.0- μ Epon sections were stained with 1% toluidine blue in saturated sodium borate (Bencosme *et al.*, '59) and 1.0- to 2.5- μ Epon sections were oxidized in a 4% Oxone solution (Siever and Munger, '68) or 2% periodic acid (McManus, '48) and stained with Schiff's reagent (Lillie, '54) and Weigert's haematoxylin (Lillie, '54).

Fifty ammocoetes of various age classes, five newly-transformed adults, four parasitic adults, and ten migrating adults were examined with the light microscope. Twenty ammocoetes, three newly transformed adults, three parasitic adults, and five migrating adults were examined with the electron microscope. Due to the small numbers of newly-transformed and parasitic adults available, one kidney from each of two specimens was prepared for light microscopic examination while the remaining kidney was prepared for electron microscopy.

Light micrographs were taken with a Leica IIIf camera using Adox KB 14 fine-grained film with a Leitz yellow-green filter (Orfil). Film was developed in Adox E 10 or Kodak Microdol-X developers. The microscope used was a Leitz Orthoplan with Plano

objectives or a Leitz Ortholux with apochromatic objectives.

The electron microscope used was a Philips EM-100C, and electron micrographs were taken on 35-mm Kodak Fine Grain Positive Film which was developed in Kodak D-11 developer.

Reconstructions of light microscopic material was performed by tracing serial sections onto 8 1/2 x 11-inch 0.0075 acetate sheets after enlargement of the sections using a Leitz XIC carbon arc microprojector.

OBSERVATIONS

GROSS MORPHOLOGY

The paired kidneys of lampreys projected ventrally into the body cavity from a dorsal mass of adipose tissue (figs. 1 to 4) and partially surrounded the gut (figs. 2, 3).

In ammocoetes the strap-shaped kidneys began at the level of the liver and extended posteriorly as much as 35 mm, the length depending upon the size of the animal, where the renal tissue disappeared and the archinephric duct continued to the cloaca (fig. 5).

There were two parts, easily detected with the naked eye, to the kidneys of newly-transformed adults. The anterior portion appeared to be located in the region previously occupied by the kidney of the largest ammocoetes and ranged in length between 30 and 34 mm while the posterior portion, which was 36 to 47 mm long, extended to the cloaca (fig. 5).

The kidneys of parasitic adults ranged in length from 14.0 to 16.5 cm while those of migrating adults were 11.5 to 14.0 cm. There appeared to be no correlation between size or sex of the animal with length of kidney in either parasitic or migrating adults. One kidney, usually the left, was always shorter than its mate. A comparison of kidney size and location in the three stages can be seen in fig. 5.

The kidneys of all three developmental stages consisted of glomera, numerous tubules, and an archinephric duct which continued to the cloaca (figs. 1 to 4). The posterior portion of the kidney of the newly-transformed adult was confined to the ventral third of the adipose projections (fig. 3) while little adipose tissue was found in the mature adult and this only at the dorsal surface (fig. 1). The anterior part of the kidney of newly-transformed adults contained degenerating glomera and tubules.

The kidneys were enveloped in a capsule of visceral peritoneum which was reflected from the parietal peritoneum (figs. 1 to 4). Its simple squamous to cuboidal mesothelium, which tended to thicken with age (figs. 6, 7), overlaid large bundles of collagenous fibrils. The cytoplasm of the mesothelial cells contained numerous smooth vesicles, free ribosomes, fibrils, and mitochondria (fig. 7). A few dense granules were present and no microvilli were seen (fig. 6). Adjacent plasma membranes were fused apically into a junctional complex and desmosomes were found at each end of large intercellular spaces (fig. 7). An electron-dense precipitate of unknown origin was usually found on the free surface (fig. 6). The cells rested on a basement membrane (fig. 6).

CIRCULATION

Blood Supply to the Glomus

Three-dimensional reconstruction on plastic sheets of kidneys perfused with India ink showed that all glomera of both ammocoetes and adults were supplied with blood from separate renal

arteries branching from the dorsal aorta (figs. 8 to 11). In first-year ammocoetes, blood entered the anterior portion of the glomus directly from a single renal artery by way of tiny anterior and posterior afferent arterioles. In one glomus the renal artery was seen to branch, one branch entering the anterior part of the glomus, the other the posterior part. In older ammocoetes the smaller anterior glomera were supplied by a single renal artery which joined a longitudinal medial artery passing along the medial surface of the glomus, periodically sending afferent arterioles into the glomus (figs. 9, 10). The longer posterior glomera of these older animals were supplied by as many as three renal arteries which all joined the medial artery before entering the glomus. The medial artery was present in every transverse sections of a glomus (fig. 12) and was often seen in sections showing no glomus suggesting that the medial arteries of all glomera are continuous.

The renal arteries of transforming larvae and adults were highly developed and contained a thick muscle layer (fig. 13A). There was a great variation in the number of renal arteries supplying the long glomus of the mature adults. For example, a 52-cm adult with kidneys 13.0 and 13.5 cm long had 17 renal arteries in each kidney showing little branching (fig. 14A) while a 51-cm adult had kidneys of 12.0 cm with 25 to 27 renal arteries showing more extensive branching (fig. 14B). This variation was common in all animals studied and was not related to the sex of the animal. In the kidney of the adult the renal arteries joined a medial artery

which extended the entire length of the glomus (fig. 11), periodically sending afferent arterioles into it (figs. 11, 13A, 13C). In addition to this branching, the renal arteries gave off as many as four other branches which passed in several directions but always arrived in the glomus; this branching was most extensive in the posterior half of the kidney (figs. 14A, B).

Serial reconstruction of a glomerulus of a 130-mm ammocoetes which had been perfused with India ink revealed the general pattern of its capillary network (figs. 15, 16). The afferent arteriole divided at the hilus of the glomus into six loops consisting of anastomosing networks of capillaries (figs. 15, 17 to 20) and constituting a single glomerulus (fig. 15); each loop was drained by a single efferent arteriole (figs. 4, 15, 17).

Blood Supply to the Tubules and its Drainage

India ink and photographic emulsion injected into the dorsal aorta just anterior to the kidneys could be traced in serial sections through the kidney to the posterior cardinal vein. Reconstructions on plastic sheets showed differences between ammocoetes and adults.

Ammocoetes

Blood from the efferent arterioles of the glomus (figs. 4, 17) flowed into capillaries and sinusoids between the tubules and islands of haemopoietic tissue (figs. 4, 10, 12). The fenestrated wall of the sinusoids consisted of simple endothelial cells (fig. 12) and large phagocytes containing cellular debris (fig. 18).

The capillaries and sinusoids in the intertubular area were bathed in blood. Blood flowed dorsally through the capillaries and sinusoids but its path varied, depending upon the size of the ammocoetes being studied.

In the 16-mm ammocoetes blood drained from the intertubular sinusoids directly into the posterior cardinal veins which were apposed to the dorsal surface of the kidneys. In ammocoetes between 16 and 60 mm the blood in the intertubular sinusoids drained into a short, thin-walled sinus connected to each posterior cardinal vein (fig. 8). In ammocoetes larger than 70 mm, blood in the intertubular sinusoids passed through a short sinus into a large subcardinal sinus which lay beneath each posterior cardinal vein. The subcardinal sinuses were usually joined below the dorsal aorta but divided when traversed by the descending renal artery, and were periodically joined to the posterior cardinal veins by short branches. The subcardinals appeared as discrete thin-walled vessels beneath the posterior cardinal vein in ammocoetes about 125 mm long (fig. 10).

Adult

A large efferent arteriole with several layers of muscle drained each loop of the elongate capillary tuft of the adult and most of these arterioles passed anteriorly between the tubules toward the archinephric duct (figs. 1, 11). A few extended dorsally amongst the tubules. The arterioles branched frequently into capillaries which flowed into narrow sinusoids which were crowded between the closely packed tubules. In most of the kidney the sinusoids were tortuous but lateral to the archinephric duct they

paralleled the straight tubules (figs. 1, 11). They were lined with squamous cells and fixed phagocytes and were filled with blood. Less haemopoietic activity was found between the tubules of adults than was seen in ammocoetes.

Two straight blood sinuses extended the entire length of the kidney beneath the capsule on both sides. The lateral subcapsular sinus extended from the position of the archinephric duct and the medial subcapsular sinus from a line just above the position of the glomus and both sinuses met at the dorsal surface to be drained by a common sinus which emptied into the subcardinal sinus (fig. 11). They were lined by a simple endothelium beneath which smooth muscle cells could occasionally be found. As in ammocoetes, the subcardinal sinus periodically communicated with the posterior cardinal vein through short branches.

Blood from the intertubular sinusoids drained into large interstitial sinuses which traversed the kidney obliquely and opened into the subcapsular sinuses (figs. 1, 11). The interstitial sinuses were large in the central regions but dorsal to the glomus, where much of the blood in the intertubular sinusoids drained into the subcapsular sinuses, they were smaller. The interstitial sinuses did not extend the length of the kidney as did the subcapsular sinus but appeared at frequent intervals.

RENAL CORPUSCLE

In transverse sections of ammocoetes one glomus appeared in the ventral half of each kidney, its position being related to

that of the archinephric duct. Anteriorly the archinephric duct was dorsal and the glomus was found at the ventral border of the kidney (figs. 2, 8); posteriorly the glomus assumed a more dorsal position to accommodate the ventral position of the duct (fig. 4).

During the growth of an ammocoete there was a gradual lengthening of the kidney and glomera as well as an increase in the number of glomera and their draining nephrons (fig. 21). In the first year of larval life each kidney contained two to five separate glomera of 90 to 870- μ in length placed end to end and each glomus was drained by three to eleven nephrons, the longer glomera having more nephrons. The smaller glomera were found anteriorly with the longer ones lined up behind, a distinction which became more pronounced as the ammocoetes increased in length (fig. 21).

In most newly-transformed and parasitic adults a single glomus extended almost the full length of the kidney in its dorsal half (figs. 11, 13A to C). Remnants of smaller glomera were often seen at the anterior tip of the adult kidney (fig. 22) but did not appear to be connected to the large glomus.

Exceptional situations were noted in two adults. In addition to the large glomus, one migrating adult showed a swelling in the posterior portion of the kidney which contained a short second glomus (fig. 23). A parasitic adult showed dorsal projections from each kidney which extended to the gut and which contained a glomus of the size seen in ammocoetes (fig. 24) but smaller than that of newly-transformed adults (fig. 25).

In the glomera of small ammocoetes, each capillary loop was surrounded by a double-walled Bowman's capsule (figs. 12, 16a) and each capsule was separated from adjacent capsules by loose connective tissue (figs. 19, 20) so that there were several Bowman's capsules for a single glomerulus (figs. 12, 16a). The visceral or podocyte layer consisted of a single layer of podocytes closely applied to the capillary endothelium (figs. 12, 18 to 20); the parietal or squamous layer of the capsule consisted of a simple squamous epithelium and was continuous with the podocyte layer and the neck segment of the tubule (figs. 19, 20). The glomus with its associated capsules constitutes the compound renal corpuscle of the ammocoetes. The number of neck segments draining a glomus was proportional to the size of the glomus (fig. 21).

In newly-transformed and parasitic adults, and occasionally in older ammocoetes, the dilated ends of the nephrons were interposed between pairs of loops resulting in a series of irregular channels whose walls closely followed the contours of the capillary knot (fig. 13C). Thus each loop excreted into two nephrons and there was no typical cup-shaped Bowman's capsule (fig. 16b). The epithelium of the capsule which invested a loop developed podocytes and resembled the podocyte layer of Bowman's capsule of ammocoetes and other vertebrates (fig. 26). The remainder of the capsule was composed of a simple squamous epithelium resembling the squamous layer of Bowman's capsule (figs. 27 to 29) and opened into the ciliated neck segment of the proximal convoluted tubule (fig. 27).

In the glomus of the adult and in the long posterior glomera of the older ammocoetes, the squamous layers surrounding two adjacent neck segments came together for a short distance to form a partition consisting of the two squamous epithelial layers enclosing loose fibrous connective tissue and a few cells (fig. 28). The two layers did not fuse but extended into the glomus to invest the capillary knot and become the podocyte layer (fig. 28).

With the electron microscope the podocytes of ammocoetes and adults were seen to be large, irregular cells with large numbers of branching cytoplasmic processes which rested on the basement membrane of the capillaries (fig. 26). The lobed nucleus of the podocytes (fig. 26) often appeared as two nuclei in section (fig. 30) and contained a single nucleolus (figs. 26, 31) and clumps of chromatin beneath the nuclear envelope (fig. 30). The nuclear envelope was frequently interrupted by pores (fig. 30). The Golgi apparatus consisted of concentrically-arranged flattened and swollen saccules with numerous closely-associated microvesicles (fig. 31) and was commonly placed at the apical pole of the cell. Irregularly-shaped mitochondria, rough-surfaced endoplasmic reticulum (rough ER), free ribosomes, and tiny, smooth, spherical vesicles were seen scattered throughout the cell (figs. 30, 31). Other structures present were dense granules (figs. 26, 30), fibrils (figs. 26, 30), and multivesicular bodies (fig. 30). All three of these inclusions, especially the fibrils, were more abundant in the adult. In the ammocoetes the fibrils, (70 to 80 $\overset{\circ}{\text{A}}$ in diameter), appeared as thin,

interweaving strands with no particular orientation (fig. 32) and were not seen in all podocytes. They were prominent in all cells of the adult and were usually concentrated around the nucleus (fig. 26). The branching processes of the podocytes ended as little feet or pedicels on the basement membrane (fig. 32) and were larger and more abundant in the adult (fig. 33). Individual pedicels were interconnected by cytoplasmic strands which appeared to form a diaphragm (fig. 32) and as many as three strands were seen to connect a pair of pedicels. The cytoplasmic processes contained a few small mitochondria, and dense granules (fig. 33). The plasma membrane surrounding them was covered by a fibrillar fuzzy material (fig. 32).

There was a gradual transition from the loosely-arranged typical podocytes to the squamous epithelial cells. The cells became flatter, their processes became less abundant and finally disappeared and tight junctions fused the adjacent cells (fig. 28).

The squamous cells contained a central nucleus, a few scattered mitochondria, a few strands of rough ER, smooth vesicles, and free ribosomes scattered throughout the remainder of the cytoplasmic matrix (fig. 29). The cells rested on a basement membrane which was continuous with that of the visceral layer and the cells of the neck segment (fig. 27).

Cilia and microvilli became more numerous and there was a gradual increase in cell height in the transition from the squamous cells to the ciliated columnar cells of the neck segment (fig. 27).

In the partition formed between two adjacent nephric capsules the basement membranes enclosed a parenchyma of stellate mesangial cells and collagenous or reticular fibrils which were continuous with the fibrils associated with the basement membranes of the squamous cells (fig. 28).

The branches of the afferent arteriole in the ammocoetes consisted of a layer of flattened endothelial cells surrounded by one or two layers of smooth muscle cells (fig. 17) while in the adult the muscle layer was three to four cells thick (fig. 34). The smaller efferent arteriole had a thinner wall (fig. 17) and its muscle layer was one or two cells thick in the transforming larva (fig. 27) and two or three cells thick in the adult.

The afferent arteriole penetrated between two capsules and was surrounded by a basement membrane and the podocyte layer (fig. 34).

A single layer of squamous endothelial cells with bulging elongate nuclei formed the wall of the capillaries and lay on a basement membrane which was common to the capillary and the podocyte layer (figs. 26, 33). The perinuclear cytoplasm of the endothelial cells consisted of a few scattered mitochondria and free ribosomes, clumps of rough ER with flattened cisternae, numerous tiny smooth vesicles, and a few granules of various electron densities (fig. 35). The well-developed Golgi apparatus was composed of flattened saccules, numerous microvesicles, and large clear vacuoles which appeared to have been pinched off from the ends of the saccules (fig. 35). A

few dense granules were usually found near the Golgi apparatus (fig. 35). The thinner portions of the endothelial cells usually contained numerous smooth vesicles and free ribosomes and occasionally mitochondria and dense granules (fig. 36). The endothelium of both ammocoetes and adult was usually complete although a small number of pores covered by a thin membrane were found (fig. 36). The basal plasma membrane of some endothelial cells of the adult showed invaginations which penetrated deep into the cytoplasm while in other cases it covered basal cytoplasmic extensions (fig. 37). Adjacent endothelial cells were fused by typical junctional complexes (fig. 37).

The lumina of the capillaries usually contained blood cells which, in the ammocoetes, were often undergoing mitosis (fig. 18). In the migrating adult the capillaries were often filled with cellular debris either in macrophages or lying free so that it was difficult to distinguish the endothelial cells under low magnification (fig. 38). That this material was degenerative was indicated by their swollen mitochondria, and remnants of chromatin and nuclear envelope. Numerous granules of varying size and electron density were present. A limiting plasma membrane could not be seen to separate the cytoplasmic structures from the contents of the lumen.

The endothelium was separated from the basement membrane by collagenous or reticular fibrils (fig. 35) and processes of mesangial cells were enclosed within infoldings of the endothelial cells (figs. 36, 38). The relatively large mesangial cells contained

a lobulated nucleus and possessed numerous cytoplasmic processes which extended in all directions following the contours of the endothelial cells (fig. 36). Mesangial cells were most abundant near the hilus of the glomus. Their cytoplasm contained a few mitochondria, a well-developed Golgi apparatus, and scattered clumps of ribosomes. The remainder of the cytoplasm consisted of a matrix of medium electron density (fig. 39).

The visceral and endothelial layers shared a common basement membrane which consisted of a dense portion (lamina densa) of 450 to 500 Å sandwiched between two less dense layers, the lamina rara externa (300 to 350 Å) on the visceral side and the lamina rara interna (1500 to 1600 Å) on the endothelial side (fig. 35). A characteristic feature of this basement membrane was the close association of the lamina densa to the podocyte layer. Collagenous or reticular fibrils were often located within the lamina rara interna (fig. 35).

TUBULAR NEPHRON

The tubular portion of the nephron of ammocoetes and adults was divided into five main segments, on the basis of cell height, stain differentiation, fine structure, and position within the kidney. Following in order from the renal corpuscle to the archinephric duct (ureteric duct) these were: neck, proximal, intermediate, distal, and collecting segments (fig. 40). Corresponding to differences in the location of the glomus within the kidneys of ammocoetes and adults, the location of the different segments were modified. Certain segments of the tubules of ammocoetes and adults were found

to be similar and will be described together; when differences in segments occur they will be described separately.

Neck Segment

The initial segment of the tubule leading from the renal corpuscle was a ciliated neck segment located in the ventral half of the kidney of ammocoetes and the dorsal half in adults (fig. 40). The total number of neck segments increased with the age of the animal and therefore with the length of the kidney (fig. 21). Usually a single neck segment opened into a proximal segment (fig. 41A) but rarely two neck segments joined a single proximal segment (fig. 41B). Each neck segment drained its own cavity in the compound capillary tuft (fig. 41A, C), either a Bowman's capsule surrounding a single loop of the glomerulus of ammocoetes, or a dilated sac interposed between two loops of the glomerulus of an adult (fig. 16a, b).

The ciliated columnar epithelial cells of the neck segment ranged in height from 7.0 to 11.0 μ in ammocoetes (fig. 41D) and from 9.0 to 20.0 μ in adults. There was a gradual transition from the simple squamous epithelium of the capsule to the tall, ciliated cells of the neck segments (fig. 27). The basement membrane separated the epithelial cells from capillaries and numerous blood cells which were often free within the intertubular connective tissue or enclosed within thin-walled sinusoids (fig. 42) and was continuous with the basement membrane of the squamous epithelium (fig. 43).

The basal, oval nuclei of the epithelial cells were oriented perpendicular to the surface and occupied most of the cell. Each contained a prominent nucleolus (fig. 43) and was limited by a

porous nuclear envelope (fig. 44).

The plasma membranes of adjacent cells were interdigitated (fig. 44) and tangential sections revealed intercellular spaces or canals (figs. 45, 46) often containing cytoplasmic projections of the epithelial cells (fig. 46). Each space was fastened by a desmosome at each end (fig. 46) and the cells were secured to adjacent cells at the apex by typical junctional complexes (fig. 46).

The cytoplasm of the cell consisted of typical cellular organelles. Mitochondria were characteristically of larger diameter than those found in cells of other segments of the tubular nephron. They were generally situated above and below the nucleus and only seldom at the sides (figs. 43, 44). They were of variable shape and size and their cristae were oriented transversely (fig. 44). The Golgi apparatus was always located above and often to the side of the nucleus (figs. 43, 45). There appeared to be no concentrations of rough ER but tiny vesicles, with ribosomes attached to their outer surface, could be seen throughout the cytoplasm (fig. 44). In addition, many free ribosomes (fig. 44) and glycogen particles (fig. 45) could be seen scattered throughout the cytoplasm. The remainder of the cytoplasm contained a few dense granules, probably lysosomes (fig. 46), and numerous smooth vesicles (fig. 44).

The cilia were usually found in clumps with the intervening areas being provided with short, irregular microvilli so that almost the entire free surface of the cell had cytoplasmic projections, (fig. 43). The deep root of each cilium consisted of an enlarged basal body (corpuscle) subtended by its fibrous extension, the electron-

dense basal plate (fig. 47) which occurred at the same height in each cilium. Above the plate a central pair of filaments appeared and the peripheral ring consisted of nine doublets (fig. 49). Near the tip of the cilium the peripheral ring was composed of nine single filaments surrounding a central pair (fig. 49).

The cytoplasm surrounding the bases of the cilia at the apex of the cell consisted of a few scattered mitochondria, multivesicular bodies (fig. 46), and numerous smooth vesicle (fig. 47). Similar vesicles also appeared in the small amount of cytoplasm surrounding the peripheral ring of filaments in the shaft of the cilium (fig. 47).

The cells of the neck segment of ammocoetes varied a great deal from one end of the kidney to the other in the amount of glycogen present within their cytoplasm. Little was found anteriorly but posteriorly (fig. 41A) the cells stained positively with the periodic acid-Schiff technique (PAS+). With the electron microscope, dark cells containing large amounts of glycogen particles, 350 to 500 Å in diameter, were seen to be interspersed between light cells containing moderate amounts (figs. 45, 50). In addition, the nucleus and cytoplasmic matrix of the dark cells were more electron dense (fig. 50). The Golgi apparatus of the dark cells was small (fig. 45) but the remainder of the cytoplasmic components were similar to those described above. The presence of glycogen did not appear to be related to seasonal activity. It was not found in the neck segments of the adult.

Proximal Segment

After a short distance the neck segment opened into the second part of the nephron (figs. 40, 41A, 51) due to the similarity

of this region to the corresponding segment in most higher vertebrates, it was termed the proximal segment.

The proximal segment of both ammocoetes and adults was distinguished from all other regions of the tubular nephron by its PAS+ brush border (fig. 41C). Two regions, the proximal pars convoluta and proximal pars recta were distinguished in the proximal segment on the basis of the epithelium lining each.

Proximal Pars Convoluta

The proximal pars convoluta comprised about one-third of the tubular area of sections of the adult kidney. It was confined to the ventral half of the kidney in ammocoetes and the dorsal half in adults.

There was an abrupt transition from the dark, ciliated cuboidal epithelial cells of the neck segment to the lighter columnar cells of the pars convoluta which possessed abundant microvilli (Fig. 51).

The cells of the pars convoluta in ammocoetes were pyramidal with a truncated apex and ranged in height from 10.0 to 16.0 μ (figs. 52 to 54). In contrast, the cells in adults tended to be more columnar and ranged in height from 18.0 to 21.5 μ (fig. 55) but were cuboidal near the neck segment (fig. 51). The nucleus was roughly spherical in outline and basal (figs. 52, 54) and often contained a nucleolus (fig. 54). Chromatin was occasionally seen at the periphery of the nucleus (fig. 56) but was more often evenly distributed in small clumps throughout. Usually the nucleus appeared pale in both light and electron microscopic preparations (figs. 52, 54). The nucleus was enclosed within a porous (fig. 57) double-layered

envelope, the outer layer of which was often studded with ribosomes (fig. 56).

Numerous closely-packed microvilli (figs. 54, 55), 1.2 to 1.4 μ in length and 0.06 to 0.09 μ in diameter, were covered with a fibrous fuzz (fig. 58) and had saccular invaginations between them at the apical surface (fig. 59). A fibrous axial core extended the entire length of each microvillus (figs. 58, 60) and penetrated into the apical cytoplasm of the cell (fig. 60). The microvilli varied from cell to cell; in some cells their plasma membranes were parallel giving the microvillus a smooth outline (fig. 60) while in other cells the microvilli contained numerous vesicles and the plasma membrane was invaginated at several points producing a rippled appearance (fig. 59). All microvilli on an individual cell were of one type or the other. The membranes of some adjacent microvilli had fused and the boundaries between them were not easily discernible (fig. 58, 59).

In addition to the microvilli, single cilia were occasionally found on the apical surface of the cells of the pars convoluta (fig. 59). Bulbous extensions of the apical cytoplasm which lacked microvilli and often contained dense granules and opaque vacuoles appeared to push out between the microvilli and may produce the cytoplasmic debris often found in the lumen (figs. 53, 61).

Laterally the cells were limited by a plasma membrane (figs. 54, 55) which was fused to that of an adjacent cell by a junctional complex at the apex and desmosomes periodically throughout the rest of the length (fig. 55). Periodic interdigitations of

the lateral plasma membranes and intercellular spaces were found (figs. 54, 55).

The base of the cell was limited by a plasma membrane which was not invaginated into folds but always contained small pockets suggestive of pinocytic vesicles (fig. 62).

The cells rested on a basement membrane (figs. 54, 55) which separated them from the thin-walled sinusoids and numerous blood cells of the intertubular *arèg.* (fig. 52).

With the light microscope few organelles could be seen above the nucleus (fig. 52) and with the electron microscope this area was shown to consist mainly of tubular dense bodies, numerous smooth vesicles, and large clear vacuoles limited by an incomplete membrane (figs. 59, 63). The apical vesicles were similar to those seen within the microvilli and were often located within the large clear vacuoles (fig. 57) or multivesicular bodies (fig. 59).

The remainder of the apical cytoplasm consisted of a few mitochondria, scattered free ribosomes, and dense granules (fig. 63).

The cells of ammocoetes often contained glycogen granules 350 to 500 Å in diameter (fig. 60). The Golgi apparatus was always located at the side of the nucleus and consisted of flattened saccules, numerous microvesicles, and a few larger clear vacuoles (fig. 56). Mitochondria near the apex of the cell were short and rod-shaped (figs. 55, 55), possessed transverse cristae (fig. 63), and had no specific orientation while those at the sides and base tended to be more elongate (fig. 53). The lateral mitochondria tended to be oriented along the longitudinal axis of the cell while those at the base showed no specific orientation (figs. 52, 53). In contract

to the ammocoetes, the mitochondria at the base of the proximal tubule cells of the parasitic adult were of various bizarre shapes and structures (fig. 64). They were usually larger in the adult but the most characteristic feature was the presence of filamentous material, crystalline structures, and elongate cristae within the mitochondria themselves, often oriented along the longitudinal axis of the mitochondria (figs. 65 to 67). Higher magnifications revealed that the mitochondrial matrix between each crista was cross-banded with electron-dense material at intervals of 180 to 200 Å (fig. 65B). At one end of the mitochondrion longitudinal striations were usually present with a periodicity of 560 Å (fig. 66); between these major striations were rows of particles, or minor striations, 90 Å apart. Mitochondrial granules were often seen (fig. 66). Occasionally cristae were seen running circularly within a mitochondrion while others had filamentous strands running longitudinally (fig. 67). Often associated with these irregular mitochondria in the adult, and rarely in the ammocoetes, were spherical bodies containing a dense flocculent material (figs. 57, 59, 66, 67). They were limited by a single membrane and were always close to rough ER and smooth vesicles (fig. 66).

In both ammocoetes and adults rough ER could be found throughout the cell (fig. 60) but the major concentrations were at the sides and below the nucleus (figs. 54, 55) and consisted of parallel layers of flattened cisternae studded with ribosomes (fig. 56). Free ribosomes were seen throughout the cells with larger numbers occurring in the adults (figs. 57, 59).

Granules of various electron densities and sizes were usually found at or near the apex of the cell (figs. 52, 53, 55, 56, 60, 61, 63). Most of the cytoplasm of the cell consisted of irregular smooth vesicles which could be grouped into two major types. Scattered throughout were tiny smooth vesicles bound by a single membrane and containing a homogeneous material of medium electron density (fig. 66). They were usually associated with larger, more electron-opaque vesicles concentrated at the base and sides of the cells (fig. 62). These large vesicles contained particulate material and appeared to be continuous with the lateral and basal plasma membranes (fig. 62). This close association of vesicles to the plasma membranes is common to proximal tubule cells of both ammocoetes and adults (figs. 54, 62).

Clumps of electron-dense material were observed lined up at intervals along the inner surface of the basal plasma membrane of the proximal tubule cells of both ammocoetes and adults (figs. 57, 64). In addition, a thin layer of fibrous material above these basal densities extended for a considerable distance across the base of the cell (fig. 57).

Proximal Pars Recta

The descent of the proximal pars convoluta into the straighter pars recta (fig. 40) was marked by a gradual decrease in cell height, lumen size, and in the extent of the brush border (fig. 68). The pars recta of ammocoetes was oriented in a ventral to dorsal direction (fig. 40) and the cells ranged in height from 7.6 to 14.3 μ , the large range being due to a gradual transition

from the taller cells of the pars convoluta. In the adult the pars recta ran in a dorsal to ventral direction (fig. 40) and the range in height of the epithelium was 9.4 to 10.9 μ . In contrast to the ammocoetes, there was an abrupt change from the pars convoluta to the lower cells of the pars recta. The cells of this segment were identified by fewer microvilli, dense granules, and clear vacuoles (figs. 68 to 72). Microvilli were usually clumped and the dense granules were much smaller (fig. 69) than in the pars convoluta (fig. 52).

The lateral plasma membrane (fig. 70) in the adult was highly invaginated and enclosed a series of intercellular spaces, each separated by a desmosome (figs. 71, 72). This space often contained wandering blood cells and cytoplasmic processes (fig. 71). The tubules were surrounded by sinusoids containing blood cells (fig. 69).

With the exception of the above-mentioned features, these cells resembled those of the pars convoluta. Mitochondria in the adult were often of irregular shapes (fig. 72). Two types of vesicles were seen and they had the same associations with the plasma membrane as in the pars convoluta (fig. 70). Rough ER was more widely concentrated at the sides than at the base of the nucleus (fig. 70). The Golgi apparatus was located above the nucleus and multivesicular bodies were common at the apex of the adult cell (fig. 72).

As has already been noted for the neck segment, the cells of both parts of the proximal segment in ammocoetes contained

greater quantities of glycogen posteriorly (fig. 60). Near the posterior tip, where it was difficult to differentiate the pars convoluta and the pars recta, dark and light cells again could be distinguished (fig. 73). Except for the absence of cilia, the dark cells resembled those of the neck segment (figs. 45, 50). Both dark and light cells possessed microvilli but the dark cells more often protruded into the lumen. The cells were separated by large intercellular spaces containing many cytoplasmic projections. Dark cells contained greater quantities of glycogen than light cells and their nuclei and cytoplasmic matrix were more electron-dense (fig. 73).

Intermediate Segment

The short intermediate segment was highly variable in structure and ranged from 250 to 500 μ in length in ammocoetes and from 200 to 3,200 μ in adults (fig. 40). It was surrounded by the tubules of the dorsal third of the kidney of ammocoetes and the tubules of the ventral third of adults (figs. 74 to 76). Its simple epithelium ranged in height from 3.1 to 8.0 μ in ammocoetes and from 3.8 to 8.8 μ in adults. Since the cells of this tubule differ widely from ammocoetes to adults, they will be considered separately here.

Ammocoetes

Two types of intermediate segments were found in ammocoetes (figs. 77, 78). The cells of the first were squamous, PAS+ (fig. 75), and showed no brush borders. The cuboidal cells of the second type were characterized by their dome-shaped protrusions of the apical surfaces (fig. 78).

An abrupt decrease in cell height and a gradual reduction in the numbers of microvilli marked the transition from the proximal pars recta to the squamous type of intermediate segment (fig. 77). The lumen commonly was filled with debris while extravasated blood cells occurred between the cells (fig. 79).

The cells had few microvilli; these were often clumped (fig. 7) and were coated with an electron-dense fuzz (fig. 80). The nucleus was flattened but invaginated. A Golgi apparatus was usually located lateral to and above the nucleus. On the whole cell organelles were not abundant (fig. 80). Mitochondria were few in number having transverse cristae and a few strands of rough ER were scattered throughout the cytoplasm (fig. 80). The apical cytoplasm contained large concentrations of 70- \AA fibrils and single glycogen particles (fig. 80); dense granules were seen throughout the cell (fig. 79).

The typical intermediate cell of the squamous type had a small amount of cytoplasm and a flattened, irregular nucleus (fig. 81), with most of the sparse organelles concentrated at its ends, although free ribosomes, dense granules, and a few strands of rough ER were scattered throughout. Bundles of 70- \AA fibrils often appeared in indentations of the nuclei while smooth vesicles appeared in large numbers at the sides of the nucleus near the plasma membrane (fig. 81). Mitochondria, which were located at the ends of the nucleus, were sparse but large and contained transverse cristae which were often angular (fig. 81). The cells were fused apically by a junctional complex and basally by desmosomes and large intercellular spaces were found (fig. 81).

Approaching the distal segment the cells of the squamous type of intermediate segment increased in height and the nucleus assumed a more oval shape (fig. 82). Microvilli were more abundant and the cytoplasm contained a large number of glycogen particles. Membrane-bound structures containing glycogen particles were also seen (fig. 82). The cytoplasm contained free ribosomes, small strands of rough ER, smooth vesicles, and mitochondria with angular cristae. The Golgi apparatus was lateral to the nucleus (fig. 82).

In the second type of intermediate segment, the dome-shaped apical protrusions (fig. 83) contained numerous free ribosomes, a few mitochondria, and often a portion of the Golgi apparatus which was largely lateral to the nucleus (figs. 84, 85) and consisted of dilated saccules and microvesicles (fig. 85). The remainder of the apical surface contained a few short microvilli covered by a fibrillar fuzz (fig. 84). The lateral plasma membranes were fused at their apices by junctional complexes (fig. 84) and the intercellular spaces were often enlarged by wandering blood cells (fig. 84). The cells rested on a basement membrane and collagenous fibrils were found between this and the closely associated sinusoidal endothelium (fig. 86).

The nucleus was usually oriented along the longitudinal axis of the cell (fig. 83) and chromatin was clumped around the inner surface of the nuclear envelope (fig. 85). Dense granules of various sizes and shapes were commonly closely associated (fig. 85). Large mitochondria with transverse cristae usually occurred at the

sides of the nucleus (fig. 86).

One of the most conspicuous features of these cells was the presence of dilated cisternae of the smooth endoplasmic reticulum (smooth ER)¹ usually found above and beside the nucleus and occasionally at the base of the cell (figs. 83, 85, 96). Dilated rough ER was occasionally seen and small vesicles were concentrated at the sides of the cells (fig. 86) but apical vesicles were not prominent (fig. 85). Numerous fibrils were found, usually concentrated around the nucleus (fig. 86). Microtubules, 250 Å in diameter, were scattered throughout (fig. 86).

Adult

The length of the intermediate segment of adults varied widely and showed no correlation with the sex of the animal or the region of the kidney from which it was taken (figs. 74, 76, 87, 88). When it was long it could often be seen running parallel to the distal and collecting segments, separated from them only by straight sinusoids (fig. 74).

Often the intermediate segment consisted of only two or three cuboidal cells which could be distinguished from the cells of the proximal and distal partes rectae by their clear cytoplasm (fig. 87). The apical surfaces of these cells bore a few irregular

¹Foot Note

The term "smooth endoplasmic reticulum (smooth ER)" has been used to denote smooth, spherical and tubular vesicles which are either dilated or fuse with one another to produce a network. The term "smooth vesicle" has been used to denote all other small, spherical to tubular vesicles which appear separate from surrounding vesicles.

microvilli which were covered by an electron-dense fuzz (fig. 89); this fuzz was absent from the microvilli of the cells of the adjacent proximal pars recta. The nucleus was spherical and centrally located (fig. 89). The Golgi apparatus consisted of a few flattened saccules and numerous microvesicles (fig. 90). Mitochondria were usually small and spherical (figs. 89, 90). In contrast to the cells of the proximal pars recta, these cells contained little rough ER and free ribosomes (fig. 89). Small spherical vesicles constituted most of the cytoplasm (figs. 89, 90). Bundles of fibrils were seen in the cytoplasm, often associated with the nucleus (fig. 90).

The larger squamous intermediate segment of adults was made up of two cell types (fig. 88). The more abundant type had an oval nucleus and a dense cytoplasmic matrix and its apical surface always reached the lumen (fig. 91). A few microvilli of irregular shape and distribution, and covered with an electron-dense fuzz, were seen on the apical surface (fig. 91). The lateral plasma membranes interdigitated slightly with those of adjacent cells and the basal plasma membranes were often involuted. The cells rested on a basement membrane with bundles of collagenous fibrils below (fig. 91). A Golgi apparatus consisting of slightly dilated saccules and microvesicles was positioned above and to one side of the nucleus (fig. 91). Relatively few mitochondria were seen and these were positioned at the ends of the nucleus. The cytoplasm also contained a few strands of rough ER, many smooth vesicles, a few dense granules, and large numbers of free ribosomes (fig. 91).

The second type of cell had a flatter nucleus, a clearer cytoplasm and only occasionally reached the lumen (fig. 92). These cells were usually seen in the transitional zone from the proximal pars recta to the intermediate segment. One to three of these cells rested on the basement membrane and were pushed between the first type. The nucleus was invaginated and irregular in outline with chromatin clumped around the inner surface of its double envelope (fig. 93). The cytoplasm contained a few mitochondria, few scattered free ribosomes, dense granules, and lipid droplets. Small, smooth, spherical vesicles were concentrated near the lateral and basal plasma membrane (fig. 93).

Distal Segment

The short intermediate segment flows into the next major segment, the distal segment. The term distal has been adopted because of its positional similarity to that of other vertebrates, not because of its structural similarity.

The distal segment of ammocoetes was located largely in the dorsal half of the kidney while in adults it was in the ventral half (fig. 40). Because of structural differences, this segment will be described separately for ammocoetes and adults.

Ammocoetes

The cells of the distal segment of ammocoetes ranged in height from 7.0 to 12.5 μ and were of two types, those PAS+ and those PAS- (figs 94A to C).

With toluidine blue, a clear distinction between a dark and a light cell was made (fig. 95). These cell types were found either intermingled in the tubule or segregated (figs. 96, 97). There

was considerable variation in the location of the dark and light cells but, generally, the dark cells were concentrated in the initial parts of the distal segment immediately following the intermediate segment. There appeared to be no large seasonal variation in the numbers of dark and light cells nor was there a variation in number according to the size of the animal.

The cells in the area of transition from the intermediate segment were classified as light cells (fig. 98). Their apical surfaces possessed a few short microvilli (fig. 99). Numerous smooth vesicles were seen near the lateral plasma membranes which interdigitated with those of adjacent cells, often producing intercellular spaces (fig. 100). The oval nucleus was often invaginated and contained numerous fibrils in the invaginations (fig. 100), closely associated with the nuclear envelope (fig. 101). Two or three Golgi apparatuses were seen and numerous mitochondria, glycogen particles, and rough ER distributed throughout the cytoplasm (fig. 99). Smooth vesicles were seen near the lateral plasma membrane (fig. 100). In this area of transition the cells contained fewer cytoplasmic vacuoles than the cells of the intermediate segment (fig. 98).

Light cells appeared to be segregated or intermingled (figs. 102, 103) among the dark cells throughout the remainder of the tubule. Because of the irregularity of occurrence of these cell types it was impossible to designate specific regions of the segment as containing all light cells, all dark cells or mixed cells. In addition, the electron microscope revealed that the terms light and dark cells of the light microscope covered a range

of cells from a type with a clear empty cytoplasm to a type with large quantities of glycogen particles and numerous closely packed organelles (figs. 102, 103). Therefore, dark cells were not of the same electron density, but they could be distinguished from light cells by large quantities of glycogen particles and numerous closely packed cytoplasmic organelles. On the other hand, light cells represented a range of cells showing an empty cytoplasm with only moderate amounts of glycogen-particles. The dark cells are not to be confused with the dark cells found in the distal segment of the mammalian kidney (Tisher et al., '68).

In contrast to the dark cells, the nucleus of the light cells was spherical with smaller amounts of chromatin and the cytoplasm was less electron-dense (figs. 102, 104). The apical surface was usually devoid of microvilli (fig. 105). Interdigitating plasma membranes separated adjacent cells (fig. 106) and enclosed wide intercellular spaces (figs. 102, 105). The nucleus usually contained a nucleolus and was limited by a porous nuclear envelope (fig. 107). Mitochondria were concentrated beside and below the nucleus (fig. 97) and appeared more swollen after glutaraldehyde-osmium tetroxide fixation than those of the dark cells (Figs. 103, 105). The cytoplasm also contained two or three Golgi apparatuses (fig. 104), scattered smooth vesicles (fig. 105) or smooth ER (fig. 106), glycogen particles (figs. 104, 106), a few strands of rough ER (fig. 104), apically situated vacuoles (fig. 108), microtubules (fig. 108), and rare tubular dense bodies (fig. 107).

The dark cells were pyramidal (figs. 109, 110) or cuboidal (fig. 111) and were limited from adjacent cells by a plasma membrane which often interdigitated with that of an adjacent cell (Fig. 112). Intercellular spaces were a constant feature and often contained cytoplasmic projections (figs. 102, 111, 112). The adjacent membranes were fused apically into a junctional complex and laterally by desmosomes (fig. 112). Intercellular spaces were separated by desmosomes and the more basal spaces appeared continuous with the spaces surrounding the tubule (figs. 113, 114). The basal cell membrane rested on a basement membrane (figs. 113, 114) and collagenous fibrils were observed in the extracellular space between the basement membrane and the closely-associated endothelial cells of the sinusoids (figs. 113, 114). The apical portion of the cells formed club-shaped cytoplasmic extensions resembling microvilli (fig. 115). These extensions often appeared fused, enclosing part of the luminal contents and suggesting phagocytosis (fig. 115). They often contained vesicles which resembled those in the apical cytoplasm (fig. 116). Microtubules, 250 \AA in diameter, were a constant feature of the apical cytoplasm (figs. 115, 117). Centrioles (fig. 116) and remnants of cilia (fig. 118) were occasionally encountered.

The nucleus was usually central (figs. 110, 111) and its outer membrane usually studded with ribosomes (fig. 117). Its content of chromatin was variable but was greater than that of the light cells. The chromatin was usually peripherally dispersed and a nucleolus was commonly present (figs. 109, 119). As in the light cells, fibrils $70 \text{ to } 80 \text{ \AA}$

in diameter were found in bundles near the nucleus and closely associated with the nuclear envelope (fig. 117).

A Golgi apparatus was usually present above and beside the nucleus and consisted of a few saccules and microvesicles (fig. 117). Mitochondria were more numerous than in the light cells (figs. 109, 110, 114) and were spherical to rod-shaped with angular transverse cristae (figs. 119) which, in cross section, occasionally appeared as triangular prisms with sides of 400 to 450 Å (fig. 119). Mitochondrial granules, 300 to 600 Å in diameter, usually accompanied these cristae (fig. 119). The angular nature of the cristae was not as pronounced after glutaraldehyde-osmium tetroxide fixation as after osmium tetroxide alone (fig. 120).

A large portion of the cytoplasm of dark cells consisted of numerous small vesicles confined to the base and sides of the cell (figs. 113, 114). The apical region appeared to be devoid of these vesicles (fig. 117) and they were reduced or absent in the most electron-dense of the dark cells (fig. 104). Tubular vesicles of similar electron density seen at the bases of dark cells were presumed to be the same type of structure (figs. 104, 110). These vesicles were assumed to be part of the smooth ER because they appeared to form continuous channels, often appearing to open into intercellular spaces or the extracellular area at the base of the cell (fig. 114) and because ribosomes were not associated with them. The cisternae were more dilated in some of the material fixed in glutaraldehyde followed by osmium tetroxide than in the material fixed in osmium tetroxide alone so that their interconnections were more readily seen. Rough ER was seen only occasionally (fig. 117).

Glycogen particles, 350 to 500 Å in diameter, were usually associated with the smooth ER, sometimes scattered throughout the cell (figs. 110, 111), sometimes forming a ring around the nucleus (fig. 109), and sometimes forming large clumps above the nucleus (fig. 121). They appeared singly, not as rosettes, and were of two electron densities in both osmium tetroxide and glutaraldehyde-osmium tetroxide preparations and appeared more spherical in the latter (fig. 122). When glutaraldehyde-osmium tetroxide sections were oxidized with 1% periodic acid, glycogen particles broke down into smaller units ranging in diameter from 38 to 78 Å, with the majority at 40 Å (fig. 123). Glycogen was not discernible in sections stained with uranyl acetate alone. In some cells, spherical membrane-bound bodies, were found above and beside the nucleus (figs. 109, 110, 112). Their matrix consisted of large quantities of glycogen particles of both electron densities (fig. 121). In addition these dense bodies contained wrapped lamellar structures and resembled myelin figures (fig. 124). Smaller membrane-bound bodies were found near the apex of these cells. Some contained glycogen particles while others contained a homogeneous matrix and appeared to be devoid of glycogen (fig. 125). The presence of glycogen in the lumen was usually accompanied by an apical blebbing of the cytoplasm in osmium fixed tissue (figs. 111, 118).

Large lipid droplets were commonly found in the cytoplasm of the dark cells (figs. 102, 111).

Adult

Two morphologically distinct parts of the distal segment

were found in the adult, the straight distal pars recta located in the ventral third of the kidney, followed by the twisted distal pars convoluta located in the middle third (fig. 126). Along with the straight collecting segment and intermediate segment, the pars recta gave the ventral third of the kidney a rayed appearance (figs. 1, 74, 127).

Distal Pars Recta

The pars recta was composed of cuboidal cells ranging in height from 12.5 to 17.0 μ with apical spherical nuclei (figs. 128 to 131). The tubules were distinguished from the collecting segment by their greater affinity for toluidine blue (fig. 128).

Varying numbers of microvilli were present from cell to cell (figs. 129 to 131) and in some cases were totally absent (fig. 130). The apical plasma membrane was covered by a layer of electron-dense fuzz (fig. 131). The lateral plasma membranes interdigitated with those of adjacent cells and often enclosed intercellular spaces (fig. 129). The basal plasma membranes rested on an electron-dense basement membrane (fig. 132). Collagenous fibrils separated the basement membrane from endothelial cells of the thin-walled sinusoids surrounding the tubules (fig. 132).

Chromatin was usually clumped near the inner surface of the nuclear envelope (figs. 129, 130) although it was sometimes evenly distributed throughout (fig. 131). A central nucleolus was often seen (fig. 130). The nuclear envelope was interrupted by pores (fig. 132) and bundles of fibrils were seen in the perinuclear cytoplasm (fig. 129).

A Golgi apparatus lying beside the nucleus consisted of flat saccules and microvesicles (fig. 131). A large number of irregularly-shaped mitochondria (fig. 129) were concentrated at the sides and below the spherical nucleus and occasionally at the apex (figs. 130, 131). Together with large numbers of anastomosing spherical to tubular smooth vesicles in the same positions they constituted most of the cytoplasm (fig. 132). The vesicles often branched and anastomosed with each other (fig. 132) and were strongly localized close to the lateral and basal plasma membranes. Small strands of rough ER and free ribosomes were scattered in small amounts throughout (fig. 132). Other cytoplasmic components encountered were dense granules (fig. 129) and multivesicular bodies (figs. 129, 130).

Distal Pars Convoluta

The cells of the pars recta gradually increased in height as the tubule extended dorsally to become the second portion of the distal segment, the pars convoluta. The region was composed of columnar cells which ranged in height from 15.0 to 23.5 μ and possessed basal nuclei (figs. 126, 133).

The apical surface of the cells contained larger numbers and more complex microvilli than the cells of the pars recta (figs. 133, 134). In the mid-dorsal part of the kidney, dome-shaped apical cytoplasmic protrusions were seen with long branching microvilli on their sides (figs. 134, 135) which resembled pseudopods rather than microvilli since their many configurations suggested pinocytosis of material from the lumen (fig. 135). The plasma membrane of the microvilli was often difficult to discern due to the presence of an electron-dense fuzzy coating (fig. 135). The

cytoplasm of these protrusions was usually devoid of smooth vesicles but contained coated vesicles, multivesicular bodies, and tiny tubular profiles which were considered to be microtubules (fig. 135). The coated vesicles appeared to be emanating from saccular invaginations at the base of the microvilli (fig. 135).

Adjacent cells were limited laterally by interdigitating plasma membranes (fig. 134) whose interdigitations were usually more extensive apically. Intercellular spaces containing cytoplasmic processes were almost always found and the adjacent plasma membranes were fused into a junctional complex above (fig. 134). Throughout the remainder of their length the lateral plasma membranes were periodically fused by desmosomes. The basal plasma membrane abutted on a basement membrane (fig. 136).

The outer layer of the double, porous envelope (figs. 136, 137) of the spherical nucleus was studded with ribosomes (fig. 136). Chromatin was concentrated in peripheral clumps and a particulate nucleolus was centrally located (fig. 136).

The Golgi apparatus was always directly above the nucleus (fig. 133) and consisted of dilated or flattened saccules and numerous microvesicles (fig. 138). Most of the cytoplasm consisted of smooth vesicles (fig. 136), smooth ER (fig. 137), and mitochondria with transverse cristae (fig. 139). The mitochondria were fairly uniformly distributed throughout and assumed many shapes and sizes (fig. 133). Larger vacuoles were seen near the apex (fig. 139). Free ribosomes appeared singly or in clumps throughout the cell and a few small strands of rough ER were seen (fig. 138). Dense granules (fig. 138), lipid droplets (figs. 135, 137), and multi-

vesicular bodies (figs. 134, 135) were frequently encountered. A centriole with an accompanying cilium commonly occurred at the apical surface (figs. 134, 139).

Collecting Segment

The collecting segments drained two or more distal segments before entering the archinephric duct (fig. 40). In ammocoetes several collecting segments joined a common collecting segment in the dorsal part of the kidney (figs. 140, 141) which was straight and ran directly to the archinephric duct (fig. 40). In adults the short tubular outpouchings of the archinephric duct received several collecting segments (fig. 142) which in turn were joined by other segments more dorsally (fig. 40).

The cells of the collecting segment were 6.3 to 12.2 μ in height in ammocoetes and 14.5 to 27.0 μ in adults. Since these cells differed structurally from ammocoetes to adults, they will be described separately.

Ammocoetes

The collecting segment consisted of pyramidal cells whose truncated apices were highly variable in structure. Occasionally the apex was dome-shaped and devoid of any cytoplasmic projections (figs. 143 to 145) while sometimes it possessed a few microvilli coated with an electron-dense fuzz (fig. 146). The interdigitating plasma membranes of adjacent cells enclosed intercellular spaces (figs. 145 to 147) and were fused apically by a junctional complex and more basally by desmosomes (fig. 146). The basal plasma membrane was adjacent to the basement membrane which

was separated by a meshwork of collagenous fibrils from the endothelial cells of the thin-walled sinusoids surrounding the tubule (fig. 146).

Chromatin was usually evenly distributed throughout the nucleus (fig. 146) and infrequently found in peripheral clumps. A central nucleolus was often found (fig. 143).

The major cytoplasmic component was an intercommunicating cisternal system of large numbers of smooth vesicles which were free of ribosomes (fig. 147). The vesicles were spherical or tubular (fig. 147) and probably represented smooth ER. Occasionally cells resembling those of the distal segment were interposed between cells of the collecting tubule so that a comparison, particularly of smooth ER, could be made (figs. 148, 149).

The Golgi apparatus was large and consisted of saccules and numerous microvesicles and was located beside the nucleus (fig. 147). The rod-shaped to spherical mitochondria (fig. 144) were abundant.

Ribosomes were scattered freely within the cytoplasm and tiny strands of rough ER were occasionally seen (fig. 147). Dense granules of many shapes and sizes were found throughout the cell (figs. 146, 148).

Adult

The straight collecting segments of the adult paralleled the tubules of the distal pars recta and the intermediate segment in the ventral portion of the kidney (figs. 74, 127, 142) but could be distinguished by their deeper basophilia (fig. 74). With toluidine

blue the cells of the collecting segment were paler and appeared to have fewer organelles than those of the distal segment (figs. 128, 150). The tubules were tightly packed being separated by small amounts of connective tissue and sinusoids.

Irregular, long cytoplasmic processes, which were coated with an electron-dense fuzz and which resembled microvilli, covered the apical surface (figs. 151, 152).

Interdigitating plasma membranes (fig. 153) were fused apically by a junctional complex (fig. 152) and laterally by desmosomes (fig. 154) and enclosed narrow intercellular spaces containing few cytoplasmic processes (fig. 153). A unique feature in the cellular attachment was the presence of large amounts of fibrous material associated with the desmosomes (fig. 155). The fibrils, 70 to 80 Å in diameter, formed an intricate web throughout the cytoplasm and constituted a large proportion of it (fig. 154). The base of the cell was closely associated with the endothelial cells of sinusoids and was separated from them by a basement membrane and collagenous fibrils (fig. 156).

Mitochondria were located beside the nucleus with only a few appearing at the apex (fig. 152, 153). A Golgi apparatus, directly above the nucleus, consisted of a few flattened saccules and numerous microvesicles (fig. 153). The remainder of the cytoplasm consisted of smooth spherical vesicles concentrated around the inner surface of the limiting plasma membrane (figs. 152, 155), free ribosomes (fig. 155), a few strands of rough ER (fig. 154) and dense granules (fig. 153).

ARCHINEPHRIC OR URETERIC DUCT

Each kidney was drained by a major duct, the archinephric or ureteric duct, into which the collecting tubules opened. In ammocoetes these ducts drained the pronephros and entered the dorsal part of the opisthonephros directly below the postcardinal vein (figs. 2, 8). Posteriorly they assumed a ventral position and united before entering the cloaca (figs, 4, 10).

The duct in adults was large and blind at the anterior end (the pronephros having disappeared), and ventrally located throughout (figs. 1, 11), and the paired ducts united before entering the cloaca.

Ammocoetes

The entire duct appeared as a simple thin-walled tube consisting of a layer of epithelium resting upon a basement membrane. On the basis of the structure of the epithelium three regions could be distinguished. The first two, an anterior and a posterior region, were contained largely within the kidney while a third region was located just anterior to the cloaca. The epithelium of the third region was continuous with that of the cloaca and was distinguished by the presence of PAS+ goblet cells. It is with the portions of the duct confined to the kidney that this study is concerned.

The epithelium was higher posteriorly and ranged from 8.3 to 16.1 μ in height. Although the anterior regions could not easily be distinguished from the collecting tubules with the light microscope, there were three differences seen with the electron

microscope. The apical surfaces of the archinephric duct were coated with a thick, electron-dense material, the epithelial cells were separated by large intercellular spaces which often contained cytoplasmic processes resembling microvilli, and their cytoplasm contained numerous dense granules of the same electron-density as the apical coat (fig. 157). The granules near the apex were small and often appeared to be connected to infolding of the apical surface (fig. 157). Toward the base the dense granules were larger (fig. 157). The nucleus was often lobed and had a Golgi apparatus of concentrically-arranged saccules and microvesicles above it (fig. 157). The remainder of the cytoplasm consisted of larger numbers of mitochondria with transverse cristae, smooth vesicles, a few strands of rough ER, and numerous free ribosomes (fig. 157).

The posterior region made up the major portion of the duct and it consisted of a stratified epithelium the cells of which were separated by large intercellular spaces (figs. 158 to 160). The apical cells were often domed so that the epithelium appeared transitional (fig. 159). The basal cells were connected only by their cytoplasmic projections or by desmosomes at each end of a large intercellular space (fig. 161).

The cells varied in their content of glycogen particles, myelin-figures, and mitochondria, and in the electron density of their nuclei and cytoplasm (fig. 160). In general the cells containing larger amounts of glycogen, myelin-figures, and closely packed mitochondria also had denser nuclei and cytoplasmic ground substance (fig. 160). These darker cells resembled the dark cells

seen in the segments of the tubule (fig. 161) and a range from light to dark in electron density was also seen in the cells of the duct (fig. 160).

Apically the cytoplasm of the lighter cells usually contained multivesicular bodies (fig. 162), and large numbers of mitochondria, while numerous smooth vesicles were concentrated near the lateral plasma membrane (fig. 161). Glycogen particles 350 to 500 Å in diameter, were evenly scattered throughout the cell and only occasionally occurred in clumps (fig. 161). Bundles of 70 Å fibrils were a common occurrence anywhere within the cytoplasm (fig. 161).

Most of the cytoplasm of the dark cells consisted of large clumps of glycogen particles, mitochondria, and myelin-figures (figs. 163, 164). The concentric membranes of the myelin-figures enclosed electron-dense deposits (fig. 164). Smooth vesicles were rare in the darker cells and occurred in or near the large Golgi apparatus (fig. 163).

The nuclei of both types were roughly spherical in outline and possessed a large nucleolus (fig. 160). The chromatin was variable in amount and usually concentrated peripherally (fig. 160). Mitochondria were spherical and often contained angular cristae (fig. 163).

Adult

The archinephric duct of newly-transformed, parasitic, and migrating adults was large and ran along the ventral border of the kidney only partially embedded in the organ (fig. 1). The ventrally-projecting portion consisted of four layers (fig. 165A):

a stratified columnar epithelium elevated into folds (figs. 165A and B, 166) surrounded by a thin layer of loose connective tissue (figs. 165A, 167), bundles of smooth muscle (figs. 165A, 168, 169), and, on the outside, a thick layer of dense collagenous connective tissue intermingled with the muscle (fig. 165A). Within the kidney the muscular and connective tissue layers of the dorsal portion of the duct were gradually reduced until only a thin layer of connective tissue separated the epithelium from the epithelium of the distal and collecting segments (figs. 74, 127). The layers beneath the epithelium in all parts of the duct were penetrated by large sinusoids which filled the contours of the invaginations of the base of the epithelium (fig. 167). A space of 2.5 to 4.0 μ (fig. 167) separated the basement membrane of the epithelium from the endothelium. The outermost layer consisted of bundles of collagenous fibrils while the smooth muscle cells contained numerous fibrils, peripheral pinocytotic vesicles, and occasional mitochondria (fig. 169).

The epithelium of the archinephric duct was intensely PAS+. The stain penetrated more deeply into the more lateral regions (fig. 1) and was strongly concentrated on the apical surface (fig. 165B). On the basis of the distribution of PAS+ material in the epithelium and on variations in structure of cells three cell types were distinguished in the epithelium: basal, intermediate, and superficial (fig. 166).

One surface of the basal cells always rested on the basement membrane and the cell never reached the lumen (fig. 170). The nucleus was found to oval (fig. 170). Interdigitating plasma

membranes of adjacent cells often surrounded intercellular spaces (figs. 168, 170). The cytoplasm contained numerous free ribosomes, mitochondria, and small strands of rough ER scattered throughout (fig. 170). Smooth vesicles were located near the lateral plasma membrane (fig. 170) and a few PAS+ granules were occasionally seen in the cytoplasm (fig. 165B).

The intermediate cells never touched the basement membrane and seldom reached the lumen (figs. 171, 172). The plasma membrane was highly invaginated (figs. 172 to 174) and often electron-dense. Large spaces, containing cytoplasmic projections resembling microvilli, often occurred between adjacent intermediate cells (figs. 166, 172). Smooth vesicles of moderate electron density were associated with these spaces just below the plasma membrane (fig. 172). The irregular, highly invaginated nucleus often contained a nucleolus and had peripheral chromatin (fig. 171). Large, dense granules, some of which stained PAS+ (fig. 165B), were associated with two or three well-developed Golgi apparatuses (fig. 171). The cell contained a large number of mitochondria (figs. 171, 172). The remainder of the cytoplasm contained scattered smooth vesicles, rough ER, free ribosomes, and 70-Å fibrils (fig. 174).

The superficial cells reached the lumen and their cytoplasm was intensely PAS+ (figs. 165A, B). Three types of cells were discerned. Type I superficial cells were characterized by the presence of numerous spherical to rod-shaped dense granules, 0.1 to 0.3 μ in diameter and 0.25 to 0.6 μ in length arranged perpendicular to the surface and interwoven with 70-Å fibrils in the apical cytoplasm (figs. 175 to 179). These granules were bound by a single

membrane (figs. 178, 179) which appeared closely associated with the apical plasma membrane (fig. 179). The apical surface contained short microvilli (fig. 177) covered by an electron-dense fibrillar to particulate fuzz (figs. 177, 178). Plasma membranes of adjacent cells interdigitated and were fused at their apices into typical junctional complexes with an apical zonula occludens and a more basal zonula adhaerens (fig. 180). Desmosomes could be found beneath the complex (fig. 180). The elongate nucleus was highly invaginated and usually oriented perpendicular to the surface (figs. 176, 176). A nucleolus was usually present and chromatin peripheral (fig. 177). A Golgi apparatus, consisting of concentrically-arranged saccules, was found at the side of the nucleus and dense granules were commonly closely associated (fig. 175). Fewer mitochondria were found than in the previous cell types (fig. 177). The rough ER was more extensive than in the basal and intermediate cells and the cisternae more dilated (fig. 175). It was largely basal and lateral but occasionally also apically located. Other cytoplasmic components were lipid droplets, large bodies containing membranous fragments (fig. 175), and large numbers of free ribosomes (fig. 179).

Flattened basal nuclei, arranged parallel to the surface of the cell, and mucous granules, packing the cytoplasm above the nuclei, characterized type II superficial cells (fig. 181). Some of the granules were membrane-bound but most had a discontinuous membrane and appeared to be losing their contents to the cytoplasmic matrix (fig. 182). These cells possessed short microvilli which were covered by an electron-dense fibrillar fuzz (fig. 182). Rough

ER, with dilated cisternae, appeared to be continuous with the nuclear envelope and occurred in close association with the Golgi apparatus at both ends of the nucleus (fig. 183). The Golgi apparatus consisted of flattened saccules with dilated ends and smooth vesicles. Numerous microvesicles lined up beneath the saccules. Mitochondria were small and sparse in these cells (figs. 181, 183).

Club-shaped type III superficial cells were occasionally encountered below the surface (fig. 184) but usually appeared superficially where both nucleus and cytoplasm showed a strong degree of electron density, a characteristic of these cells (fig. 185). The major cytoplasmic components were tightly-packed, membrane-bound vesicles of various electron densities (fig. 185). Profiles of mitochondria could be seen between the vesicles as well as a Golgi apparatus (fig. 185). All organelles were outlined by an electron-dense material (fig. 185). Projections from these cells appeared between the interlocking interdigitations of the plasma membrane of adjacent cells and also appeared on the luminal surface (fig. 185). An electron-dense coat covered the apical projections (fig. 185).

GROWTH AND DEGENERATION

In addition to the structural changes occurring during development in the renal corpuscle, tubules, and blood vessels, the two closely-related processes of growth and degeneration were also examined.

Growth

In ammocoetes a posterior proliferation of nephrogenic

tissue (figs. 186 to 189) was accompanied by an anterior degeneration of tubules and glomera resulting in a more posterior position of the kidneys.

The posterior tip of the kidney consisted of the archinephric duct and one or two groups of rapidly dividing, undifferentiated cells which were closely associated with the parietal peritoneum (fig. 186). The cells often pushed into the wall of the archinephric duct producing an invagination. Slightly more anteriorly could be seen small tubules with narrow lumina and composed of closely packed cuboidal cells, many of which were in mitosis (fig. 187). These cells were intensely PAS+ as were the cells of the archinephric duct (fig. 187). In 0.5- μ sections the cells were seen to be separated by large intercellular spaces and their cytoplasm contained numerous large droplets which stained with toluidine blue with the same intensity as droplets occurring in the cells of the intertubular area (fig. 189). A little ahead of this region the tubules were more differentiated and were accompanied by a mass of cells which was presumed to represent a renal corpuscle and which surrounded a knot of capillaries (fig. 188).

The apical surfaces of the tubular cells possessed a few short microvilli (figs. 190, 191) and an occasional cilium with an accompanying centriole (fig. 192). The lateral plasma membranes were fused apically with those of adjacent cells into a junctional complex but were usually separated below this by large intercellular spaces and only occasionally attached by desmosomes (fig. 193). These intercellular spaces appeared to be continuous with the extra-

cellular spaces at the base of the cell (fig. 194). The basal plasma membrane rested on a basement membrane and only a thin layer of collagenous fibrils separated it from the endothelium of the sinusoids which possessed many pinocytotic vesicles (fig. 194).

The outer layer of the nuclear envelope was studded with ribosomes (fig. 195) and associated with fibrils 70-Å in diameter (fig. 195). The cells contained two or three Golgi apparatuses, each consisting of parallel arrays of microvesicles and tiny saccules (fig. 195).

The structure of the numerous mitochondria was the most conspicuous feature of these cells. There were many shapes and sizes but all contained angular, prismatic cristae which often appeared in cross section as equilateral triangles with sides of 400 to 450 Å (figs. 192, 197A, B). Many were arranged in a star-shaped hexagonal pattern (figs. 197A, B) with the prisma parallel to the edge of the mitochondrion and their bases facing inside so that the apices of the triangles became the points of the star. The inside became a hexagonal tube, 900 Å in diameter, which always contained a single row of mitochondrial granules, each 300 to 350 Å in diameter, and as much as 1000 Å long, (figs. 191, 197C, and D, 198). Some micrographs suggested that the granules were connected by thin, electron-dense strands (fig. 197C). The granules appeared to possess a substructure which was beyond the resolution of the electron microscope used (fig. 197). Not all the cristae within a mitochondrion were arranged hexagonally nor were they found to run in the same plane (fig. 197D). Six parallel cristae formed the hexagonal structure

enclosing a single row of granules as described above. More than six parallel cristae were oriented so that one of the sides of the original prisms contributed to the formation of a second hexagon surrounding its own row of granules (fig. 198).

The remainder of the cytoplasm consisted of large amounts of smooth ER (fig. 196) and glycogen particles (fig. 194) scattered throughout. Often the smooth vesicles appeared tubular near the base of the cell and were seen to be closely associated to bundles of thin fibrils (fig. 196). Rough ER and free ribosomes were scattered throughout in small amounts (fig. 195). Large lipid droplets (figs. 193, 194), autophagic vacuoles (figs. 192, 196), multivesicular bodies (figs. 191, 195) were constant features.

Degeneration

Four phases of degeneration were observed in the kidney during the life cycle of the lamprey. These did not include the changes which may have resulted from infection or infestation of parasites. The first phase occurred in ammocoetes, the second at transformation, the third throughout adult life, and the fourth during spawning migration.

Ammocoetes and Newly-transformed Adults

Posterior growth of the kidney in ammocoetes was accompanied by anterior degeneration; at transformation the entire kidney of the ammocoetes degenerated and a new posterior kidney formed (figs. 3, 25, 199A to C). The processes of degeneration were considered to be separate because in ammocoetes it appeared to be a slow gradual process while at transformation it appeared much more sudden, the largest ammocoetes observed showing no evidence indicating

the massive degeneration which was forthcoming. Although the processes proceeded at a different rate, both processes were similar morphologically and occurred in three states, with the most advanced degeneration being located more anteriorly. At first the inter-tubular area was invaded by large numbers of phagocytes (figs. 199B). This was followed by an accumulation of PAS+ material in the lumen, at the base of the tubules, and within the renal corpuscle (fig. 199B). The final stage was the reduction of the most anterior areas to a mass of debris-containing phagocytes and a PAS+ amorphous material (fig. 199C).

Adult

The process of degeneration continued up to the death of the lamprey following spawning. The anterior tip of the adult kidney was always characterized by the presence of degenerating tubules and renal corpuscles (figs. 22, 200, 201). No large accumulations of phagocytes but rather thick-layers of an amorphous material surrounded the tubules, many of which were shrunken (fig. 201). Material in the lumen and the thick basement membrane of the tubules were PAS+ (fig. 200). Remnants of renal corpuscles could be identified by their draining neck segments but they seldom contained any capillaries or visceral epithelium and were surrounded by the amorphous material (fig. 22).

Migrating Adult

Degeneration occurred in the kidney during the migration to the spawning beds. Beginning posteriorly, it had not proceeded to the same degree in all animals studied. In some animals, phagocytes had invaded both the intertubular area and the lumina of the

of the tubules (fig. 202) while in others the entire kidney capsule enclosed a mass of closely packed phagocytes (fig. 203). The renal corpuscle was usually missing in these areas. Regions which had not undergone this invasion showed an increased amount of PAS+ material in their lumina, as in the anterior part of the parasitic adult kidney. Even tissues which appeared superficially healthy showed structural changes in epithelial cells when viewed with the electron microscope. In the renal corpuscle there appeared to be an increased amount of collagenous tissue between the basement membrane of the epithelial cells and the capillary endothelium as well as an estimated increase in numbers of mesangial cells. The capillary lumina often contained phagocytes (figs. 38, 204). In the proximal segment the cells contained granules of a variety of shapes and sizes (fig. 205). The cells of the distal segment were characterized by the presence of large basal autophagic vacuoles (fig. 206) containing mitochondria, and vesicles (fig. 207). Few organelles appeared in the cytoplasm. The distal cells also contained an unusual type of dense body showing a crystalline matrix (fig. 208). It was spherical and appeared to be composed of concentrically arranged parallel membranes on one side while at the other side parallel membranes were seen to run in two directions and intersect at an angle of 60 to 65° giving it a crystalline appearance. In the archinephric duct, huge vacuoles containing debris were commonly found between the epithelial cells (fig. 209). The superficial cells contained large lipid droplets and unidentified irregularly dense bodies which may have represented poorly preserved lipid droplets.

(fig. 210). The endothelial cells of the sinusoids contained large amounts of lipid (fig. 205) and small lipid-like droplets were seen in the intertubular area between the basement membrane of the tubules and the endothelium (fig. 211).

CELLS OF THE INTERTUBULAR AREA

Many types of cells were found in the intertubular area and have been described previously: fibroblasts, wandering blood cells, developing blood cells, endothelial cells, and phagocytes. Two other types, pigment cells and intertubular cells, warrant consideration.

Pigment Cells

Pigment cells were found concentrated in the dorsal and peripheral portions of the kidney in both ammocoetes and adults and gave these regions a dark appearance (fig. 5). The granules did not take up any of the stains used and appeared yellow-brown and resembled melanin (fig. 212). The granules were hard and difficult to section. The cells were stellate, and the many branching processes extended in several directions in the interstitium (figs. 212, 213). The nucleus was eccentrically placed in the perikaryon and contained a prominent nucleolus (fig. 214). Most of the cytoplasm was packed with the membrane-bound granules with a few vesicles between them (fig. 215).

Intertubular Cells

Elongate, often stellate, intertubular cells were found only in ammocoetes in the dorsal parts of the kidney near the PAS+ portions of the distal segment and near the undifferentiated tubules

of the posterior regions (figs. 212, 213). These cells were closely associated with the sinusoidal endothelium, fibroblasts, pigment cells, and the tubules. They usually occurred in clusters with each cell having an electron-dense coating surrounding its limiting plasma membrane (fig. 216). The spherical to ovoid nucleus occasionally contained a transverse band of chromatin (fig. 217). The Golgi apparatus was located at one end of the nucleus and consisted of the usual saccules and microvesicles (fig. 217). Mitochondria were large and contained transverse cristae and distinct mitochondrial granules (fig. 216) and were located either at the ends of the nucleus (fig. 217) or closely associated with the large lipid droplets which were characteristic of the cytoplasm of these cells. The size of the droplets varied from cell to cell; often they were inconspicuous (fig. 216) but sometimes they were the major component of the cytoplasm (fig. 212). The cells of the posterior region were distinguished from the dorsal cells by their large clumps of glycogen particles which could be found in all parts of the cytoplasm (figs. 216, 218). Little or no glycogen particles were found in the dorsal cells (figs. 215, 219, 220). Mitochondria were smaller in the dorsal cells and the major cytoplasmic component was the large lipid droplets (fig. 215).

The remainder of the cytoplasm of both types consisted of smooth (figs. 216, 219) and rough (figs. 216, 220) ER, free ribosomes (fig. 219), and autophagic vacuoles (figs. 216, 218).

DISCUSSION

During the life of P. marinus three separate kidneys appear. An anterior pronephros and a more posterior opisthonephros coexist during the major portion of the larval life. At transformation the opisthonephros of the ammocoetes degenerates while an adult opisthonephros forms and it appears that the ammocoetes kidney does not contribute to the formation of the adult kidney. This had been suggested by Wheeler (1899), who in the absence of histological evidence, compared the position of the kidneys with that of muscle segments of ammocoetes prior to transformation and showed that the kidney of the adult is not the one which is present in the ammocoetes. The formation of the new kidney in the adult may be an example of the tendency of vertebrate kidneys to take a more posterior position within the body cavity in their evolutionary development (Torrey, '64). On the other hand, it may suggest that the ammocoetes kidney was not a sufficient organ for the demands of water conservation in the change from a freshwater to a marine habitat in the anadromous ancestor of the Great Lakes lamprey.

The opisthonephric kidneys of both ammocoetes and adult are well developed excretory organs possessing features common to most vertebrate kidneys; a renal corpuscle and a segmented tubular nephron.

Renal Corpuscle

The fusion of the glomera in the ammocoetes to form the unique elongate glomus of the adult was suggested by Wheeler (1899) who considered that the anterior glomera disappear and that the more posterior elongate glomera fuse to produce a single glomus in older ammocoetes and adults. In contrast, the present investigation shows no single long glomus in older ammocoetes but a series of small, isolated, degenerating anterior glomera followed by a few long posterior ones which disappear at transformation. It appears that glomera become larger by the addition of glomeruli posteriorly but this process does not proceed at the same rate in all individuals so that animals of similar length and therefore of similar age (Thomas, '62), show varying degrees of anterior atrophy and posterior fusion. Similar variations in developmental rate of lampreys have already been noted in the ovary (Lewis and McMillan, '65). The larvae appear to reflect the transition from the primitive condition of segmentally-arranged, unfused glomeruli, as seen in the myxinoids (Gerard, '54) to the more advanced, fused glomus of the adult, although they do not contribute to the formation of the latter.

The word glomus was adopted in the present work to distinguish the fused capillary tuft of the lamprey from a simple glomerulus. Torrey ('39) referred to this tuft in the opisthonephros of the ammocoetes as a "glomus or an elaborate glomerular colony" while Gerard ('54) called it a "pseudoglomus" and referred to the capillary knot of the pronephros of the ammocoetes as a "glomus".

Both workers used the term glomus to indicate the compound nature of the capillary tuft. Wheeler (1899) recognized this fusion of glomeruli and referred to the "compound glomerulus" of both ammocoetes and adults. Although there have been no reports of the fine structure of the pronephric glomus, our own observations on ammocoetes and work by Christensen ('64) on Ambystoma indicate that it is not surrounded by a typical Bowman's capsule, a significant difference between the pronephric glomus and the opisthonephric glomus.

The interconnections of the capillary tufts through the medial artery appears to be unique to the lamprey. The renal arteries pass ~~down~~ ^{ventrally} to the glomera at irregular intervals from the dorsal aorta to a medial artery. The medial artery may be an adaptation to equalize the blood flow in the elongate glomus, an hypothesis which is reinforced by the observation that the medial artery was not seen in the tiny anterior glomeruli of the smallest ammocoetes where the supply from the renal arteries would be sufficient.

Boyer ('55, '56) has shown that the afferent arteriole of the mammalian glomerulus divides at the hilus into five loops whose numerous branches anastomose with those of other loops and are drained by a single efferent arteriole. This is similar to the arrangement in the lamprey where the afferent arteriole divides into five or six branches. A unique feature of the lamprey, however, is the presence of five or six efferent arterioles for each afferent arteriole and these drain blood to the intertubular area.

The uninvaginated capsule of older ammocoetes and adults is simply a protrusion of the expanded end of a nephron between the loops of the capillary tuft. This simple method is made possible by the compound nature of the glomus; the formation of more complex Bowman's capsules is unnecessary to provide each capillary tuft with an envelope of podocytes and access to a nephron. Wherever the capsule comes into contact with capillaries, typical podocytes develop; elsewhere a simple squamous epithelium is found. The presence of podocytes in organs of excretion appears to be wide spread in the glomeruli of vertebrates and they have also been reported in such diverse locations as the antennal gland of the crayfish (Kummel, '64a, '64b), crab (Schmidt-Nielsen et al., '68b), in the end-sac of the brine shrimp (Tyson, '66, '68), and in the labial gland of a springtail (Altner, '68) where no Bowman's capsules are found but in which filtration is believed to be occurring (Tyson, '68).

The renal corpuscles of ammocoetes possess several Bowman's capsules for each glomus with each capsule surrounding a single loop of the capillary tuft. The multiple Bowman's capsules of the renal corpuscles of ammocoetes are not unique among the vertebrates for they have been reported in the hagfish, Myxine glutinosa where Bowman's capsules are found to envelope each glomerulus of the glomus (Nash, '31). It is likely that multiple Bowman's capsules in M. glutinosa and the ammocoetes of P. marinus, and the multiple dilated ends of nephrons of adult P. marinus are a reflection of the size of the glomus rather than a primitive condition from which all vertebrate renal corpuscles evolved.

The electron microscope reveals a similarity between the cells of the renal corpuscle of the lamprey and those described for other vertebrates, both embryonic (Leeson, '57, '59, '60; Pak Poy, '57, '58; Christensen, '64; De Martino and Zamboni, '66; Gibley and Chang, '67) and adult (summarized by Rosen and Tisher, '68). The laminae rarae of the glomus constitute nine-tenths of the total thickness of the basement membrane whereas in the rhesus monkey they comprise only one-tenth (Rosen and Tisher, '68). The close association of the basement membrane to the visceral epithelium appears to be common to both the English sole (Bulger and Trump, '68) and the lamprey but appears to be lacking in higher vertebrates (Rosen and Tisher, '68). The significance of these discrepancies is unknown although it may be partially the result of variations in fixation. The basement membrane is the principal barrier in ultrafiltration (Farquhar et al., '61; Faith and Trump, '66) and variations in its structure may reflect variations in functions. The presence of numerous smooth vesicles and multivesicular bodies in podocytes indicate the possibility of absorption of materials from the urinary space between the cells as has been suggested in other animals (Dick and Kurtz, '68).

The capillary endothelium of the glomera of both ammocoetes and adults lack the numerous fenestrations described in the glomeruli of higher vertebrates (eg. Rhodin, '62, '63a, '63b). The capillaries in the glomeruli of the English sole are also thick and possess only a few pores suggesting that a low filtration rate may exist (Bulger and Trump, '68). The thickened endothelium,

with few fenestrations, resembles the condition described in the human foetal mesonephros (De Martino and Zamboni, '66) where low blood pressure, correlated with the absence of a juxtaglomerular apparatus, produces a low filtration rate and fluid transfer is presumed to occur by pinocytosis across the endothelial cells. A similar condition may exist in the lamprey which lacks a juxtaglomerular apparatus (Capr  ol and Sutherland, '68) but whose glomerular capillary endothelium contains pinocytotic vesicles. Bulger and Trump ('69) have shown granulated arteriolar cells (juxtaglomerular cells) in the English sole and goldfish and have suggested that the cells may secrete renin, an enzyme elaborated by the juxtaglomerular apparatus of higher vertebrates and involved in blood pressure regulation (for review see Biava and West, '66). Renin has also been shown to be present in a variety of other marine and freshwater teleosts as well as in aglomerular marine teleosts which lack a juxtaglomerular apparatus (Mizogami et al., '68; Oguri and Sokabe, '68). The relationship between thickened endothelium with few pores and lack of a juxtaglomerular apparatus in lampreys requires further investigation.

The Tubule

The earliest descriptions of the tubular nephron of the lamprey recognized only three regions: the ciliated funnel, a glandular portion with a brush border (the proximal segment), and a terminal portion which was continuous with the archinephric duct (Wheeler, 1899; Regaud and Policard, '01, '02a, '02b, '02c). Later work has shown two regions in the proximal segment on the basis of the number of cytoplasmic granules (Gerard, '54) and has delineated

a third segment immediately following the proximal segment and leading into a collecting duct (Bentley and Follett, '63). Vinnichenko ('66) has described the fine structure of five regions in the tubule of migrating Lampetra fluviatilis: neck, proximal, connecting, distal, and collecting. The present study has shown that in both ammocoetes and adult of P. marinus the tubular nephron is divided into neck, proximal, intermediate, distal, and collecting segments. In addition, the proximal segments of ammocoetes and adults and the distal segments of adults are further subdivided into pars recta and pars convoluta.

Differences are noted between the ammocoetes and adults of P. marinus in the placement of the segments of the nephron within the kidney which are related to differences in the position of the glomus. The dorsal portion of the adult kidney contains the renal corpuscle, proximal segment, and part of the distal segment and corresponds roughly to the cortex of the mammalian kidney. The ventral half can be compared to the medulla and contains the intermediate segment, most of the distal segment, the collecting ducts, and the archinephric duct. The straight parallel arrangement of the distal, intermediate, and collecting tubules in this region is reminiscent of the medullary rays of mammals where it increases the efficiency of osmoregulation by establishing a counter-current exchange mechanism (Gottschalk, '61). This arrangement of tubules may be the site of the tubular sodium and potassium exchange described in the adults of L. fluviatilis (Bentley and Follett, '63). Hickman ('65) has suggesting that the distal segment is the site of sodium and chloride reabsorption in freshwater teleosts and most authors

investigating kidney function in ammocoetes agree that a similar mechanism probably exists (Wikgren, '53, Hardisty, '56; Morris, '56, '60; Bentley and Follett, '63; Read, '67).

Neck Segment

The ciliated neck segment resembles the pronephric nephrostome as described, for example, in larvae of Ambystoma (Christensen, '64) but, since it does not drain the coelome, it cannot be given this name. A similar segment has also been noted in the opisthonephros of teleosts (Bulger and Trump, '68) and probably serves to move the glomerular filtrate down the nephron, as was suggested earlier by Regaud and Policard ('02a). Its absence in amniotes may be a reflection of the higher blood pressure which would produce sufficient hydrostatic force to move the filtrate.

Cells of the neck segment appear to be engaged in other functions as is suggested by their close association with capillaries and sinusoids and their well-developed organelles: mitochondria, Golgi apparatus, smooth vesicles, rough ER, and free ribosomes. The presence of microvilli and multivesicular bodies suggests an absorptive function and the Golgi apparatus, rough ER, and free ribosomes, secretion. In addition to providing energy for ciliary activity, the large mitochondria could supply the energy requirements of transport as is suggested by the intercellular spaces.

Proximal Segment

The cells of the proximal segment of the lamprey resemble those of other vertebrates (Sjöstrand and Rhodin, '53; Maunsbach, '64; Bulger, '65; Bulger and Trump, '65a; Ericsson et al., '65;

Tisher et al., '66; Bulger and Trump, '68; Olsen and Ericsson, '68). The most obvious similarity is the presence of a brush border which reflects the absorptive function of the proximal segment (Fawcett, '62). Organs in invertebrates performing similar functions, such as the filter chamber of insects (Gouranton, '68), the antennal gland labyrinth (Schmidt-Nielsen et al., '68) green gland labyrinth (Anderson and Beams, '56), and the efferent duct of the maxillary gland (Tyson, '69) of crustaceans show similar structural features. Christensen ('64) reported the existence of irregular interconnected microvilli in the proximal segment of Ambystoma larvae. Similar microvilli were seen occasionally in the proximal cells of the lamprey. The presence within them of numerous tiny vesicles similar to those seen at the apex of the cell suggests that the microvilli might be involved in pinocytosis. Those vesicles were not seen in material fixed in glutaraldehyde and post fixed in osmium tetroxide, an observation which supports the opinion of Maunsbach ('66) that they are artifacts resulting from fixation in osmium tetroxide.

Cilia have been reported on the epithelium of the proximal tubule in a variety of vertebrates (Latta et al., '61; Fujimoto, '64; Tisher et al., '66; De Martino and Zamboni, '66; Duffy and Suzuki, '68) where they have been considered to be a remnant of the pronephric nephrostome (Latta et al., '61; De Martino and Zamboni, '66). They may be found anywhere in the tubule and may aid in the flow of material in the lumen (Olsen and Ericsson, '68).

Bulbous protrusions of the apex of the proximal epithelial cells are common in most species studied (Tyson, '69) and their presence in lampreys, as in other vertebrates, can probably be

accounted for by delayed fixation (Longley and Burstone, '63; Trump and Ericsson, '65; Davis and Schmidt-Nielsen, '67).

Flocculent bodies, usually associated with mitochondria in adults and occasionally in ammocoetes, are bound by a single membrane, lack internal vacuoles, and are closely associated with the rough ER. They resemble the renal microbodies described in cells of the proximal tubule of mammals (Rhodin, '54; Ericsson, '64; Ericsson and Trump, '66; Langer, '68; Tisher et al., '68) except that they lack the crystalline "nucleoid", a factor which may be related to the method of fixation (Langer, '68; Tisher et al., '68). It has been suggested that renal microbodies contain enzymes such as uricase, which is normally present in large quantities in the liver (for review see Tisher et al., '68). The presence of microbodies in the proximal segment of a teleost (Bulger and Trump, '68) demonstrate that they also exist in lower vertebrate kidneys.

The flocculent bodies should be distinguished from the many dense granules which are found in the cells of the proximal tubule. Gerard ('36, '54) described "yellow granules of a chromolipid nature" in the cells of the proximal tubule in the lamprey which probably correspond to the dense granules described in the present investigation. He noted a decrease in number and size of the yellow granules in descending the proximal segment corresponding to the decrease in size and number of dense granules, observed in the present study. He also felt that the majority if not all of these granules were "granules of arthrocytosis", that is, the result of absorption, concentration, and retention of all colloids brought

into contact with the apical pole of the cells. Arthrocytosis of colloids differs from the resorption of diffusible substances since it is accompanied by a prolonged retention of the substances resorbed. It is likely that these dense granules are lysosomes or protein absorption droplets, as has been suggested for the hagfish ureteric duct (Ericsson, '67; Ericsson and Seljelid, '68) and mammalian proximal cells (Straus, '57; Miller, '60; Ericsson and Trump, '64; Miller and Palade, '64; Graham and Karnovsky, '66) and are the result of concentration and dehydration of material absorbed from the lumen (Trump, '61).

Although no physiological evidence on absorption and secretion has been obtained in this study, structural features suggest the proximal segment probably absorbs filtered proteins and other macromolecules from the lumen as has been suggested for a freshwater teleost (Hickman, '68). The appearance of bag-like depressions at the base of the microvilli, dense tubules, multivesicular bodies, and vacuoles is similar to the condition of proximal cells shown to be involved in endocytosis (Ericsson and Trump, '66; Graham and Karnovsky, '66; Ericsson and Seljelid, '68).

Intermediate Segment

Until the studies of Bentley and Follett ('63) and Vinnichenko ('66) the connective region between the proximal and distal segments in the lamprey had been overlooked. Both these studies were performed on migrating L. fluviatilis and little information is available other than it consists of flat epithelial cells containing a few mitochondria and microvilli (Vinnichenko, '66).

Three types of tubular connective regions or intermediate segments have been described between the proximal and distal tubules of vertebrates: the ciliated intermediate segment as seen in some fishes (Edwards, '35), amphibians (Christensen, '64), reptiles (Anderson, '60), and some birds (Marshall, '34); the nonciliated looped segment of the loop of Henle in some birds (Gibley and Chang, '67) and most mammals (Rhodin, '58a, '58b, '62, '63a; Osvaldo and Latta, '65; Bulger and Trump, '66; Bulger et al., '67; Darnton, '69); and the nonciliated straight segment of lampreys and some fishes (Edwards, '35). The segment in P. marinus ammocoetes and adults often appears longer than that described in teleosts, amphibians, reptiles, and some birds and mammals (Marshall, '34). The adult segment often appears longer than the loop of Henle of some birds and mammals (Marshall, '34).

The low cuboidal to squamous epithelium of the intermediate segment of P. marinus suggests that it may correspond to the thin descending limb of the loop of Henle of mammals. The structure of these cells suggests, as in the loop of Henle, that the segment is involved in more than conduction of fluid down the tubule which appears to be the only function of ciliated intermediate segment (Christensen, '64). Both the ammocoetes and adults have two types of segments; one possessing low cuboidal cells and another squamous cells.

In the cuboidal cells the presence of dilated cisternae of the rough and smooth ER, numerous free ribosomes, well-developed Golgi apparatus, lysosome-like granules, and microvilli suggest activity. The absence of apical vesicles and multivesicular bodies

indicate that this activity is secretory rather than absorptive. The squamous cells of ammocoetes and adults also contain these organelles in abundance but in addition often contain multivesicular bodies which appear in cells involved in endocytosis (Ericsson and Trump, '66). The thin limbs of the loop of Henle are characterized by their paucity of organelles (for review see Darnton, '69) yet they are actively transporting sodium (Jamison et al., '67). If the cells of the intermediate segment of P. marinus transport sodium, they appear to be better equipped for there is an abundance of mitochondria and smooth vesicles.

The presence in adults of a second squamous cell type which seldom reaches the lumen is not clearly understood. This cell is characterized by its paucity of organelles and its irregular flattened nucleus, It may be that it serves only as a support for the thin superficial cells, for its few organelles do not suggest a similar activity.

Distal Segment

The distal segment is well developed in freshwater teleosts (Tampi, '59) and absent from marine forms (Smith, '59; Ogawa, '62; Beitch, '63; Bulger and Trump, '68). Using the above criteria, the presence of a distal segment in P. marinus of the Great Lakes as well as in the marine form (personal observation) suggest that P. marinus may have originated in a freshwater habitat. Hickman ('65) has stated that the presence of a distal segment in a freshwater teleost may be related to the fact that this segment is the site of urine dilution by reabsorption of sodium and chloride without the accompaniment of water. It is probable that the presence of a

distal segment in P. marinus is the key to its euryhaline nature, as has been suggested by Smith ('59) and Tampi ('59) for euryhaline teleosts, but more information on its function must be obtained.

The two regions of the distal tubule in the adult lamprey correspond in location to the pars recta and pars convoluta of the mammalian segment (Tisher et al., '68) but such a distinction is absent in ammocoetes. The pars recta and pars convoluta of mammals and lampreys are also similar in the height of the epithelium but the fine structure of the cells differ.

Characteristic of distal cells in amphibians (Bargmann et al., '55; Fawcett, '58; Karnovsky, '63; Christensen, '63, '64) and mammals (Rhodin, '58a, '58b; Ericsson et al., '65; Tisher et al., '68; Trump and Bulger, '68) is the presence of infoldings of the basal plasma membrane which are lacking in lampreys. In contrast, the distal cells of P. marinus possess intercellular spaces, a feature they share in common with reptiles (Anderson, '60; Davis and Schmidt-Nielsen, '67; Schmidt-Nielsen and Davis, '68a).

The distal cells of both the pars recta and pars convoluta of adults possess an abundance of smooth vesicles and mitochondria and have little rough ER but they vary in their numbers of microvilli and multivesicular bodies. The microvilli of the cells of the pars convoluta are elongate and club-shaped and the apical cytoplasm possesses numerous multivesicular bodies characteristic of cells involved in endocytosis (Ericsson and Seljelid, '68). In addition, the cells of the pars convoluta often possess domed apices, as do the cells in the human mesonephros (De Martino and Zamboni, '66),

but this may be the result of delayed fixation (Tisher et al., '68). The presence of large numbers of mitochondria, apical vesicles, and smooth vesicles in the cells of both regions more closely resembles the condition found in the mammalian collecting duct (Myers et al., '66) than the distal segment (Tisher et al., '68). The similarity between the human mesonephric distal cells and the metanephric collecting cells has been noted previously (De Martino and Zamboni, '66) and may suggest a common function.

The cells of the distal segments of ammocoetes were unlike those of adults and both differed from any other vertebrate. The segment of ammocoetes possesses a range of cells from those with large concentrations of glycogen particles (dark cells) to those with relatively few or no glycogen particles (light cells). The light cells most closely resemble the adult distal cells in the large amounts of spherical, smooth vesicles and mitochondria, and in the small amount of rough ER, but differ in the absence of microvilli. The dark cells, in addition to the glycogen particles, possess irregular club-shaped microvilli and tubular smooth ER. The irregular nature of the microvilli suggest that they may be involved in the engulfment of material from the lumen, as was suggested in the cells of the pars convoluta of the adult. The fusion of the tips of adjacent microvilli to enclose a vacuole does not appear to be the result of fixation procedures and it is felt that perfusion of the animal with a suitable tracer, such as horse radish peroxidase (for review see Graham and Karnovsky, '66) or ferritin (Ericsson and Seljelid, '68), may show these cells to be absorptive.

Vinnichenko ('66) appears to be the only investigator to have described the distal segment of the lamprey. The scant information provided by his study of autumn migrating Lampetra fluviatilis suggests a segment structurally different from that of ammocoetes and adult P. marinus with no divisions into pars recta and pars convoluta. This does not seem unreasonable when the structural variations among nephrons of teleosts is considered (summarized by Bulger and Trump, '68). The distal segment of L. fluviatilis contains cells with a "vacuolated cytoplasm" which are poor in inclusions and the Golgi apparatuses are "féebly" developed. P. marinus distal cells do not contain a vacuolated cytoplasm, but instead possess an extensive system of smooth vesicles and a well-developed Golgi apparatus. Common features shared by distal cells of these two species are the presence of abundant mitochondria and small microvilli.

Collecting Segment

The collecting tubule of higher vertebrates is actively involved in urine formation and is not simply a conducting vessel (Grantham et al., '69). The presence in cells of the collecting segment of the lamprey of a well-developed Golgi apparatus, microvilli, mitochondria, intercellular spaces, and smooth ER, features also described in the collecting segments of a teleost (Bulger and Trump, '68) and mammals (Rhodin, '63a; Ericsson et al., '65; Bulger and Trump, '66; Myers et al., '66), suggest that they too may be involved in urine formation.

The collecting segments of ammocoetes and adults lack

mucous granules which are a constant feature in this region of some teleosts (Bulger and Trump, '68) and reptiles (Anderson, '60), and also lack the four cell types described in L. fluviatilis (Vinnichenko, '66). The cells of the collecting segments of P. marinus do not contain the extensive rough ER of the English sole (Bulger and Trump, '68) but possess an extensive system of smooth ER, which is highly developed in ammocoetes.

The complex cytoskeleton of fibrils is one of the most striking features of the cells of the adult and resembles that seen in the epidermis of the lamprey where it may function in support (Fawcett, '66). The fibrils are part of the cell web and emanate from the desmosomes and junctional complexes providing a strong support for the tubular cells. The reason why such an intricate system is restricted to the collecting segment of adults is not understood.

The Archinephric Duct

The role of the archinephric duct in kidney development and function has long been a subject of interest (Wheeler, 1899). Three basic functions have been attributed to it: providing an inductive stimulus for renal differentiation, an excretory duct or drainage system for the nephrons of lower vertebrates, and contributing to the formation of male genital ducts in amniotes (Torrey, '64). Despite the knowledge of its importance to kidney function and urogenital development, very little is known of its structure.

The paired archinephric ducts of ammocoetes can be divided into two morphologically distinct regions, an anterior portion which

is similar to the collecting duct, and a posterior portion which contains large amounts of glycogen particles and resembles the posterior tubules, especially the distal segment. These resemblances probably result from the fact that the duct is formed from the union of the distal extremities of the most anterior nephrons (Torrey, '64).

The archinephric duct of ammocoetes is replaced at transformation by a new duct to which it bears no resemblance. It is assumed that the adult duct is a modification of that portion of the duct which extends from the ammocoetes kidney to the cloaca, since the duct of ammocoetes disappears at transformation. The presence of the layer of smooth muscle, like that beneath the collecting duct of the English sole (Bulger and Trump, '68), suggests that the adult duct is able to contract, aiding in the expulsion of urine.

The archinephric duct of both ammocoetes and adults resembles the transitional epithelium of the urinary tract of man (Monis and Zambrano, '68) in its division into basal, intermediate, and superficial layers and the presence of intercellular spaces which are most prominent in the epithelium of ammocoetes. The intercellular spaces, together with the presence of smooth vesicles, multivesicular bodies, microvilli, numerous mitochondria, and the close relationship of the sinusoidal epithelium make it appear likely that the archinephric duct of ammocoetes is able to transport fluids and is probably involved in the formation of urine, as in the urinary tract of man (Monis and Zambrano, '68).

In the adult the epithelium can be divided into three cell types on the basis of location, organelles, and their numbers

of PAS+ granules. A progressive increase in the number of granules is seen from the base to the surface of the epithelium. Superficial type I cells resemble ~~mucus~~-secreting cells seen in the epidermis of Protopterus (Kitzan and Sweeney, '68) in the arrangement of the granules beneath the apical plasma membrane and their staining character. Type II superficial cells resemble goblet cells seen in many vertebrates (for review see Kitzan and Sweeney, '68; Toner, '68) with the characteristic basal nuclei and apical cytoplasm filled with large PAS+ mucous droplets. The type III cells appear to be degenerating as indicated by their pycnotic nuclei and the electron density of the cytoplasm features which have been shown to be characteristic for degenerating cells (Myers et al., '66). On the other hand, these cells may be involved in holocrine secretion with a development of cells from the base of the epithelium to death at the apex. Autoradiographic studies using tritiated thymidine would show whether a cell progression occurs as has been described in the mucus-secreting cells of the mouse intestine (Merzel and Leblond, '69) where the basal cells accumulate carbohydrates, push up to become intermediate cells and, on reaching the lumen, become type I cells which then shrink to produce type II and finally type III cells. It may also be that there are three types of superficial cells each producing its own secretion.

Mucous granules, as seen in the tubular nephron and collecting duct of the English sole (Bulger and Trump, '68) and the conducting portion of the reptile kidney (Anderson, '60), suggest that mucus is a secondary product of the cells, for the fine structure

of the cells indicates that they are actively involved in urine formation. In contrast, the superficial cells of the archinephric duct of adult lampreys appear to be engaged wholly in the production of mucus.

The Cell Coat

Almost all cells of the nephron in the kidney of P. marinus have a fibrillar fuzzy coat of variable thickness. It is particularly prominent on the processes of the podocytes as well as in the collecting segment and archinephric duct of adults and the intermediate and collecting segments of ammocoetes. This cell coat is thick in the archinephric duct of adults and resembles the enteric surface coat of the cat in that the coat appears as branching filaments covering the microvilli (Ito, '65). The external coats of most cells have been shown to be rich in carbohydrates (Rambourg and Leblond, '67) and this probably accounts for the intense PAS+ staining of the apical surface of these cells in the archinephric duct, although the apical mucous granules would account for the intense staining of the apical cytoplasm. Ito and Revel ('64) have demonstrated that the coat is the product of the cell which it covers and is not a mucous secretion; the PAS+ covering of the archinephric duct of adult P. marinus, therefore, is probably mainly a thick cell coat rather than a secretion of the superficial cells.

Cytoplasmic Fibrils

Cytoplasmic fibrils are common in most cells of the nephron of the lamprey kidney and are usually located in bundles near the

nucleus, although in the proximal segment they were found lying parallel to the basal plasma membrane. The fibrils of the proximal segment correspond in location to the myosin-like fibrils described in the nephron of the rat by Pease ('68) who suggested that its cells were myoepithelial. The bundles of fibrils located near the nucleus and often closely associated to the nuclear envelope likely represent tonofilaments which have been described as a fundamental component of cytoplasm (Fawcett, '66) and are probably supportive.

The Golgi Apparatus

The Golgi apparatus of podocytes and all parts of the tubular nephron, with the possible exception of the posterior undifferentiated tubules of ammocoetes, consists of a few microvesicles and highly dilated saccules indicating activity, probably reflecting its role in secretion (Fawcett, '66). In the posterior undifferentiated tubules and often in dark cells of the various segments of the tubular nephron of ammocoetes, it consists of large numbers of vesicles and only a few tiny, flattened saccules. The structure of the Golgi apparatus in these cells may reflect its role in glycogen synthesis as has been suggested for other glycogen-containing cells (Karrer and Cox, '60).

The similarity of the Golgi apparatus of the superficial type II cells of the archinephric duct of the adult to that described by Neutra and Leblond ('66) in goblet cells of rat leaves little doubt that vesicles of mucus are being pinched off from the ends of the saccules. We must know more of the functions of other

regions of the nephron to determine the role of their Golgi apparatuses.

Renal Glycogen

The identification of glycogen using the electron microscope has been well documented (Revel et al., '60; Drochmans, '62; Biava, '63; Revel, '64; Perry and Waddington, '66). The oxidation of 350- to 500-Å glycogen granules to 38- to 78-Å particles with periodic acid by the method of Perry and Waddington ('66) serves as a positive identification and leaves little doubt that the PAS+ material of the tubules of ammocoetes contains glycogen. Glycogen occurs in the human nephron (Biava, '63; Biava et al., '66; Witzleben, '60) and in the excretory system of an invertebrate (Bonga and Boer, '69) but no reports have described such large quantities in normal vertebrate renal tissues as is seen in ammocoetes.

Glycogen is associated with the smooth ER in varying quantities from small amounts in light cells to large amounts in the dark cells. The small amounts of the light cells may indicate a reduced rate of glycogen metabolism or depleted stores of glycogen.

The renal glycogen of ammocoetes and other forms (Biava, '63; Biava et al., '66; Witzleben, '69; Bonga and Boer, '69) is monoparticulate. In ammocoetes it is often contained within membrane-bound bodies. These bodies are identical to bodies found in human renal tubules in Pompe's disease (Witzleben, '69), the result of an inborn metabolic error where the lysosomal enzyme, α -glucosidase, is absent and the lysosomes store glycogen. These bodies are not found in the proximal segment of the human nephron, even in Pompe's

disease, where the enzyme has been suggested to occur, or in the lamprey. Perhaps the enzyme is absent in the distal tubules of ammocoetes.

Glycogen is characteristic of undifferentiated and developing cells (for example, Thomson and Binster, '66; Lentz and Trinkaus, '67; Rybiska, '67; Garant, '68) and its presence in ammocoetes may reflect the undifferentiated nature of these cells in a developing animal. The concentrations were highest in the least differentiated regions so that the light cells, with the smallest amounts of glycogen, could be considered the most highly differentiated cells. The range of electron densities from dark to light cells may indicate the continuing process of differentiation.

The presence of glycogen in the cells may also reflect the nutritional state of the animal; since no seasonal variations in concentration were noted, however, this suggestion seems unlikely.

Smooth and Rough Endoplasmic Reticulum

In most epithelial cells of the kidney of ammocoetes and adults of P. marinus, free ribosomes are scattered throughout the cytoplasm and are accompanied by smooth vesicles and smooth ER. Large concentrations of rough ER are seen only in the proximal segment although small amounts were scattered throughout most cells.

Smooth ER is characterized by its lack of ribosomes and its tubular reticulate form and it is often divided into cisternal and tubular types (see Locke, '69, for discussion). The appearance of smooth ER and other cell membranes is often dependent on the fixative used (see Bulger, '65; Bulger and Trump, '65b, for examples

and review) and cytoplasmic smooth vesicles may result from fragmentation of plasma membranes or perhaps from smooth ER. The tubular cells of P. marinus lack infoldings of the basal plasma membrane so that it seems unlikely that the numerous smooth vesicles are the result of fragmentation of the plasma membrane. Cells of the distal segment of ammocoetes when fixed in veronal acetate-buffered osmium tetroxide contain both smooth vesicles and smooth ER in close association. After fixation in glutaraldehyde and postfixation in osmium tetroxide the cytoplasm contains an anastomosing network of smooth ER with few smooth vesicles. This suggests that a major portion of the smooth vesicles are part of the smooth ER. The tubular smooth ER and the smooth vesicles in the cells of the distal segment of the adult are also believed to be part of the same system.

A similar condition of abundant smooth ER and sparse rough ER is found in the ureteric duct of the hagfish (Ericsson, '67) and in the tubules of the glomerular kidney of a marine teleost (Olsen and Ericsson, '68) but not in other teleosts (Bulger and Trump, '68). Abundant smooth ER does not appear to be characteristic of kidneys of higher vertebrates although there is more smooth ER in human proximal tubules than in distal tubules (Tisher et al., '68).

The close association between abundant tubular smooth ER and the presence of cells which contain glycogen has also been observed in the reno-pericardial system of the pond snail (Bonga and Boer, '69) and supports the hypothesis that the smooth ER is involved in glycogen metabolism (Porter and Bruni, '59; DeMan and

Blok, '66). The well-developed smooth ER of P. marinus, especially that of the distal cells, is remarkably similar to that which is considered characteristic of actively transporting cells such as the "chloride cells" of fish (Philpott and Copeland, '63; Pêtrick and Bucher, '69) and "flask-shaped cells" of Xenopus mesonephros (Spannhof and Jonas, '69). These similarities suggest that the tubular cells of P. marinus may be involved in the transport of ions.

Intercellular Spaces

Infoldings of the basal plasma membrane are absent from the kidney tubules of P. marinus. Such infoldings, in close association with mitochondria, are related to the passive transport of water through a cell following the active transport of sodium (Pease, '56) and are found in the proximal and distal tubules of many vertebrates (see summaries of Bulger, '65; Davis and Schmidt-Nielsen, '67; Gibley and Chang, '67; Schmidt-Nielsen and Davis, '68) as well as the loop of Henle of mammals (Osvaldo and Latta, '66) and in the excretory tubules of some invertebrates (for example Gouranton, '68; Tyson, '69).

Basal infoldings are lacking in the proximal tubules of the chick (Gibley and Chang, '67) and the proximal and distal tubules of the crocodile (Davis and Schmidt-Nielsen, '67; Schmidt-Nielsen and Davis, '68). In both of these there are large intercellular spaces similar to those seen in the lamprey, and, in their studies on gall bladder, Diamond and Tormey ('66) have concluded that these spaces serve the same transport function as the basal infoldings. The intercellular spaces seen in the archinephric

duct of ammocoetes closely resemble those of the "partially specialized secretory cells" of the avian salt gland (Ernst and Ellis, '69) and both contain interdigitating folds between cells. The intercellular spaces are small compared to those of the crocodile and lack the numerous microvilli. Intercellular spaces in collecting tubules of the rabbit have been shown to be related to water transport and the width of this space is dependent upon the rate of flow (Grantham et al., '69). It may be that the presence of intercellular spaces in the tubules of lampreys is related to water transport. The apparent continuity of the intercellular space with the extracellular space at the base of the epithelium in the tubules of the lamprey has also been demonstrated in the tubular epithelium of the rabbit, where it likely serves as a path for the diffusion of ions into the intercellular space in order to maintain a higher osmolality than that in the cell and lumen to facilitate continuous diffusion (Grantham et al., '69).

Mitochondria

Mitochondria occur in large numbers in almost all epithelial cells of the nephron indicating an active turnover of energy (Fawcett, '66). They are most abundant in the intermediate, distal, and collecting segments and the archinephric duct of ammocoetes and in the distal segment of adults where they probably provide energy for active transport. In the proximal segment of adults the cristae are often longitudinal or circular and the matrix contains filaments or a periodic structure of a crystalline appearance. Intramitochondrial filaments and crystalline structures have been described in the thick limb of Henle in rats and in many other tissues and may

reflect some metabolic activity or may be the result of injury or degeneration (see Suzuki and Mostofi, '67, for review). In adult lampreys, these filaments and crystalline structures may indicate more advanced degeneration or a greater susceptibility to injury. Longitudinal cristae have been shown to result from reduced activity of cytochrome oxidase during a summer starvation period in the frog (Karnovsky, '63) and their presence in adult lampreys may reflect the nutritional states. Longitudinal cristae are highly elaborated in salt absorbing cells of the crab gill where it has been suggested they form "mitochondrial pumps" which aid in transport of ions (Copeland Fitzjarrell, '68); the longitudinal cristae seen in the present investigation may be related to a specific activity.

Large numbers of mitochondria are also characteristic of cells rich in glycogen and may be involved in providing energy for its synthesis as well as for active transport. Their cristae are often angular and prismatic, a characteristic of the active tissues in which they have been found (Revel et al., '63).

Prismatic cristae were seen occasionally in the distal segment of ammocoetes but were more common in the undifferentiated tubules of the posterior tip of the kidney. The sides of the prisms were 400 to 450 Å long, comparable to those described in the pancreatic islets of the lizard (Burton and Vensel, '66) and blood cells of the crayfish (Shivers, '67), but larger than those of astrocytes of the hamster which measured 250 to 330 Å (Blinzinger et al., '65) and smaller than those of the cricothyroid muscle of the bat (Revel et al., '63). The arrangement of the cristae to form a tube is

similar to that described in the bat muscle but instead of having the apices of the triangular prisms meeting in the centre of the tube, the apices form the points of a star while the bases form a hexagonal tube (fig. 198). A feature not previously described is the linear arrangement of the intramitochondrial granules within the tube formed by the prismatic cristae. Mitochondrial granules are considered to be the site of binding of ions (Peachey, '64) necessary for the regulation of the internal environment of the mitochondrion (Fawcett, '66). This tube of granules may represent a more adequate unit for the performance of this function or be a reflection of the undifferentiated state of the cells in which they are found.

Circulation

The lamprey shares its lack of a renal portal system with mammals, and, in part, birds (Siller and Hindle, '69). The tubules of the lamprey kidney are supplied with blood from the glomus through a system of efferent arterioles, capillaries, and sinusoids while, in mammals, blood from the efferent arteriole passes to the venules by way of capillaries (Edwards, '56). The bird appears to be intermediate in condition between the mammalian system and the renal portal system (Siller and Hindle, '69). It has been suggested that the renal portal system of teleosts, amphibians, and reptiles is an adaptation to water conservation in that the glomerular filtration pressure can be reduced without affecting the blood supply to the tubules (Hoar, '66). The absence of a renal portal system in lampreys may be evidence for the existence of a different mechanism

for osmoregulation from that seen in most fishes.

The capillaries and sinusoids of the intertubular area lack the numerous fenestrations commonly seen in mammalian endothelial cells (Rhodin, '62). Transport of material across endothelial cells in the lamprey may occur by way of the abundant pinocytotic vesicles and may be necessary due to low blood pressure (De Martino and Zamboni, '66).

The condition of multiple efferent arterioles for each single afferent arteriole seems to be unique to the cyclostomes; this has also been reported for the hagfish, M. glutinosa (Nash, '31), and may be due to the large glomus found in both animals.

The paralleling of the straight tubules and sinusoids of the adult lamprey is similar to that seen in the loop of Henle, collecting tubules, and vasa recta of the mammalian renal medulla. In mammals the vasa recta operates as a counter-current diffusion exchanger minimizing the loss of solute from the medulla by creating a higher osmotic gradient (Gottschalk, '61). It may be that the sinusoids are simply following the course of the tubules in lampreys or that this, as in mammals, is related to the establishment of an osmotic gradient necessary for transport.

The circulation of the adult is distinguished from that of the ammocoetes by its more complex system of sinusoids and sinuses. The presence of a subcapsular sinus which drains all the interstitial sinuses and intertubular sinusoids is a feature not previously reported in vertebrate kidneys and closely resembles the central vein in the liver lobules of mammals.

The development of a subcardinal sinus is probably

necessitated by the increase in size of the kidney in older ammocoetes and adults. The drainage of blood from the intertubular sinuses directly into the posterior cardinal veins in young ammocoetes may not be a sufficient method of venous drainage for the large kidneys.

The present investigation confirms the observations of Torrey ('38) that the ammocoetes kidney is a site for haemopoietic activity.

Growth and Degeneration

The present investigation supports the earlier view (Wheeler, 1899) that the kidney of ammocoetes grows by a posterior proliferation of nephrogenic tissue accompanied by an anterior degeneration. The differentiating cells of the posterior tubules are unlike any cells of the kidney except for the glycogen-rich dark cells. An autoradiographic study would aid in determining whether a sequence exists between the cells of the posterior tip of the kidney to the dark and light cells found more anteriorly.

The kidney of the newly-transformed adult resembles that of the parasitic adult except that its tubules and glomus are confined to the ventral tip of the adipose projections. It differs from the ammocoetes kidney in that it extends to the cloaca, it contains a single glomus, and its tubules resemble those of the adult. It is assumed that the kidney of the newly-transformed adult reaches the size seen in parasitic adults by a proliferation of the existing tissue. Examination of animals from transformation to maturity would solve this problem.

The immense anterior region of degenerating renal tissue of the newly-transformed adult, which had been overlooked in the literature (Gerard, '54), appears to be in the position previously occupied by the kidney of ammocoetes.

Phagocytic invasion is characteristic of regressing tissue (for example Brown, '46; Lewis and McMillan, '75; Braekevelt and McMillan, '67) and may arise from the circulation or by differentiation from existing mesenchymal cells in response to the destruction of the tissue by lysosomal enzymes rather than the phagocytes themselves initiating the destruction (Weber, '64). The lamprey kidney is an excellent subject for the investigation of tissue regression; an ultrastructural and histochemical study of the role of lysosomes in this process would be useful in dispelling some of the mystery which surrounds these inclusions.

At the anterior tip of the adult kidney the tubules and glomera are enveloped by large amounts of amorphous material. This process is not accompanied by phagocytic invasion as in ammocoetes, but resembles hyalinization, an advanced form of degeneration seen in many tissues (Moorehead, '65). It is not known whether this represents a more advanced stage in the degeneration of the ammocoetes kidney which begins at transformation or whether it is a degeneration of the adult kidney.

A final period of degeneration occurs during the spawning migration. Initially the tubular epithelium accumulates lysosome-like granules, autophagic vacuoles, and lipid droplets. This resembles changes which accompany senility and which may result from the inability of cells to remove accumulated metabolic wastes (eg. Youson

and van Heyningen, '68). The accumulation of lipid may be the result of the absence of lysosomal lipase (eg. Toth, '68). Increased mesangium is characteristic of human renal abnormalities and may indicate decreased filtration (for reviews see Faith and Trump, '66; Fisher et al., '69). Accumulation of biliverdin within the kidney of migrating L. fluviatilis may result in the death of the animal (Lanzing, '59). Some of the changes occurring in the epithelial cells of the kidney of P. marinus may result from an accumulation of biliverdin since Sawyer and Roth ('54) have found large quantities in the urine of migrating adults.

Advanced degenerating changes of necrosis is followed by an invasion of phagocytes. A similar pattern has been noted in the gut of lamprey (Battle and Hayashida, '65). Early atrophy of the gut can be accounted for by the cessation of feeding but it would seem that kidney function would be essential until the time of death. Perhaps this is evidence for reduced kidney function during this stage in the life of the lamprey or it may be the result of toxic effects produced by changes occurring in the liver (Lanzing, '59).

Intertubular Tissue

The term intertubular cells was adopted for a group of cells which have not been described in the kidney of lamprey and whose function is unknown. Several types of cells are found in the interstitium of the kidneys of a variety of vertebrates. Interstitial cells are present among the tubules of higher vertebrates and although their function is not known they appeared to be able to phagocytose

material from the interstitium and undergo structural changes during dehydration of the animal (Bulger and Trump, '66). The intertubular cells of the ammocoetes share some morphological features of the interstitial cells: the presence of lipid droplets, stellate shape, the presence of an electron-dense coat morphologically similar to a basement membrane, and the abundance of the organelles (see Bulger and Trump, '66 for comparison). One of the main differences is the absence of glycogen from interstitial cells of the rat (Bulger and Trump, '66).

Interrenal or adrenal cortical cells are often seen in the intertubular spaces of vertebrate kidneys (see Gorbman and Bern, '66) and the intertubular cells of the lamprey may be migrants from the interrenal tissue which is located near the kidneys around the dorsal aorta (Sterba, '62) or the postcardinal vein (Gorbman and Bern, '66). The cells resemble each other in their large amounts of smooth ER, lipid droplets, and mitochondria, but the intertubular cells lack the tubular mitochondrial cristae (Long and Jones, '67a, '67b; Yoshimura et al., '68) of interrenal cells. Glycogen has also been reported in adrenal cortical cells (Long and Jones, '67b) and interrenal cells (Picheral, '68).

These intertubular cells can also be compared to immature adipose cells (Dyer, '68) in their large accumulations of glycogen and lipid droplets. Growth of the kidney may be predisposed by a growth of the adipose network in which the renal tissue is situated and thus would explain the presence of immature adipose cells. The main difference between adipose cells and intertubular cells is the

presence of the electron-dense coat beneath the limiting plasma membrane of the latter.

This electron-dense coat resembles the basement membrane of epithelial cells raising the possibility that the intertubular cells are epithelial remnants of the mesonephric cord described by Wheeler (1899). In their abundance of glycogen and lipid, the intertubular cells resemble the cells of the undifferentiated tubules in the posterior regions of the kidney which are derivatives of this cord.

Epilogue

The present investigation has shown that the kidney of the "primitive" vertebrate, P. marinus, is as highly evolved from the archinephros as those of higher vertebrates and that it is probably able to perform all of the functions which have been attributed to them.

SUMMARY

1. The kidney of ammocoetes of Petromyzon marinus grows by a posterior proliferation of nephrogenic tissue accompanied by anterior degeneration. At transformation a new kidney is formed.
2. Degeneration of kidney tissue occurs at four stages: in the anterior regions throughout larval life; in the entire ammocoetes kidney at transformation; in the anterior regions throughout adult life; in the entire kidney during the post-spawning migration. Large quantities of amorphous material appear in the interstitium during anterior degeneration of the adult. The other stages involve necrosis followed by the invasion of phagocytes.
3. Kidneys of ammocoetes contain several glomera placed end to end which increase in number and become longer posteriorly with age. A single glomus extends almost the entire length of the adult kidney.
4. A glomus is composed of several fused glomeruli. In ammocoetes each glomerulus consists of five to six capillary loops surrounded by its own Bowman's capsule. In adults Bowman's capsules are not seen but the dilated ends of the nephron are interposed between the capillary loops. In both ammocoetes

and adults the capillary endothelium is thick and is surrounded by a layer of podocytes; elsewhere a simple epithelium is found.

5. The tubular nephron of both ammocoetes and adults is divided into five regions: neck, proximal, intermediate, distal, and collecting segments. Further subdivisions occur in the proximal segment of both and in the distal segment of the adult.
6. In the adult, straight tubules of the distal, collecting, and intermediate segments parallel straight sinusoids; this may indicate a counter-current mechanism related to ion transport.
7. Large amounts of smooth endoplasmic reticulum and mitochondria in the distal segments of adults and ammocoetes and in the collecting segment of ammocoetes may reflect a mechanism for ion transport while intercellular spaces in most segments suggest water transport.
8. A range in the glycogen content of cells of every segment in ammocoetes may reflect variations in the degree of differentiation or metabolic activity between the cells.
9. The archinephric duct of ammocoetes consists of a stratified epithelium and the structure of its cells and the presence of intercellular spaces suggest that it is probably involved in urine formation. The duct in adults is composed of four layers. A layer of smooth muscle probably indicates peristaltic expulsion of urine while the epithelium secretes mucus.

10. A renal portal system is lacking. A medial artery extends the length of the kidney apposed to the glomera and is periodically supplied with blood from renal arteries. Blood enters the glomus through afferent arterioles from the medial artery and leaves through several efferent arterioles which branch into capillaries and sinusoids to supply the tubules. Intertubular sinusoids are drained by a system of sinuses which becomes more complex in the adult.
11. The cells of the tubules in the proliferating region of the ammocoetes kidney contain numerous mitochondria with parallel prismatic cristae which form a hexagonal tube containing rows of mitochondrial granules.
12. The intertubular tissue of the kidney of ammocoetes appears to be involved in haemopoiesis but it also contains many other types of cells. One of these, an intertubular cell, may be epithelial.
13. The kidney of the lamprey is not primitive but appears as highly evolved from the archinephric type as the kidneys of higher vertebrates; it is probably able to perform most of the functions attributed to them.

LITERATURE CITED

- Altner, H. 1968 Die Ultrastruktur der Labialnephridien von Onychiurus quadriocellatus (Collembola). J. Ultrastructure Res. 24: 349-366.
- Anderson, E. 1960 The ultramicroscopic structure of a reptilian kidney. J. Morphol. 106: 205-241.
- Anderson, E. and H.W. Beams 1956 Light and electron microscope studies on the "green gland" of Cambarus sp. Proc. Iowa Acad. Sci. 63: 681-685.
- Applegate, V.C. 1950 Natural History of the Sea Lamprey, Petromyzon marinus, in Michigan. U.S. Fish Wildlife Serv., Spec. Sci. Rep. Fisheries, no. 55, 237 pp.
- Bargmann, W., A. Knoop, and T.H. Schiebler 1955 Histologische, cytochemische und elektronenmikroskopische Untersuchungen am Nephron (mit Berücksichtigung der Mitochondrien). Z. Zellforsch. 42: 386-422.
- Battle, H.I. and K. Hayashida 1956 Comparative study of the intraperitoneal alimentary tract of parasitic and non-parasitic lampreys from the Great Lakes region. J. Fisheries Res. Bd. Canada 22: 289-306.

- Beitch, I. 1963 A histomorphological comparison of the urinary systems in serranid fishes, Roccus saxatilis and Roccus americanus. Chesapeake Sci. 4: 75-83.
- Bencosme, S.A., R.S. Stone, H. Latta, and S.C. Madden 1959
A rapid method for localization of tissue structures or lesions for electron microscopy. J. Biophys. Biochem. Cytol. 5: 508-511.
- Bentley, P.J. 1962 Permeability of the skin of the cyclostome Lampetra fluviatilis to water and electrolytes. Comp. Biochem. Physiol. 6: 95-97.
- Bentley, P.J. and B.K. Follett 1962 The action of neurohypophysial and adrenocortical hormones on sodium balance in the cyclostome Lampetra fluviatilis. Gen. Comp. Endocrinol. 2: 329-335.
- Bentley, P.J. and B.K. Follett 1963 Kidney function in a primitive vertebrate, the cyclostome Lampetra fluviatilis. J. Physiol. (London) 169: 902-918.
- Biava, C. 1963 Identification and structural forms of human particulate glycogen. Lab. Invest. 12: 1179-1197.
- Biava, C. and M. West 1966 Fine structure of normal human juxtaglomerular cells. I. General structure and intercellular relationship. Amer. J. Pathol. 49: 679-721.
- Biava, C., A. Grossman, and M. West 1966 Ultrastructural observations on renal glycogen in normal and pathologic human kidneys. Lab. Invest. 15: 330-356.

- Blinzinger, K., N.B. Rewcastle, and H. Hager 1965 Observations on prismatic-type mitochondria within astrocytes of the Syrian hamster brain. *J. Cell Biol.* 25: 293-303.
- Bonga, S.E.W. and H.H. Boer 1969 Ultrastructure of the renopericardial system in the pond snail *Lymnaea stagnalis* (L.). *Z. Zellforsch.* 94: 513-529.
- Boyer, C.C. 1955 Plastic reconstruction of the human renal glomerulus from serial sections. *Anat. Rec.* 121: 427.
- Boyer, C.C. 1956 The vascular pattern of the renal glomerulus as revealed by plastic reconstruction from serial sections. *Anat. Rec.* 125: 433-442.
- Braekevelt, C.R. and D.B. McMillan 1967 Cyclic changes in the ovary of the brook stickleback *Eucalia inconstans* (Kirtland) *J. Morphol.* 123: 373-396
- Brown, E.M. 1946 The histology of the tadpole tail during metamorphosis. *Amer. J. Anat.* 78: 79-113.
- Bulger, R.E. 1965 The fine structure of the aglomerular nephron of the toadfish, *Opsanus tau*. *Amer. J. Anat.* 117: 171-191.
- Bulger, R.E. and B.F. Trump 1965a A light and electron microscopic study of the mesonephric kidney of the English sole, *Parophrys vetulus*. *Anat. Rec.* 151: 445.
- Bulger, R.E. and B.F. Trump 1965b Effects of fixatives on tubular ultrastructure of the aglomerular midshipman, *Porichthys notatus*, and the glomerular flounder, *Parophrys vetulus*. *J. Histochem. Cytochem.* 13: 719.

- Bulger, R.E. and B.F. Trump 1966 Fine structure of the rat renal papillae. *Amer. J. Anat.* 118: 685-721.
- Bulger, R.E. and B.F. Trump 1968 Renal morphology of the English sole (Parophrys vetulus). *Amer. J. Anat.* 123: 195-226.
- Bulger, R.E. and B.F. Trump 1969 Ultrastructure of granulated arteriolar cells (juxtaglomerular cells) in kidney of a fresh and a salt water teleost. *Amer. J. Anat.* 124: 77-87.
- Bulger, R.E., C.C. Tisher, C.H. Myers, and B.F. Trump 1967 Human renal ultrastructure. II. The thin limb of Henle's loop and the interstitium in healthy individuals. *Lab. Invest.* 16: 124-141.
- Burton, P.R. and W.H. Vensel 1966 Ultrastructural studies of normal and alloxan-treated islet cells of the pancreas of the lizard, Eumeces fasciatus. *J. Morphol.* 118: 91-118.
- Capréol, S.V. and L.E. Sutherland 1968 Comparative morphology of juxtaglomerular cells. I. Juxtaglomerular cells in fish. *Can. J. Zool.* 46: 249-255.
- Christensen, A.K. 1963 Fine structure of an exceptional kidney in the salamander, Batrachoseps. *J. Cell Biol.* 19: 13A.
- Christensen, A.K. 1964 The structure of the functional pronephros in larvae of Ambystoma opacum as studied by light and electron microscopy. *Amer. J. Anat.* 115: 257-277.
- Copeland, D.E. and A.T. Fitzjarrell 1968 The salt absorbing cells in gills of the blue crab (Callinectes sapidus Rathbun) with notes on modified mitochondria. *Z. Zellforsch.* 92: 1-22.

- Darnton, S.J. 1969 A possible correlation between ultrastructure and function in the thin descending and ascending limbs of the loop of Henle of rabbit kidney. *Z. Zellforsch.* 93: 516-524.
- Davis, L.E. and B. Schmidt-Nielsen 1967 Ultrastructure of the crocodile kidney (*Crocodylus acutus*) with special reference to electrolyte and fluid transport. *J. Morphol.* 121: 255-276.
- De Man, J.C.H. and A.P.R. Blok 1966 Relationship between glycogen and a granular ER in rat hepatic cells. *J. Histochem. Cytochem.* 14: 135-141.
- De Martino, C. and L. Zamboni 1966 A morphological study of the mesonephros of the human embryo. *J. Ultrastructure Res.* 16: 399-427.
- Diamond, J.M. and J. McD. Tormey 1966 Role of long extracellular channels in fluid transport across epithelium. *Nature* 210: 817-820.
- Dick, B.W. and S.M. Kurtz 1968 Protein absorption from the urinary space by glomerular visceral epithelium. *Lab. Invest.* 19: 412-420.
- Drochmans, P. 1962 Morphologie du glycogène. Étude au microscope électronique de colorations négative du glycogène. *J. Ultrastructure Res.* 6: 141-163.
- Duffy, J.L. and Y. Suzuki 1968 Ciliated human renal proximal tubular cells. Observations in three cases of hypercalcaemia. *Amer. J. Pathol.* 53: 609-616.

- Dyer, R.F. 1968 Morphological features of brown adipose cell maturation in vivo and in vitro. Amer. J. Anat. 123: 255-282.
- Edwards, J.G. 1935 The epithelium of the renal tubule in bony fish. Anat. Rec. 63: 263-279.
- Edwards, J.G. 1956 Efferent arterioles of glomeruli in the juxtamedullary zone of the human kidney. Anat. Rec. 125: 521-530.
- Ericsson, J.L.E. 1964 Absorption and decomposition of homologous hemoglobin in renal proximal tubule cells. An experimental light and electron microscopic study. Acta Pathol. Microbiol. Scand. 168 (Supl.): 1-121.
- Ericsson, J.L.E. 1967 Fine structure of ureteric duct epithelium in the north Atlantic hagfish (Myxine glutinosa L.). Z. Zellforsch. 83: 219-230.
- Ericsson, J.L.E. and R. Seljelid 1968 Endocytosis in the ureteric duct epithelium of the hagfish (Myxine glutinosa L.). Z. Zellforsch. 90: 263-272.
- Ericsson, J.L.E. and B.F. Trump 1964 Electron microscopic study of the epithelium of the proximal tubule of the rat kidney. I. The intracellular localization of acid phosphatase. Lab. Invest. 13: 1427-1456.
- Ericsson, J.L.E. and B.F. Trump 1966 Electron microscopic studies of the epithelium of the proximal tubule of the rat kidney. III. Microbodies, multivesicular bodies, and the Golgi apparatus. Lab. Invest. 15: 1610-1633.

- Ericsson, J.L.E., and B.F. Trump, and J. Weibel 1965 Electron microscopic studies of the proximal tubule of the rat kidney. II. Cytosegrosomes and cytosomes; their relationship to each other and to the lysosome concept. *Lab. Invest.* 14: 1341-1365.
- Ericsson, J.L.E., A. Bergstrand, G. Andres, H. Bucht, and G. Cinotti 1965 Morphology of the renal tubular epithelium in young, healthy humans. *Acta Pathol. Microbiol. Scand.* 63: 361-384.
- Ernst, S.A. and R.A. Ellis 1969 The development of surface specialization in the secretory epithelium of the avian salt gland in response to osmotic stress. *J. Cell Biol.* 40: 305-321.
- Faith, G.C. and B.F. Trump 1966 The glomerular capillary wall in human disease: acute glomerulonephritis, system lupus erythematosus and preeclampsia-eclampsia. *Lab. Invest.* 15: 1682-1719.
- Farquhar, M.G., S.L. Wissig, and G.E. Palade 1961 Glomerular permeability. I. Ferritin transfer across the normal glomerular capillary wall. *J. Exp. Med.* 113: 47-66.
- Fawcett, D.W. 1958 Structural specializations of the cell surface. In: *Frontiers in Cytology*, S.L. Palay, Ed. Yale Univ. Press, New Haven, Chapter 3, pp. 19-41.
- Fawcett, D.W. 1962 Physiologically significant specializations of the cell surface. *Circulation* 26: 1105-1125.
- Fawcett, D.W. 1966 *The Cell. An Atlas of Fine Structure.* W.B. Saunders Co., Philadelphia, 448 pp.

- Fisher, E.R., V. Pardo, R. Paul, and T.T. Hayashi 1969 Ultra-structural studies in hypertension. IV. Toxemia of pregnancy. *Amer. J. Pathol.* 55: 109-131.
- Fraser, E.A. 1950 The development of the vertebrate excretory system. *Biol. Rev.* 25: 159-187.
- Fujimoto, T. 1964 Ciliary fine structure of epithelium of the renal tubule in urodele, *Triturus ensicauda*, with special reference to the so called "dense granules" in the basal body. *Arch. Histol. Jap.* 25: 248-252.
- Gage, S.H. 1928 The lake and brook lampreys of New York State - life history and economics. In: Biological Survey of the Oswego River System, N.Y. Cons. Dept. Suppl., 17th Ann. Rep., pp. 158-191.
- Garant, P.R. 1968 Glycogen storage within undifferentiated cells of the dental papilla: electron microscopic findings. *J. Dent. Res.* 47: 699-703.
- Gerard, P. 1936 Contributions apportées par l'histophysiologie comparée à la connaissance de la fonction rénale chez les vertébrés. *Ann. Physiol. Physicochim. Biol.* 12: 587-618.
- Gerard, P. 1954 Appareil excreteur. In: *Traité de zoologie*, P.P. Grassé, Ed. 12: 974-1043.
- Gibley, C.W., Jr., and J.P. Chang 1967 Fine structure of the functional mesonephros in the eight-day chick embryo. *J. Morphol.* 123: 441-462.
- Gorbman, A. and H.A. Bern 1966 A Textbook of Comparative Endocrinology. Wiley, New York, 468 pp.

- Gottschalk, C.W. 1961 Micropuncture studies of tubular function in the mammalian kidney. *The Physiologist* 4: 35-55.
- Gouranton, J. 1968 Ultrastructures en rapport avec un transit d'eau. Étude de la "chambre filtrante" de Cicadella viridis L. (Homoptera, Jassidae). *J. Microscop.* 7: 559-574.
- Graham, R.C. and M.J. Karnovsky 1966 The early stages of absorption of injected horseradish peroxidase in the proximal tubules of mouse kidney: ultrastructural cytochemistry by a new technique. *J. Histochem. Cytochem.* 14: 291-302.
- Grantham, J.J., C.E. Ganote, M.B. Burg, and J. Orloff 1969 Paths of transtubular water flow in isolated renal collecting tubules. *J. Cell Biol.* 41: 562-576.
- Gritzka, T.L. 1963 The ultrastructure of the proximal convoluted tubule of a euryhaline teleost, Fundulus heteroclitus. *Anat. Rec.* 145: 235-236.
- Hardisty, M.W. 1956 Some aspects of osmotic regulation in lampreys. *J. Exp. Biol.* 33: 431-437.
- Hatta, S. 1900 Contributions of the morphology of cyclostomata. II. On the development of the pronephros and segmental duct. *J. Coll. Sci. Imp. Univ. Tokyo* 13: 311-346.
- Hickman, C.P., Jr. 1965 Studies on renal function in freshwater teleost fish. *Trans. Roy. Soc. Can.* 3 (Ser. 4, Sect. 3): 213-236.
- Hickman, C.P., Jr. 1968 Urine composition and kidney tubular function in southern flounder, Paralichthys lethostigma, in sea water. *Can. J. Zool.* 46: 439-455.

- Hoar, W.S. 1966 General and Comparative Physiology. Prentice Hall, Englewood Cliffs, N.J., 815 pp.
- Hyman, L.H. 1949 Comparative Vertebrate Anatomy. U. of Chicago Press, Chicago, 544 pp.
- Inukai, T. 1929 Die Vorniere (pronephros) auf ihrer höchsten Entwicklungsstufe bei Neunaugen [Lampetra (Petromyzon) fluviatilis und planeri]. Z. Zellforsch. 19: 139-162.
- Ito, S. 1965 The surface coat of enteric microvilli. J. Cell Biol. 27: 475-491.
- Ito, S. and J.P. Revel 1964 Incorporation of radioactive sulfate and glucose on the surface coat of enteric microvilli. J. Cell Biol. 23: 44A.
- Jamison, R.L., C.M. Bennett, and R.W. Berliner 1967 Counter-current multiplication by the loop of the Henle. Amer. J. Physiol. 212: 357-366.
- Jordan, H.E. and C.C. Speidel 1930 Blood formation in cyclostomes. Amer. J. Anat. 46: 355-391.
- Karnovsky, M.J. 1963 The fine structure of mitochondria in the frog nephron correlated with cytochrome oxidase activity. Exp. Mol. Pathol. 2: 347-366.
- Karrer, H.E. and J. Cox 1960 Electron microscopic observations on developing chick embryo liver. The Golgi complex and its possible role in formation of glycogen. J. Ultrastructure Res. 4: 149-165.
- Kerr, J.G. 1919 Textbook of Embryology. Vertebrata with the Exception of Mammalia, Vol. II. (Cited by Hyman, 1949).

- Kitzan, S.M. and P.R. Sweeney 1968 A light and electron microscope study of the structure of Protopterus annectens epidermis. I. Mucus production. *Can. J. Zool.* 46: 767-772.
- Kummel, G. 1964a Morphologischer Hinweis auf einen Filtrationsvorgang in der Antennendrüse von Cambarus affinus Say. (Crustacea, Decapoda). *Naturwissenschaften* 51: 200-201.
- Kummel, G. 1964b Das Cblomsäckchen der Antennendrüse von Cambarus affinis Say. (Decapoda, Crustacea). *Zool. Beitr.* 10: 227-252.
- Langer, K.H. 1968 Feinstrukturen der Mikrokorper (Microbodies) des proximalen Nierentubulus. *Z. Zellforsch.* 90: 432-446.
- Lanzing, W.J.R. 1959 Studies on the river lamprey, Lampetra fluviatilis, during its anadromous migration. Thesis, Universiteit te Utrecht, 82 pp.
- Latta, H., A.B. Maunsbach, and S.C. Madden 1961 Cilia in different segments of the rat nephron. *J. Biophys. Biochem. Cytol.* 11: 248-252.
- Leeson, T.S. 1957 The fine structure of the mesonephros of the 17-day rabbit embryo. *Exp. Cell Res.* 12: 670-672.
- Leeson, T.S. 1959 An electron microscopic study of the mesonephros and metanephros of the rabbit. *Amer. J. Anat.* 105: 165-195.
- Leeson, T.S. 1960 The electron microscopy of the developing kidney. An investigation into the fine structure of the mesonephros and metanephros of the rabbit. *J. Anat. (London)* 94: 100-106.
- Lentz, T.L. and J.P. Trinkaus 1967 A fine structural study of cytodifferentiation during cleavage, blastula, and gastrula stages of Fundulus heteroclitus. *J. Cell Biol.* 32: 121-138.

- Lewis, J.C. and D.B. McMillan 1965 The development of the ovary of the sea lamprey (Petromyzon marinus L.). J. Morphol. 117: 425-465.
- Lillie, R.D. 1942 An improved acid hematoxylin formula. Stain Technol. 17: 89.
- Lillie, R.D. 1954 Histopathologic Technic and Practical Histochemistry. The Blakiston Company, New York, 501 pp.
- Locke, M. 1969 The ultrastructure of the oenocytes in the molt/ intermolt cycle of an insect. Tissue and Cell 1: 103-154.
- Long, J.A. and A.L. Jones 1967a Observations of the fine structure of the adrenal cortex of man. Lab. Invest. 17: 355-370.
- Long, J.A. and A.L. Jones 1967b The fine structure of the zona glomerulosa and the zona fasciculata of the adrenal cortex of the opossum. Amer. J. Anat. 120: 463-488.
- Longley, J.B. and M.S. Burstone 1963 Intraluminal nuclei and other inclusions as agonal artifacts of the renal proximal tubule. Amer. J. Pathol. 42: 643-655.
- Luft, J.H. 1961 Improvements in epoxy resin embedding methods. J. Biophys. Biochem. Cytol. 9: 409-414.
- MacDonald, T.H. 1959 Estimates of length of larval life in three species of lamprey found in Great Britain. J. Animal Ecol. 28: 293-298.
- Marshall, E.K., Jr. 1934 The comparative physiology of the kidney in relation to theories of renal secretion. Physiol. Rev. 14: 133-159.

- Marshall, E.K., Jr. and H.W. Smith 1930 The glomerular development of the vertebrate kidney in relation to habitat. Biol. Bull. 59: 135-153.
- Maunsbach, A.B. 1964 Ultrastructure of different segments within the rat renal proximal tubule. Anat. Rec. 148: 387.
- Maunsbach, A.B. 1966 The influence of different fixatives and fixation methods on the ultrastructure of rat kidney proximal tubule cells. I. Comparison of different perfusion fixation methods and of glutaraldehyde, formaldehyde and osmium tetroxide fixatives. J. Ultrastructure Res. 15: 242-282.
- McManus, J.F.A. 1948 Histological and histochemical uses of periodic acid. Stain Technol. 23: 99-108.
- Merzel, J. and C.P. LeBlond 1969 Origin and renewal of goblet cells in the epithelium of the mouse small intestine. Amer. J. Anat. 124: 281-306.
- Miller, F. 1960 Hemoglobin absorption by the cells of the proximal convoluted tubule in mouse kidney. J. Biophys. Biochem. Cytol. 8: 689-718.
- Miller, F. and G.E. Palade 1964 Lytic activities in renal protein absorption droplets. An electron microscopical cytochemical study. J. Cell Biol. 23: 519-552.
- Millonig, G. 1962 Further observations on a phosphate buffer for osmium solutions in fixation. Proc. Fifth Int. Congr. Electron Microscop., Vol. 2, S.S. Breese, Jr., Ed. Academic Press, New York, p. 8.

- Mizogami, S., M. Oguri, H. Sokabe, and H. Nishimura 1968 Presence of renin in the glomerular kidney of marine teleosts. *Amer. J. Physiol.* 215: 991-994.
- Monis, B. and D. Zambrano 1968 Transitional epithelium of urinary tract in normal and dehydrated rats. A histochemical and electron microscopic study. *Z. Zellforsch.* 85: 165-182.
- Moorehead, R.P. 1965 *Human Pathology*. McGraw-Hill, Blakiston Division, New York, 1676 pp.
- Morris, R. 1956 The osmoregulatory ability of the lamprey (*Lampetra fluviatilis* L.) in sea water during the course of its spawning migration. *J. Exp. Biol.* 33: 235-248.
- Morris, R. 1957 Some aspects of the structure and cytology of the gills of *Lampetra fluviatilis* L. *Quart. J. Microscop. Sci.* 98: 473-485.
- Morris, R. 1960 General problems of osmoregulation with special reference to Cyclostomes. *Symp. Zool. Soc. Lond.* No. 1, 1-16.
- Myers, C.H., R.E. Bulger, C.C. Tisher, and B.F. Trump 1966 Human renal ultrastructure. IV. Collecting ducts of healthy individuals. *Lab. Invest.* 15: 1921-1950.
- Nash, J. 1931 The number and size of glomeruli in the kidneys of fishes with observations on the morphology of the renal tubules of fishes. *Amer. J. Anat.* 47: 425-445.
- Neutra, M. and C.P. Leblond 1966 Synthesis of the carbohydrate of mucus in the Golgi complex as shown by electron microscope radioautography of goblet cells from rats injected with glucose-H³. *J. Cell Biol.* 30: 119-136.

- Ogawa, M. 1962 Comparative study on the internal structure of the teleostean kidney. Sci. Rep. Saitama Univ., Ser. B. 4: 107-129.
- Oquri, M. and H. Sokabe 1968 Juxtaglomerular cells in the teleost kidneys. Bull. Jap. Soc. Sci. Fisheries 34: 882-888.
- Olsen, S. and J.L.E. Ericsson 1968 Ultrastructure of the tubule of the aglomerular teleost, Neophis ophidion. J. Zellforsch. 87: 17-30.
- Osvaldo, L. and H. Latta 1966 The thin limb of the loop of Henle. J. Ultrastructure Res. 15: 144-148.
- Pak Poy, R.K.F. 1957 Electron microscopy of the amphibian renal glomerulus. Austral. J. Exp. Biol. Med. Sci. 35: 583-594.
- Pak Poy, R.K.F. 1958 Electron microscopy on the piscine (Carassius auratus) renal glomerulus. Austral. J. Exp. Biol. Med. Sci. 36: 191-209.
- Parks, H.F. and W. McFarland 1966 Ultrastructure of tubular and ductal epithelium of mesonephric kidney of hagfish. Anat. Rec. 154: 480.
- Peachey, L.D. 1964 Electron microscopic observations on the accumulation of divalent cations in intramitochondrial granules. J. Cell Biol. 20: 95-111.
- Pease, D.C. 1956 Infolded basal plasma membranes found in epithelia noted for their water transport. J. Biophys. Biochem. Cytol. 2 (Suppl.): 203-208.
- Pease, D.C. 1964 Histological Techniques for Electron Microscopy Academic Press, New York, 381 pp.

- Pease, D.C. 1968 Myoid features of renal corpuscles and tubules. *J. Ultrastructure Res.* 23: 304-320.
- Perry, M.M. 1967 Identification of glycogen in thin sections of amphibian embryos. *J. Cell Sci.* 2: 257-264.
- Perry, M.M. and C.H. Waddington 1966 The ultrastructure of the cement gland in Xenopus laevis. *J. Cell Biol.* 1: 193-200.
- Petrík, P. and O. Bucher 1969 A propos des "chloride cells" dans les épithélium des lamelles branchiales du poisson rouge. *Z. Zellforsch.* 96: 66-74.
- Philpott, C.W. and D.E. Copehand 1963 Fine structure of chloride cells from three species of Fundulus. *J. Cell Biol.* 18: 389-404.
- Picheral, B. 1968 Les tissus élaborateurs de hormones stéroïdes chez les amphibiens urodèles. II. Aspects ultrastructuraux de la glande interrénale de Salamandra salamandra (L.) étude particulière du glycogène. *J. Microscop.* 7: 907-926.
- Porter, K.R. and C. Bruni 1959 An electron microscope study of the effects of 3' - Me- DAB on rat liver cells. *Cancer Res.* 19: 997-1009.
- Rambourg, A. and C.P. Leblond 1967 Electron microscope observations on the carbohydrate-rich cell coat present at the surface of cells in the rat. *J. Cell Biol.* 34: 27-54.

- Read, L.J. 1968 A study of ammonia and urea production and excretion in the freshwater-adapted form of the Pacific lamprey, Entosphenus tridentatus. *Comp. Biochem. Physiol.* 26: 455-466.
- Regaud, Cl. and A. Policard 1901 Notes histologiques sur la sécrétion rénale. *C.R. Soc. Biol. Paris* 53: 1186-1188.
- Regaud, Cl. and A. Policard 1902a Notes histologiques sur la sécrétion rénale. II. Le segment cilié du tube urinifère de la lamproie. *C.R. Soc. Biol. Paris* 54: 91-93.
- Regaud, Cl. and A. Policard 1902b Notes histologiques sur la sécrétion rénale. III. Le segment à bordure en brosse du tube urinifère de la lamproie. *C.R. Soc. Biol. Paris* 54: 129-131.
- Regaud, Cl. and A. Policard 1902c Notes histologiques sur la sécrétion rénale. IV. Les diverticules glandulaires du tube contourné de la lamproie. *C.R. Soc. Biol. Paris* 54: 554-555.
- Revel, J.P. 1964 Electron microscopy of glycogen. *J. Histochem. Cytochem.* 12: 104-114.
- Revel, J.P., D.W. Fawcett, and C.W. Philpott 1963 Observations of mitochondrial structure. Angular configurations of the cristae. *J. Cell Biol.* 16: 187-195.
- Revel, J.P., L. Napolitano, and D. Fawcett 1960 Identification of glycogen in electron micrographs of thin tissue sections. *J. Biophys. Biochem. Cytol.* 8: 575-589.
- Reynolds, E.S. 1963 The use of lead citrate at high pH as an electron-opaque stain in electron microscopy. *J. Cell Biol.* 17: 208-212.

- Rhodin, J. 1954 Correlation of ultrastructural organization and function in normal and experimentally changed proximal convoluted tubular cells of the mouse kidney. Aktiebolaget Godvil, Stockholm, 76 pp.
- Rhodin, J. 1958a Anatomy of kidney tubules. Int. Rev. Cytol. 7: 485-534.
- Rhodin, J. 1958b Electron microscopy of the kidney. Amer. J. Med. 24: 661-675.
- Rhodin, J. 1962 The diaphragm of capillary endothelial fenestrations. J. Ultrastructure Res. 6: 171-185.
- Rhodin, J. 1963a Structure of the kidney. In: Diseases of the Kidney, M.B. Strauss and L.G. Welt, Eds. Little, Brown, and Co., Boston, 1033 pp.
- Rhodin, J. 1963b An Atlas of Ultrastructure. W.B. Saunder Co., Philadelphia, 222 pp.
- Robertson, J.D. 1954 The chemical composition of the blood of some aquatic chordates including members of the Tunicata, Cyclostomata, and Osteichthyes. J. Exp. Biol. 31: 424-442.
- Rosen, S. and C.C. Tisher 1968 Observations on the rhesus monkey glomerulus and juxtaglomerular apparatus. Lab. Invest. 18: 240-248.
- Rybicksa, K. 1967 Embryogenesis in Hymenolepsis diminuta. II. Glycogen distribution in embryos. Exp. Parasitol. 20: 98-105.

- Sabatini, D.D., K. Bensch, and R.J. Barnett 1963 Cytochemistry and electron microscopy. The preservation of cellular ultrastructure and enzymatic activity by aldehyde fixation. *J. Cell Biol.* 17: 19-58.
- Sawyer, W.H. and W.D. Roth 1954 The storage of biliverdin by the liver of the migrating sea lamprey, *Petromyzon marinus*. *Anat. Rec.* 120: 741.
- Schmidt-Nielsen, B. and L.E. Davis 1968a Fluid transport and tubular intercellular spaces in reptilian kidneys. *Science* 159: 1105-1108.
- Schmidt-Nielsen, B., K.H. Gertz, and L.E. Davis 1968b Excretion and ultrastructure of the antennal gland of the fiddler crab, *Uca mordax*. *J. Morphol.* 125: 473-496.
- Shivers, R.R. 1967 Fine structure of crayfish optic ganglia. *U. Kansas Sci. Bull.* 47: 677-733.
- Siever, A.C. and B.L. Munger 1968 The use of oxone to facilitate specific tissue stainability following osmium fixation. *Anat. Rec.* 162: 43-51.
- Siller, W.G. and R.M. Hindle 1969 The arterial blood supply to the kidney of the fowl. *J. Anat.* 104: 117-135.
- Sjöstrand, F.S. and J. Rhodin 1953 The ultrastructure of the proximal convoluted tubules of the mouse kidney as revealed by high resolution electron microscopy. *Exp. Cell Res.* 4: 426-456.
- Smith, H.W. 1959 *From Fish to Philosopher*. Little, Brown, and Co., Boston, 264 pp.

- Spannhof, L. and L. Jonas 1969 Elektronenmikroskopische Untersuchungen zur Genese und Sekretbildung in den Flaschenzellen der Urniere vom Krallenfrosch. *Z. Zellforsch.* 95: 134-142.
- Sterba, G. 1962 Die Neunaugen. Handbuch der Binnentischerei Mitteleuropas Vol. II, E. Schweizerbart'sche Verlagsbuchhandlung, Stuttgart.
- Strauss, W. 1957 Segregation of an intravenously injected protein by "droplets" of the cells of rat kidney. *J. Biophys. Biochem. Cytol.* 3: 1037-1040.
- Suzuki, T. and F.K. Mostofi 1967 Intramitochondrial filamentous bodies in the thick limb of Henle of the rat kidney. *J. Cell Biol.* 33: 605-623.
- Tampi, P.R.S. 1959 On the renal unit in some common teleosts. *Proc. Indiana Acad. Sci. (Sect. B)* 50: 88-104.
- Thomas, M.L.H. 1962 Observations on the Ecology of Petromyzon marinus L. and Entosphenus lamottei (Le Seur) in the Great Lakes Watershed. M.S.A. Thesis, University of Toronto, 214 pp.
- Thomson, J.L. and R.L. Binster 1966 Glycogen content of perimplantation mouse embryos. *Anat. Rec.* 155: 97-102.
- Thorson, T.B. 1959 Tricaine methanesulfonate (MS222) as an anesthetic for sea lamprey, Petromyzon marinus. *Copeia* 2: 163-165.
- Tibbles, J.J. 1961 Preparations for lamprey control in Lake Huron. Fisheries Res. Bd. Can., Progr. Rept. Biol. Station and Technol. Unit, London, Ontario. 2: 32-35.

- Tisher, C.C., R.E. Bulger, and B.F. Trump 1966 Human renal ultrastructure. I. Proximal tubule of healthy individuals. Lab. Invest. 15: 1357-1394.
- Tisher, C.C., R.E. Bulger, and B.F. Trump 1968 Human renal ultrastructure. III. Distal tubule of healthy individuals. Lab. Invest. 18: 655-668.
- Tisher, C.C., R.M. Rinkel, S. Rosen, and E.M. Kendig 1968 Renal microbodies in the rhesus monkey. Lab. Invest. 19: 1-6.
- Toner, P.G. 1968 Cytology of intestinal epithelial cells. Int. Rev. Cytol. 24: 233-343.
- Torrey, T.W. 1938 The absorption of colloidal carbon from the body cavity of ammocoetes. A study of the structure and function of the larval kidneys and blood forming tissues. J. Morphol. 63: 163-178.
- Torrey, T.W. 1964 Morphogenesis of the vertebrate kidney. In: International Conference of Organogenesis. Holt, Rinehart, and Winston, New York, 559-579.
- Toth, S.E. 1968 Review Article. The origin of lipofuscin age pigments. Exp. Gerontol. 3: 19-30.
- Trump, B.F. 1961 An electron microscope study of the uptake, transport and storage of colloidal material by the cells of the vertebrate nephron. J. Ultrastructure Res. 5: 291-310.
- Trump, B.F. and R.E. Bulger 1967 Studies of cellular injury in isolated flounder tubules. I. Correlation between morphology and function of control tubules and observations of autophagocytosis and mechanical cell damage. Lab. Invest. 16: 453-482.

- Trump, B.F. and J.L.E. Ericsson 1965 The effect of the fixative solution on the ultrastructure of cells and tissues. A comparative analysis with particular attention to the proximal convoluted tubule of the kidney. *Lab. Invest.* 14: 1245-1323.
- Tyson, G.E. 1966 Gross morphology and fine structure of the maxillary gland of the brine shrimp, Artemia salina. *Amer. Zool.* 6: 555.
- Tyson, G.E. 1968 The fine structure of the maxillary gland of the brine shrimp, Artemia salina: the end-sac. *Z. Zellforsch.* 86: 129-138.
- Tyson, G.E. 1969 The fine structure of the maxillary gland of the brine shrimp, Artemia salina: the efferent duct. *Z. Zellforsch.* 93: 151-163.
- Urist, M.R. and K.A. van de Putte 1967 Comparative biochemistry of the blood of fishes: identification of fishes by the chemical composition of serum. In: Sharks, Skates, and Rays, P.W. Gilbert, R.F. Mathewson, and D.P. Rall, Eds. Johns Hopkins Univ. Press, Baltimore, pp. 2271-285.
- Vinnichenko, L.N. 1966 Elektronomikroskopisheskoe issedtvanie pochki minogi. In: *Electronnaya Mikroskopiya Kletok Zhivot Nykh.* Nauka, Moscow, pp 5-25.
- Vladykov, V.D. 1950 Larvae of eastern American lampreys (Petromyzontidae). I. Species with two dorsal fins. *Natur. Canadien* 77: 79-95.

- Wladykov, V.D. 1960 Description of young ammocoetes belonging to two species of lampreys: Petromyzon marinus and Entosphenus lamottei. J. Fisheries Res. Bd. Can. 17: 267-290.
- Watson, M.L. 1958 Staining of tissue sections for electron microscopy with heavy metals. J. Biophys. Biochem. Cytol. 4: 475-478.
- Weber, R. 1964 Ultrastructural changes in regressing tail muscles of Xenopus larvae at metamorphosis. J. Cell. Biol. 22: 481-487.
- Wikgren, J.B. 1953 Osmotic regulation in some aquatic animals with special reference to the influence of temperature. Acta Zool. Fenn. 71: 1-102.
- Witzleben, C.L. 1969 Renal cortical tubular glycogen localization in glycogenosis type II-(Pompe's disease). Lab. Invest. 20: 424-429.
- Wheeler, M.W. 1899 The development of the urogenital organs of the lamprey. Zool. Jahrb. Abt. Anat. Ontog. Tiere 13: 1-88.
- Yoshimura, F., K. Harumiya, N. Suzuki, and S. Totsuka 1968 Light and electron microscopic studies on the zonation of the adrenal cortex in albino rats. Endocrinol. Jap. 15: 20-52.
- Youson, J.H. and H.E. Van Heyningen 1968 Dense granules (lysosomes?) and crystals in the thyroids of senile rats. Amer. J. Anat. 122: 377-396.
- Zetterqvist, H. 1956 The Ultrastructural Organization of the Columnar Absorbing Cells of the Mouse Jejunum. Dept. Anat., Karolinska Institutet, Stockholm (Cited by Pease, '64).

THE MORPHOLOGY OF THE OPISTHONEPHRIC KIDNEY OF THE GREAT
LAKES LAMPREY, Petromyzon marinus (L.)

by

John Harold Youson

Department of Zoology

PART II: Figures 1 to 220

Submitted in partial fulfillment
of the requirements for the degree of
Doctor of Philosophy

Faculty of Graduate Studies
The University of Western Ontario
London, Canada.
August, 1969

In all legends of figures the fixative, embedding material,
and stain are listed in that order.

Abbreviations used for the stains:

Periodic acid-Schiff	PAS
Acid haemalum	AH
Haematoxylin	H
Orange G	OG
Toluidine blue	TB
Oxone-Schiff	OxS
Uranyl acetate	UA
Lead Citrate	LC

Fixatives:

Bouin's fluid	Bouin
Osmium tetroxide buffered with veronal acetate	Osmium
Phosphate buffered glutaraldehyde and post-fixation in phosphate buffered osmium tetroxide	Glutaraldehyde-Osmium



In all legends of figures the fixative, embedding material,
and stain are listed in that order.

Abbreviations used for the stains:

Periodic acid-Schiff	PAS
Acid haemalum	AH
Haematoxylin	H
Orange G	OG
Toluidine blue	TB
Oxone-Schiff	OxS
Uranyl acetate	UA
Lead Citrate	LC

Fixatives:

Bouin's fluid	Bouin
Osmium tetroxide buffered with veronal acetate	Osmium
Phosphate buffered glutaraldehyde and post-fixation in phosphate buffered osmium tetroxide	Glutaraldehyde-Osmium

Figure 1: Light micrograph of a transverse section of the kidney; parasitic adult.

The kidney is enveloped by a capsule of parietal peritoneum and connective tissue (CA) and is composed of tubules (T), a glomus (GL), and an archinephric duct (AD). Adipose tissue (AT) is found at the dorsal surface and a large sinusoid (S) traverses the ventral part of the kidney obliquely. An efferent arteriole (arrow) drains a loop of the glomus.

Bouin, Tissuemat, PAS-AH-OG

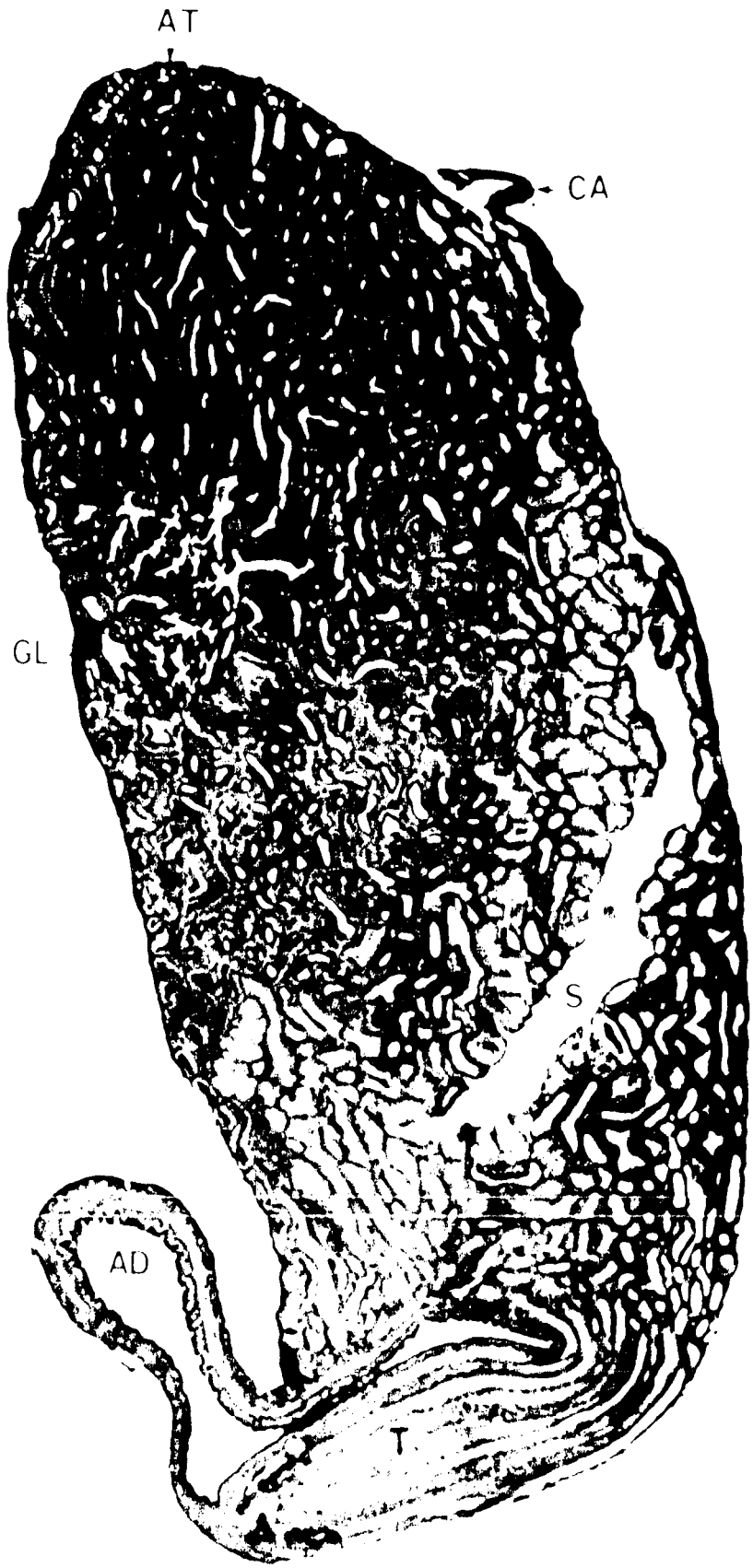


Figure 2: Light micrograph of a transverse section at the level of the anterior portion of the kidneys; 55-mm ammocoetes.

Seen in the section are the notoderm (NC), dorsal aorta (DA), posterior cardinal vein (PC), and gut (G). The kidneys project ventrally from a dorsal mass of adipose tissue (AT). In the anterior part of the kidneys the archinephric ducts (AD) are dorsal while the glomera (GL) are at the ventral tip.

Bouin, Tissuemat, PAS-AH-OG

X 145

Figure 3: Light micrograph of a transverse section through one of the paired kidneys and the gut (G); newly-transformed adult.

The renal tissue is confined to the ventral third of the adipose projection with the remainder being made up of adipose tissue (AT). The glomus (GL) is more ventrally located than in the mature adult. The archinephric duct (AD) is located at the ventral tip. The remainder of the renal tissue consists of tubules (T) and the kidney is enveloped in a capsule (CA). The gut (G) is lateral to the kidney.

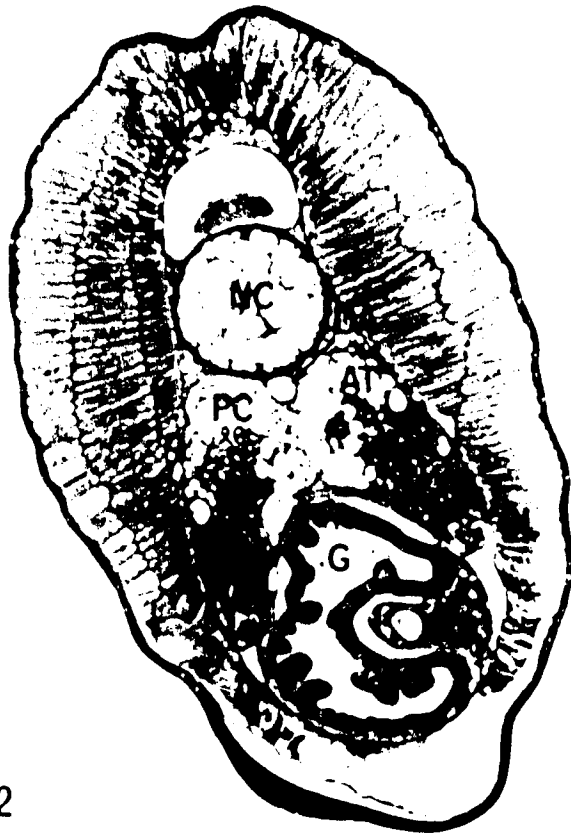
Bouin, Tissuemat, PAS-AH-OG

A 170

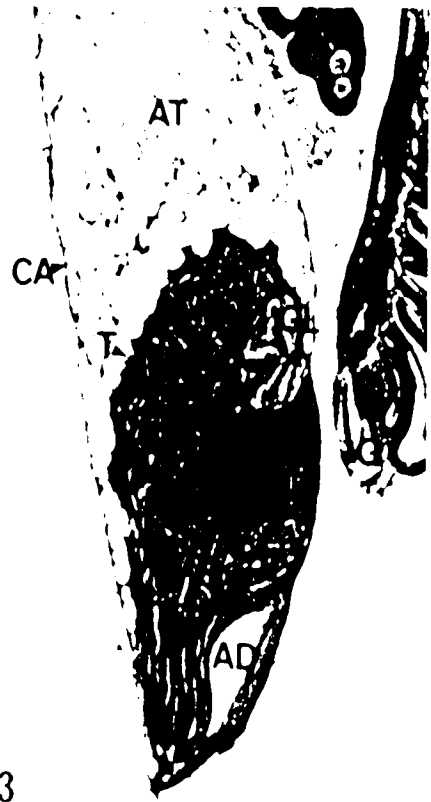
Figure 4: Light micrograph of a transverse section through the posterior region of the paired kidneys; 79-mm ammocoetes.

The archinephric duct (AD) is at the ventral tip while the glomus (GL) is in a more medial location. The remainder of the kidney is composed of loosely arranged tubules (T), between which are found blood sinusoids (S), and a dorsal mass of adipose tissue (AT). The kidney is enclosed within a capsule (CA). An efferent arteriole (arrow) drains one loop of the glomus.

Bouin, Tissuemat, PAS-AH-OC



2



3



4

Figure 5: A comparison of the kidneys from three stages in the life of the lamprey. X 9

These kidneys had been previously fixed in Bouin's fluid.

- A. A ventral view of the posterior half of the paired kidneys of a parasitic adult. Gonad (GD) lies in the midline between the kidneys and a portion of the gut (G) is represented.
- B. A ventral view of the kidneys of a newly transformed adult; (a) represents the degenerating ammocoetes kidney while a posterior portion (b) extends to the cloaca and the renal tissue is represented by a strip of tissue at the ventral tip (arrow).
- C. Lateral view of the kidneys of a 126-mm ammocoetes (a). This is to be compared in size and location with the newly transformed adult kidney (B). Note that it does not extend to the cloaca (arrow).

ANTERIOR



POSTERIOR

Figure 6: Electron micrograph of the kidney capsule; 85-mm ammocoetes.

The capsule is covered by a layer of squamous cells which often contain dense granules (DG). A basement membrane (BM) separates the epithelial cells from large bundles of collagenous fibrils (CO). A dense precipitate is seen at the apical surface (arrows).
Osmium, Epon, UA-IC

X 16,700

Figure 7: Electron micrograph showing the junction between two adjacent epithelial cells of the kidney capsule; parasitic adult.

The cytoplasm of the cells contains mitochondria (M), ribosomes (R), smooth vesicles (SV), and fibrils (FI) and the surface of the cells shows accumulations of a dense precipitate (arrows). The plasma membrane of adjacent cells are fused apically into a junctional complex (JC). Desmosomes (DS) are found at each end of large intercellular spaces (IS). A portion of a fibroblast (FB) is also seen.

Osmium, Epon, UA-LC

X 20,000

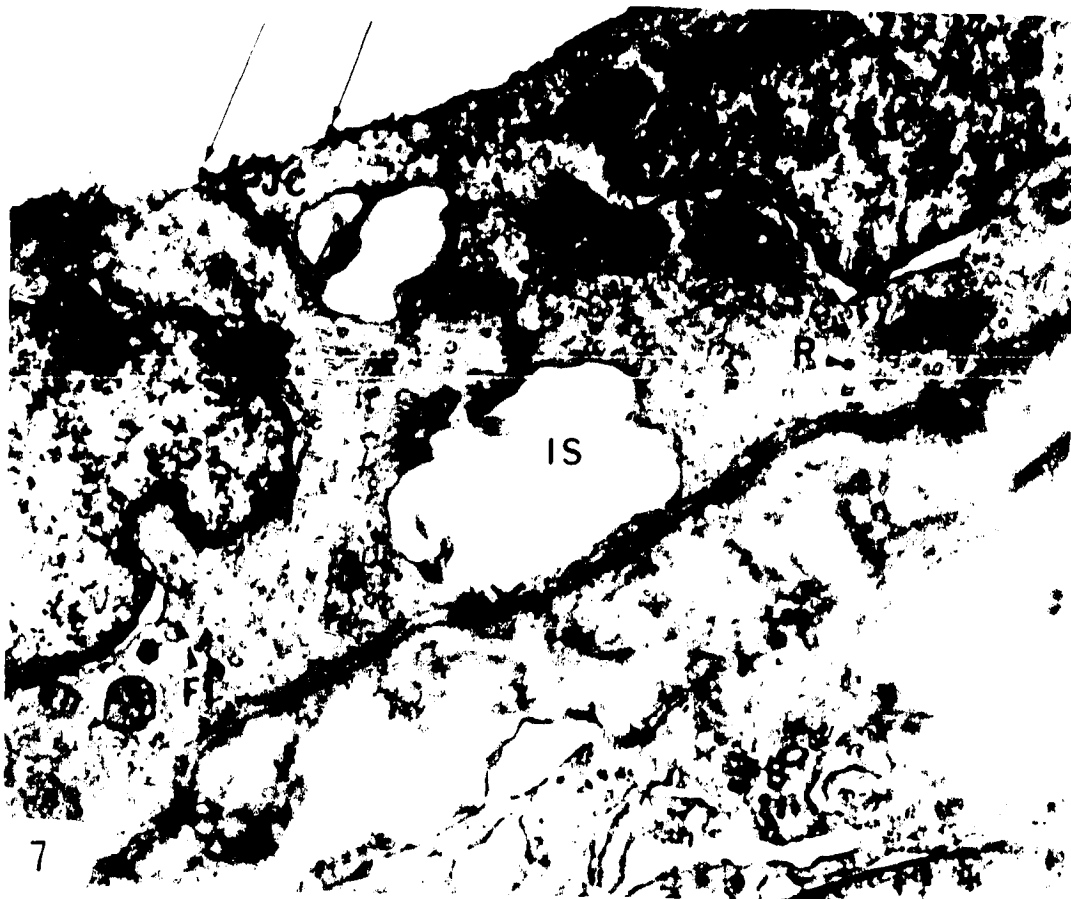
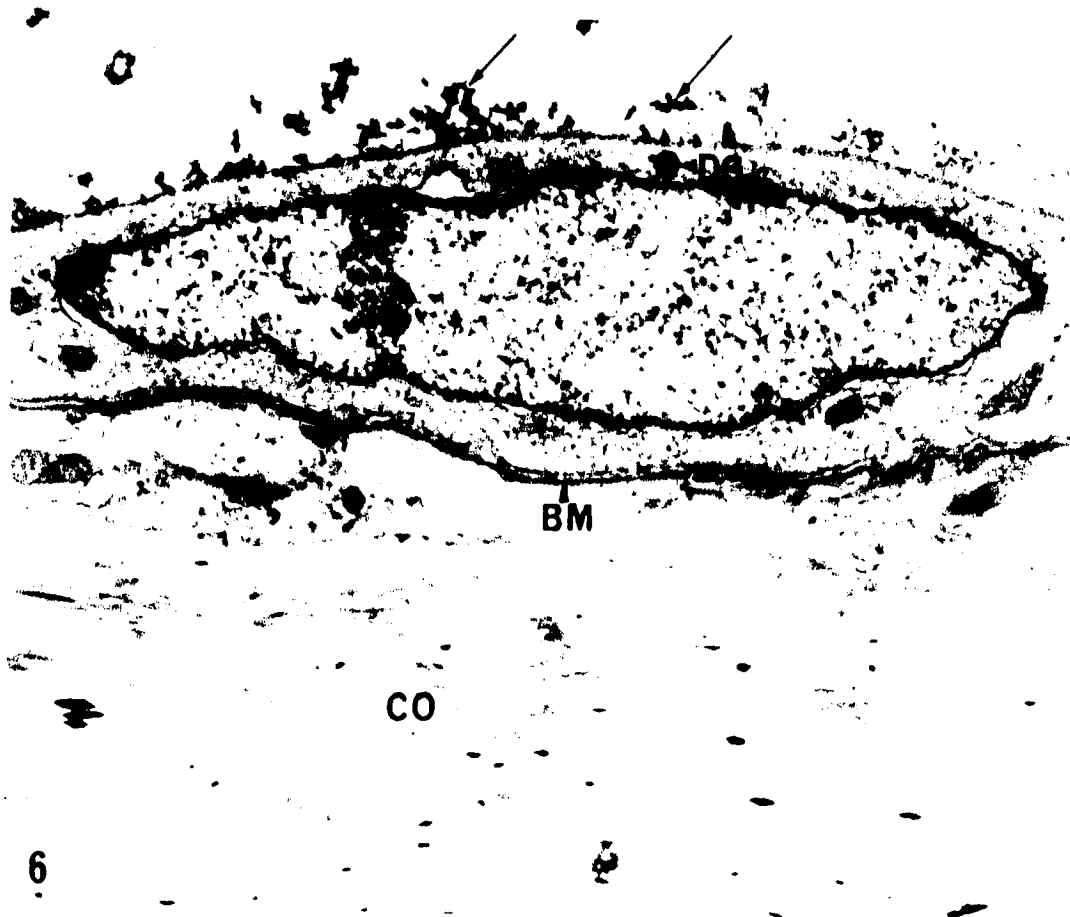


Figure 8: Light micrograph of a transverse section through the anterior portion of the kidney; 33-mm ammocoetes. The renal artery (RA) extends from the dorsal aorta (DA) to the glomus (GL). Blood from the inter-tubular area drains into a large sinus (S) connected to the posterior cardinal vein (arrow).
Bouin, Tissuemat, PAS-AH-OG

X 641

Figure 9: Light micrograph of a frontal section through the glomus; 95-mm ammocoetes. The renal artery (RA) leads into the medial artery (MA) and the medial artery branches into the afferent arterioles (AA) which penetrate into the glomus (GL).
Bouin, Tissuemat, PAS-AH-OG

X 570



Figure 10: A three-dimensional reconstruction of a portion of the kidney of a 125-mm ammocoetes showing the circulation to the glomus and tubules, and its drainage. Blood is traced from the dorsal aorta through the renal and medial arteries. Blood enters the glomus through afferent arterioles and leaves through several efferent arterioles which immediately branch into capillaries and then sinusoids. Blood from these intertubular sinusoids drains into the subcardinal sinus dorsally through a short sinus. The subcardinal sinus periodically drains into the posterior cardinal vein.

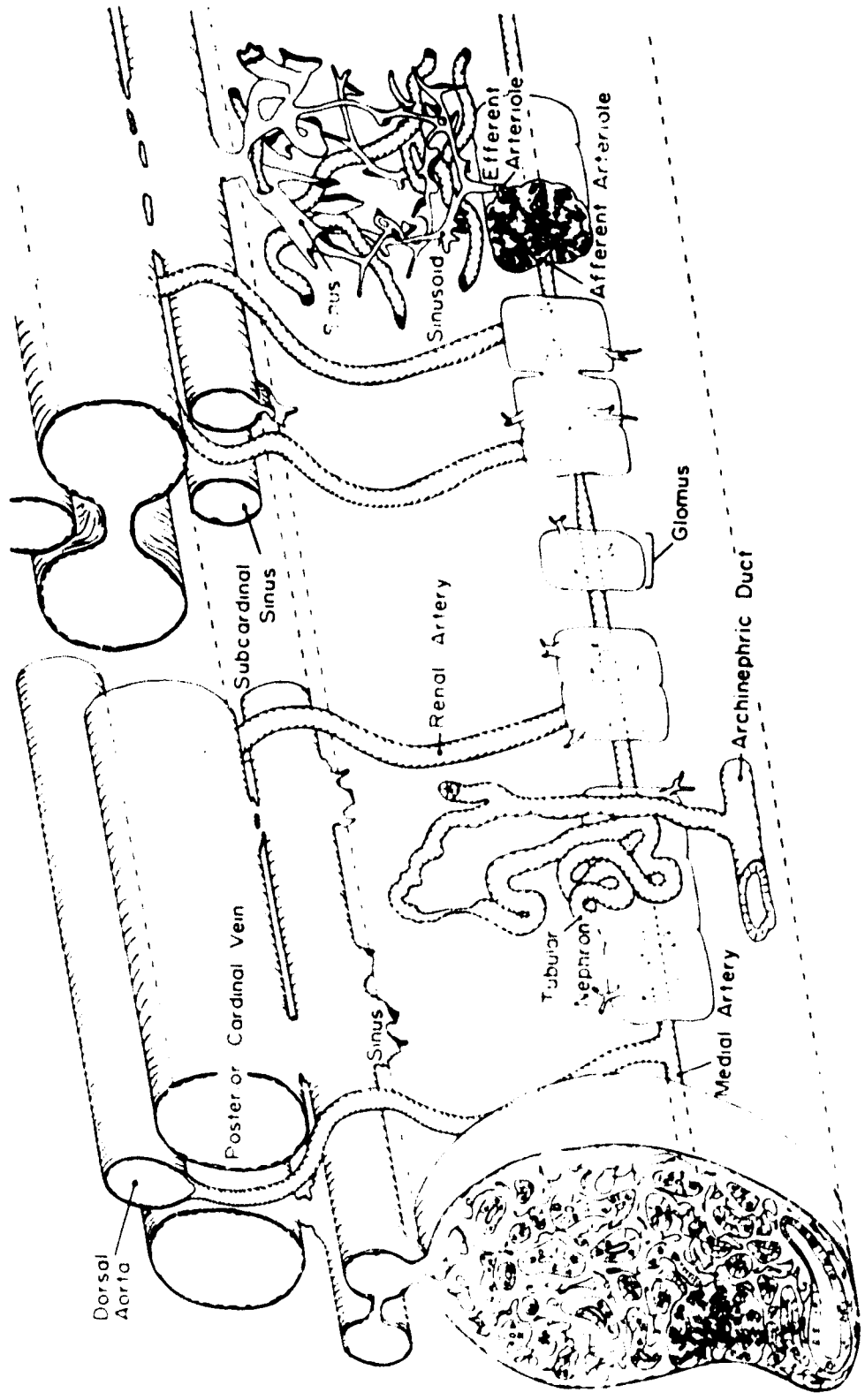


FIG. 10

- Figure 11: A three-dimensional reconstruction of a portion of the kidney of a parasitic adult showing the circulation to the glomus and tubules, and its drainage.
- A. A transverse section through the region of the kidney.
 - B. A three-dimensional view of the medial and lateral subcapsular sinuses and a portion of the glomus.
 - C. With tubules removed the circulation is traced from the dorsal aorta through renal and medial arteries into the glomus through afferent arterioles. Several efferent arterioles drain the loops of the glomus and branch into capillaries and sinusoids in the intertubular area. Blood is picked upon the large interstitial sinuses which flow into the subcapsular sinuses. Blood reaches the posterior cardinal vein through subcardinal sinuses which communicate with it and the subcapsular sinuses.

Figure 12: Light micrograph of a transverse section of the kidney;
125-~~mm~~ ~~ammocoetes~~.

This 2.0- μ section shows that the loops (L) of an individual glomerulus are surrounded by their own Bowman's capsules. Each capsule is composed of an outer squamous layer (SL) and an inner podocyte layer (PL) and the epithelium is continuous with a neck segment (NS). The large medial artery (MA) is seen. The tubules are surrounded by sinusoids lined with simple endothelial cells (arrow).

Osmium, Epon, TB

X 1,900



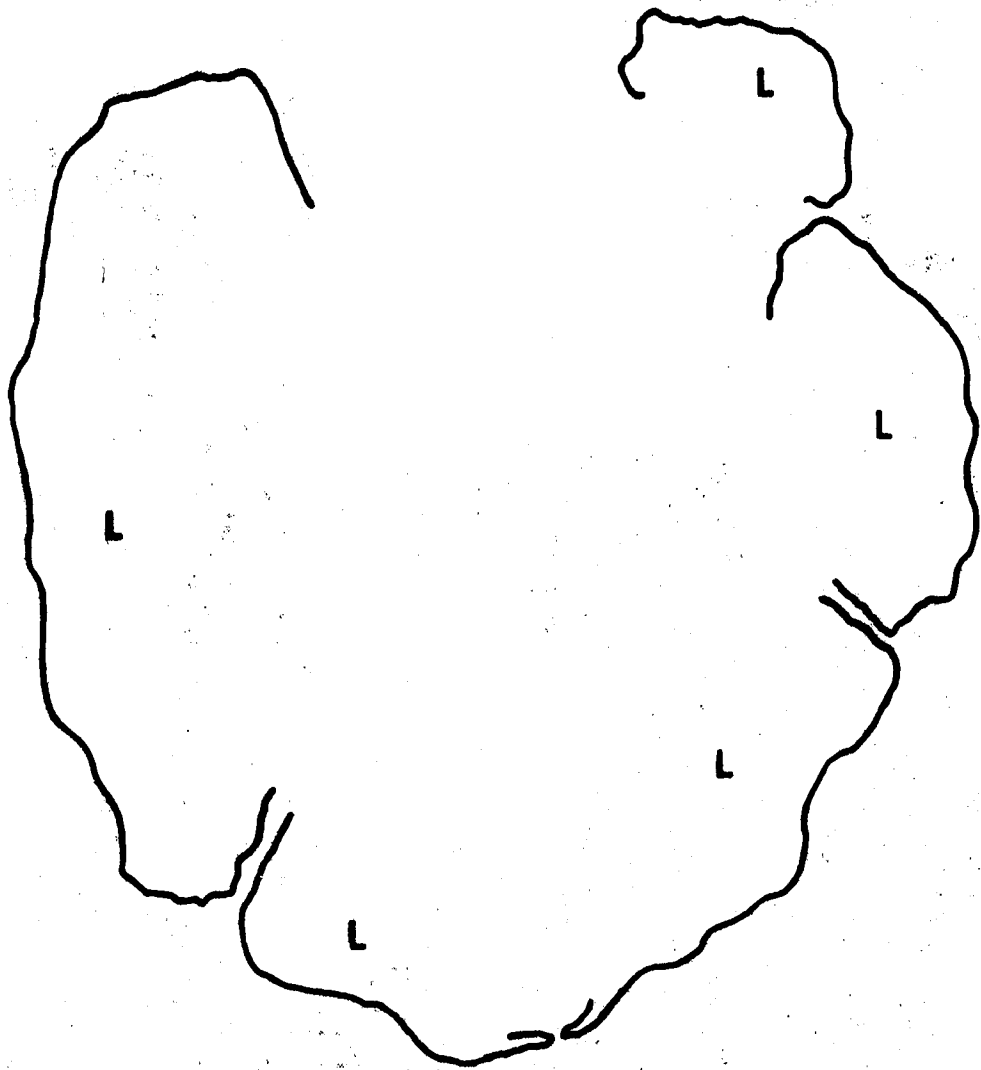


Figure 13: Light micrographs of portions of the kidney; parasitic adults.

Bouin, Tissuemat, PAS-AH-OG

A. Transverse section through the dorsal half showing the large glomus (GL) supplied by a renal artery (RA) which enters a medial artery (MA). The glomus is composed of several capillary loops which anastomose with each other. Between the loops are cavities, each drained by a tubule (T).

X 160

B. Frontal section through the dorso-medial surface of the kidney showing the long glomus which is composed of individual looped glomeruli. The loops fuse with one another and with those of other glomeruli to produce a continuous vascular cord. Two glomeruli are outlined; the upper one is divided by the medial artery.

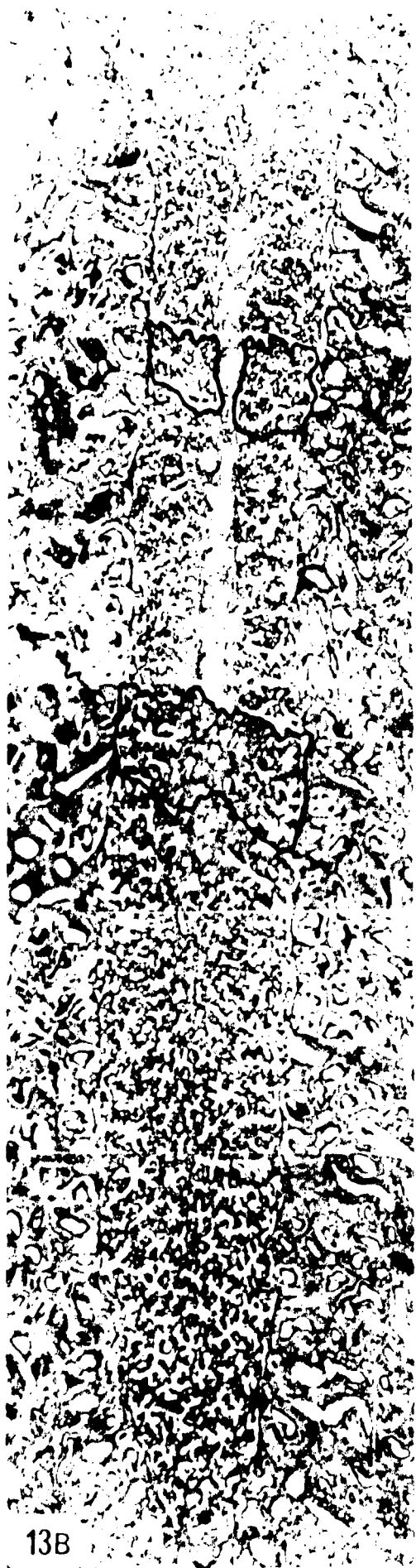
X 160

C. High magnification of a frontal section with one glomerulus outlined. The afferent arteriole (AA) branches to produce the loops.

X 420



13A



13B



13C

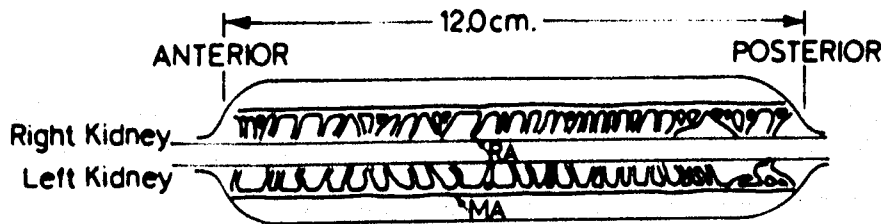
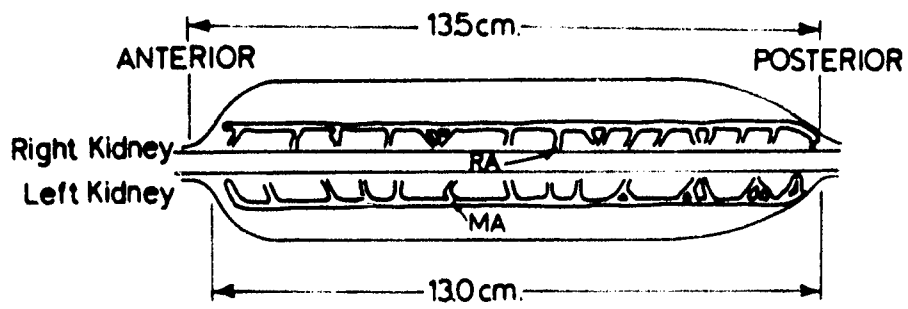
Figure 14: Reconstructions of the dorsal-lateral aspect of the kidneys of two adult male lampreys showing the variation in number and distribution of the renal arteries. Branching of the renal arteries is more frequent at the posterior end of the kidneys.

- A. Kidneys of a 52-cm adult showing 17 renal arteries (RA) supplying a medial artery (MA) on each side.
- B. Kidneys of a 51-cm adult showing 25 and 27 renal arteries (RA) supplying a medial artery (MA).

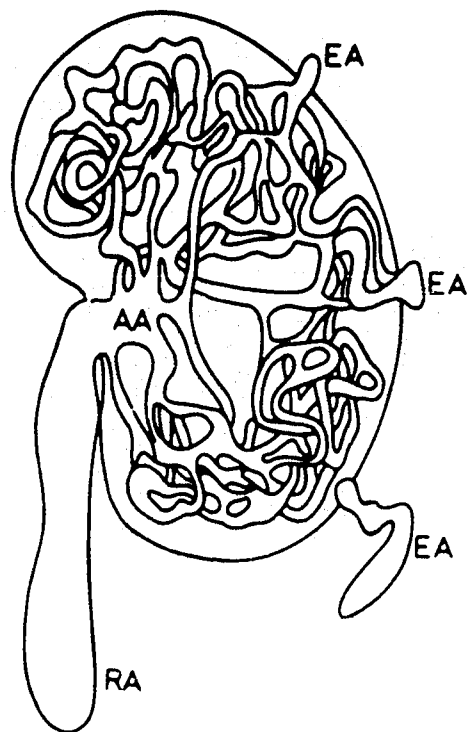
Figure 15: A three-dimensional reconstruction of a glomerulus within the glomus of a 135-mm ammocoetes. The afferent arteriole (AA) divides at the hilus into six loops consisting of anastomosing networks of capillaries; each loop is drained by its own efferent arteriole (EA).

Figure 16: Diagrams of the capsules surrounding the capillary tufts of ammocoetes and adults.

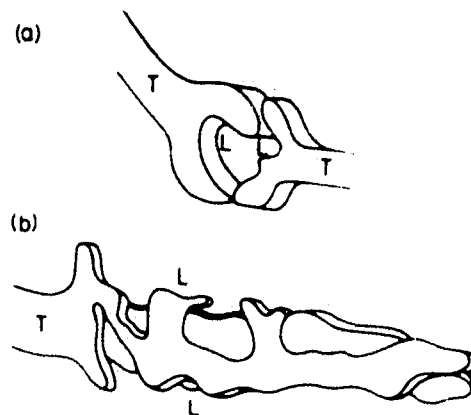
- A. In ammocoetes the loops (L) of the tuft are enveloped by Bowman's capsules which are separated from each other by connective tissue.
- B. In older ammocoetes, newly-transformed adults, and adults, the dilated end of the tubule (T) lies between the loops (L) of the tuft. Anastomoses between individual loops penetrate this capsule.



14



15



16

Figure 17: Light micrograph of a 0.5- μ section of the renal corpuscle; 40-mm ammocoetes.

The thin-walled efferent arteriole (EA) has penetrated the squamous layer (SL) of Bowman's capsule. The much larger afferent arteriole (AA) is located near the centre of the glomerus. A layer of podocytes (PL) surrounds the capillaries (CP).

Osmium, Epon, TB

X 4,100

Figure 18: Light micrograph of a 0.5- μ oblique section through the glomerus of the kidney; 40-mm ammocoetes.

Portions of three loops are found in this section. The two largest are separated by a cavity (arrow) and are enclosed within an inner podocyte layer (PL) which surrounds capillaries, and an outer squamous layer (SL). The small loop is separated from the other two by its squamous layer and that of the large loop. A blood cell in mitosis (MC) is seen in the lumen of one capillary. Phagocytes (PH) are seen in the intertubular area.

Osmium, Epon, TB

X 1,400

Figure 19: Light micrograph of a 0.5- μ longitudinal section through two Bowman's capsules of the compound renal corpuscle; 98-mm ammocoetes.

This section shows the loose connective tissue containing a capillary (CP) and collagenous fibrils (CO) which separate the two renal corpuscles. The squamous layer (SL) is continuous with the epithelium of the neck segment (NS) and the podocyte layer (PL) is closely applied to the capillaries (CP).

Osmium, Epon, TB

X 4,500

Figure 20: Light micrograph of a 0.5- μ longitudinal section of the compound renal corpuscle of a 98-mm ammocoetes.

The cells of the short squamous layer (SL) are continuous with the cells of the podocyte layer (PL) and with those of the neck segment (NS). The adjacent neck segments are separated by loose connective tissue containing a capillary (CP) and collagen (CO). The podocyte layer surrounds the capillaries (CP).

Osmium, Epon, TB

X 4,500

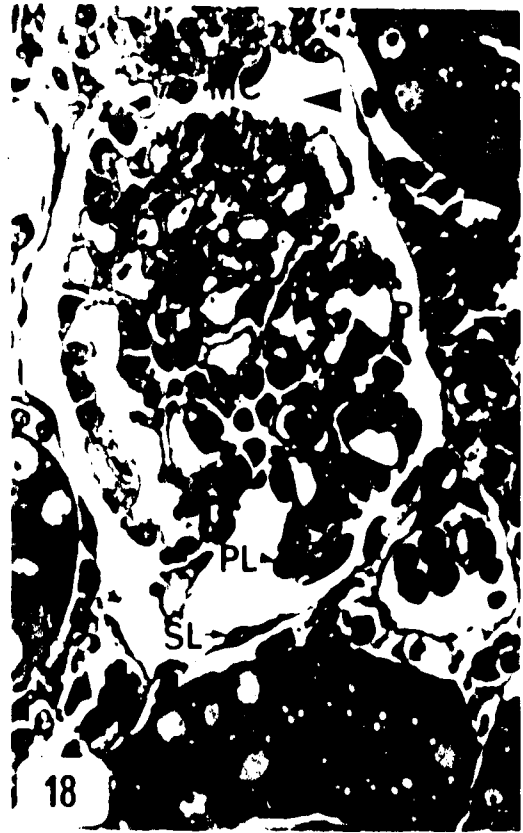
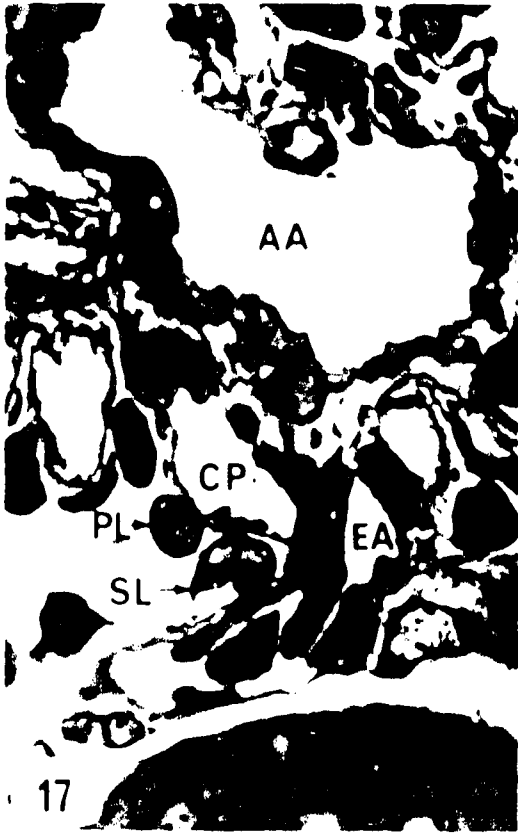
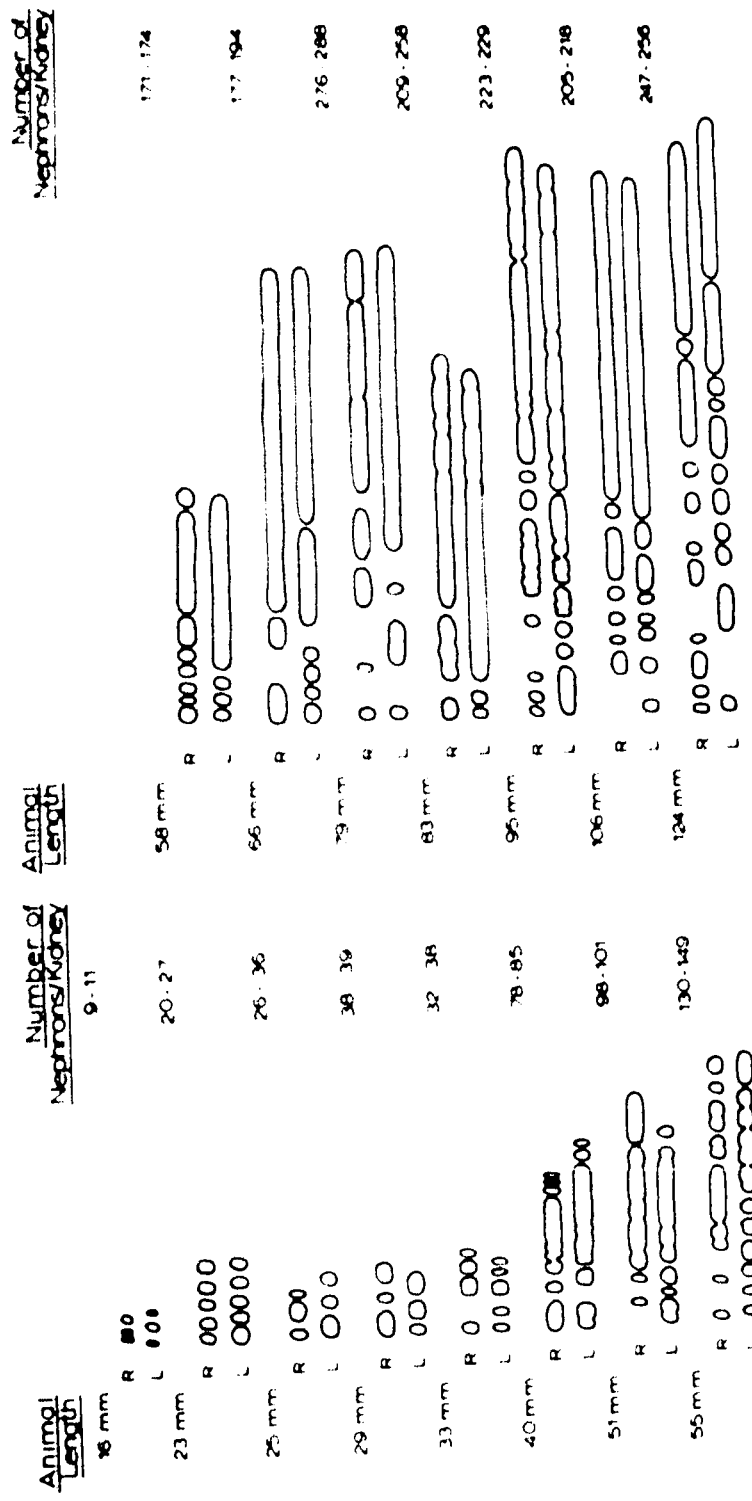


Figure 21: Diagram showing the arrangement, distribution, and size of the renal corpuscles in various stages of ammocoetes.

There is a gradual lengthening of the more posterior corpuscles and an increase in their number as the animal increases in body length. The anterior regions are at the left in each case. The total number of nephrons per kidney is greater in the larger animals.



Scale 100μm
Legend R=Right L=Left

FIG. 21

Figure 22: Light micrograph of a transverse section through the anterior tip of the kidney; parasitic adult. Degenerating glomeruli (GLR) are seen, one of which is being drained by a neck segment (NS). An artery (A) passes close by. A tubule (T) is seen to be surrounded by thick layers of connective tissue (CT).

Bouin, Tissuemat, PAS-AH-OG

X 1,070

Figure 23: Light micrograph of a transverse section through the posterior region of the kidney showing two glomera; migrating adult. The main glomus (GL) is dorsal and its medial artery (MA) sends a branch (B) to the more ventral secondary glomus (GL'). The archinephric duct (AD) is in a more medial position.

Bouin, Tissuemat, PAS-AH-OG

X 120

Figure 24: Light micrograph of a portion of the kidney; parasitic adult. A dorsal projection containing a glomus (GL') and tubules (T) is seen. The glomus is smaller than the normal glomus (GL). A medial artery (MA) is seen in the large glomus.

Bouin, Tissuemat, PAS-AH-OG

X 490

Figure 25: Light micrograph of a frontal section through the newly-formed posterior portion of the kidney; newly-transformed adult.

The long glomerulus (GL) lies beneath adipose tissue (AT).

A renal artery (RA) sends branches anteriorly and posteriorly forming a medial artery (MA).

Bouin, Tissuemat, PAS-AH-OG



Figure 26: Electron micrograph of the central region of the renal corpuscle; parasitic adult.

Podocytes (PL) surround capillaries (CP) and contain a highly indented nucleus (N) with a prominent nucleolus (n). The podocytes have numerous cytoplasmic projections (CY) which rest on a basement membrane (BM). Bundles of fibrils (FI) are often located near the nucleus. Dense granules (DG) are common.

Osmium, Epon, UA-LC

X 6,500



Figure 27: Electron micrograph of a portion of the renal corpuscle showing the three regions of the dilated end of the tubule; newly-transformed adult.

The short squamous layer (SL) rests on a basement membrane (BM) which is continuous with that of the cells of the neck segment (NS) and the podocyte layer (PL). A transition from the tall ciliated cells of the neck segment to the flattened squamous cells and eventually to the podocytes with their cytoplasmic processes (CY) can be seen. An efferent arteriole with endothelial cells (END) lining the lumen and overlying smooth muscle cells (SM) is also seen.

Osmium, Epon, UA-LC

X 8,400



Figure 28: Electron micrograph of a portion of a renal corpuscle; parasitic adult.

The invaginating squamous layers (SL) rest on their own basement membranes (BM). The two layers are separated by loose connective tissue containing collagenous fibrils (CO) and cytoplasmic projections of mesangial cells (CY). There is a gradual progression from the ovoid podocytes (CL) with numerous cytoplasmic projections to spherical podocytes (CU) to squamous cells. The cuboidal cells are connected by tight junctions (arrow) but the columnar cells are separate. Foot processes of the podocytes (P) lie along the basement membrane.

Osmium, Epon, UA-LC

X 4,500

Figure 29: Electron micrograph of part of a squamous cell from the renal corpuscle; newly-transformed adult.

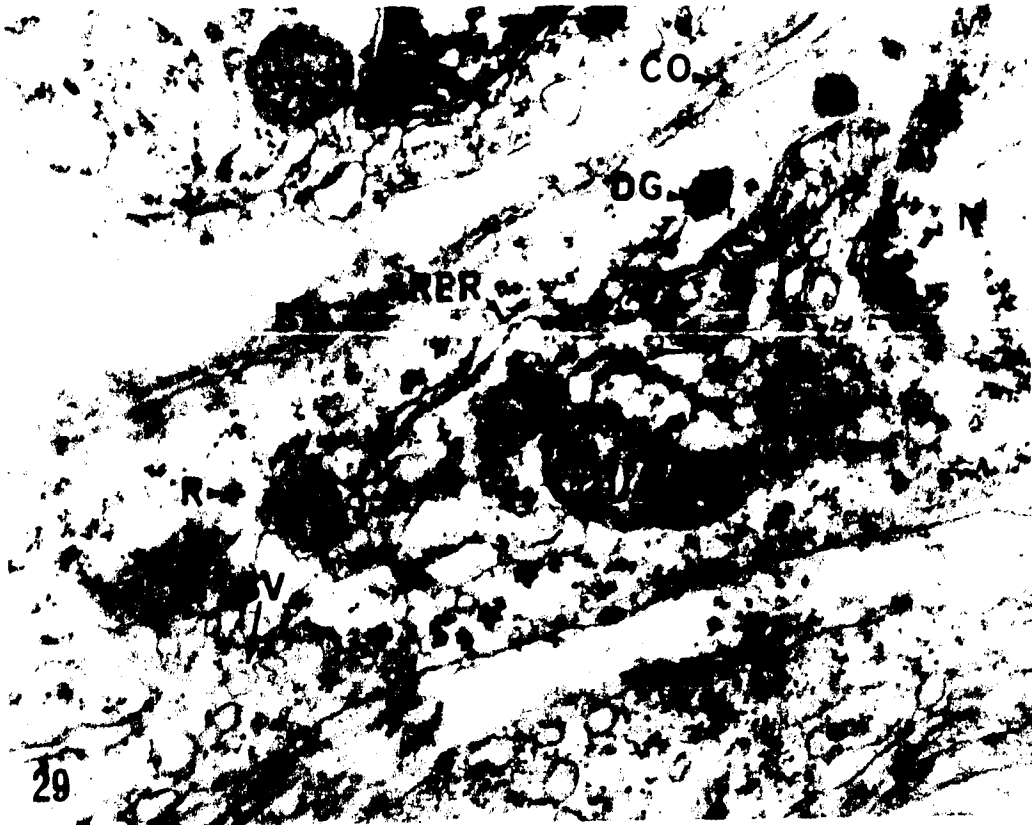
The nucleus (N), a few scattered irregular mitochondria (M), strands of rough ER (RER), and scattered free ribosomes (R) are seen. The remainder of the cytoplasm is taken up by a few dense granules (DG) and tiny smooth vesicles (SV). This micrograph was taken near the point of exit of an efferent arteriole and its accompanying connective tissue so that collagen fibrils (CO) can be seen near the basement membrane (BM).

Osmium, Epon, UA-LC

X 28,900



28



29

Figure 30: Electron micrograph of a podocyte from the renal corpuscle; parasitic adult.

This cell probably contains a single bilobed nucleus (N) whose lobes appear separate in this section. The cytoplasm contains many free ribosomes (R), fine fibrils (FI), scattered mitochondria (M), smooth vesicles (SV), dense granules (DG), and a few strands of rough ER (RER). A multivesicular body (MVB) is seen above the nucleus. The nuclear envelope is interrupted by nuclear pores (arrow) and chromatin (CH) is located in clumps at the periphery of the nucleus.

Osmium, Epon, UA-LC

X 11,900

Figure 31: Electron micrograph of the renal corpuscle; newly-transformed adult.

Two podocytes rest on two capillaries (CP) and are separated from the endothelium by a basement membrane (BM). The podocytes have a large nucleus (N) and often show a nucleolus (n). A Golgi apparatus (GA), when present, is usually located at the opposite pole from the endothelium and consists of concentrically-arranged, swollen saccules (S) and numerous microvesicles (MS). Throughout the remainder of the cytoplasm are found flattened rough ER (RER), mitochondria (M) and smooth vesicles (SV).

Osmium, Epon, UA-LC

X 12,700



Figure 32: Electron micrograph of a portion of a podocyte; newly-transformed adult.

Abundant in the cytoplasm are free ribosomes (R) and numerous interweaving fibrils 70-80 Å in diameter (FI). The pedicels of the cell (P) line the basement membrane (BM). Individual pedicels are often connected by a thin diaphragm (arrow) and are coated with a fuzzy material (FZ).

Osmium, Epon, UA-LC

X 45,000

Figure 33: Electron micrograph of a podocyte; parasitic adult.

Many branching cytoplasmic processes (CY) end as pedicels (P) on the basement membrane (BM). These cytoplasmic projections often contain mitochondria (M) and dense granules (DG). This cell covers a portion of the endothelial surfaces of two capillaries (CP). A mesangial cell (MS) is also seen in this section.

Osmium, Epon, UA-LC

X 5,800

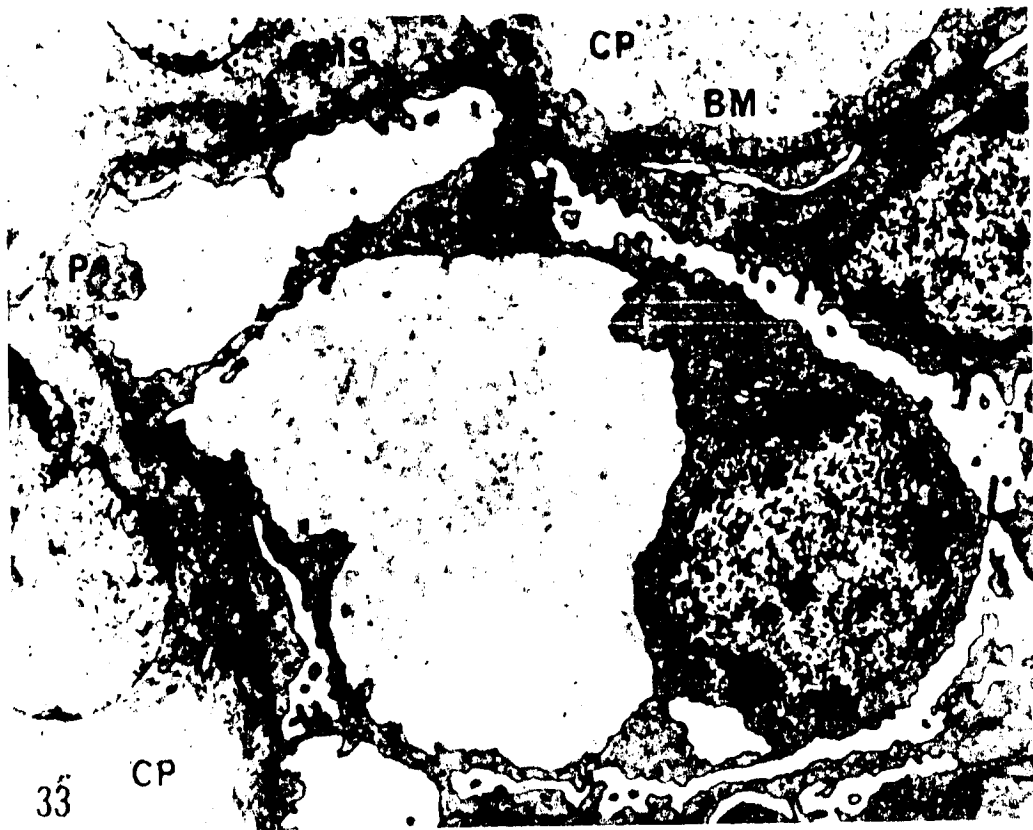


Figure 34: Electron micrograph through the afferent arteriole of the renal corpuscle; parasitic adult.

The lumen contains numerous red blood cells (RBC) and is lined by flattened endothelial cells (END). Beneath the endothelium are three to four layers of smooth muscle (SM) with large amounts of collagen (CO) between the layers. The arteriole is separated from the podocyte layer (PL) by a basement membrane (BM).

Osmium, Epon UA-LC

X 4,500

Figure 35: Electron micrograph showing the relationship between the endothelium and the podocyte layer in the renal corpuscle; parasitic adult.

The cytoplasm of the endothelial cell is composed of thin strands of rough ER (RER), dense granules (DG), smooth vesicles (SV), and free ribosomes (R). The Golgi apparatus consists of flattened saccules which often appear swollen at the ends (arrows). The cell is limited at the base by a plasma membrane (PM) beneath which is found the lamina rara interna (LRI) containing fine fibrillar material and collagen fibrils (CO). A lamina densa (LD) is located between the lamina rara interna and the lamina rara externa (LRE). The three layers constitute the basement membrane.

Osmium, Epon, UA-LC

X 36,600



Figure 36: Electron micrograph showing the different cell types in the renal corpuscle; parasitic adult. Cells of the podocyte layer (PL), mesangium, and the endothelium (END) are closely related. Between the thin endothelial cells and the podocytes are cytoplasmic processes (CY) of mesangial cells and the basement membrane (BM). The endothelium contains numerous smooth vesicles (SV). Fenestrations (arrow) are seldom seen.

Osmium, Epon, UA-LC

X 38,100

Figure 37: Electron micrograph showing the endothelium in the renal capsule; parasitic adult. Cytoplasmic extensions (arrows) of the base of the endothelium are a common feature. Note also the invagination (I) of the base of the endothelium. Adjacent cells are fused by junctional complexes (JC).

Osmium, Epon, UA-LC

X 23,400

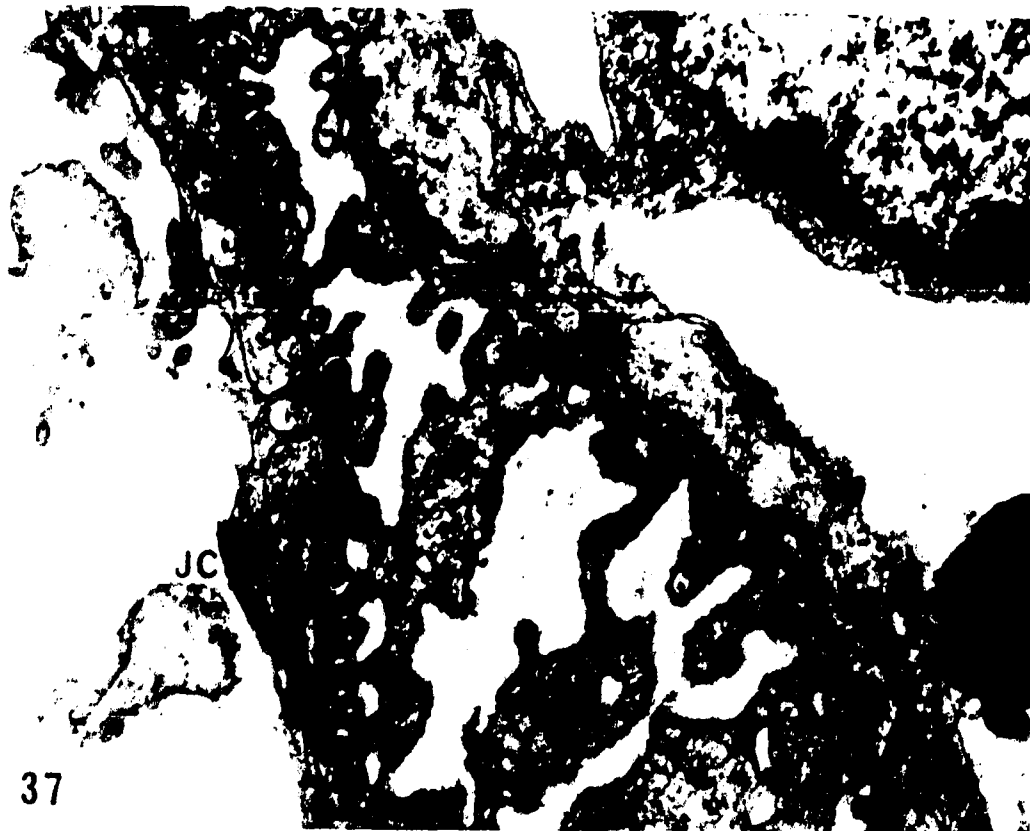


Figure 38: Electron micrograph showing a capillary in the renal corpuscle; migrating adult.

The lumen of a capillary is filled with cellular debris consisting of dense granules of various electron densities (DG), swollen mitochondria (M), dense chromatin-like material (CH), and possible remnants of a nuclear envelope (NE). Mesangial cells (MS) separate the endothelium (END) from the basement membrane (BM) and podocytes (PL).

Osmium, Epon, UA-LC

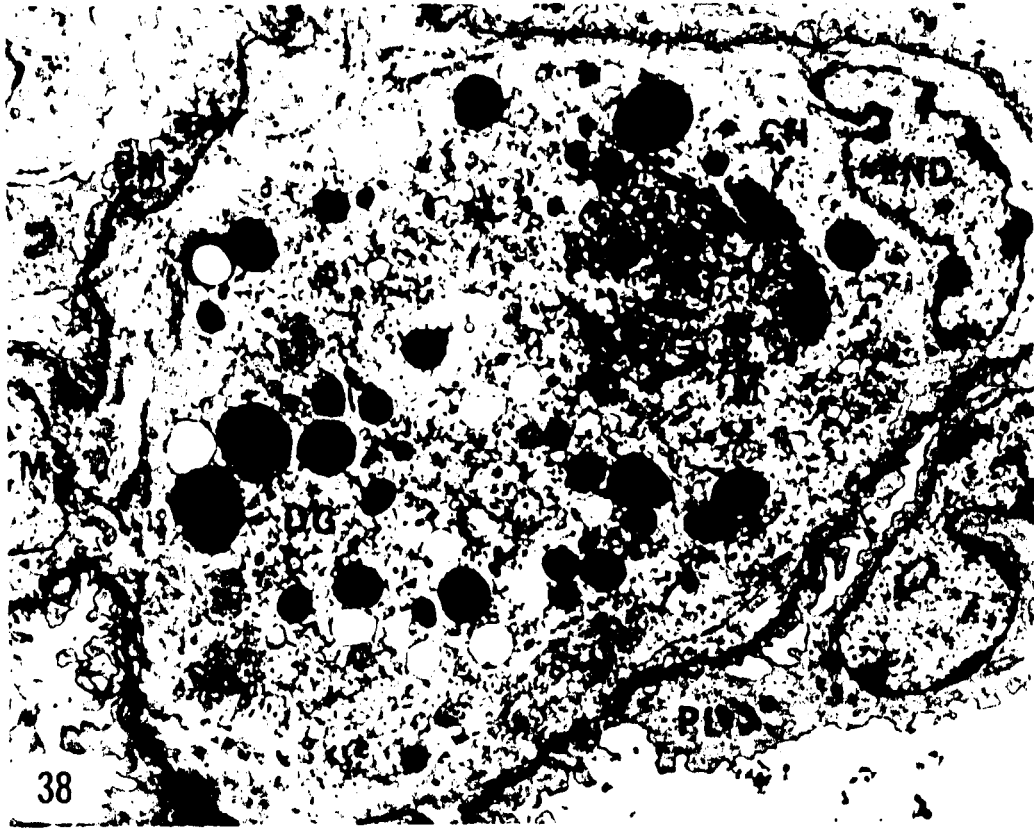
X 5,000

Figure 39: Electron micrograph of the renal corpuscle showing several mesangial cells in the intercapillary area; parasitic adult.

The mesangial cells (MS) have a lobed nucleus (N) and many branching cytoplasmic processes (CY). The cytoplasm consists of a Golgi apparatus (GA), a few mitochondria (M), clumps of free ribosomes (R), and areas of a matrix of medium electron density (arrows).

Osmium, Epon, UA-LC

X 5,000






Figure 40: A comparison of the tubular nephron of the ammocoetes (A) and adult (B).

The location of the various segments in these diagrams of cross sections of the kidney is related to the position of the glomus.

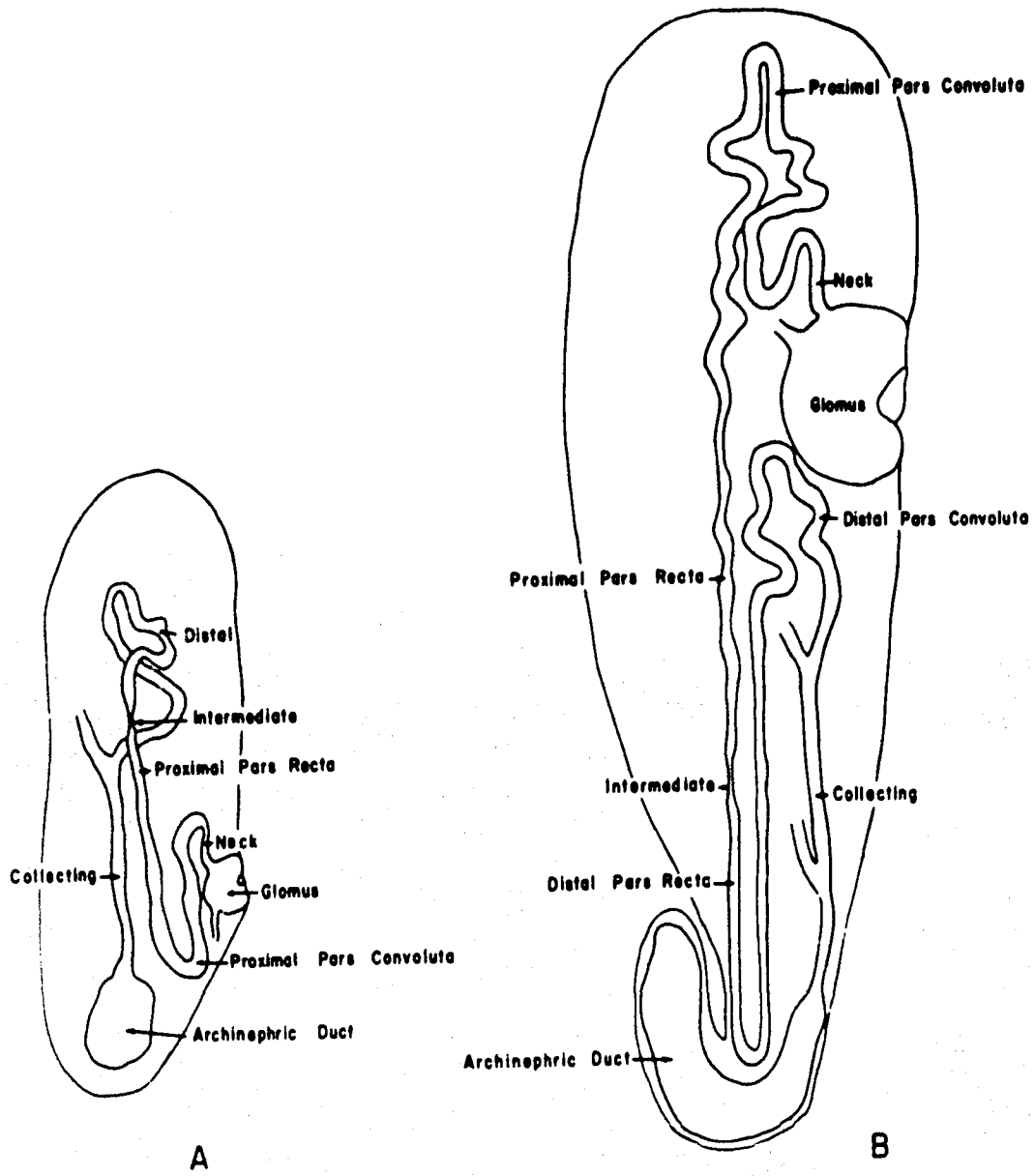


FIG. 40

Figure 41: Light micrographs of neck segments.

- A. Posterior region of the kidney; 29-mm ammocoetes.
A neck segment (NS) drains the cavity of the glomus (GL). Its epithelium is continuous with the squamous layer (SL) of Bowman's capsule and the cells of the proximal pars convoluta (PC). The neck cells are PAS+.

Bouin, Tissuemat, PAS-AH-OG

X 1,400

- B. Two confluent neck segments (NS) drain the cavities of two separate loops of a glomus; 55-mm ammocoetes.

Bouin, Tissuemat, PAS-AH-OG

X 1,200

- C. Junction of the squamous layer (SL) and the neck segment (NS); parasitic adult.

Note the PAS + brush border (BB) in the cells of the pars convoluta.

Bouin, Tissuemat, PAS-AH-OG

X 2,700

- D. This 0.5- μ section shows a neck segment consisting of ciliated columnar epithelium and surrounded by thin walled sinusoids (S); 98-mm ammocoetes.

Osmium, Epon, TB

X 4,200

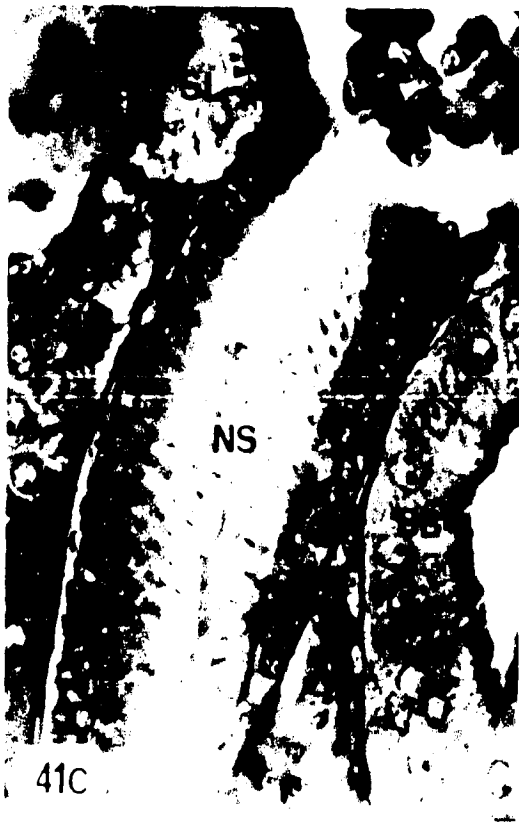
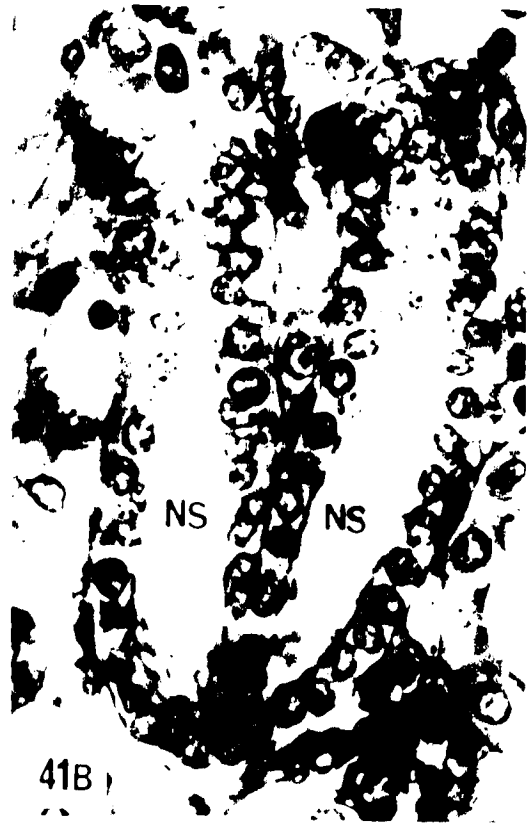
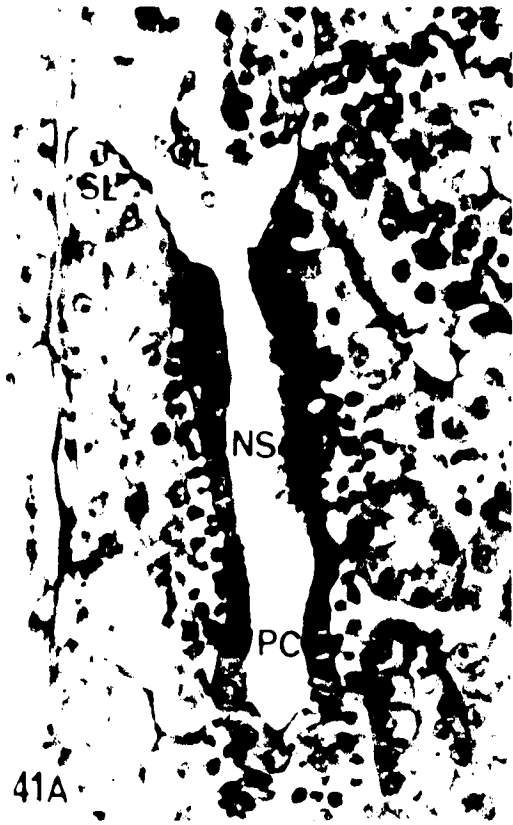


Figure 42: Electron micrograph of a longitudinal section of a ciliated neck segment; newly-transformed adult.

A basement membrane (BM) separates the epithelium from the capillaries (CP), sinusoids (S), and blood cells (BC) free in the intertubular area.

Osmium, Epon, UA-LC

X 7,000



Figure 43: Electron micrograph of a longitudinal section of a ciliated neck segment near the renal corpuscle; newly-transformed adult.

The cells of the neck segment rest on a basement membrane (BM) which is continuous with that of the squamous layer (SL). The neck cells contain a large nucleus with a prominent nucleolus (n). Large mitochondria (M) are seen above and below the nucleus but seldom at the sides. A Golgi apparatus (GA) is usually located above and to one side of the nucleus. Microvilli (arrow) and cilia (CL) occur in separate clusters on these cells.

Osmium, Epon, UA-LC

X 9,500

Figure 44: Electron micrograph of the base of two ciliated neck cells; 62-mm ammocoetes.

The cells are limited laterally by an interdigitating plasma membrane (PM). A basement membrane (BM) is seen beneath the basal plasma membrane. The cytoplasm of the cells contains large elongate mitochondria with transverse cristae (CR). The remainder of the cytoplasm is composed of smooth vesicles (SV), free ribosomes (R), and rough ER (RER). Nuclei are limited by a porous double-layered envelope (NE).

Osmium, Epon, UA-LC

X 36,700

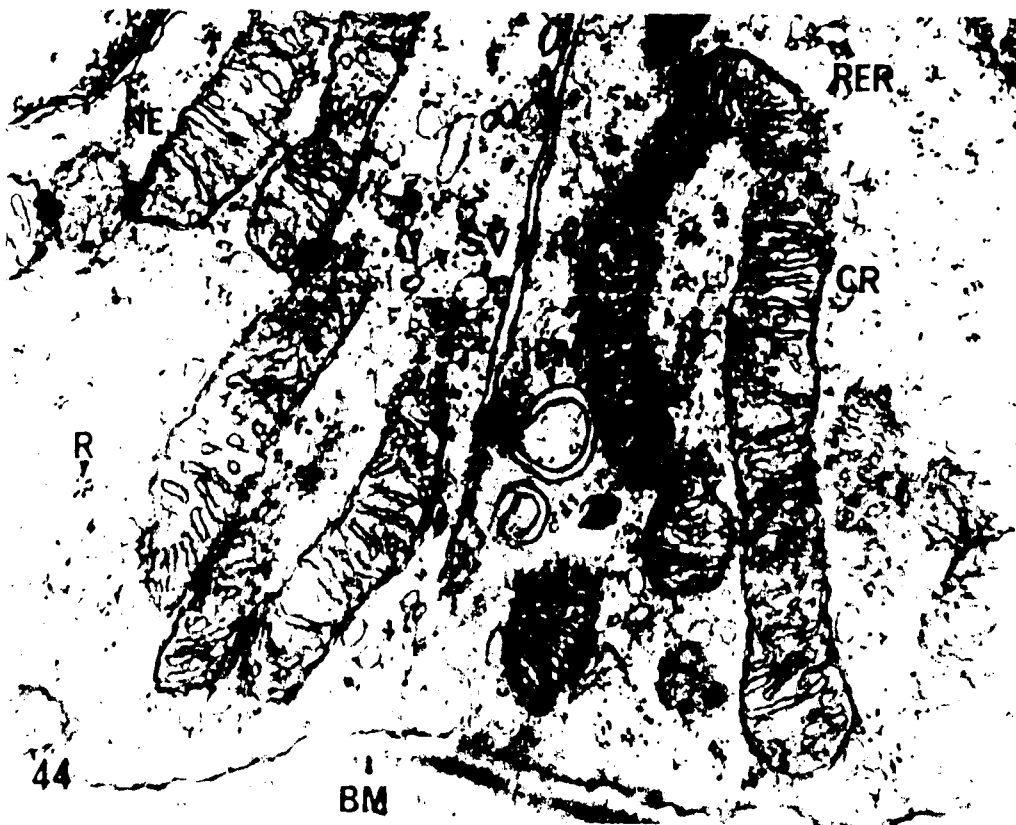
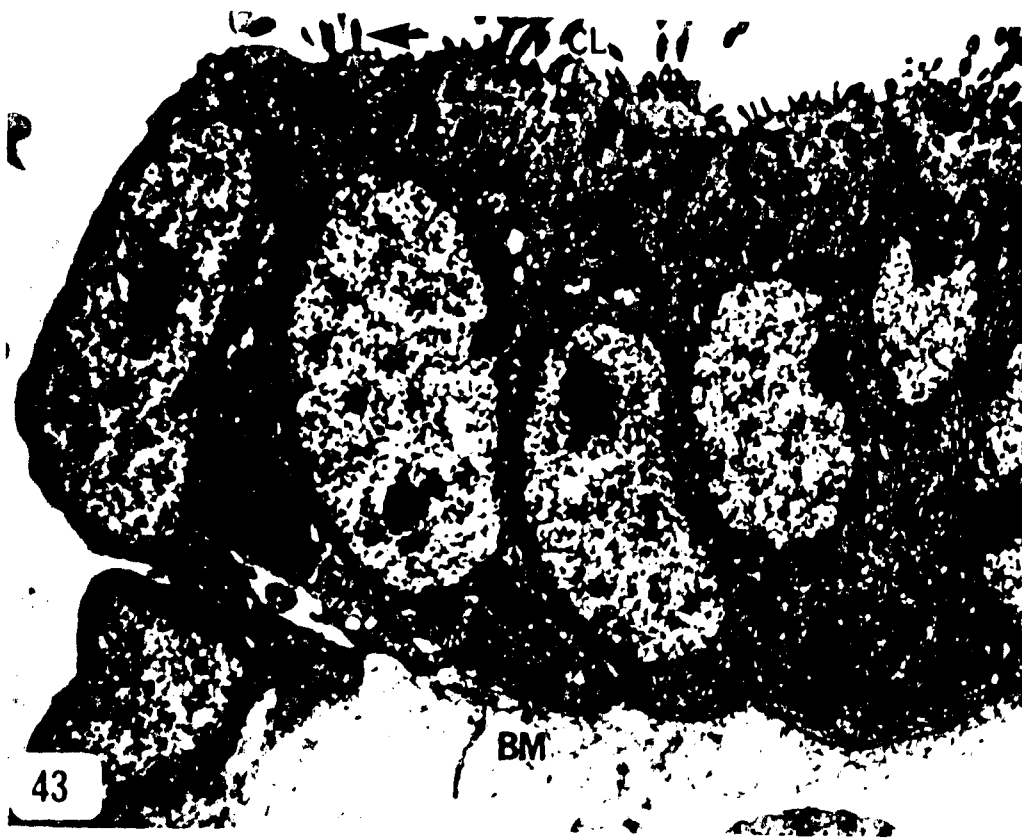


Figure 45: Electron micrograph of three adjacent neck cells;
85-mm ammocoetes.

Intercellular spaces (IS) are present between the cells
and a light and a dark cell possess a Golgi apparatus
(GA) and glycogen (GLY).

Glutaraldehyde—Osmium, Epon, UA-LC

X 16,700

Figure 46: Electron micrograph of cells of the neck segment;
60-mm ammocoetes.

Longitudinal sections of cilia show the hollow basal
body (BA) and rootlets (RT). Intercellular spaces (IS)
have desmosomes (DS) at each end and contain cytoplasmic
projections (CY) which resemble the microvilli (MV).

Dense granules (DG) and multivesicular bodies (MVB) can
be seen in the cytoplasm. Cells are fused apically by
a junctional complex (JC).

Osmium, Epon, UA-LC

X 16,700

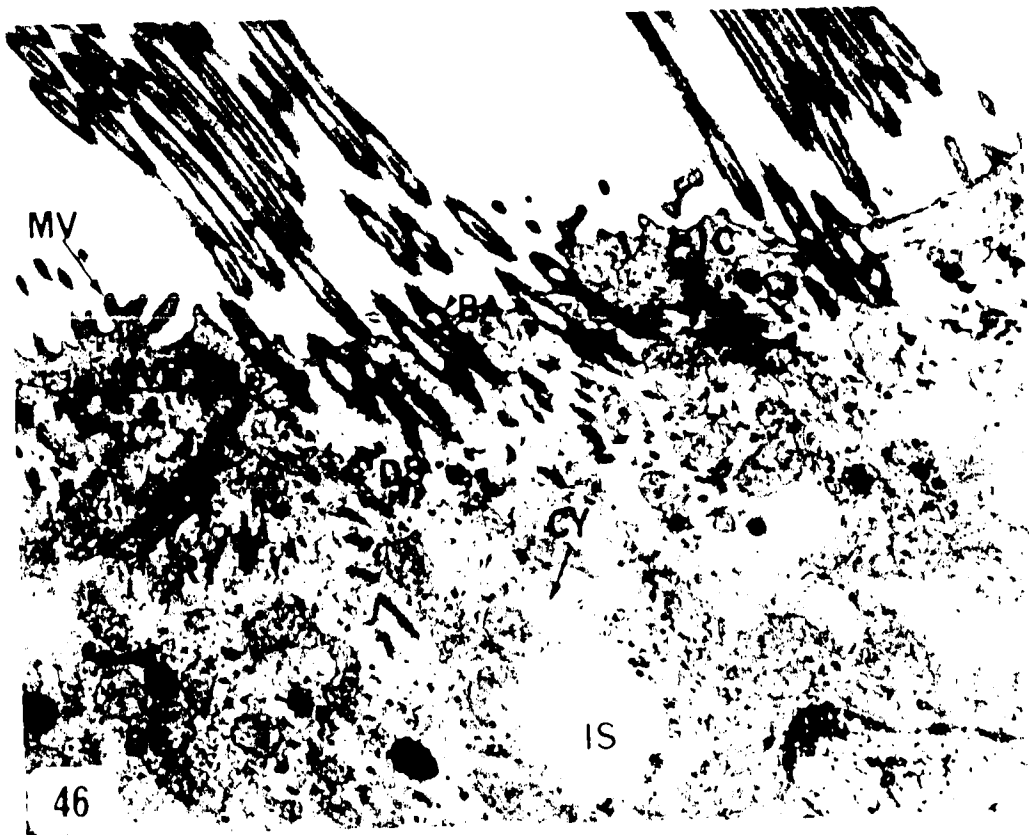


Figure 47: Electron micrograph of longitudinal sections of cilia from neck cells; newly-transformed adult.

The deep root of each cilium consists of an enlarged basal body (BA) subtended by the fibrous basal foot (BF) which branches into rootlets (RT). Above the surface of the cell the shaft of the cilium is enclosed within the plasma membrane (PM) and contains a transverse basal plate (BP) at the same level in each cilium.

Above the plate two longitudinal central filaments (CF) are surrounded by a small amount of cytoplasm containing vesicles (arrows) and a peripheral ring of longitudinal filaments. Vesicles (SV) were also found in the apical cytoplasm.

Osmium, Epon, UA-LC

X 45,000

Figure 48: Electron micrograph of transverse section of the basal bodies of several cilia from neck cells; 60-min ammocoetes.

The basal body consists of a peripheral ring of nine triplets (arrows) and has a hollow centre. Transverse sections through the basal feet (BF) show an electron-dense fibrous material and their fibrous extensions, the rootlets (RT).

Osmium, Epon, UA-LC

X 75,000

Figure 49: Electron micrograph of transverse section of cilia from neck cells; 95-mm ammocoetes.

Most cilia are sectioned in the middle of the shaft (e.g. A, B, C) revealing a peripheral ring of nine doublet filaments surrounding a central pair. A few cilia are sectioned near the tip (e.g. D, E) showing a peripheral ring of nine singlet filaments surrounding the central pair.

Osmium, Epon, UA-LC

X 40,800

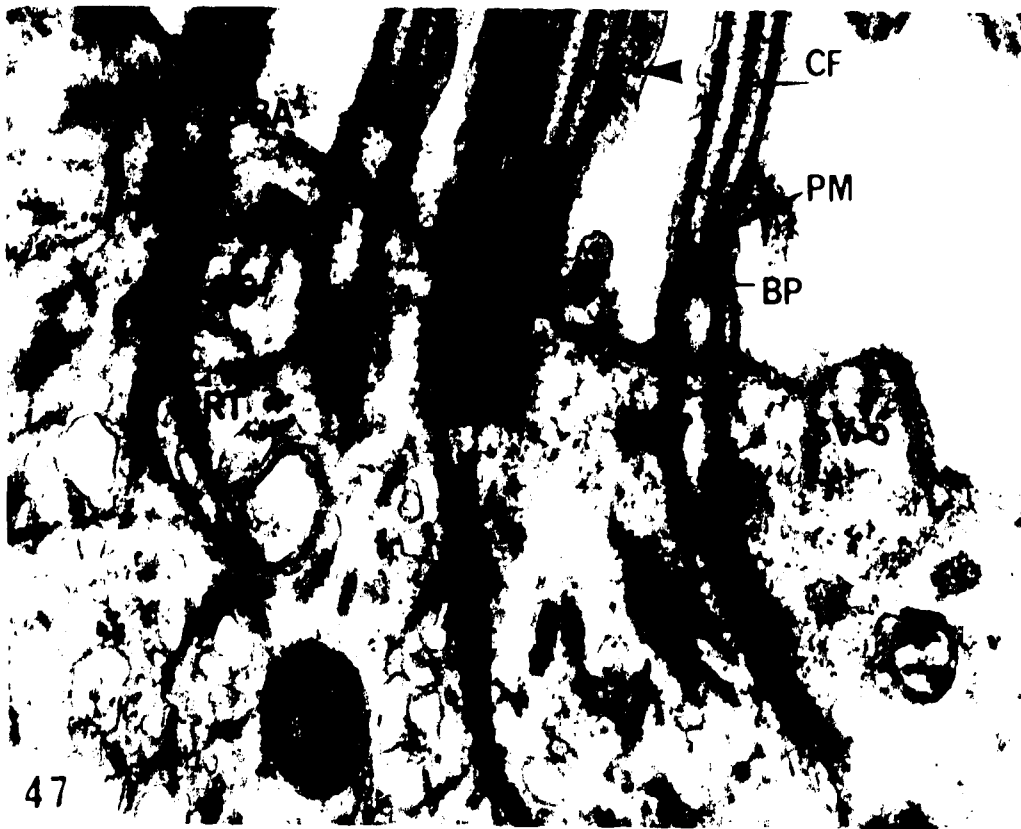


Figure 50: Electron micrograph of the base of several ciliated neck cells showing light (LC) and dark cells (DC); 85-mm ammocoetes.

The nucleus (N) and cytoplasmic matrix are more electron-dense in the dark cell which contains more glycogen (GLY).
Glutaraldehyde-Osmium, Epon, UA-LC

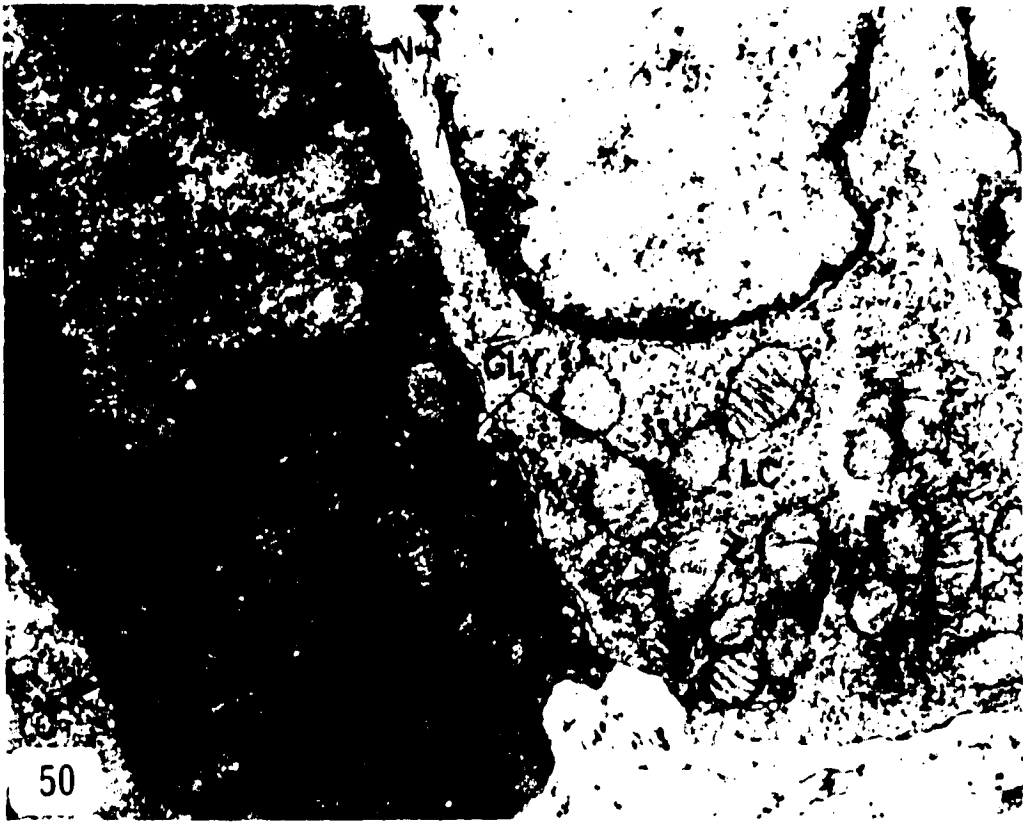
X 21,800

Figure 51: Electron micrograph showing the neck (NS) and proximal pars convoluta (PC); newly-transformed adult.

The cells of the neck segment are the more electron dense. Cilia give way to the brush border of the proximal cells. A dark cell with a brush border (DBB) is adjacent to a light cell with a brush border (LBB) marking the end of the transition from neck to proximal cells.

Osmium, Epon, UA-LC

X 5,700



Figures 52 and 53: Light micrographs of the proximal pars convoluta;
98-mm ammocoetes.

Osmium, Epon, TB

52: The tubules are surrounded by thin-walled sinusoids (S) and are composed of pyramidal cells with brush borders (BB) and basal nuclei (N). Large dense granules (DG) are seen in the cytoplasm.

X 3,500

53: Large dense granules (DG) are often found in bulbous protrusions (BT) from the apices of the cells.

X 3,300

Figure 54: Electron micrograph of cells of the proximal pars convoluta: 46-mm ammocoetes.

Numerous microvilli (MV) cover the apical surface. Cells are limited laterally by interdigitating plasma membranes (PM) and basally by a plasma membrane associated with numerous smooth vesicles (SV). The basal nucleus contains a conspicuous nucleolus (n). The apical cytoplasm contains a few clear vacuoles (CV), rod-shaped mitochondria (M), and multivesicular bodies (MVB). The Golgi apparatus (GA) and strands of rough ER (RER) are at the side of the nucleus. A basement membrane (BM) separates the cell from a sinusoid (S).

Osmium, Epon, UA-LC

X 9,000

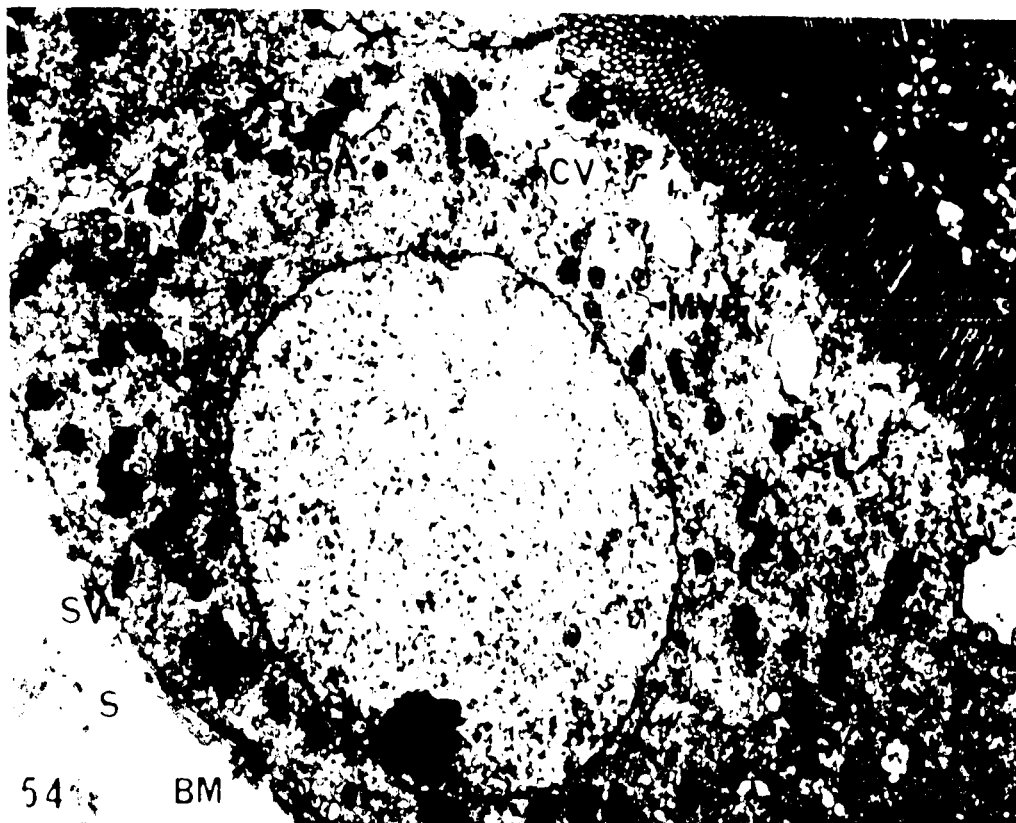
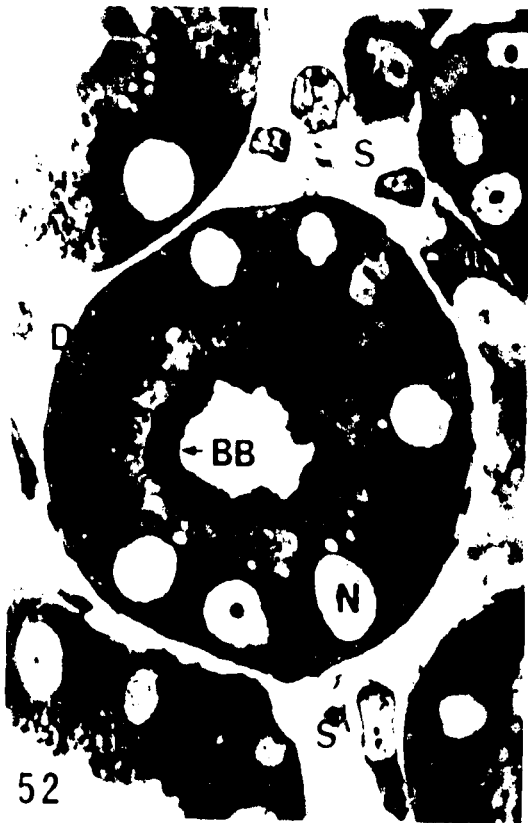


Figure 55: Electron micrograph of cells from the proximal pars convoluta; parasitic adult.

Columnar cells have central to basal nuclei with conspicuous nucleoli (n). Microvilli (MV) cover their apices. Interdigitating adjacent plasma membranes (PM) are fused apically by junctional complexes (JC) and laterally by desmosomes (DS). The cell rests on a basement membrane (BM). The cytoplasm contains irregular mitochondria (M) throughout, a Golgi apparatus (GA) and numerous dense granules (DG) above the nucleus, and parallel strands of rough ER (RER) below.

Osmium, Epon, UA-LC

X 5,800

Figure 56: Electron micrograph of a portion of a cell from the proximal pars convoluta; newly-transformed adult.

The outer layer of the nuclear membrane is studded with ribosomes (R). Clumps of chromatin (CH) are seen. The Golgi apparatus consists of flattened saccules (SA), microvesicles (MS), and a few clear vacuoles (CV). Dense granules (DG), rough ER (RER), and mitochondria (M) are also seen.

Osmium, Epon, UA-LC

X 38,000



Figure 57: Electron micrograph of the base of a cell from the proximal pars convoluta; 40- μ m ammocoetes. The basal plasma membrane (PM) has periodic accumulations of dense material on its inner surface (arrows) and parallel fibrils are seen above it (FI). The nuclear envelope is interrupted by pores (NP). A large clear vacuole contains small vesicles (SV). Ribosomes (R) and a rare flocculent body (FB) are seen.

Osmium, Epon, UA-LC

X 27,200

Figure 58: Electron micrograph of cross sections of microvilli from a section cut parallel to the apical surface of a cell from proximal pars convoluta; 74- μ m ammocoetes. Arrows indicate points of fusion of microvilli. Each microvillus has a central filamentous core (FC), a limiting plasma membrane (PM), and a coat of fuzzy material (FZ).

Osmium, Epon, UA-LC

X 99,000

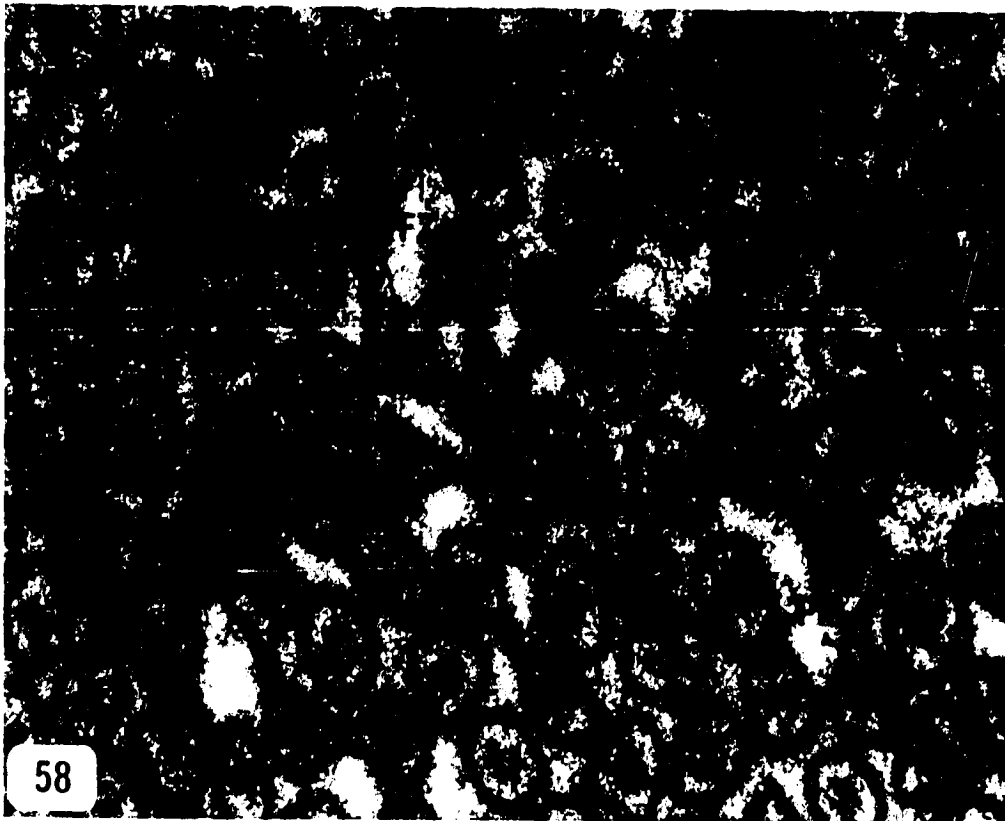


Figure 59: Electron micrograph of the apex of a cell from the proximal pars convoluta; parasitic adult.

Microvilli (MV) are irregular in shape and are often fused for a short distance (arrow); bag-like depressions (BD) are seen at the base of each. A single cilium (CL) is seen. The apical cytoplasm consists of dense tubular structures (DT), opaque smooth vesicles (SV), mitochondria (M), clear vacuoles (CV), rough ER (RER), a multivesicular body (MVB), a flocculent body (FB), and scattered clusters of free ribosomes (R).

Osmium, Epon, UA-LC

X 17,000

Figure 60: Electron micrograph of the apex of a cell from the proximal pars convoluta; 85-mm ammocoetes.

A filamentous core (FC) from the microvilli (MV) extends into the apical cytoplasm. Also seen are dense granules (DG), glycogen particles (GLY), rough ER (RER), and microtubules (MT).

Glutaraldehyde-Osmium, Epon, UA-LC

X 23,500

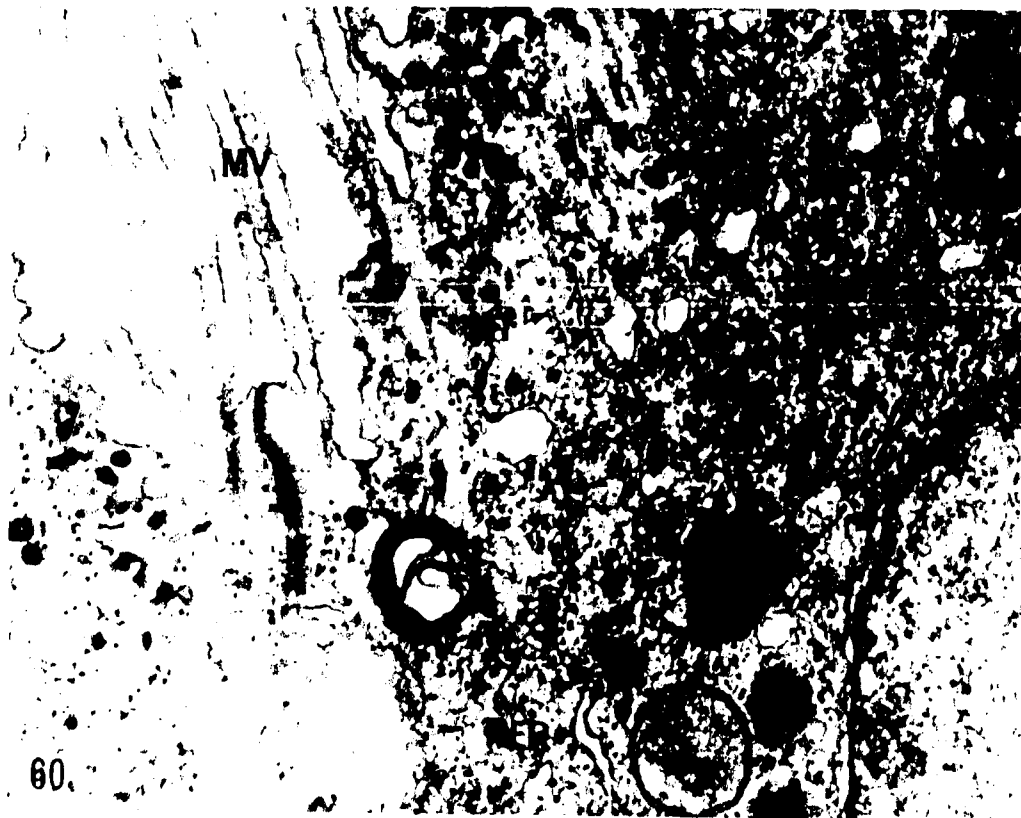


Figure 61: Electron micrograph of an apical bulbous protrusion of a cell from the proximal pars convoluta; 98-~~mm~~ ammocoetes.

The protrusion lacks the microvilli seen on the remainder of the apical surface of the cell (MV) but contains dense granules (DG), clear vacuoles (CV), smooth vesicles (SV), and mitochondria (M).

Osmium, Epon, UA-LC

X 7,100

Figure 62: Electron micrograph of the base of a cell from the proximal pars convoluta; 62-~~mm~~ ammocoetes.

Two types of vesicle are seen. Small, smooth vesicles (SV) are scattered throughout the cytoplasm and often are associated with the basal plasma membrane (arrows).

The large irregular vesicles (LV) usually contain a particulate material resembling that in the inter-cellular spaces (IS).

Osmium, Epon, UA-LC

X 16,700

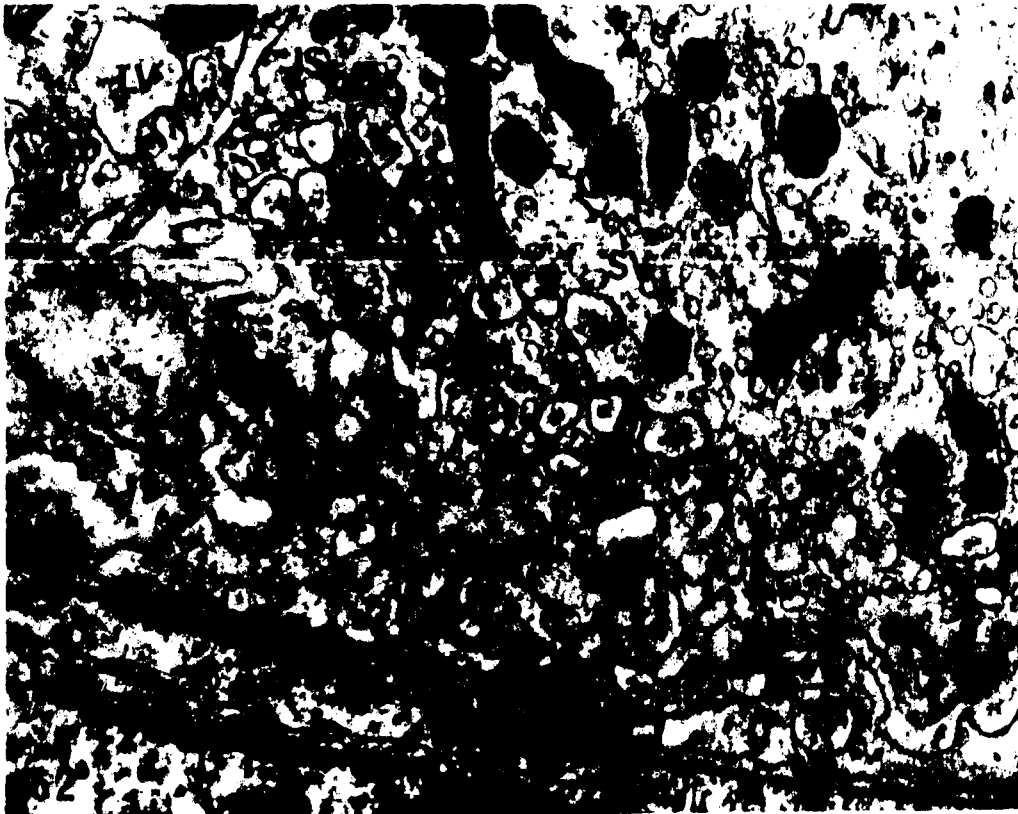


Figure 63: Electron micrograph of an oblique section of the apex of several cells from the proximal pars convoluta; parasitic adult.

Cells contain dense granules (DG), mitochondria (M), and porous clear vacuoles (arrows) containing dense deposits (DD) or smooth vesicles (SV). Microvilli (MV) are out in several planes.

Osmium, Epon, UA-LC

X 14,700

Figure 64: Electron micrograph of the base of a cell from the proximal pars convoluta; parasitic adult.

Large irregular mitochondria (M) are oriented along the longitudinal axis of the cell. Clumps of dense material (arrows) are distributed along the inner surface of the basal plasma membrane.

Osmium, Epon, UA-LC

X 7,100

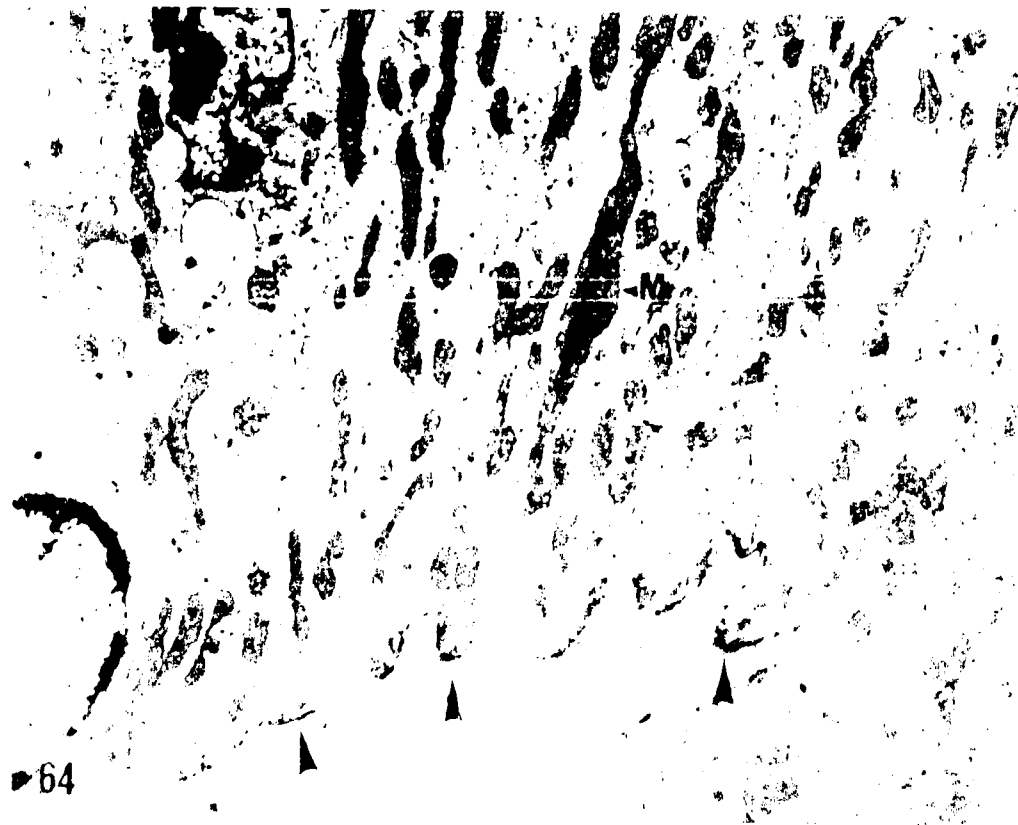
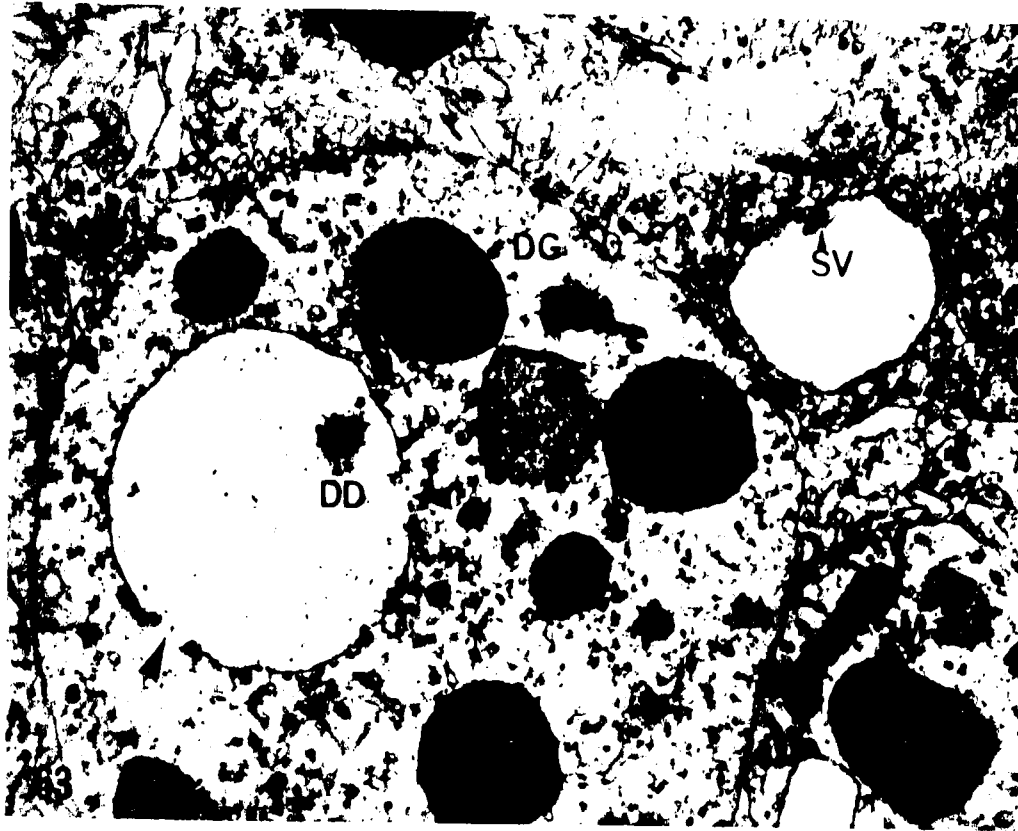


Figure 65A: Electron micrograph of the basal cytoplasm of a cell from the proximal pars convoluta; parasitic adult.

Most mitochondria have transverse cristae (CR) but one has cristae running longitudinally (arrow); striations (ST) are seen at one end of this mitochondrion.

Osmium, Epon, UA-LC

X 20,300

Figure 65B: Electron micrograph of one of the mitochondria shown in Fig. 65A; parasitic adult.

Between each longitudinal crista (CR) the matrix (arrows) is cross-banded with a periodicity of 180 to 200 Å.

Osmium, Epon, UA-LC

X 138,800

Figure 66: Electron micrograph of the basal cytoplasm of a cell from the proximal pars convoluta; parasitic adult.

Transverse cristae are seen in most mitochondria while one has longitudinal cristae. Major striations (ST) at one end of this mitochondrion have a periodicity of 560 \AA while minor striations between have a periodicity of 90 \AA . Mitochondrial granules (MG) are seen in all mitochondria.

Flocculent bodies (FB) are limited by a single membrane and are usually associated with rough ER (RER). A large number of small smooth vesicles (SV) are seen in the cytoplasm.

Osmium, Epon, UA-LC

X 24,500

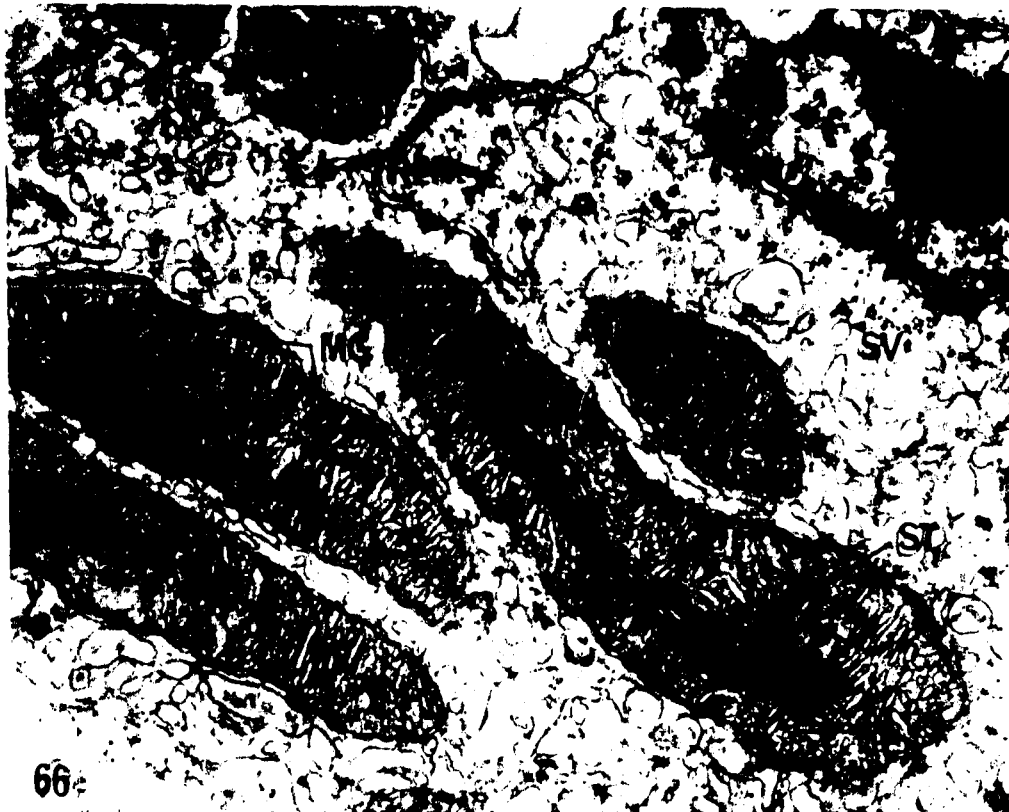


Figure 67: Electron micrograph of a cell of the proximal pars convoluta; parasitic adult.

Cristae occur in whorls in one mitochondrion and are arranged longitudinally in one (arrows). One mitochondrion has obliquely-arranged cristae (CR) and filamentous material (FM) at one side. Note flocculent bodies (FB).

Osmium, Epon, UA-LC

X 18,400

Figure 68: Light micrograph showing the cuboidal epithelium of the proximal pars recta; parasitic adult. The proximal pars recta (PPR) is contrasted with the taller cells and more highly developed brush border (BB) of the epithelium of the pars convoluta (PC).

Bouin, Tissuemat, PAS-AH-OG

X 2,000

Figure 69: Light micrograph at a 0.5- μ section showing two tubules from the proximal pars recta; 98-mm ammocoetes.

Brush border (BB) is poorly developed. A few dense granules (DG) are scattered throughout the cells. The tubules are surrounded by sinusoids (S) containing blood cells (BC).

Osmium, Epon, TB

X 4,200

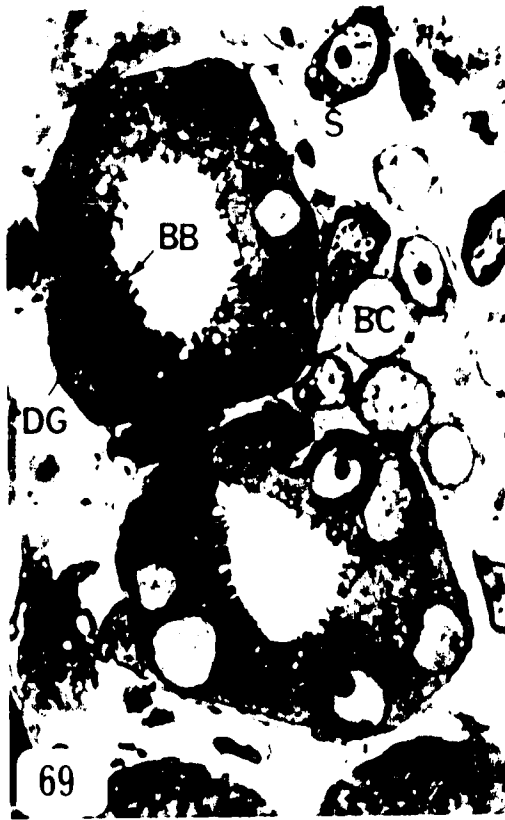


Figure 70:

Electron micrograph of cells from the proximal pars recta; 98-mm ammocoetes.

The microvilli (MV) and clear vacuoles (CV) are few in number. The plasma membranes (PM) of adjacent cells interdigitate and large vesicles (LV) are associated with them. Mitochondria (M) are seen at the sides of the nucleus (N) as well as rough ER (RER) and smooth vesicles (SV).

Osmium, Epon, UA-LC

X 10,700

Figure 71:

Electron micrograph of cells from the proximal pars recta; parasitic adult.

Microvilli (MV) are seen at the apex of the cell as well as small dense granules (DG) and a lipid droplet (LD). The cells are limited laterally by interdigitating plasma membranes and intercellular spaces (IS) containing cytoplasmic projections (CY). A wandering blood cell (BC) is seen in the intercellular space.

Osmium, Epon, UA-LC

X 6,500

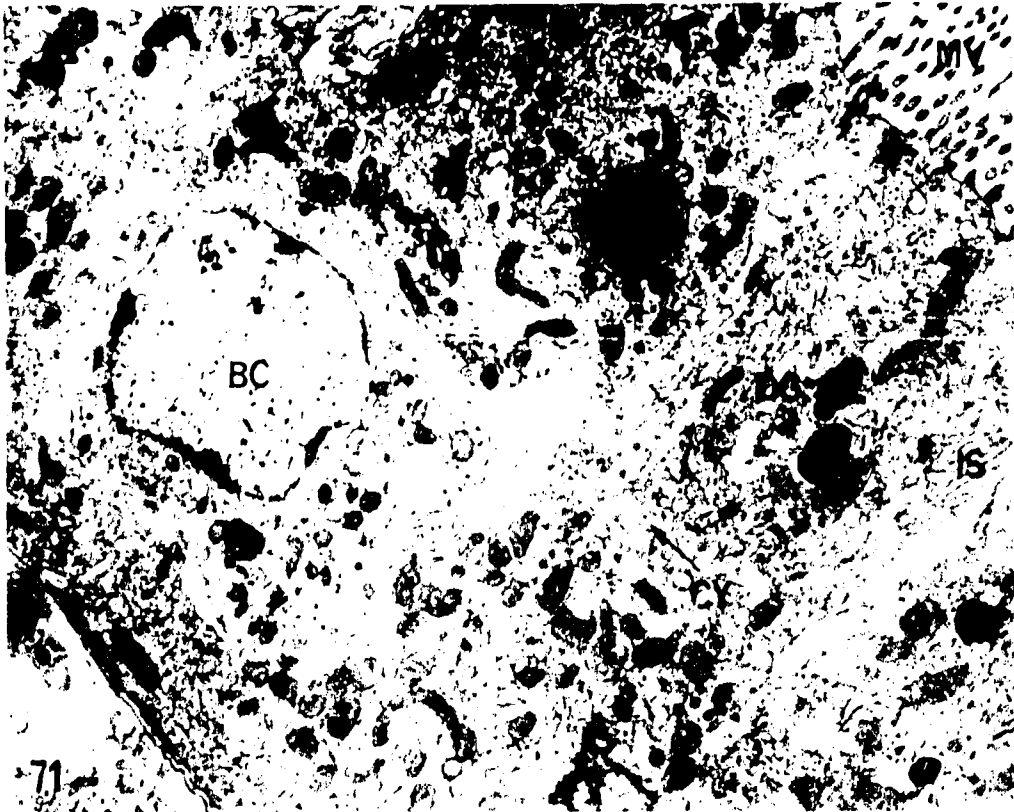
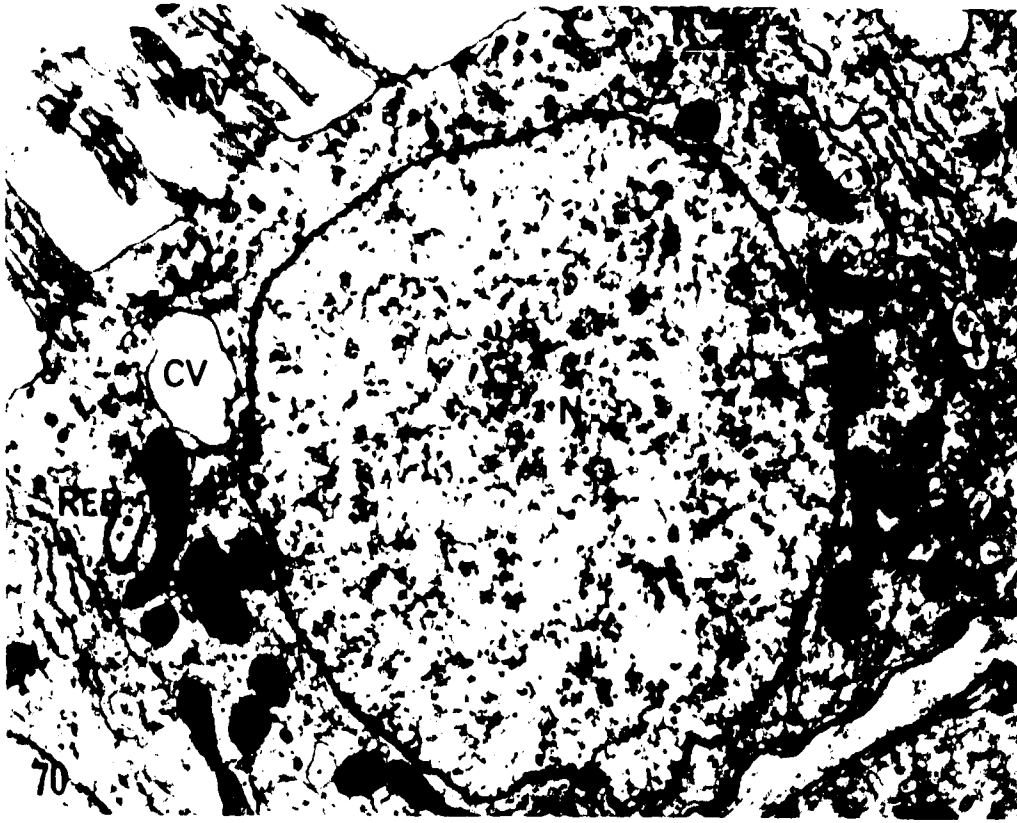


Figure 72:

Electron micrograph of cells from the proximal pars recta; parasitic adult.

The apex has a few microvilli (MV) and several multivesicular bodies (MVB). Plasma membranes are fused laterally by desmosomes (DG) and intercellular spaces (IS) are seen between the cells. An irregular nucleus with a prominent nucleolus (n) is centrally located with a Golgi apparatus (GA) above. Irregularly-shaped mitochondria (M) and flocculent bodies (FB) are present.

Osmium, Epon, UA-LC

X 8,600

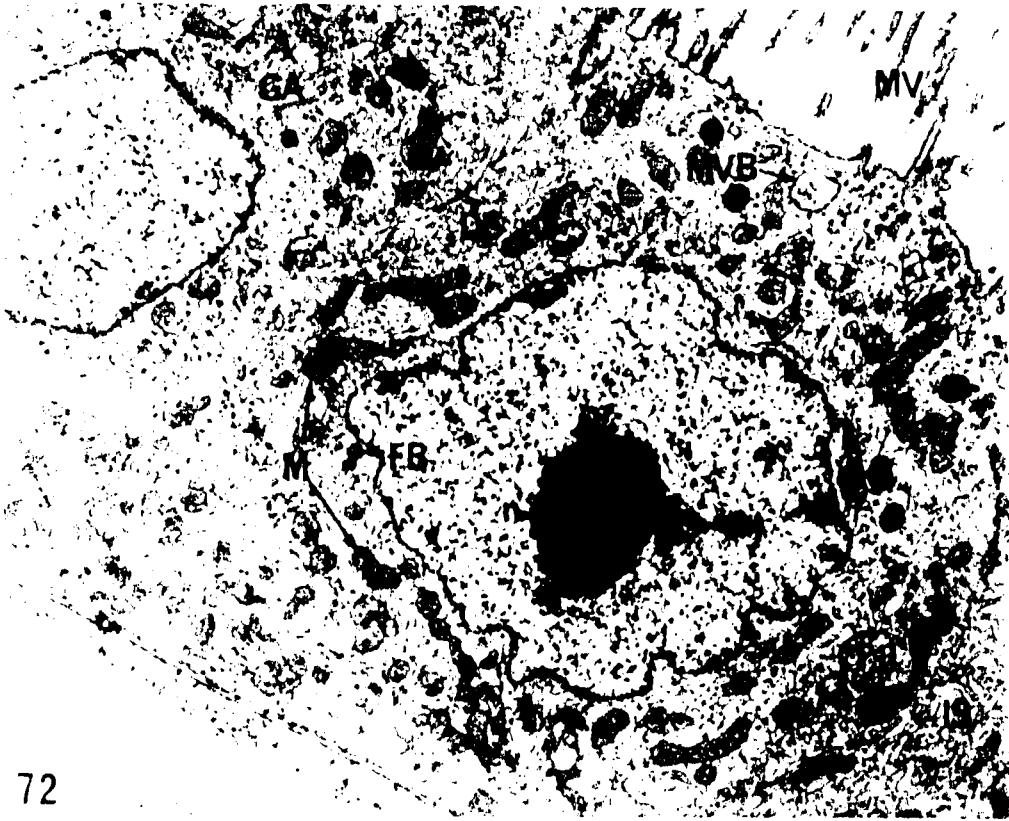
Figure 73:

Electron micrograph of cells from the proximal segment; posterior portion of the kidney of an 85-mm ammocoetes.

The tubule consists of light (LC) and dark cells (DC) both possessing apical microvilli (MV). Cells are separated by intercellular spaces (IS) containing cytoplasmic projections (CY). Dark cells contain more glycogen (GLY) and their nucleus (N) and cytoplasmic matrix are more electron dense.

Glutaraldehyde-Osmium, Epon, UA-LC

X 7,000



72



73

Figure 74: Light micrograph of the ventral portion of the kidney; parasitic adult.

Straight intermediate segments (I) run parallel to the distal pars recta (DPR) and collecting (C) segments, and are separated from them by narrow sinusoids (S). One intermediate segment is continuous with the proximal pars recta (PPR) while another is seen continuous with the distal pars recta which contains a cell in mitosis (arrow). A portion of the archinephric duct (AD) is also seen.

Bouin, Tissuemat, PAS-H-OG

X 2,400



Figure 75: Light micrograph of the dorsal portion of the kidney;
83-mm ammocoetes.
The PAS + intermediate segments (I) are seen between
the proximal pars recta (PPR) and distal (D) segments.
Bouin, Tissuemat, PAS-AH-OG

X 1,540

Figure 76: Light micrograph of the ventral portion of the
kidney; parasitic adult.
Three intermediate segments (I) are seen between
the proximal pars recta (PPR) and distal pars
recta (DPR).
Bouin, Tissuemat, PAS-AH-OG

X 2,000

Figure 77: Light micrograph of the junction of proximal pars
recta and intermediate segment; 125-mm ammocoetes.
This 0.5- μ section shows the transition of cells
of the proximal pars recta (PPR) into the squamous
cells of one type of intermediate segment (I).
Osmium, Epon, TB

X 4,700

Figure 78: Light micrograph of an intermediate segment;
129-mm ammocoetes.
This 0.5- μ section shows an intermediate segment
(I) with cuboidal cells with a dome-shaped apex.
Osmium, Epon, TB

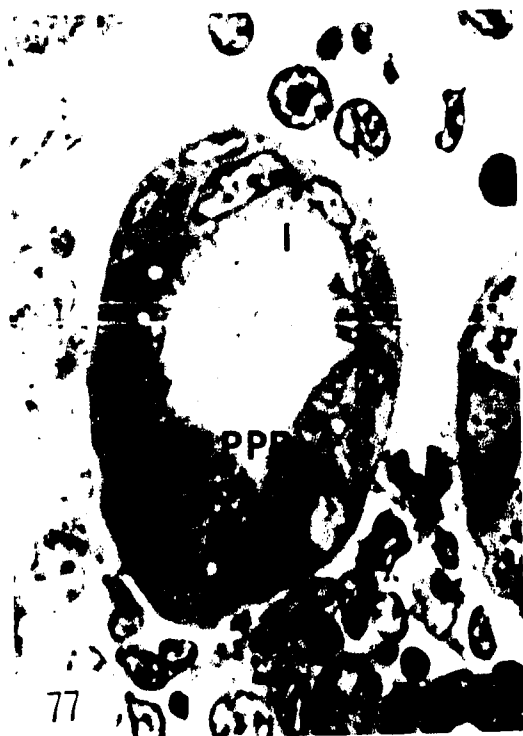
X 3,600



75



76



77



78

Figure 79: Electron micrograph of a transverse section of an intermediate segment; 85-mm ammocoetes. Cells possess a flattened, elongate nucleus with a large nucleolus (n). The cytoplasm contains large dense granules (DG) and apical microvilli (MV). A portion of a blood cell (BC) is seen in the intercellular space (IS) and the lumen (LU) contains debris. Glutaraldehyde-Osmium, Epon, UA-LC

X 10,400



BC

MV

CG

Figure 80: Electron micrograph of one of the cells in Fig. 76;
85-mm ammocoetes.

The nucleus is flattened and invaginated. The cytoplasm contains mitochondria (M), fibrils (FI), rough ER (RER), glycogen (GLY), and a Golgi apparatus (GA). Apical microvilli are often clumped and are coated with fuzz (FZ).

Glutaraldehyde-Osmium, Epon, UA-LC

X 15,900

Figure 81: Electron micrograph of a squamous intermediate cell; 105-mm ammocoetes.

The flattened elongate nucleus (N) contains cytoplasmic fibrils (FI) in invaginations of the membrane. Mitochondria possess angular cristae, and smooth vesicles (SV) are located near the lateral plasma membrane. Dense granules (DG), ribosomes (R), and rough ER (RER) are scattered throughout the cytoplasm. Adjacent cells are fused apically by a junctional complex (JC) and laterally by desmosomes (DS). An intercellular space (IS) is seen. The cell rests on a basement membrane (BM).

Osmium, Epon, UA-LC

X 20,000

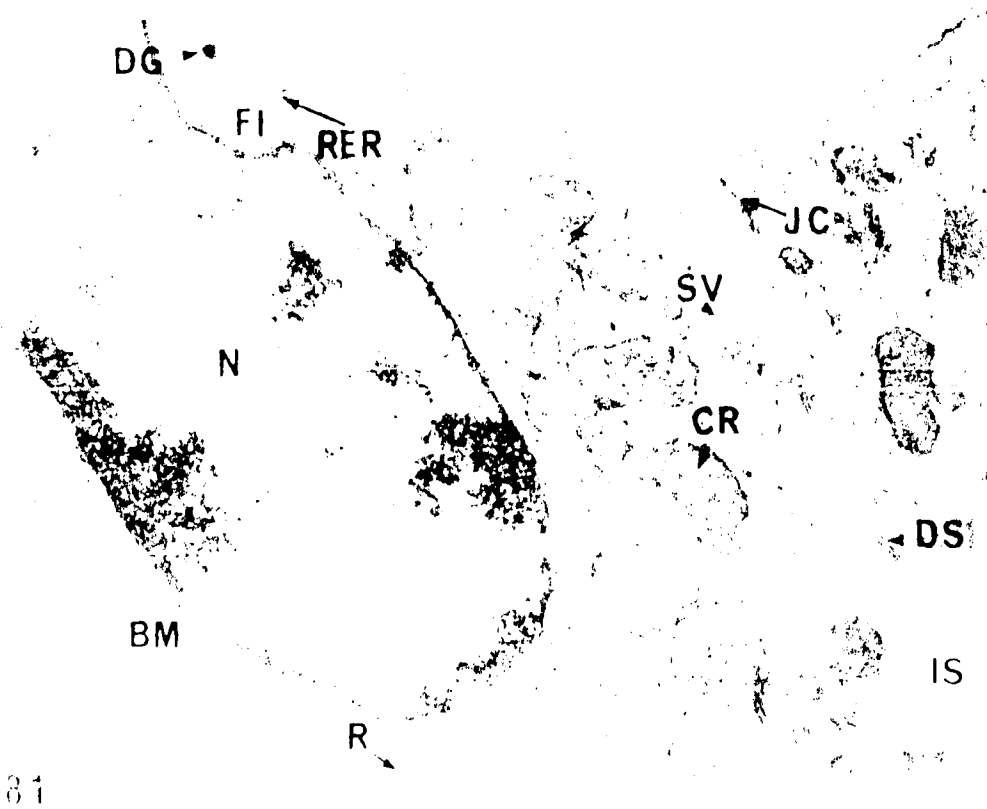
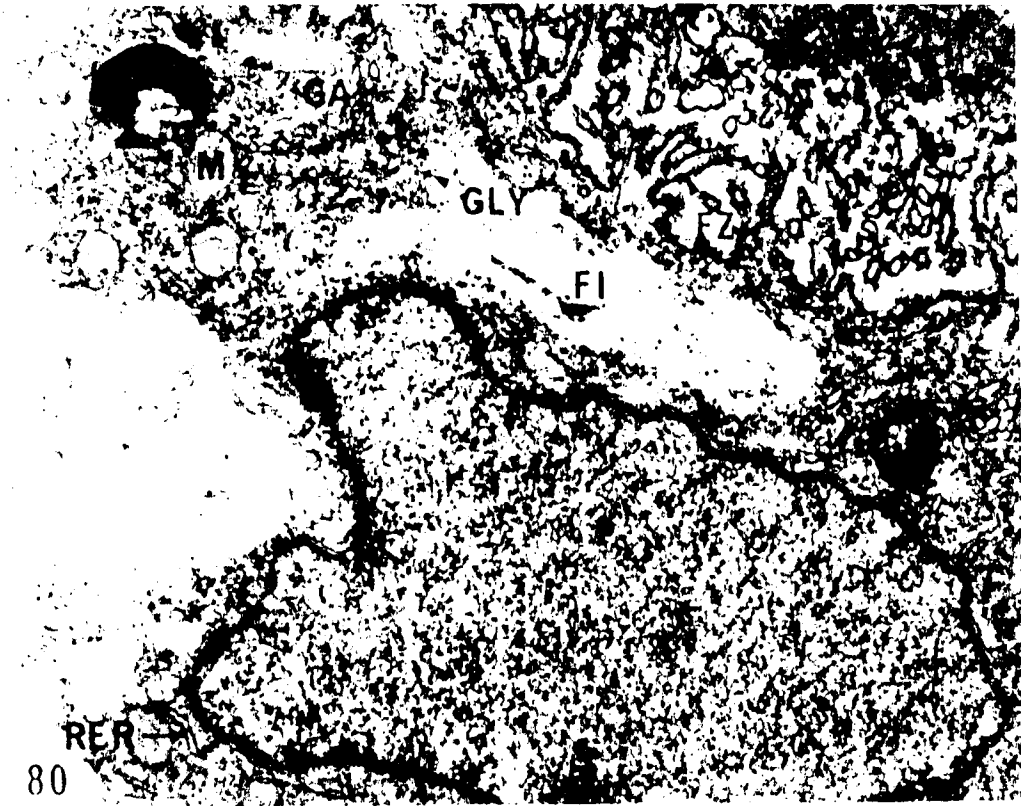


Figure 82: Electron micrograph of a transitional intermediate cell near the distal segment; 117-mm ammocoetes. The nucleus (N) is oval and the apical surface of the cell contains a few microvilli (MV). The cytoplasm contains numerous free ribosomes (R), rough ER (RER), mitochondria (M), glycogen particles (GLY), and a Golgi apparatus (GA). A dense body (DB) containing glycogen particles is also seen.

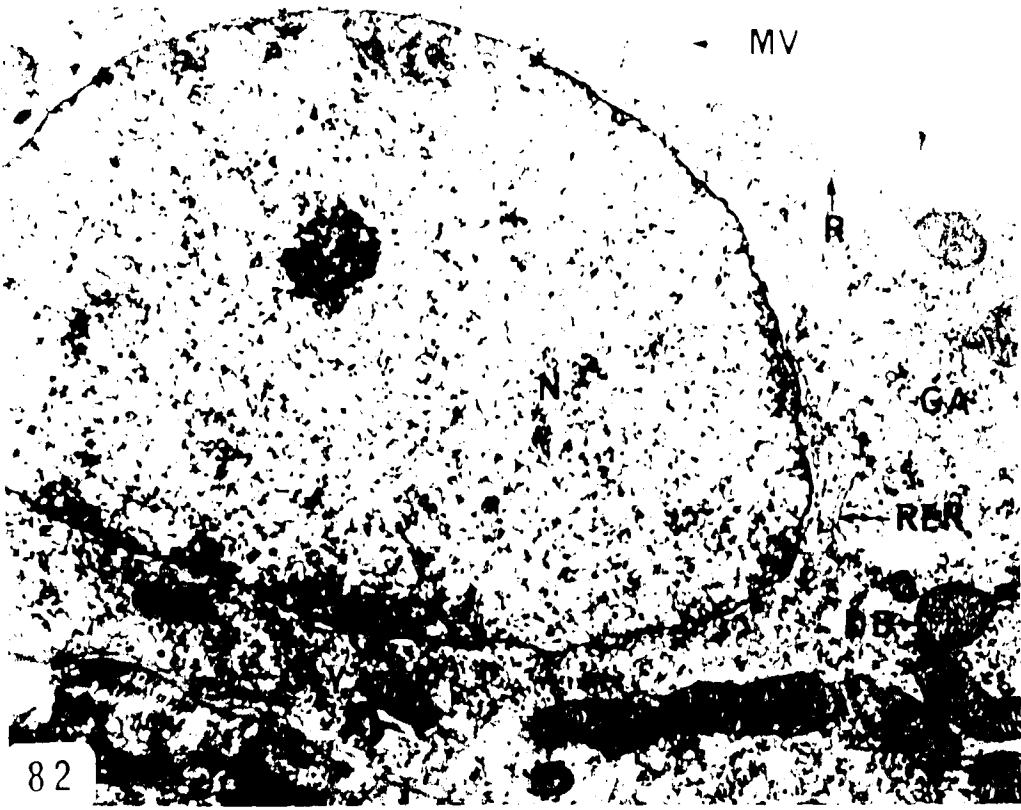
Osmium, Epon, UA-LC

X 11,900

Figure 83: Electron micrograph of the cuboidal type intermediate segment; 129-mm ammocoetes. The cells have dome-shaped protrusions and the nuclei (N) are oriented along the long axis of the cell. The cytoplasm is vacuolated (V). Wandering blood cells (BC) are seen in the intercellular areas.

Osmium, Epon, UA-LC

X 7,100



82



83

Figure 84: Electron micrograph of one of the cells in Fig. 83 showing the cytoplasmic components; 129-mm ammocoetes.

Adjacent cells are fused apically by a junctional complex (JC) and intercellular spaces are often swollen due to the presence of wandering blood cells (BC). The apical surface has a few short microvilli which are coated with a fuzzy fibrillar material (FZ). The cytoplasm contains bundles of fibrils (FI), a large Golgi apparatus (GA), and mitochondria (M).

Osmium, Epon, UA-LC

X 10,700

Figure 85: Electron micrograph showing the apex of a cuboidal intermediate cell; 129-mm ammocoetes.

A Golgi apparatus consists of dilated saccules (SA) and microvesicles (MI); dense granules (DG) are closely associated. Smooth (SER) and rough ER (RER) are found in the cytoplasm. The nucleus has peripherally located clumps of chromatin (CH) and the nuclear envelope is interrupted by pores (arrow).

Osmium, Epon, UA-LC

X 14,600

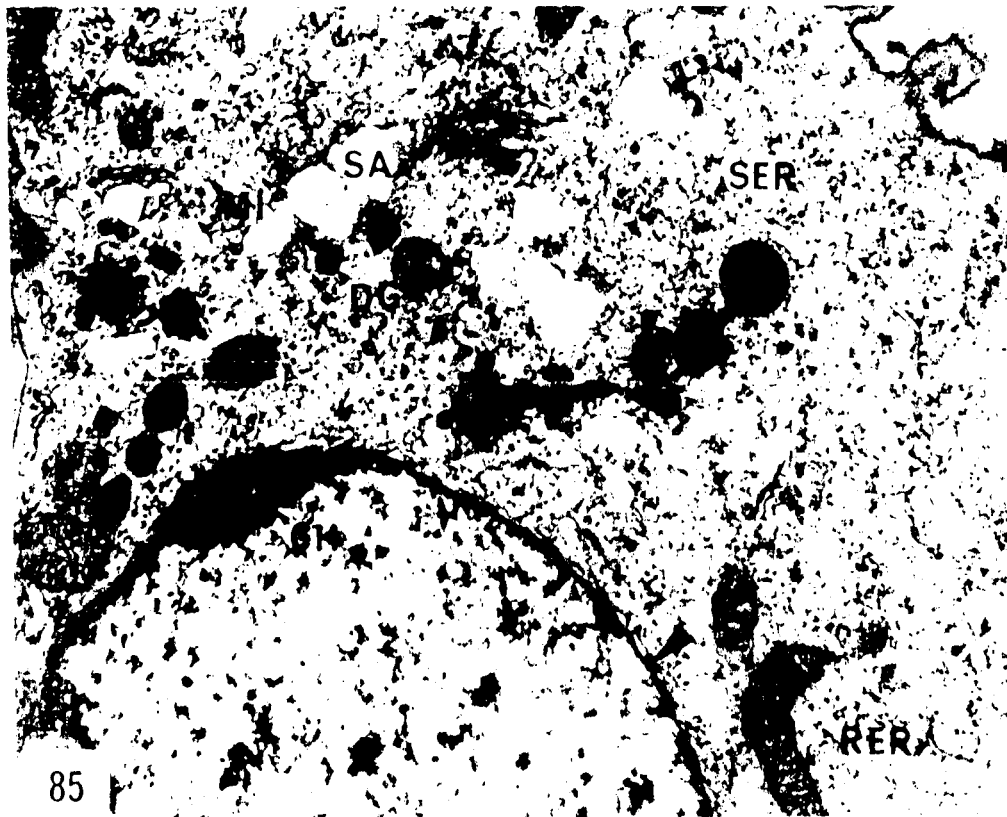
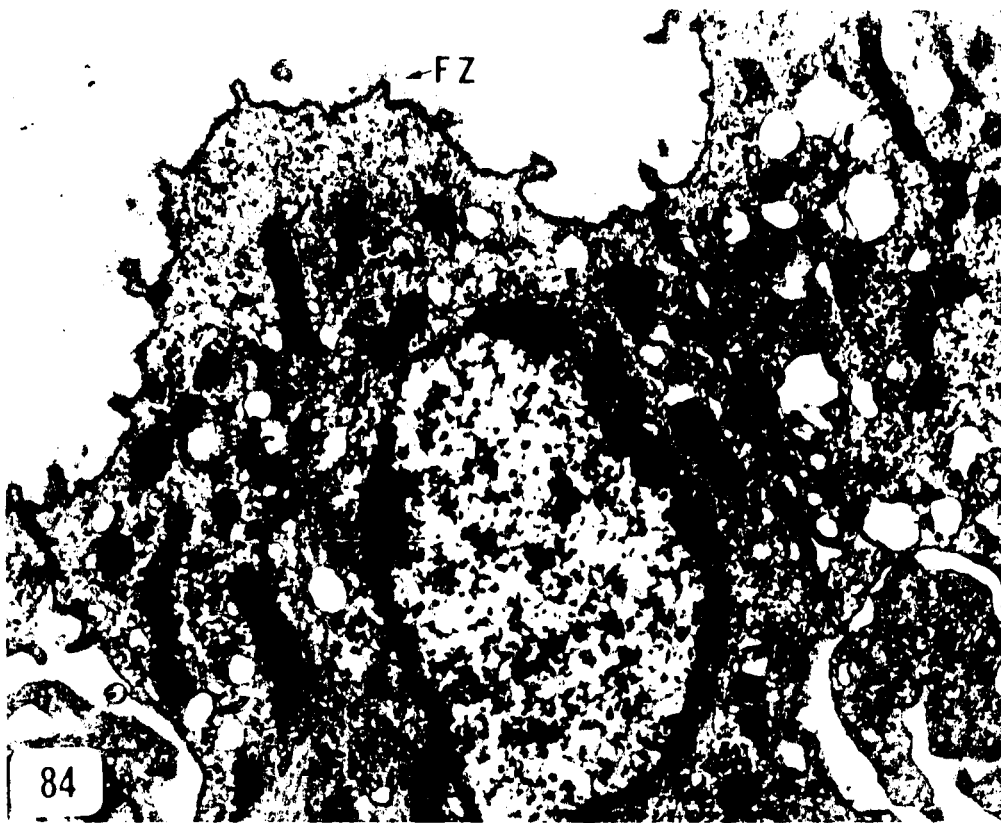


Figure 86: Electron micrograph of a cuboidal intermediate cell; 129-mm ammocoetes.

The cytoplasm contains dilated rough (RER) and smooth ER (SER), mitochondria (M), fibrils (FI), microtubules (MT), and small vesicles (SV) near the plasma membrane. The cell rests on a basement membrane (BM) and a space containing collagenous fibrils (CO) separates it from the sinusoidal endothelium (END).

Osmium, Epon, UA-LC

X 16,700

Figure 87: Light micrograph of a short cuboidal intermediate segment; parasitic adult.

In this 0.5- μ section the intermediate segment (I) is seen between the proximal pars recta (PPR) and distal pars recta (DPR) segments.

Osmium, Epon, TB

X 3,500

Figure 88: Light micrograph of a long squamous intermediate segment; parasitic adult.

In this 0.5- μ section the intermediate segment (I) leads into the distal pars recta (DPR).

Osmium, Epon, TB

X 3,900

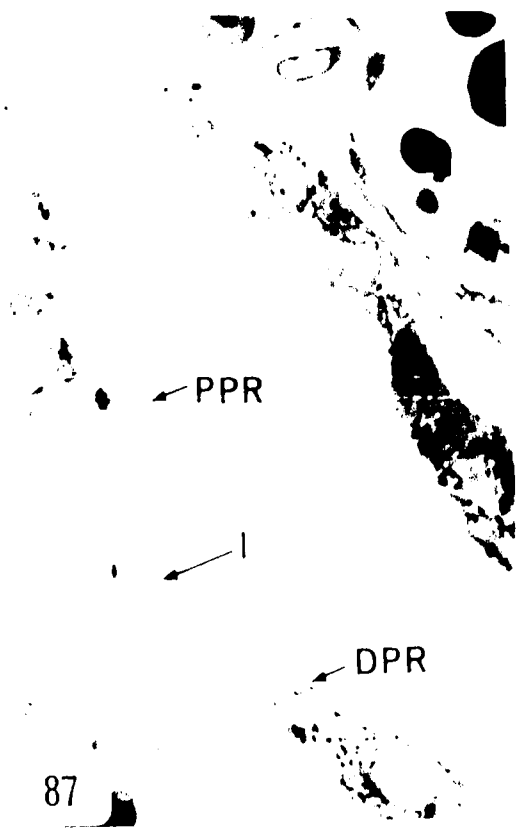
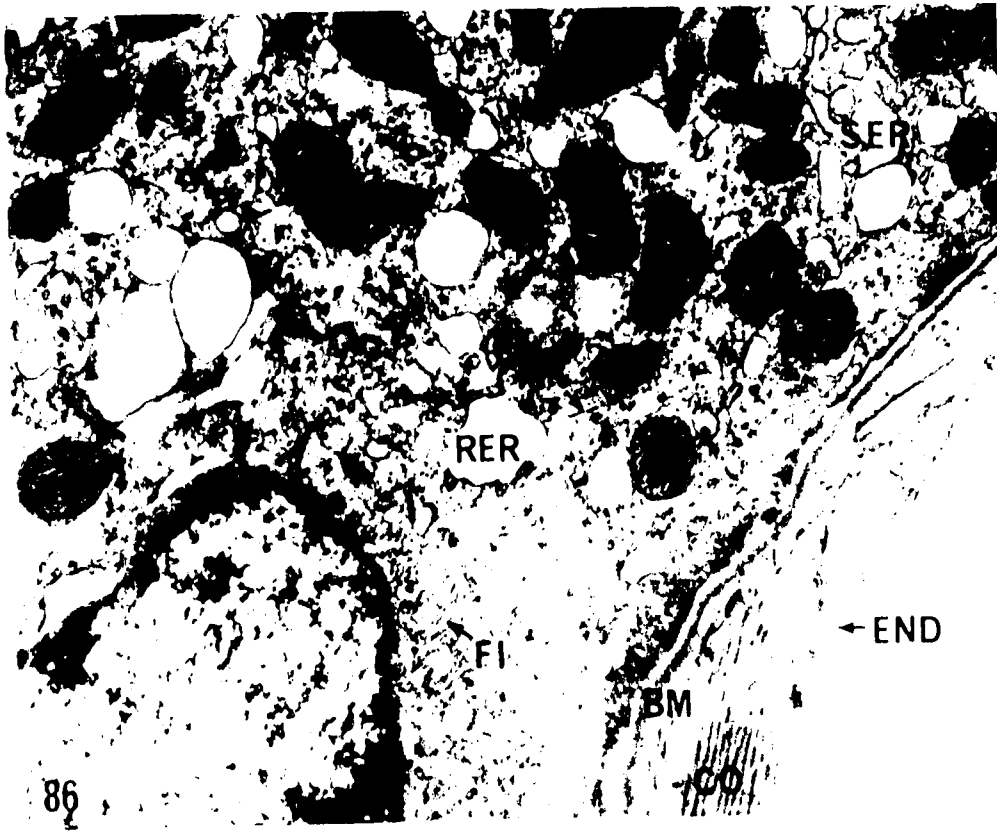


Figure 89: Electron micrograph of adjacent cells of the proximal pars recta (PPR) and the intermediate segment; parasitic adult.

The cuboidal intermediate cells have a few microvilli coated with an electron dense fuzz (FZ). Mitochondria (M) are small and the cytoplasm contains numerous fibrils (FI) and smooth vesicles (SV). The nucleus (N) is spherical and centrally located.

Osmium, Epon, UA-LC

X 13,800

Figure 90: Electron micrograph of a cuboidal intermediate cell; parasitic adult.

This micrograph shows a close association of fibrils (FI) to the nuclear envelope (NE), and a Golgi apparatus (GA), numerous smooth vesicles (SV) and mitochondria (M).

Osmium, Epon, UA-LC

X 48,900

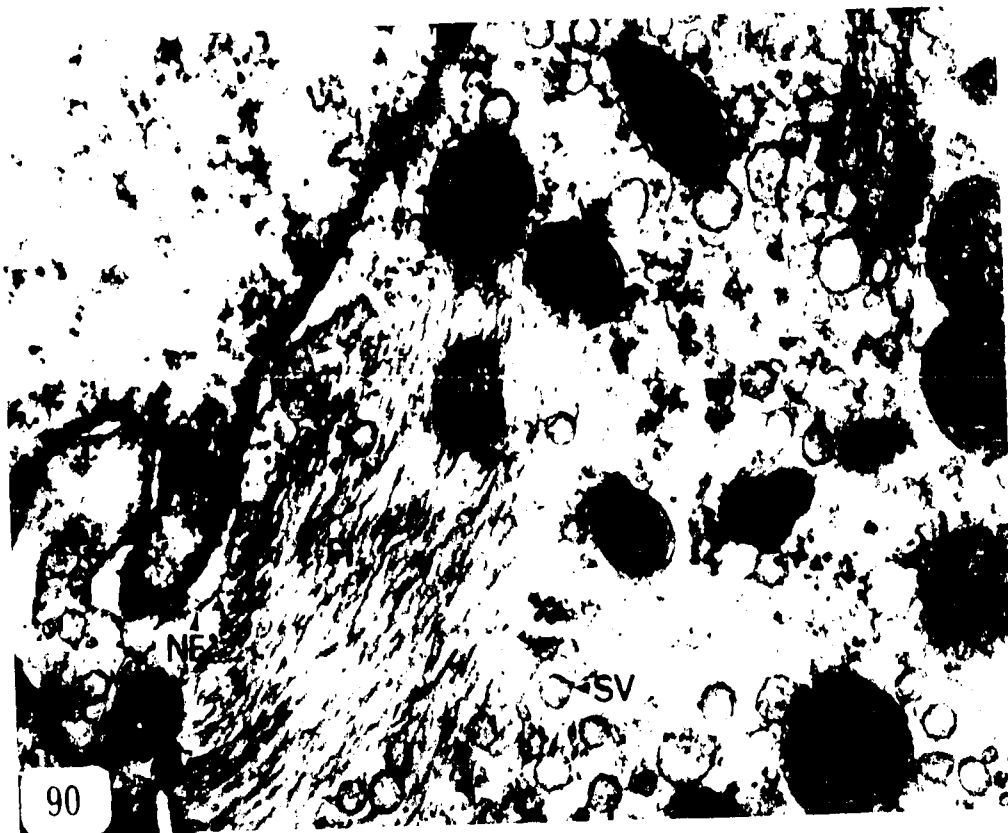
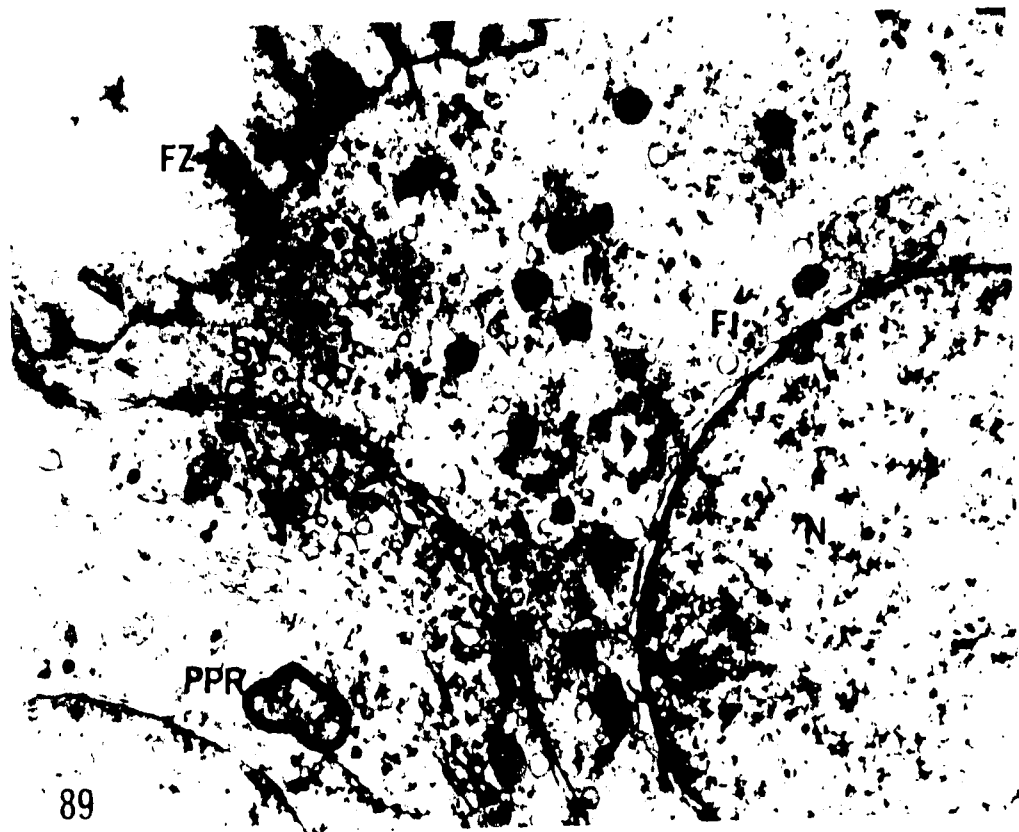


Figure 91: Electron micrograph of a squamous intermediate cell; parasitic adult.

Mitochondria (M), dense granules (DG), and the Golgi apparatus (GA) are situated lateral to the elongate nucleus (N). The apex contains a few microvilli coated with fuzz (FZ), rough ER (RER), ribosomes (R), smooth vesicles (SV), and multivesicular bodies (MVB). A lipid droplet (LD) is seen in this section. Beneath the cell are found bundles of collagenous fibrils (CO).

Osmium, Epon, UA-LC

X 13,700

Figure 92: Electron micrograph of a squamous intermediate segment showing the two cell types; parasitic adult.

The basally located cells have an elongate irregular nucleus (N), few mitochondria (M) and large lipid droplets (LD).

Osmium, Epon, UA-LC

X 7,100



Figure 93: Electron micrograph of a portion of Fig. 92 showing the basally located cells of a squamous intermediate segment; parasitic adult.

The nucleus (N) is enclosed within a nuclear envelope, the outer membrane of which is coated with ribosomes (R). The cytoplasm contains a few mitochondria (M), dense granules (DG), and smooth vesicles (SV) near the lateral and basal plasma membranes.

Osmium, Epon, UA-LC

X 32,600



Figure 94: Light micrograph of the distal segment showing light and dark cells.

A. 83-mm ammocoetes.

One cell type (DC) is intensely PAS+ while the other type (LC) is unstained.

Bouin, Tissuemat, PAS-AH-OG

X 3,100

B. 118-mm ammocoetes.

This 2.0- μ section shows several light cells (LC) among dark cells (DC). Note also the darkly staining intertubular cells (arrows).

Glutaraldehyde-Osmium, Epon, OxS-H

X 3,100

C. 118-mm ammocoetes.

This 2.0- μ section shows a light cell (LC) among dark cells (DC).

Glutaraldehyde-Osmium, Epon, OxS-H

X 4,700

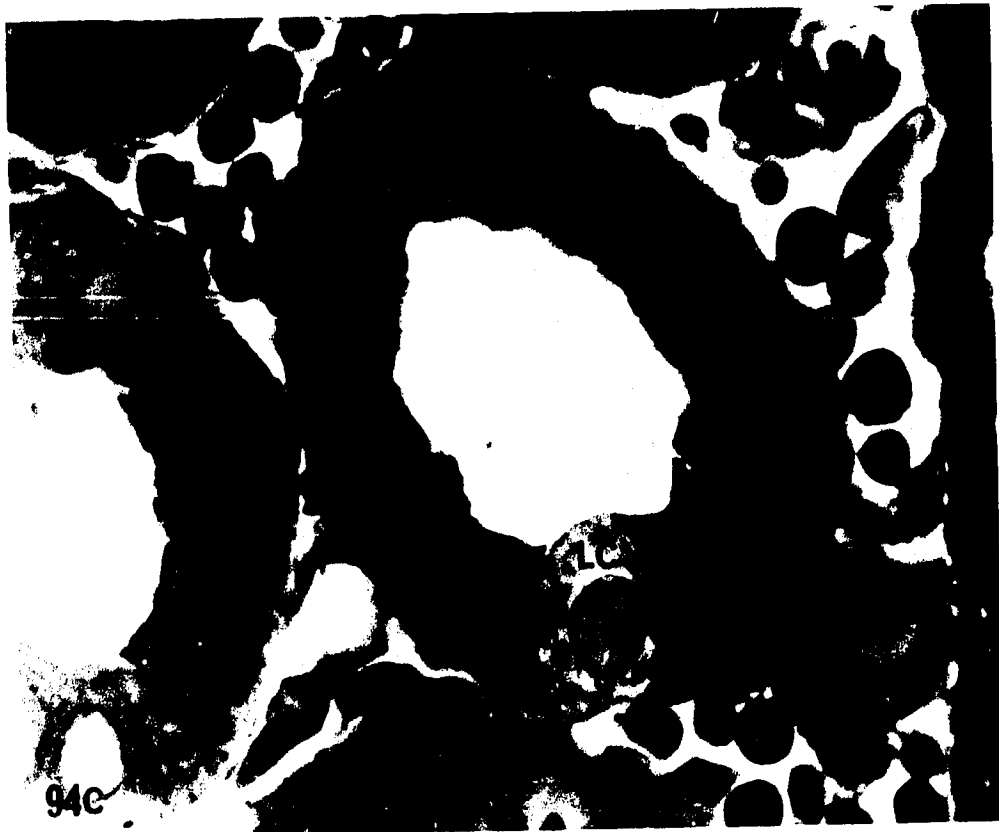


Figure 95: Light micrograph of the distal segment; 65-mm ammocoetes.

This 0.5- μ section shows the distal segment to be composed of two cell types, a light (LC) and a dark (DC). The light cell is to be compared with the large cells of the collecting segment (C).

Osmium, Epon, TB

X 3,300

Figure 96: Light micrograph of distal segments; 83-mm ammocoetes.

This 0.5- μ section shows the tubules to be separated by large sinusoids (S) and are made up of light cells (LC) and dark cells (DC).

Osmium, Epon, TB

X 500

Figure 97: Light micrograph of distal segments; 98-mm ammocoetes.

This 0.5- μ section shows that the light cells (LC) have few mitochondria while the darker cells (DC) have numerous basally located mitochondria (arrows).

Osmium, Epon, TB

X 4,700

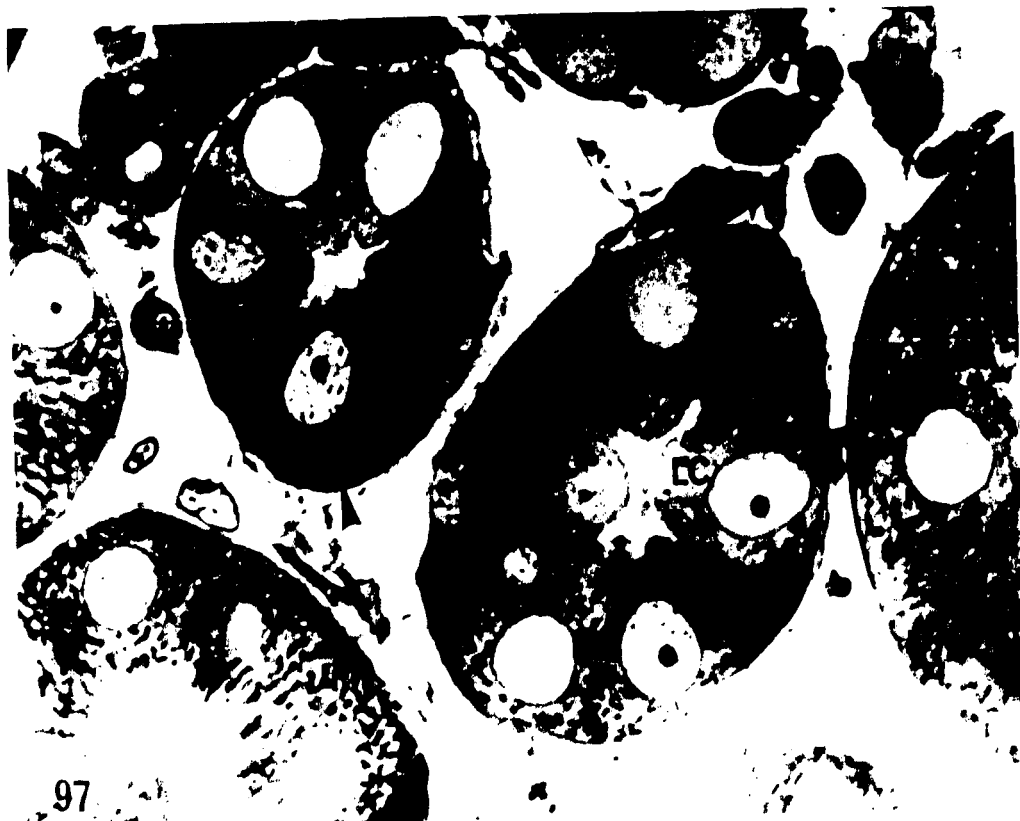


Figure 98: Electron micrograph of the transition zone from intermediate to distal segment; 129-mm ammocoetes. The light distal cells (LC) have fewer vacuoles (V) than the intermediate cells (I). Note the elongate to oval nuclei (N) of the distal cells in this region.

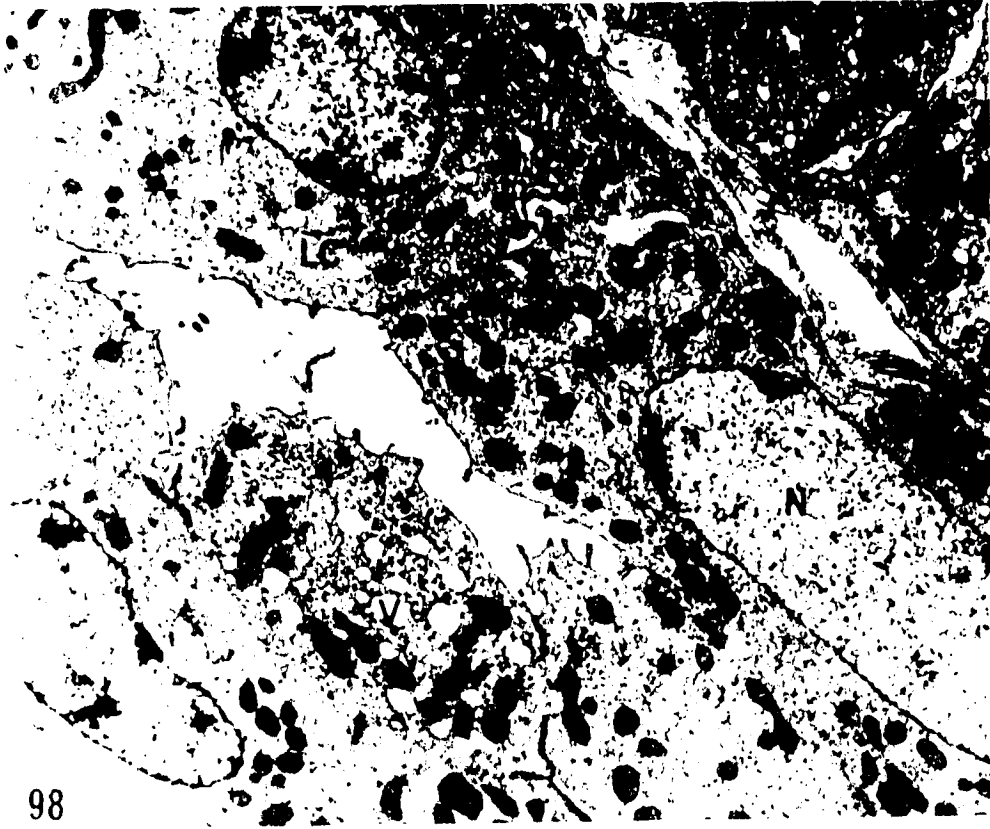
Osmium, Epon, UA-LC

X 7,500

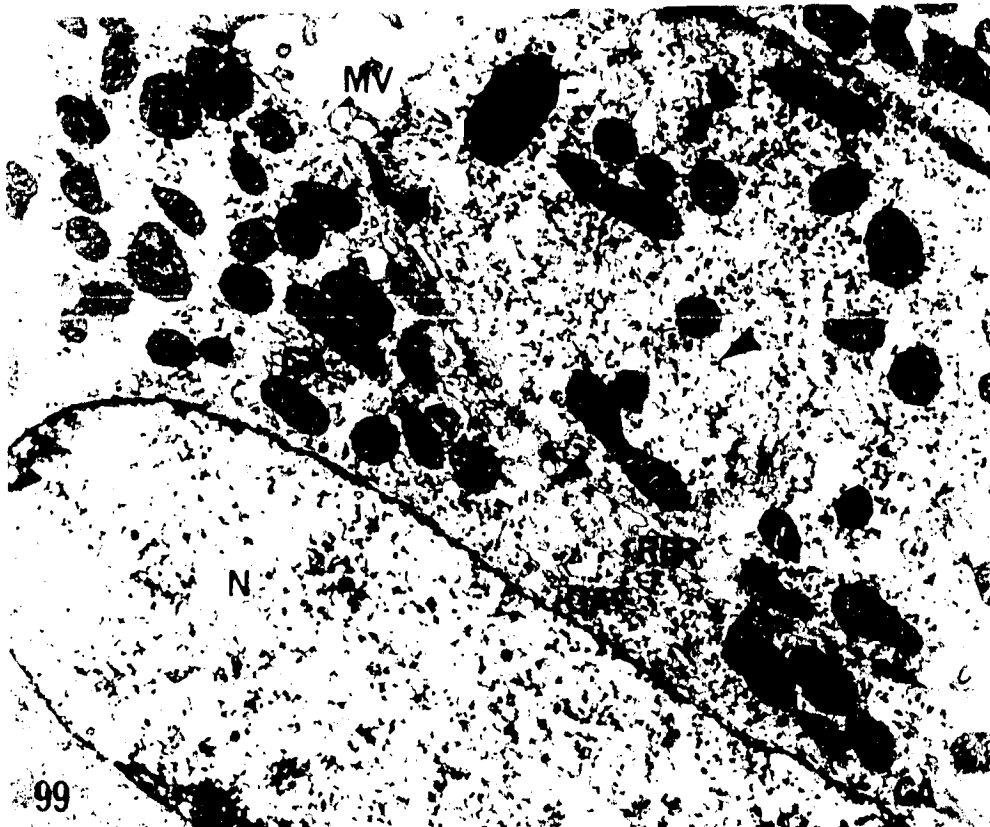
Figure 99: Electron micrograph of a portion of Fig. 96 showing a transitional distal cell; 129-mm ammocoetes. The nucleus (N) is elongate and the cytoplasm consists of numerous mitochondria (M), glycogen particles (arrows), three Golgi apparatuses (GA), a few strands of rough ER (RER), and a few short apical microvilli (MV).

Osmium, Epon, UA-LC

X 11,900



98



99

Figure 100: Electron micrograph of a light cell from the transition zone between the distal and intermediate segments; 129-mm ammocoetes.

The nucleus (N) is invaginated and fibrils are located in this invagination (arrows). Smooth vesicles (SV) are located in the cytoplasm close to the lateral plasma membrane. Intercellular spaces (IS) are found between cells.

Osmium, Epon, UA-LC

X 10,800

Figure 101: Electron micrograph of a portion of Fig. 100; 129-mm ammocoetes.

A close association of the 70-80 Å cytoplasmic fibrils (FI) to the nuclear envelope (arrow) is seen.

Osmium, Epon, UA-LC

X 43,500

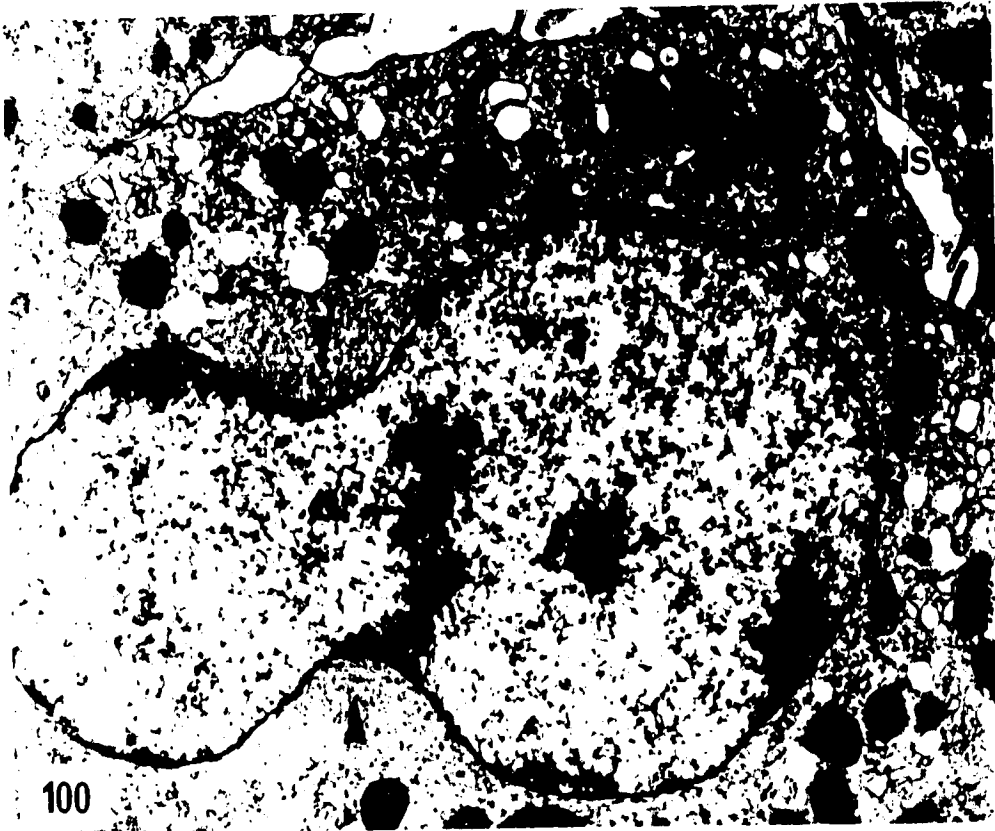


Figure 102: Electron micrograph of cells from a distal segment;
74-mm ammocoetes.

The segment is composed of light (LC) and dark cells (DC). Intercellular spaces with cytoplasmic projections (CY) are found between the cells. The nucleus (N) of the dark cells is centrally located. Note the presence of large lipid droplets (LD).

Osmium, Epon, UA-LC

X 7,100

Figure 103: Electron micrograph showing the range of electron densities in cells of the distal segment; 85-mm ammocoetes.

A dark cell (DC) is contrasted with a light cell (LC). The remainder of the cells are between these two in their densities. Intercellular spaces (IS) are found between the cells and their cytoplasm contains numerous mitochondria (M).

Glutaraldehyde-Osmium, Epon, UA-LC

X 7,800

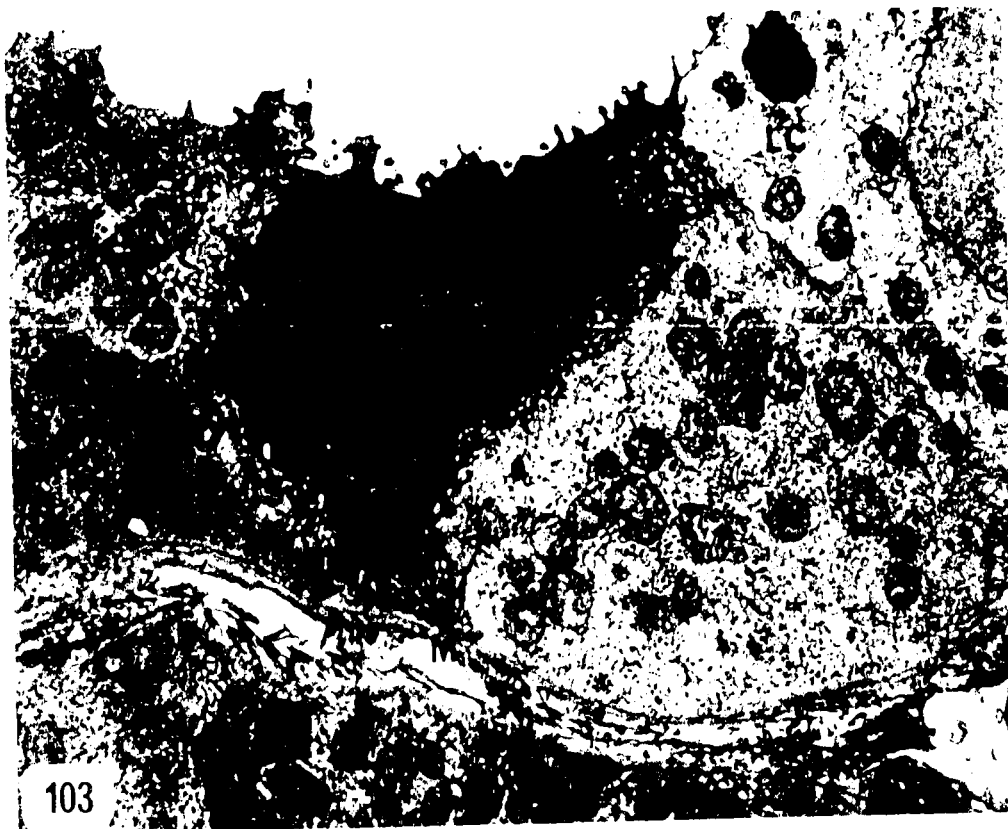
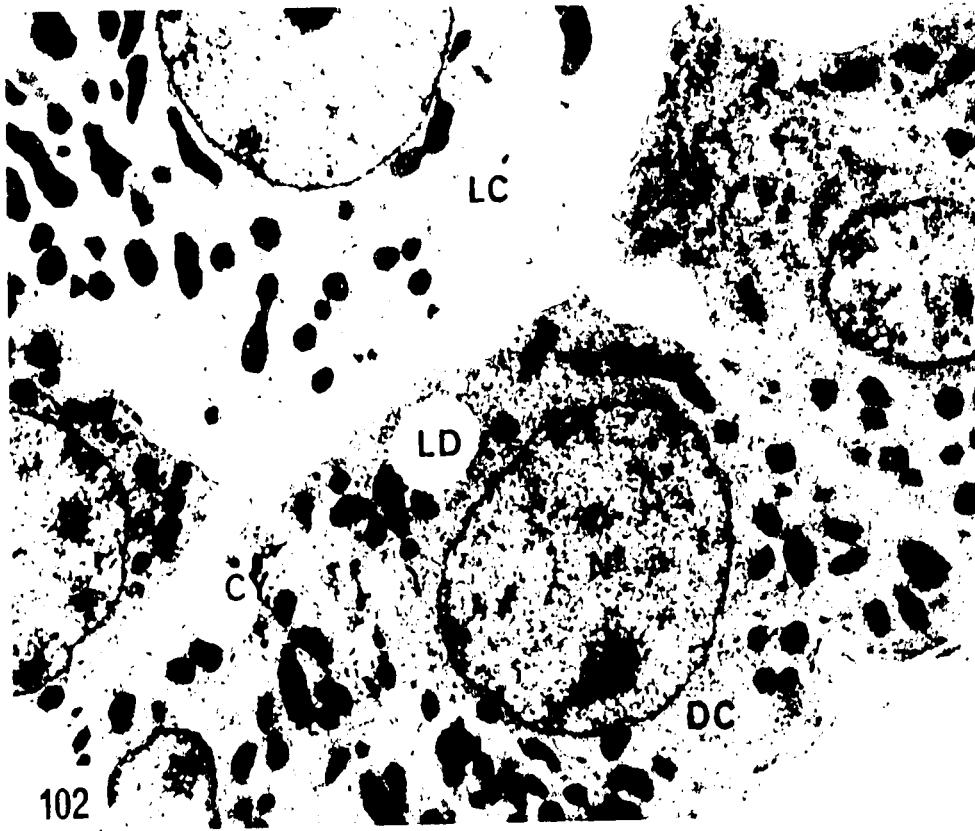


Figure 104:

Electron micrograph of cells of the distal segment; 46-mm ammocoetes.

A light cell is seen amongst several dark cells.

The cytoplasm of the light cell contains three or four Golgi apparatuses (GA), dense granules (DG), glycogen particles (GLY), and a few strands of rough ER (arrow). Note the tubular smooth ER (SER) in the dark cell.

Osmium, Epon, UA-LC

X 11,900

Figure 105:

Electron micrograph of a light cell from the distal segment; 98-mm ammocoetes.

The nucleus (N) is pale and the cytoplasm consists of mitochondria (M) and smooth vesicles (SV).

An intercellular space (IS) is seen. Note the absence of glycogen particles as compared to the previous micrograph.

Osmium, Epon, UA-LC

X 10,800

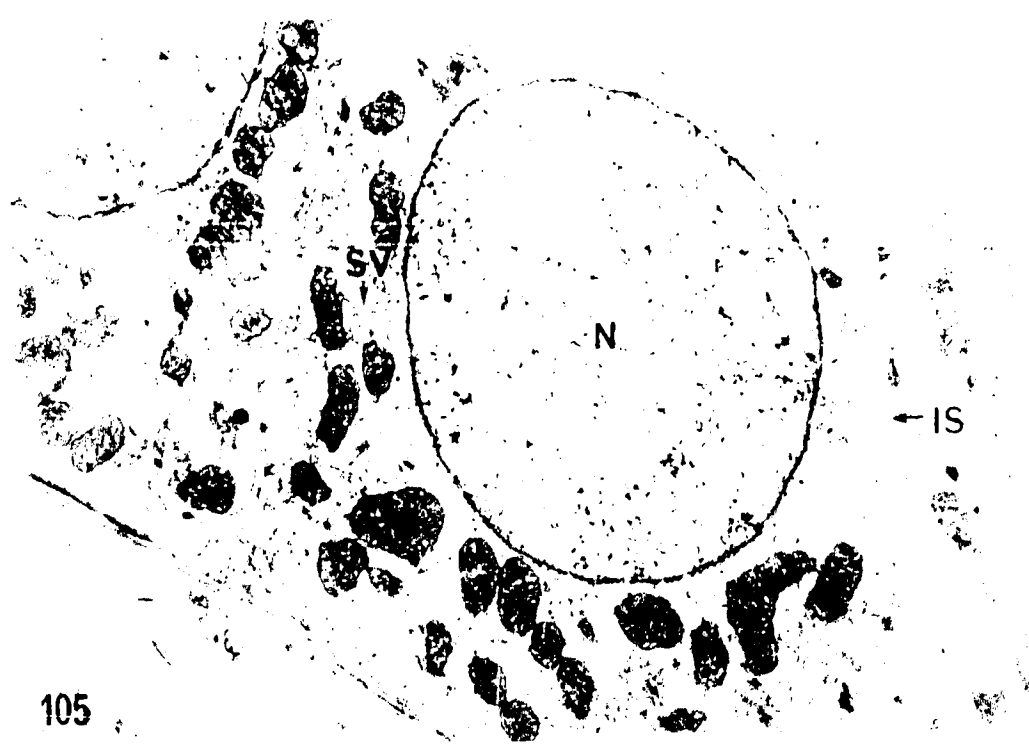


Figure 106: Electron micrograph of the bases of light and dark cells of the distal segment; 85-mm ammocoetes.

The light and dark cells are limited by interdigitating plasma membranes (PM). The light cell has larger amounts of smooth ER (SER) but less glycogen (GLY) than the dark cell.

Glutaraldehyde-Osmium, Epon, UA-LC

X 16,700

Figure 107: Electron micrograph of light cells in the distal segment; 110-mm ammocoetes.

The nucleus is limited by a nuclear envelope which is often interrupted by pores (arrow). The nucleus contains a nucleolus (n). In the cytoplasm are found mitochondria (M), glycogen particles (GLY), and tubular dense bodies (DB).

Osmium, Epon, UA-LC

X 19,300

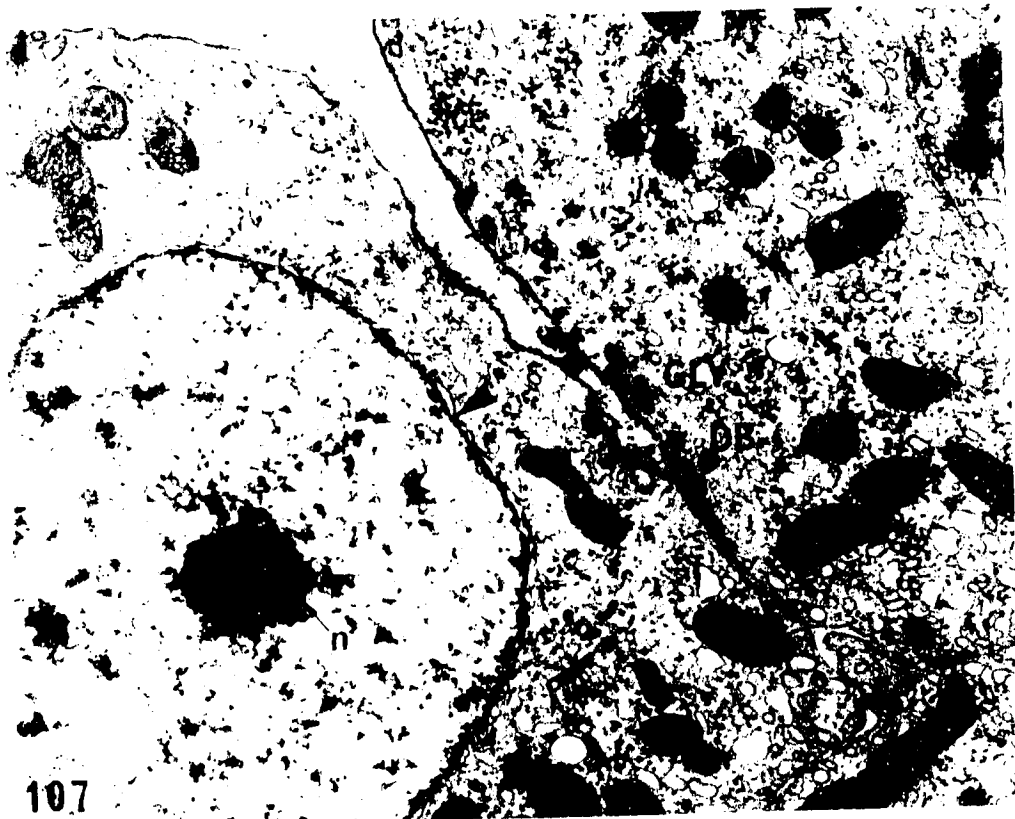


Figure 108: Electron micrograph of the apical surface of a light cell from the distal segment; 40-mm ammocoetes.

The apical surface contains no microvilli. Glycogen particles (GLY), vacuoles (V), and microtubules (MT) are seen in the apical cytoplasm.

Osmium, Epon, UA-LC

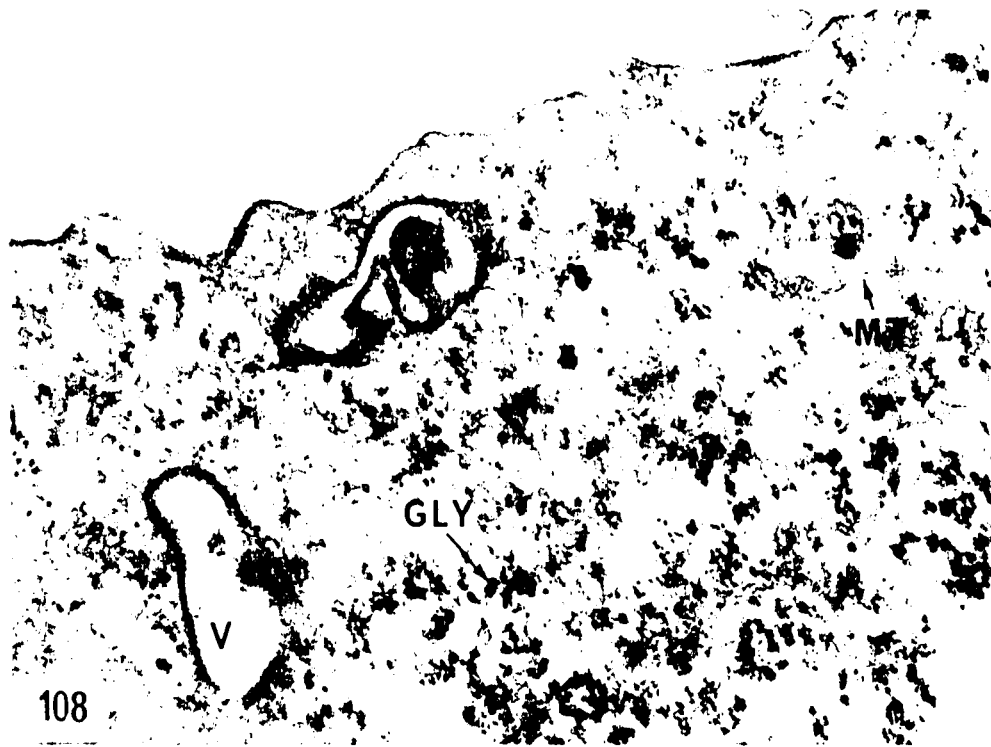
X 50,800

Figure 109: Electron micrograph of dark cells in the distal segment; 40-mm ammocoetes.

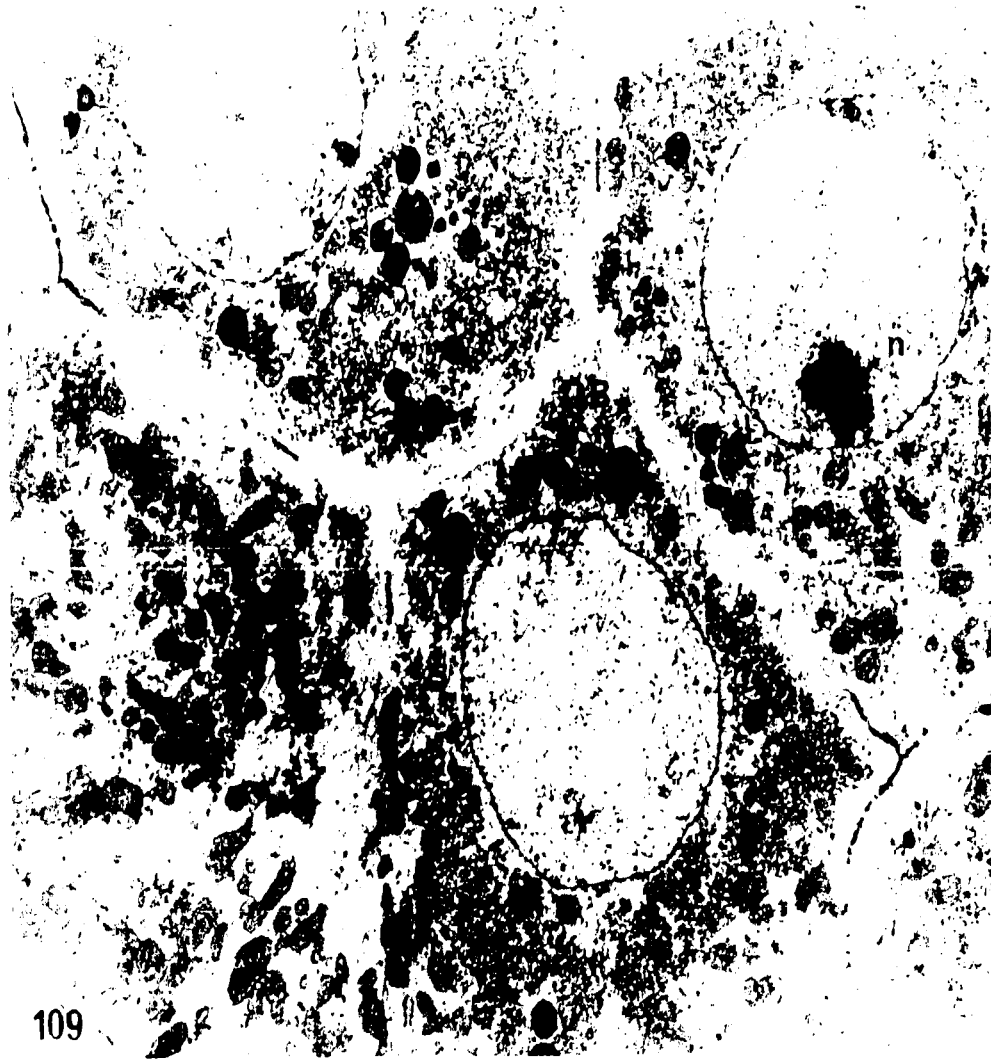
The nuclei are spherical and often contain a nucleolus (n). The cytoplasm contains large accumulations of glycogen particles (GLY), numerous mitochondria (M), and spherical dense bodies (DB).

Osmium, Epon, UA-LC

X 5,300



108



109

Figure 110: Electron micrograph of pyramidal dark cells in the distal segment; 40-mm ammocoetes.

The nucleus (N) is roughly spherical and centrally located. Mitochondria (M) and glycogen particles (GLY) are numerous, and a dense body (DB) is seen above the nucleus. One cell contains large quantities of tubular smooth ER (SER). The apical surface contains a few microvilli (MV).

Osmium, Epon, UA-LC

X 12,100



←MV

DB

N

SER

Figure 111: Electron micrograph of cuboidal dark cells from the distal segment; 129-mm ammocoetes.

The centrally located nucleus contains a nucleolus (n) and the cells are separated by intercellular spaces (IS) which often contain cytoplasmic projections (CY). The cytoplasm contains large lipid droplets (LD) as well as large quantities of glycogen particles (GLY) often contained within apical cytoplasmic protrusions (AB).

Osmium, Epon, UA-LC

X 9,800

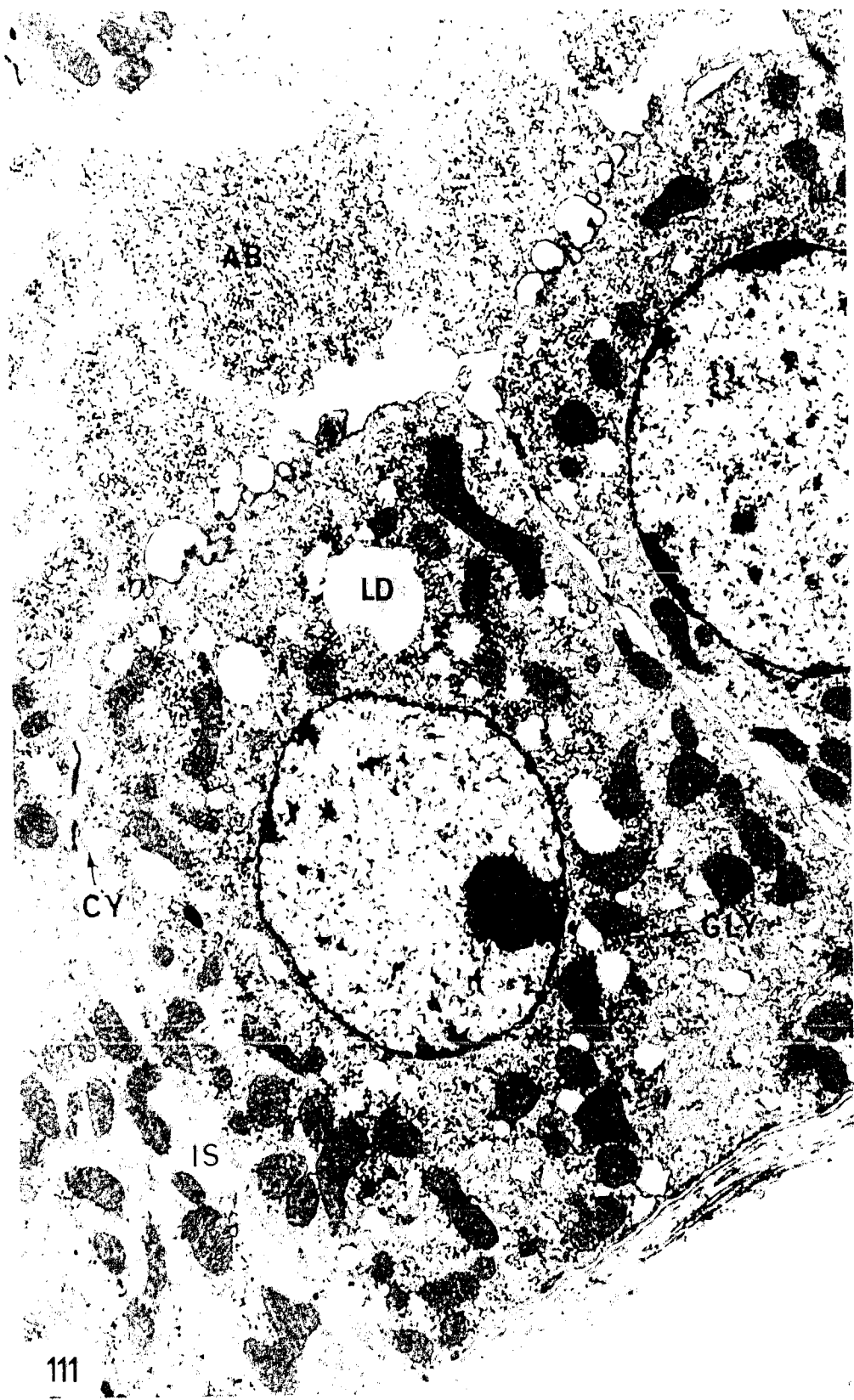


Figure 112: Electron micrograph of the apical surface of several dark cells in the distal segment; 110- μ m ammocoetes.

Adjacent cells are limited by invaginating plasma membranes which also enclose intercellular spaces (arrow). Cells are fused apically by a junctional complex (JC) and laterally by desmosomes (DS). The cytoplasm contains dense bodies (DB).

Osmium, Epon, UA-LC

X 20,100

Figure 113: Electron micrograph of the base of two dark cells in the distal segment; 125- μ m ammocoetes.

Adjacent cells adhere by desmosomes (DS) and are separated by large intercellular spaces (IS) which appear to be continuous with the extracellular space (arrow) above the basement membrane (BM). Collagenous fibrils (CO) are found between the basement membrane and the sinusoidal endothelium (END). The cytoplasm contains spherical, smooth vesicles (SV) and the nuclear envelope is interrupted by a pore (NP).

Osmium, Epon, UA-LC

X 27,200

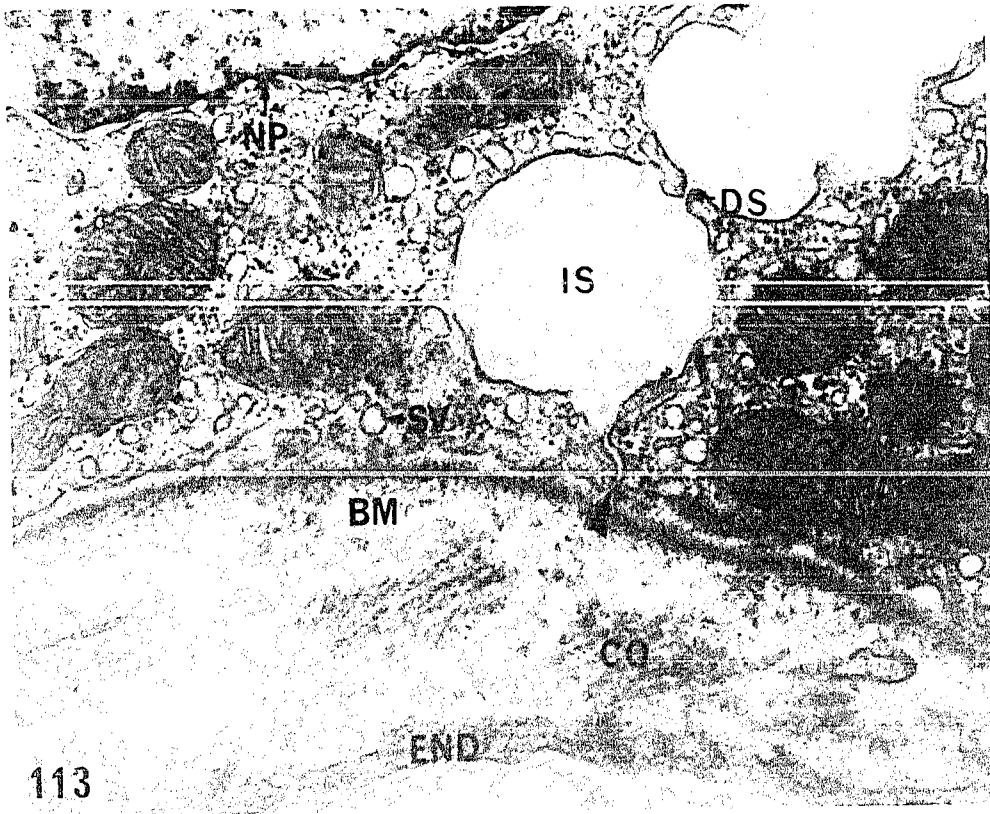
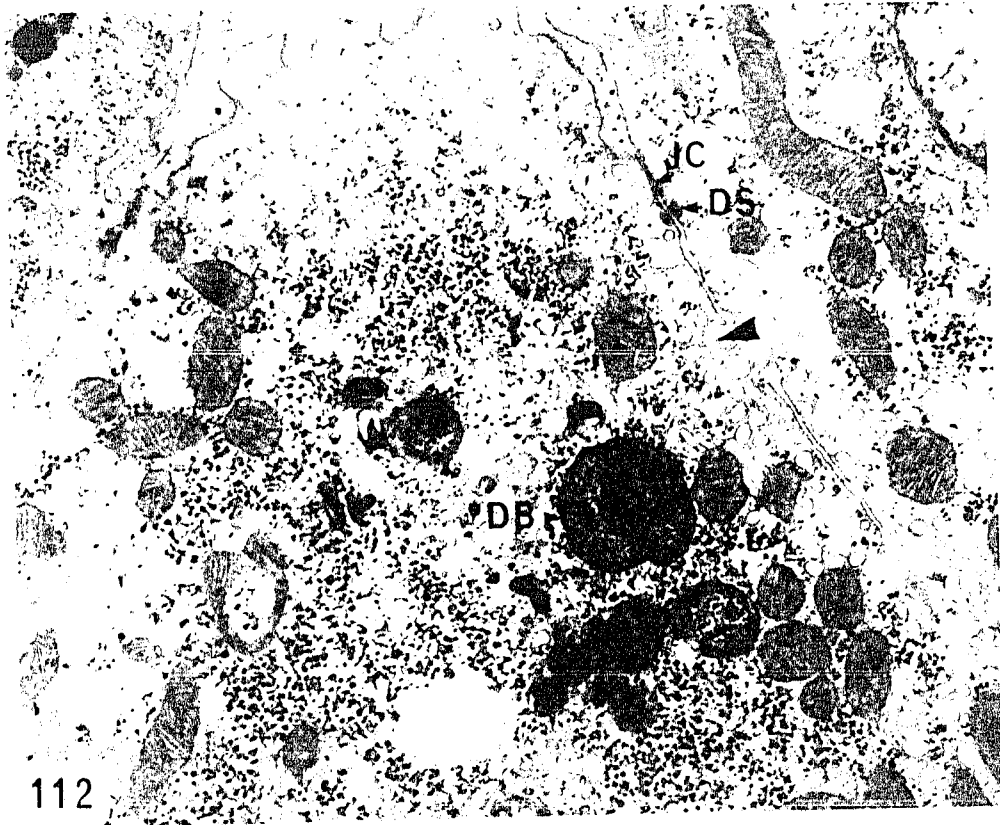


Figure 114: Electron micrograph of the base of a dark cell from the distal segment; 118-mm ammocoetes. Mitochondria (M) are large. Anastomosing cisternae of the smooth ER (SER) appear to communicate with the extracellular (ES) and intercellular spaces (IS). Glycogen particles (GLY) are found in the cytoplasm. The cell rests on a basement membrane (BM) and collagen fibrils (CO) are found between it and the closely associated endothelium (END).

Glutaraldehyde-Osmium, Epon, UA-LC

X 18,400

Figure 115: Electron micrograph of the apical surface of a dark cell from the distal segment; 98-mm ammocoetes.

Club-shaped microvilli (MV) and a large vacuole are seen at the apical surface (arrow). The mitochondrial cristae (CR) are angular. A transverse section of a microtubule (MT) is also seen.

Osmium, Epon, UA-LC

X 34,400

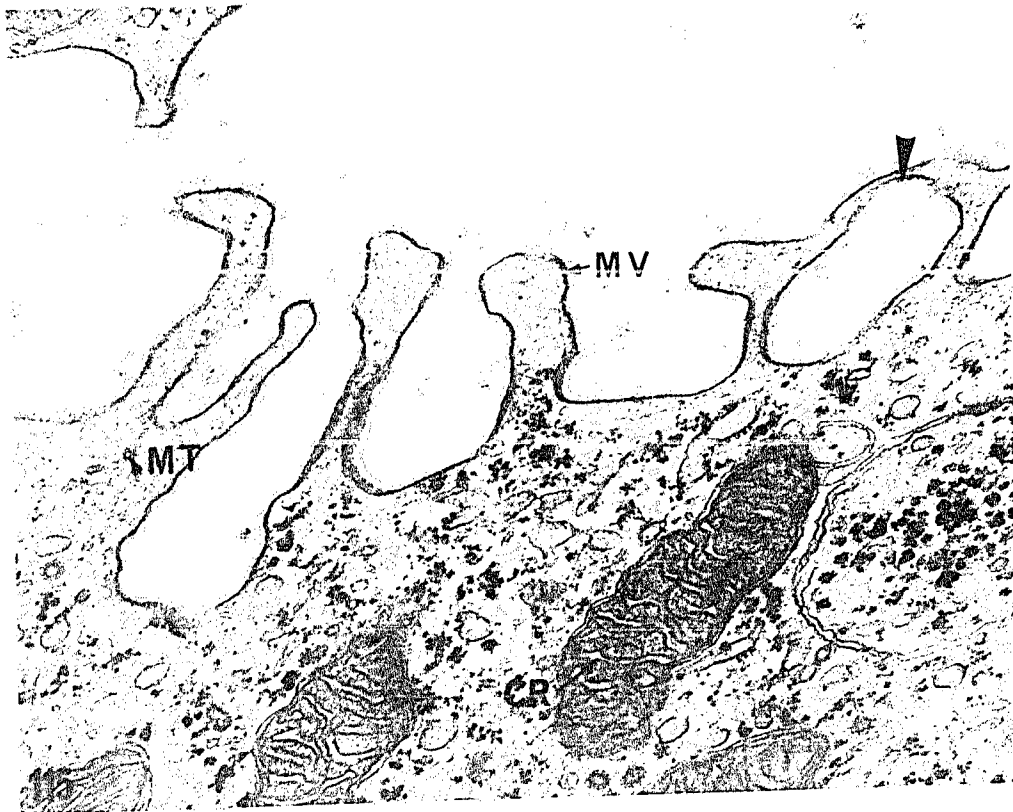
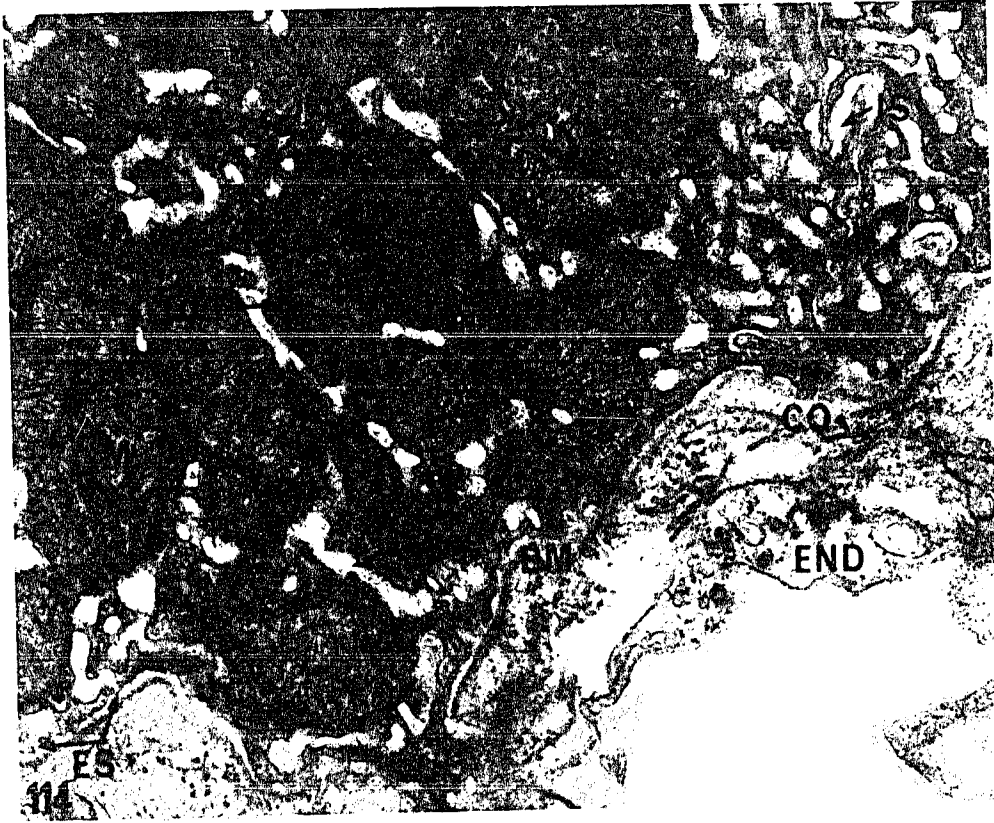


Figure 116: Electron micrograph of the apical surface of a dark cell from the distal segment; 98-mm ammocoetes.

A club-shaped cytoplasmic projection appears to contain pinocytotic vesicles (PV). A centriole (CT) is seen in the apical cytoplasm.

Osmium, Epon, UA-LC

X 45,000

Figure 117: Electron micrograph of the apical surface of a dark cell from the distal segment; 110-mm ammocoetes.

The nucleus is surrounded by a nuclear envelope, the outer layer of which is studded with ribosomes (R). Above the nucleus are found bundles of fibrils (FI) and a Golgi apparatus (GA). In the remainder of the cytoplasm are found rough ER (RER), and microtubules (MT).

Osmium, Epon, UA-LC

X 34,400

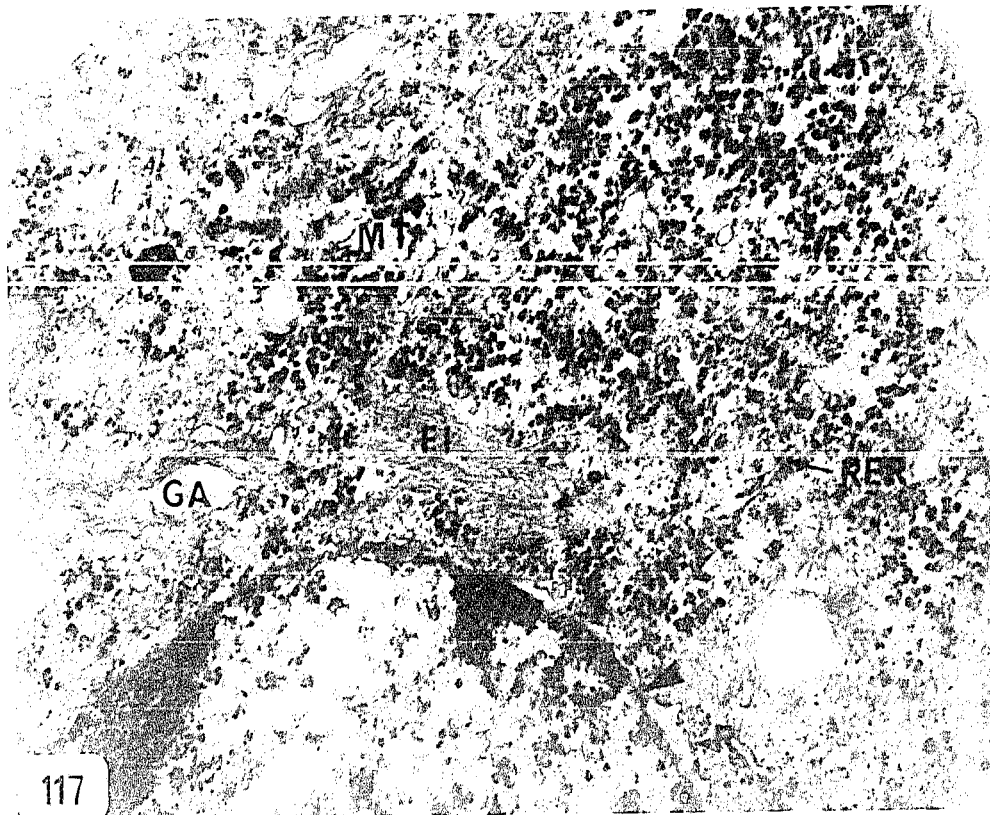
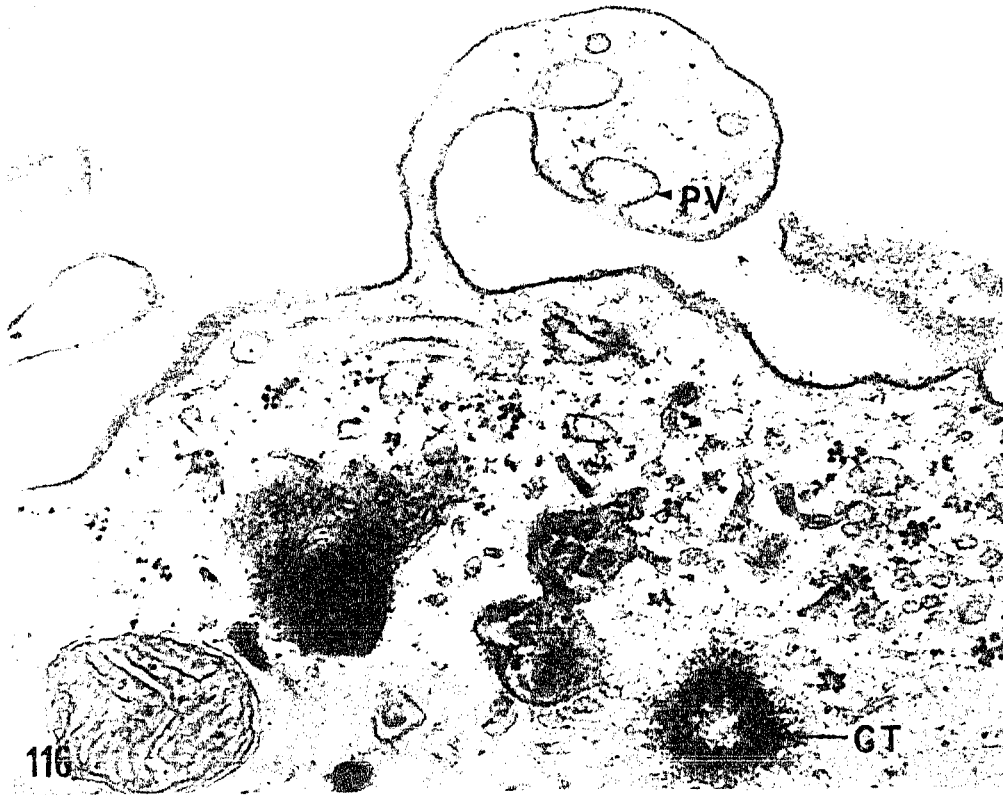


Figure 118: Electron micrograph of the apical surface of dark cells and the lumen of a distal segment; 129-mm ammocoetes.

Glycogen particles (GLY) and a cilium (CL) are found in the lumen.

Osmium, Epon UA-LC

X 11,900

Figure 119: Electron micrograph of a mitochondrion from a dark cell of the distal segment; 125-mm ammocoetes.

Cristae (CR) in transverse section appear as triangular prisms. Mitochondrial granules (arrows), 300-400 \AA in diameter, are also seen.

Osmium, Epon, UA-LC

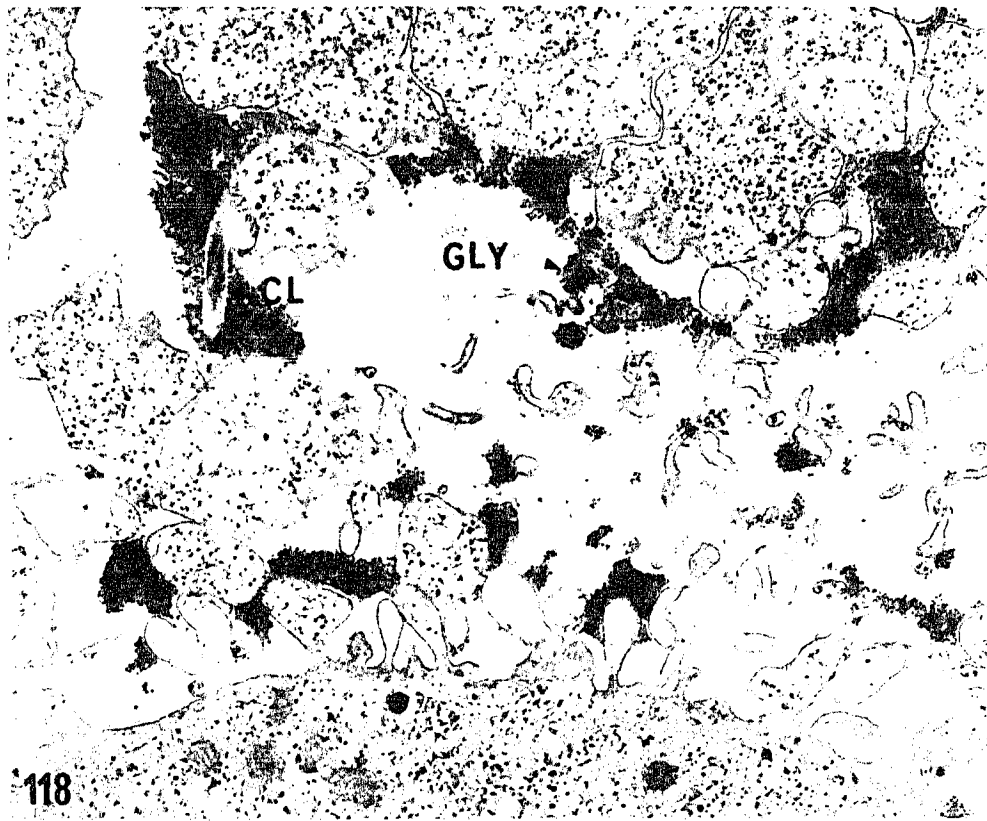
X 81,100

Figure 120: Electron micrograph of a mitochondrion from a dark cell of the distal segment; 118-mm ammocoetes.

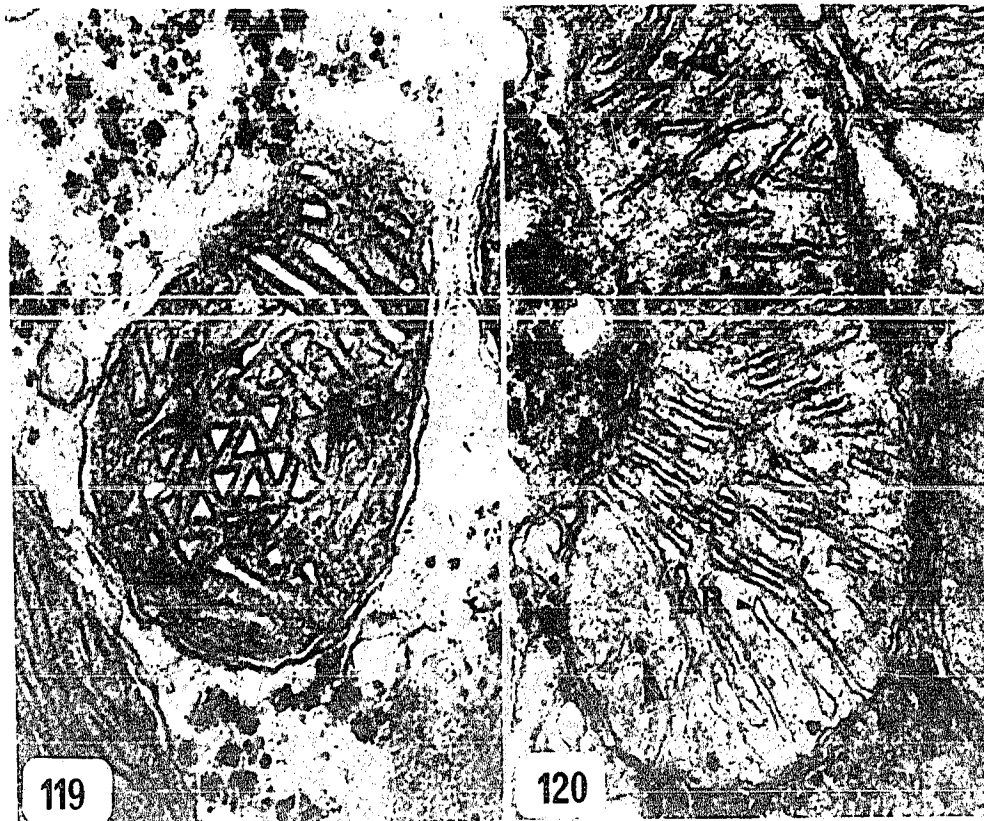
Cristae (CR) are angular and prismatic but not as regular as in the previous micrograph. The matrix contains mitochondrial granules (arrows).

Glutaraldehyde-Osmium, Epon, UA-LC

X 48,900



118



119

120

Figure 121: Electron micrograph of a portion of a dark cell from the distal segment; 40-mm ammocoetes. Glycogen particles (GLY) are of two electron densities and they are also found within membrane-bound dense bodies (DB).
Osmium, Epon, UA-LC

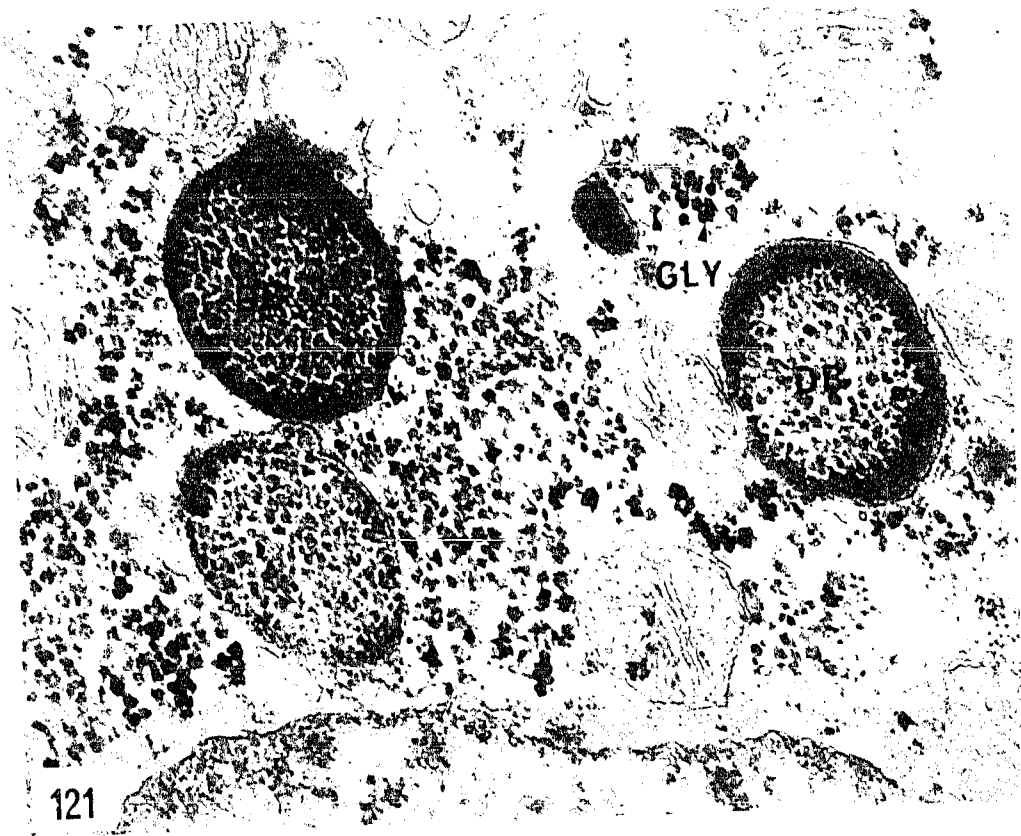
X 57,000

Figure 122: Electron micrograph of the 350-500 \AA glycogen particles in the dark cells of the distal segment; 118-mm ammocoetes.
Glutaraldehyde-Osmium, Epon, LC

X 103,000

Figure 123: Electron micrograph of an adjacent section to that of Fig. 122 showing glycogen after oxidation with periodic acid; 118-mm ammocoetes. The 300-500 \AA particles (Fig. 122) have dispersed into 37-78 \AA particles.
Glutaraldehyde-Osmium, Epon, LC

X 103, 000



121



122



123

Figure 124: Electron micrograph of dense bodies from a dark cell of the distal segment; 40-mm ammocoetes. The dense bodies contain glycogen particles (GLY) and dense wrapped lamellar structures (arrows).

Osmium, Epon, UA-LC

X 49,000

Figure 125: Electron micrograph of dense bodies from a dark cell of the distal segment; 110-mm ammocoetes.

Some dense bodies contain glycogen particles (DB) while others have a homogeneous electron density. Glycogen particles (GLY) are also found in the lumen.

Osmium, Epon, UA-LC

X 32,700

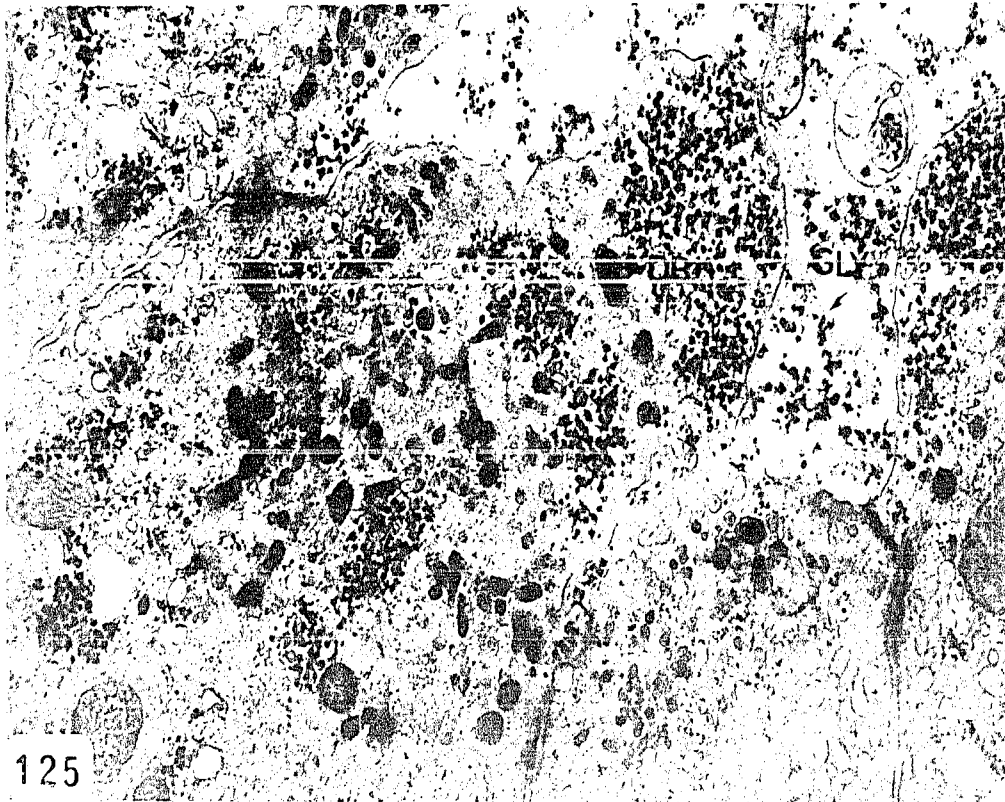
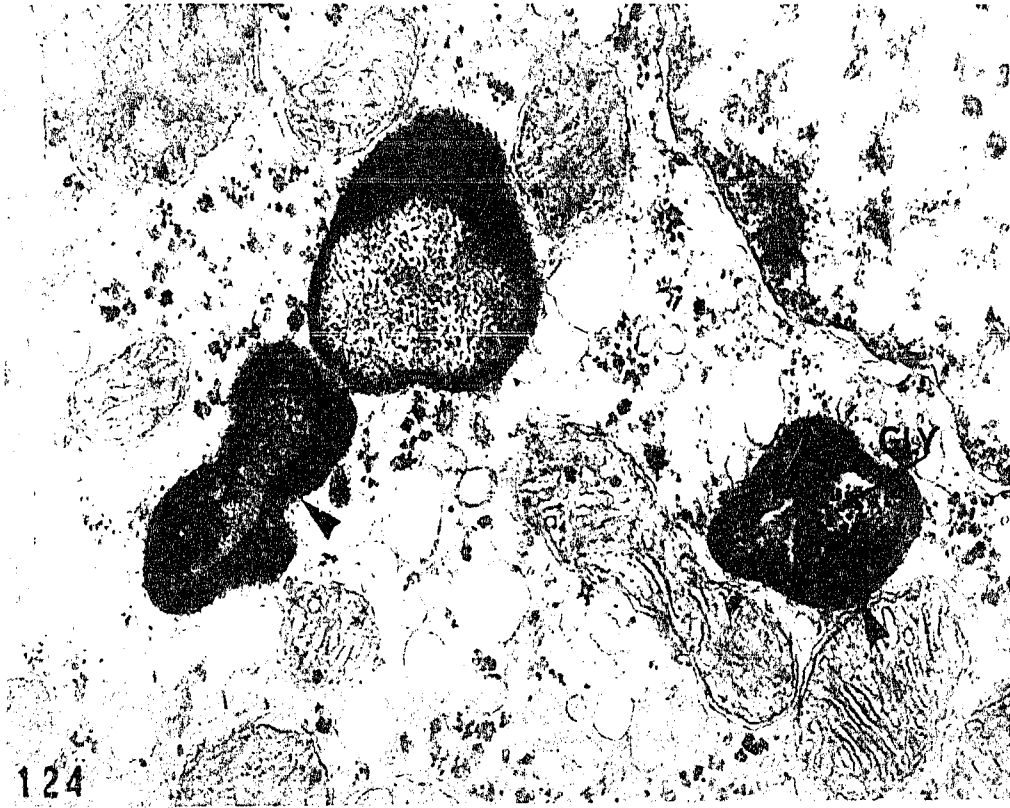


Figure 126: Light micrograph of the middle third of the kidney; parasitic adult.

The cells of the distal pars recta (DPR) are cuboidal in outline and the segment is relatively straight. The distal pars convoluta (DPC) is twisted and the cells columnar. A portion of the proximal pars recta (PPR) is also seen.

Bouin, Tissuemat, PAS-AH-OG

X 1,760

Figure 127: Light micrograph of the ventral portion of the kidney; parasitic adult.

The distal partes rectae (DPR) are lined up parallel to the collecting tubules (C). The archinephric duct (AD) is also seen.

Bouin, Tissuemat, PAS-AH-OG

X 600

Figure 128: Light micrograph of the distal pars recta; parasitic adult.

In this 0.5- μ section darker cells of the distal pars recta (DPR) are contrasted with the paler cells of the collecting duct (C). The nuclei (N) of distal cells are apically to centrally located.

Osmium, Epon, TB

X 4,700

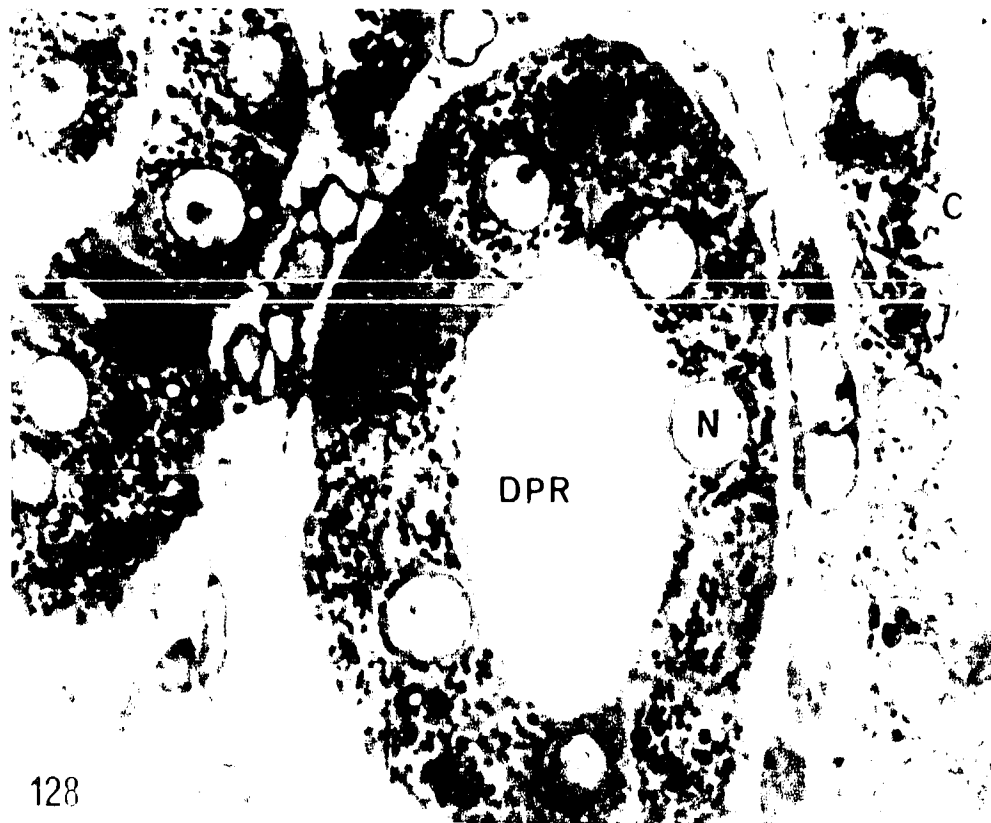


Figure 129: Electron micrograph of a cell from the distal pars recta; parasitic adult.

The apical nucleus contains peripheral clumps of chromatin (CH). Intercellular spaces (IS) are found between the cells. In the cytoplasm are mitochondria (M), bundles or fibrils (FI), dense granules (DG), and multivesicular bodies (MVB). A few microvilli are seen at the apex.

Osmium, Epon, UA-LC

X 7,800

Figure 130: Electron micrograph of a cell from the distal pars recta; parasitic adult.

The apical nucleus contains a central nucleolus (n) and peripheral clumps of chromatin (CH).

In the cytoplasm are found mitochondria (M), spherical to tubular smooth vesicles (SV), and a multivesicular body (arrow).

Osmium, Epon, UA-LC

X 11,900

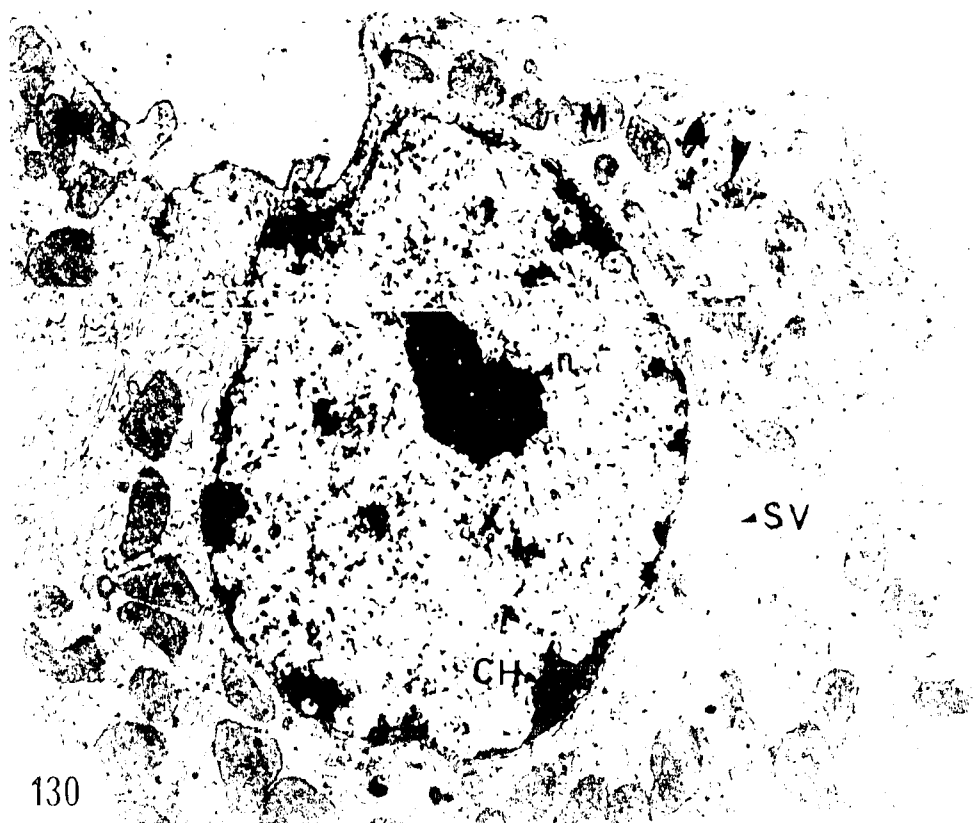
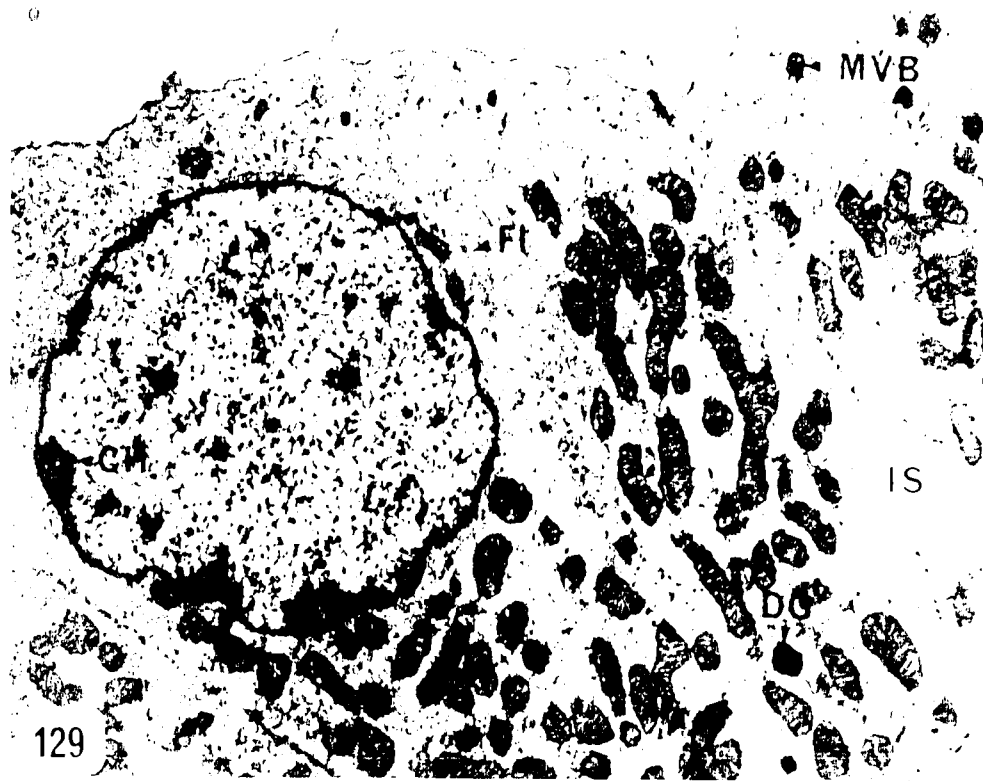


Figure 131: Electron micrograph of a cell from the distal pars recta; parasitic adult.

The central spherical nucleus contains evenly distributed chromatin (CH). A Golgi apparatus (GA) is lateral to the nucleus. Mitochondria (M) are seen in rare occasion at the apex of the cell. Microvilli are coated with fuzz (FZ).

Osmium, Epon, UA-LC

X 10,500

Figure 132: Electron micrograph of the base of the cell seen in Fig. 131; parasitic adult.

The nuclear envelope is frequently interrupted by pores (arrows). The cytoplasm contains a few strands of rough ER (RER) and free ribosomes (R). Smooth vesicles are spherical to tubular and appear to branch and anastomose with one another forming a smooth ER (SER). Collagenous fibrils (CO) are located between the basement membrane (BM) and the sinusoidal endothelium (END).

Osmium, Epon, UA-LC

X 15,000

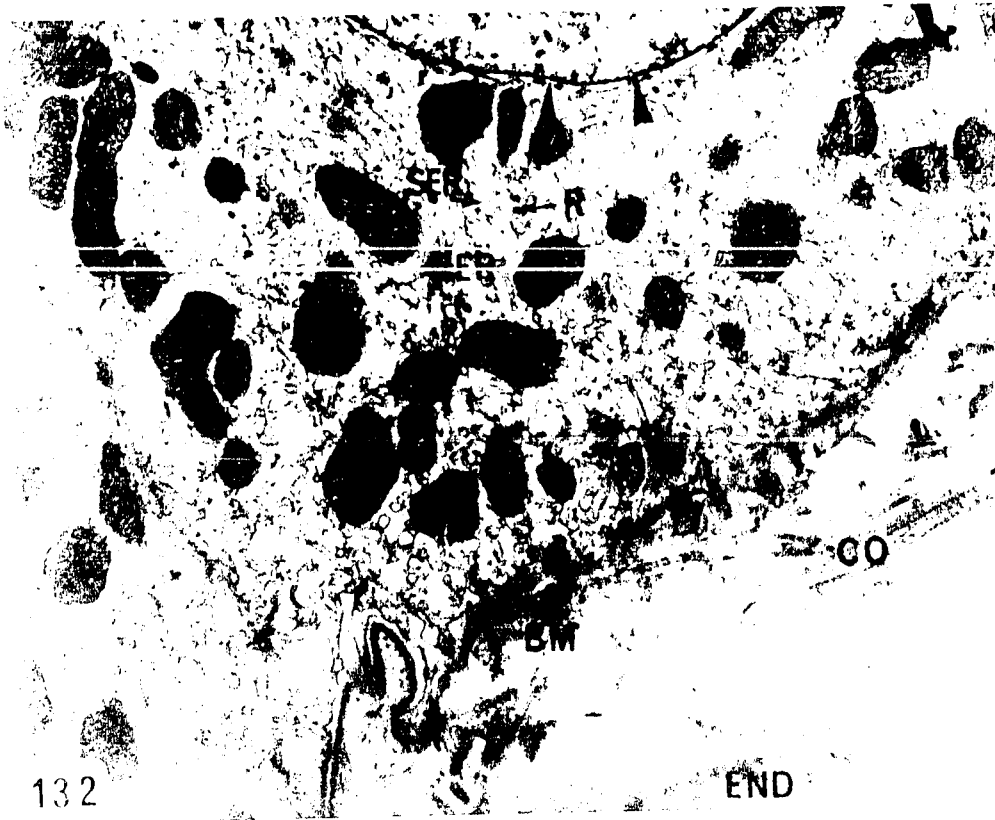


Figure 133: Electron micrograph of columnar cells of the distal pars convoluta; parasitic adult. A Golgi apparatus (GA) is seen directly above the spherical basal nucleus (N) and mitochondria are often of bizarre shapes (arrow). The microvilli (MV) are elongate.

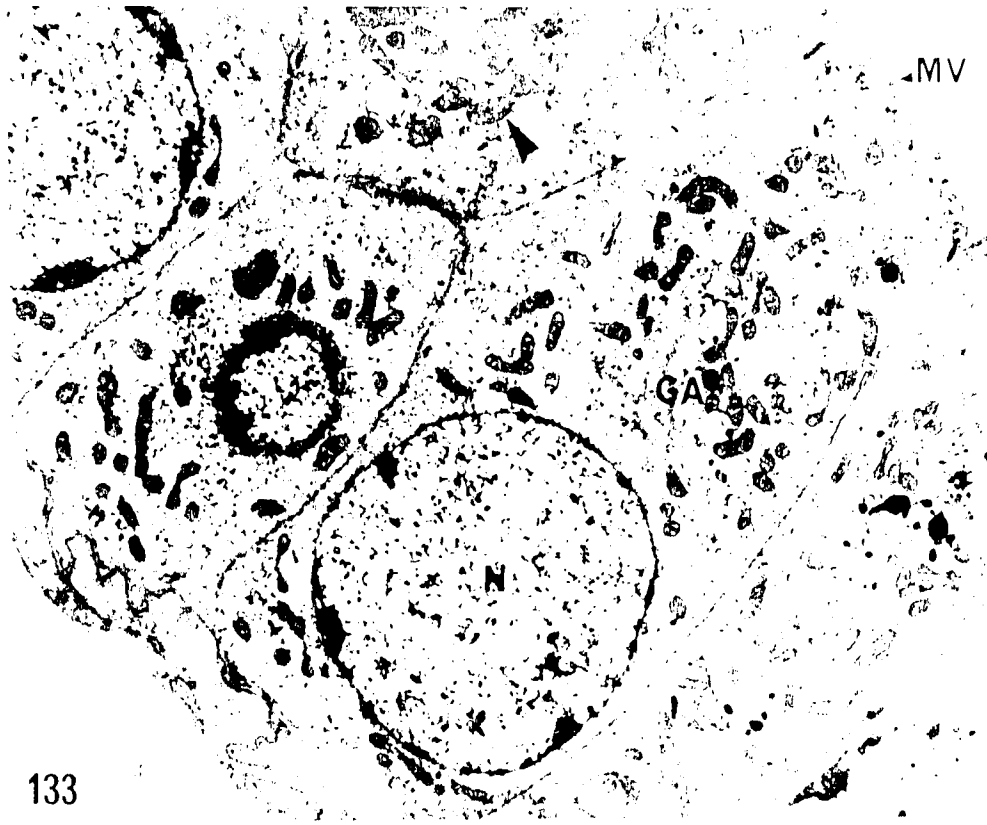
Osmium, Epon, UA-LC

X 7,100

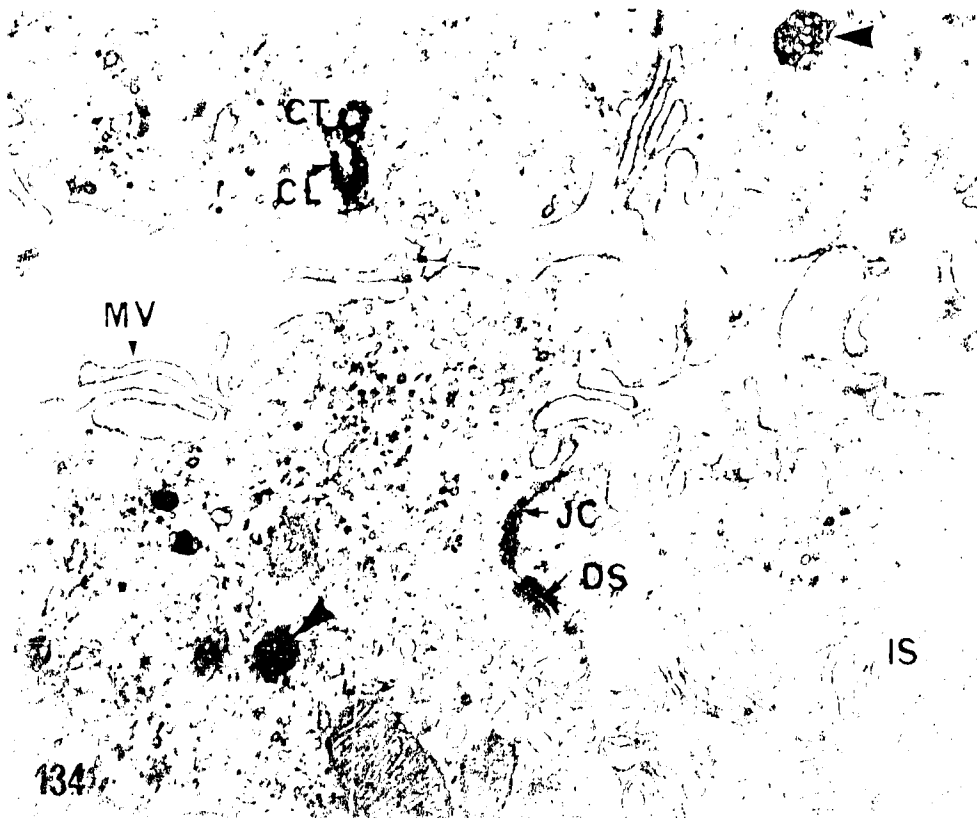
Figure 134: Electron micrograph of the apical surface of several cells of the distal pars convoluta; parasitic adult. The sides of the dome-shaped protrusions possess microvilli (MV). Adjacent cells are fused apically by a junctional complex (JC), desmosomes (DS) immediately below, and are separated by intercellular spaces (IS). A centriole (CT) and an accompanying cilium (CL) are seen below the apical surface. These cells contain numerous multivesicular bodies (arrows).

Osmium, Epon, UA-LC

X 20,000



133



134

Figure 135: Electron micrograph of the apex of two adjacent cells of the distal pars convoluta; parasitic adult.

The microvilli are coated with an electron-dense fuzzy material (FZ). The cytoplasm contains a lipid droplet (LD), numerous microtubules (MT), a multivesicular body (MVB), and coated vesicles (arrows).

Osmium, Epon, UA-LC

X 27,000

Figure 136: Electron micrograph of the base of a cell from the distal pars convoluta; parasitic adult.

The outer layer of the porous (arrows) nuclear envelope is studded with ribosomes (R) while the inner layer is lined with clumps of chromatin (CH); a particulate nucleolus (n) is central. The cell rests on a basement membrane (BM) and smooth vesicles (SV) overlie the basal plasma membrane.

Osmium, Epon, UA-LC

X 20,100

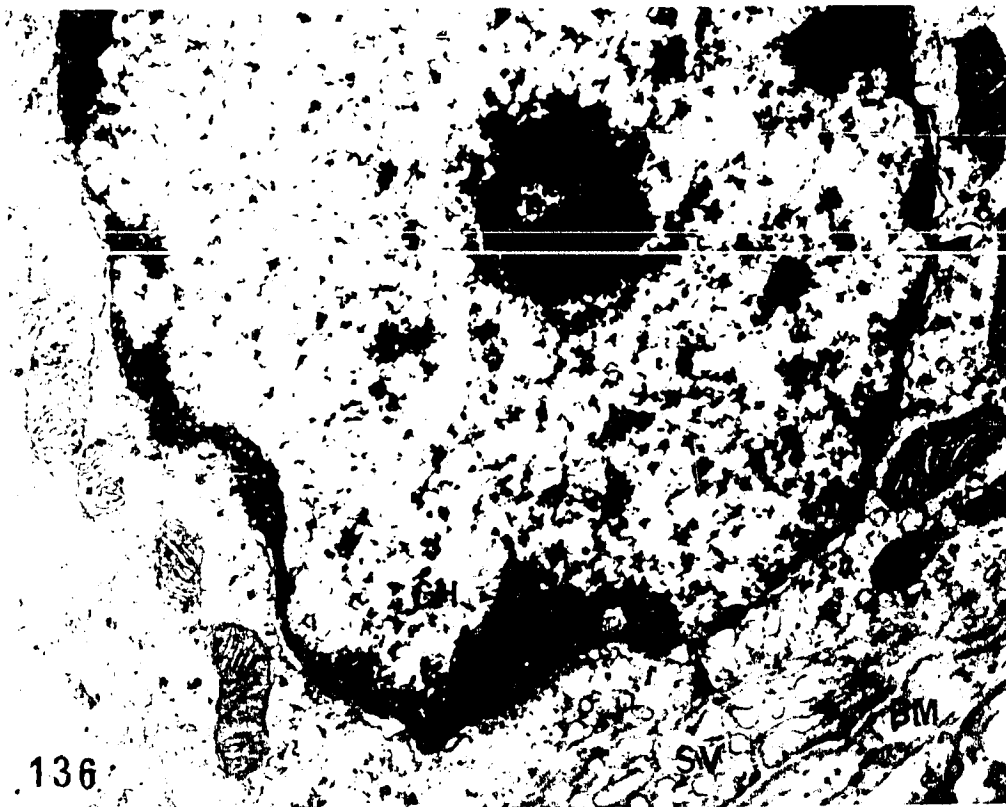


Figure 137: Electron micrograph of a tangential section through cells of the distal pars convoluta; parasitic adult.

The cytoplasm contains elongate mitochondria (M), spherical to tubular smooth ER (SER), free ribosomes (R), small strands of rough ER (RER), and a lipid droplet (LD).

Osmium, Epon, UA-LC

X 11,900

Figure 138: Electron micrograph of a tangential section through cells of the distal pars convoluta; parasitic adult.

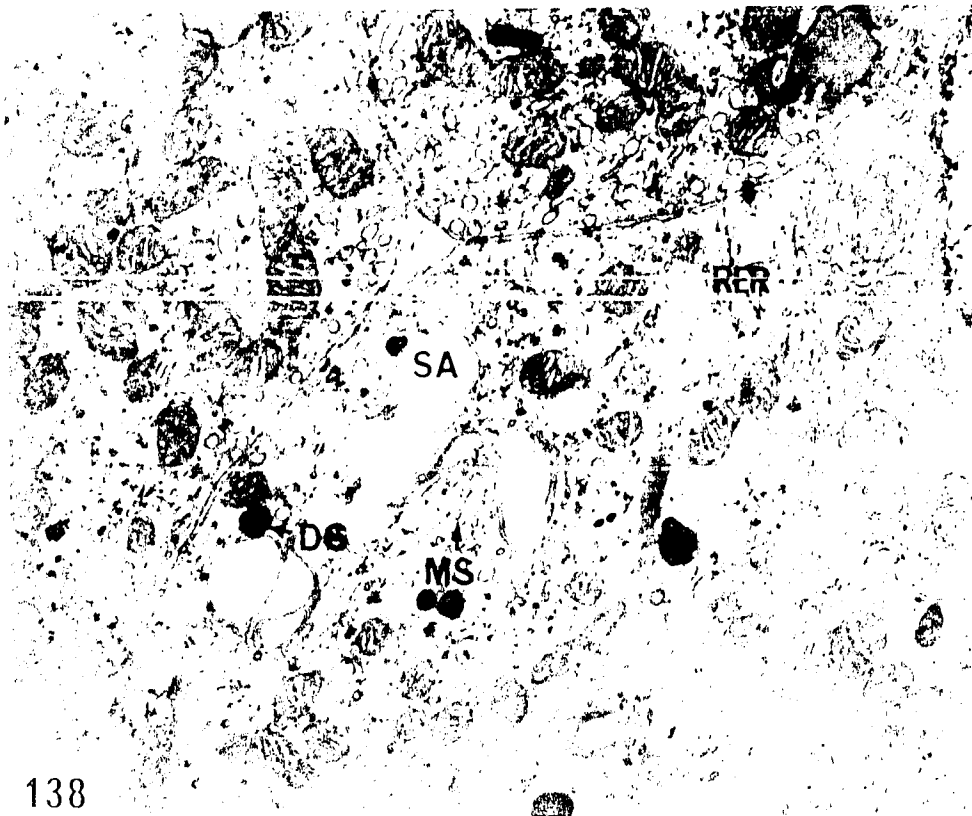
The Golgi apparatus consists of swollen saccules (SA) and microvesicles (MS). Dense granules (DG) are seen near the Golgi apparatus and rough ER (RER) is scattered throughout the cytoplasm.

Osmium, Epon, UA-LC

X 19,300



137



138

Figure 139: Electron micrograph of the apical surface of a cell of the distal pars convoluta; parasitic adult.

The apical cytoplasm contains mitochondria with transverse cristae (CR), vacuoles (V), free ribosomes (R), and a cilium (CL).

Osmium, Epon, UA-LC

X 42,200

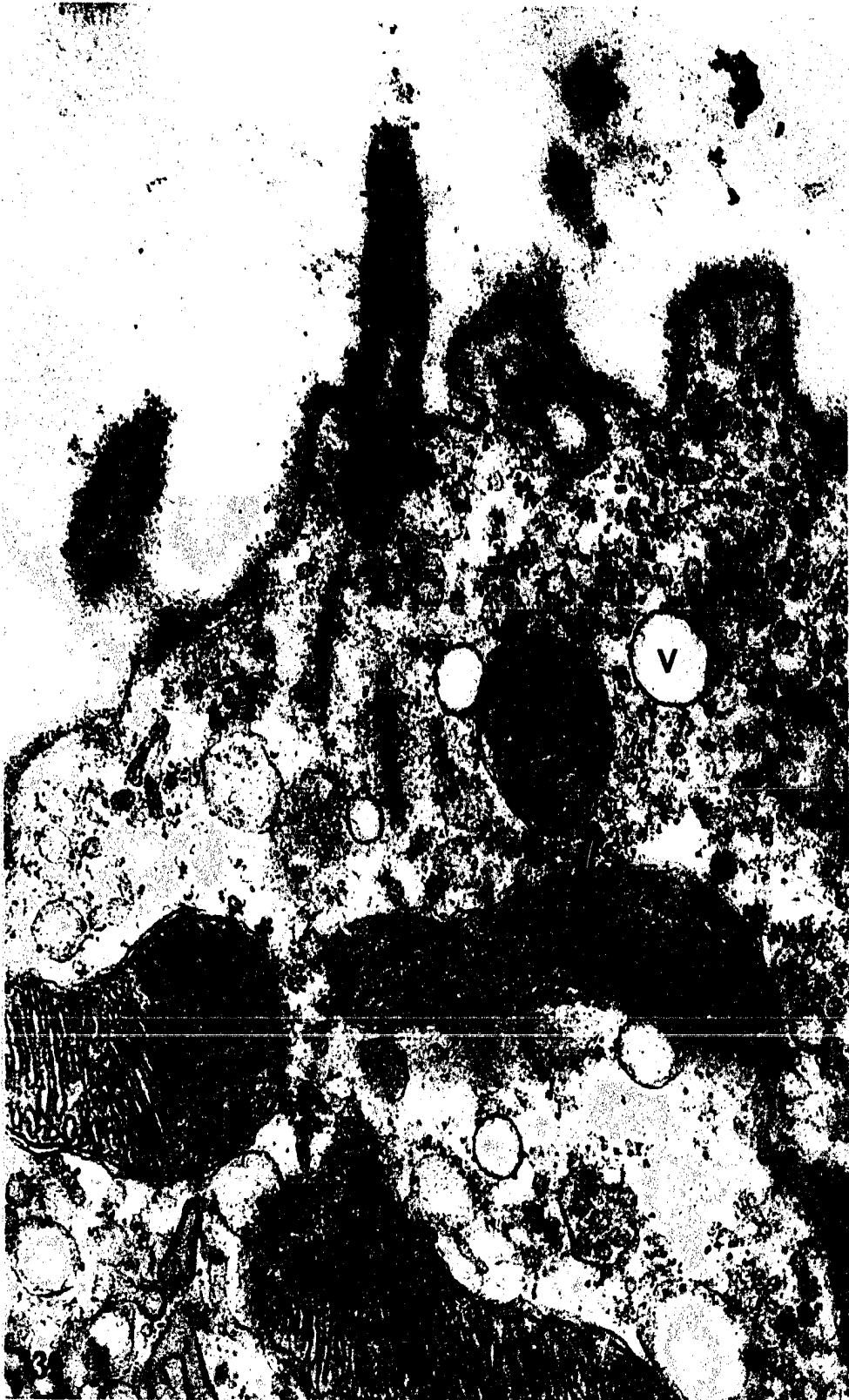


Figure 140: Light micrograph of a collecting segment; 83-mm ammocoetes.

Several collecting segments (C) are draining into a larger collecting tubule (C'). Also seen are a distal segment (D) and the proximal pars recta (PPR).

Bouin, Tissuemat, PAS-AH-OG

X 1,250

Figure 141: Light micrograph from the middle portion of the kidney; 98-mm ammocoetes.

A 0.5- μ section showing tubules of the proximal pars convoluta (PPC) and distal segments (D) one of which is continuous with the collecting segment (C).

Osmium, Epon, TB

X 1,730

Figure 142: Light micrograph of a portion of the ventral part of the kidney; parasitic adult.

The paralleling of distal pars recta (DPR) and collecting segments (C) is seen. Two collecting segments join a common collecting segment (C') which is continuous with the archinephric duct (not seen in this micrograph).

Bouin, Tissuemat, PAS-AH-OG

X 1,000

Figure 143: Light micrograph of a collecting segment near the archinephric duct; 98-mm ammocoetes. In this 0.5- μ section a dark cell (DC) is seen in both the collecting segment (C) and the archinephric duct (AD). Note the central nucleolus (n) in a cell of the collecting segment.

Osmium, Epon, TB

X 3,500

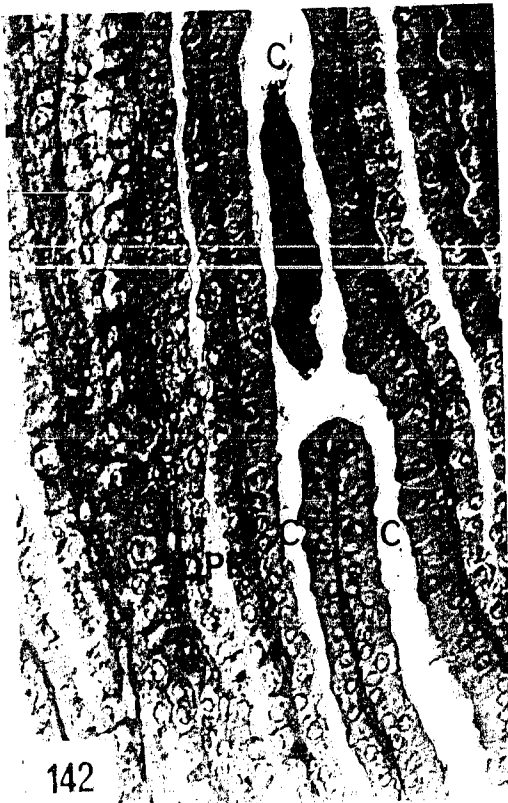
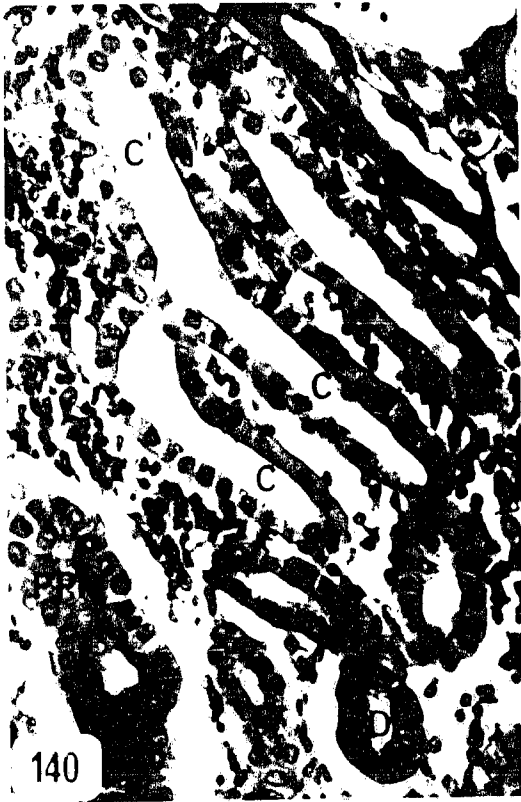


Figure 144: Electron micrograph of cells from a collecting segment; 74-mm ammocoetes.

The spherical nucleus is central and the dome-shaped apex of the cell is devoid of microvilli (arrow). Mitochondria (M) are spherical or rod-shaped.

Osmium, Epon, UA-LC

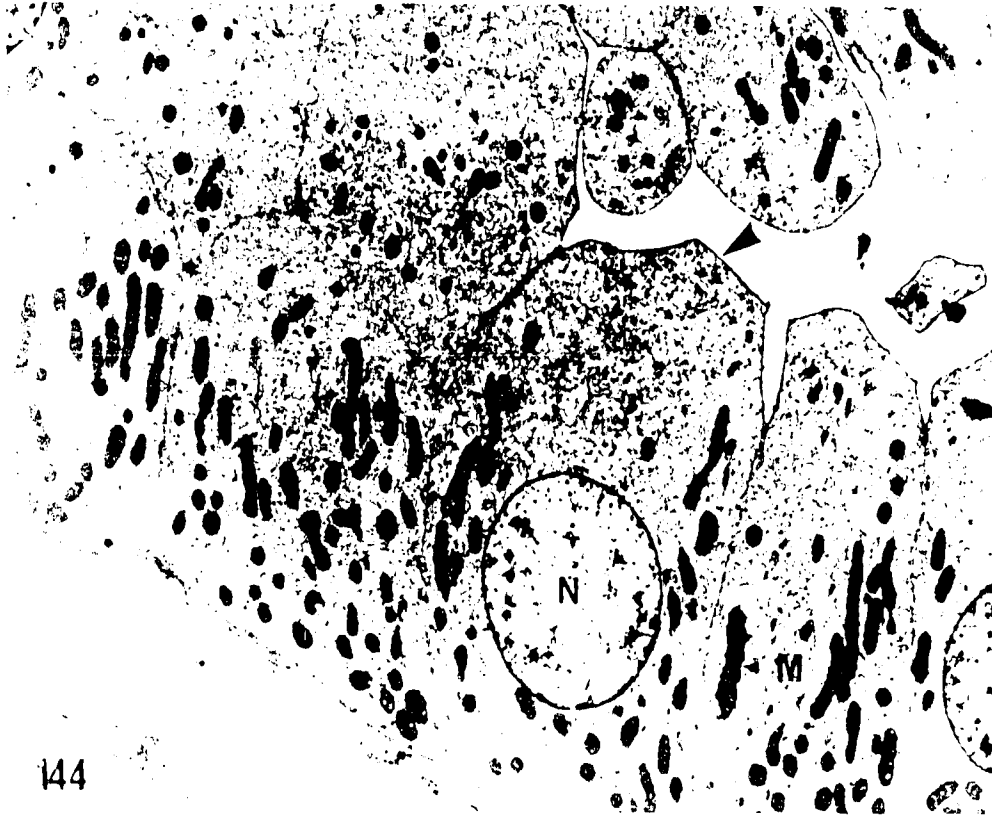
X 5,000

Figure 145: Electron micrograph of the apices of cells of the collecting segment; 74-mm ammocoetes.

The domed apices are covered with an electron-dense fuzzy coating (FZ). Intercellular spaces (IS) are found between adjacent cells.

Osmium, Epon, UA-LC

X 14,250



144



145

Figure 146:

Electron micrograph of several cells in the collecting segment; 98-mm ammocoetes. Adjacent cells are fused by an apical junctional complex (JC). Desmosomes (DS) are seen at each end of intercellular spaces (IS) between the cells. A few microvilli, coated with fuzz (FZ), are found at the apex. Collagenous fibrils (CO) are found between the basement membrane (BM) and the sinusoidal endothelial cells (END). Nuclear chromatin (CH) is evenly distributed, and dense granules (DG) are found in the cytoplasm.

Osmium, Epon, UA-LC

X 9,700

Figure 147:

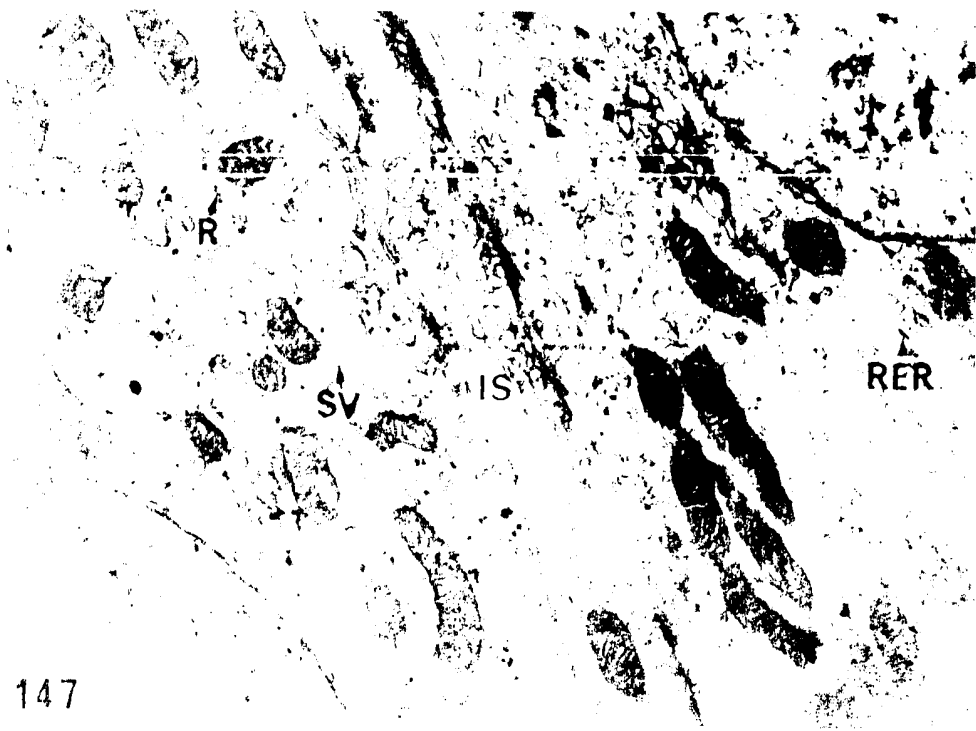
Electron micrograph of several cells of a collecting segment; 98-mm ammocoetes. A large number of smooth vesicles (SV), a few strands of rough ER (RER), and free ribosomes (R) occur in the cytoplasm. Intercellular spaces (IS) are found between cells. A Golgi apparatus (GA) is seen lateral to the nucleus.

Osmium, Epon, UA-LC

X 16,900



END
146



147

Figure 148:

Electron micrograph of several cells from the collecting segment; 125-mm ammocoetes.

A cell similar to that of the distal tubule (D) is found between two cells of the collecting segment (C). The collecting cells contain dense granules (DG) and large mitochondria (M).

Osmium, Epon, UA-LC

X 13,000

Figure 149:

Electron micrograph of several cells from the collecting segment; 74-mm ammocoetes.

A dark distal cell with abundant smooth ER (SER) is seen between two cells of the collecting segment (C).

Osmium, Epon, UA-LC

X 19,300

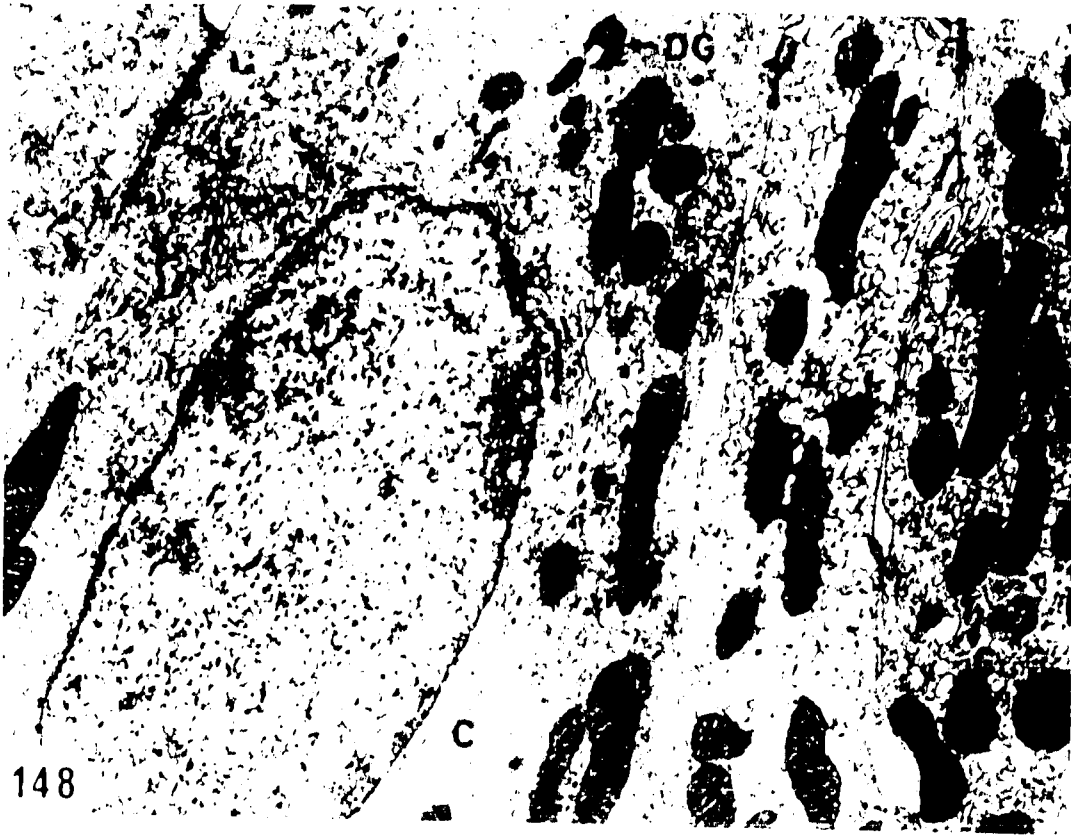


Figure 150: Light microrgraph from the ventral part of the kidney; parasitic adult.

In this 0.5- μ section the collecting segment (C) is contrasted with the distal pars recta (DPR). The tubules are surrounded by sinusoids (S). The nucleoli (n) are usually eccentric in the nuclei of the collecting cells.

Osmium, Epon, TB

X 5,600

Figure 151: Electron micrograph of cells from the collecting segment; parasitic adult.

The cells are closely associated with sinusoids (S). The nucleus (N) is central to basal and the apices of the cells possess irregular microvilli (arrow).

Osmium, Epon, UA-LC

X 9,000

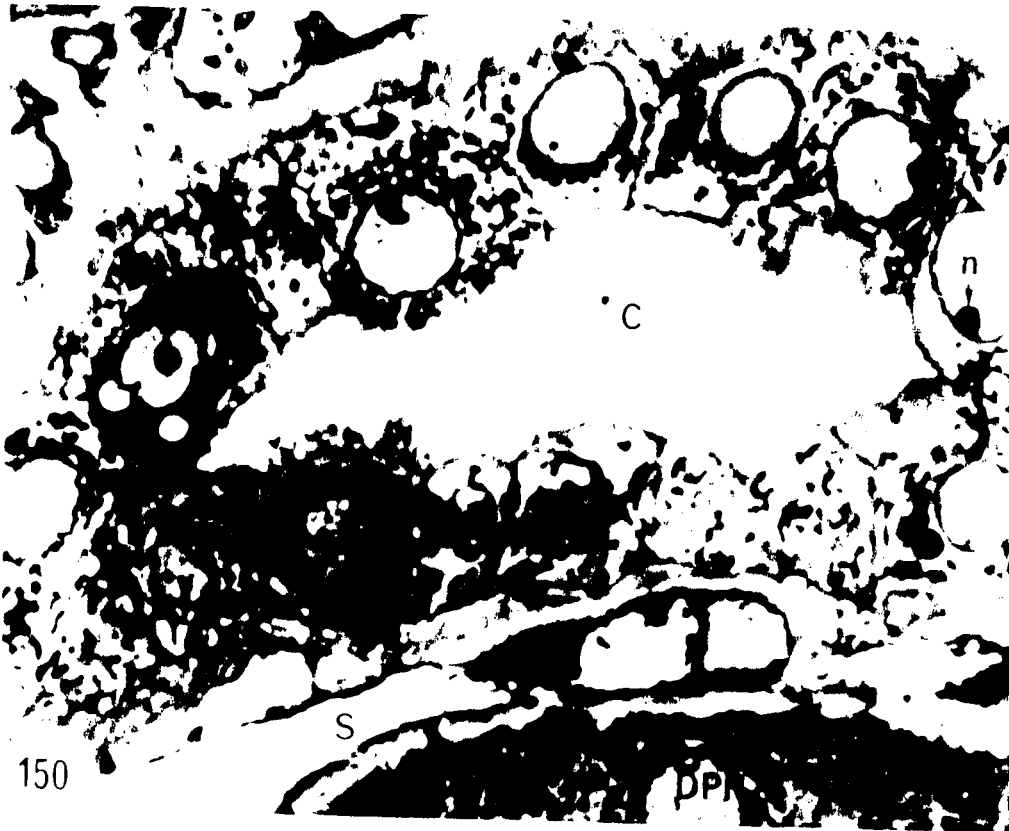


Figure 152: Electron micrograph of the apical surfaces of two adjacent cells from a collecting segment; parasitic adult. The microvilli are covered by an electron dense fuzzy coating (FZ). Adjacent plasma membranes are fused apically into a junctional complex (JC) and smooth vesicles (SV) are seen below the surface.

Osmium, Epon, UA-LC

X 34,000

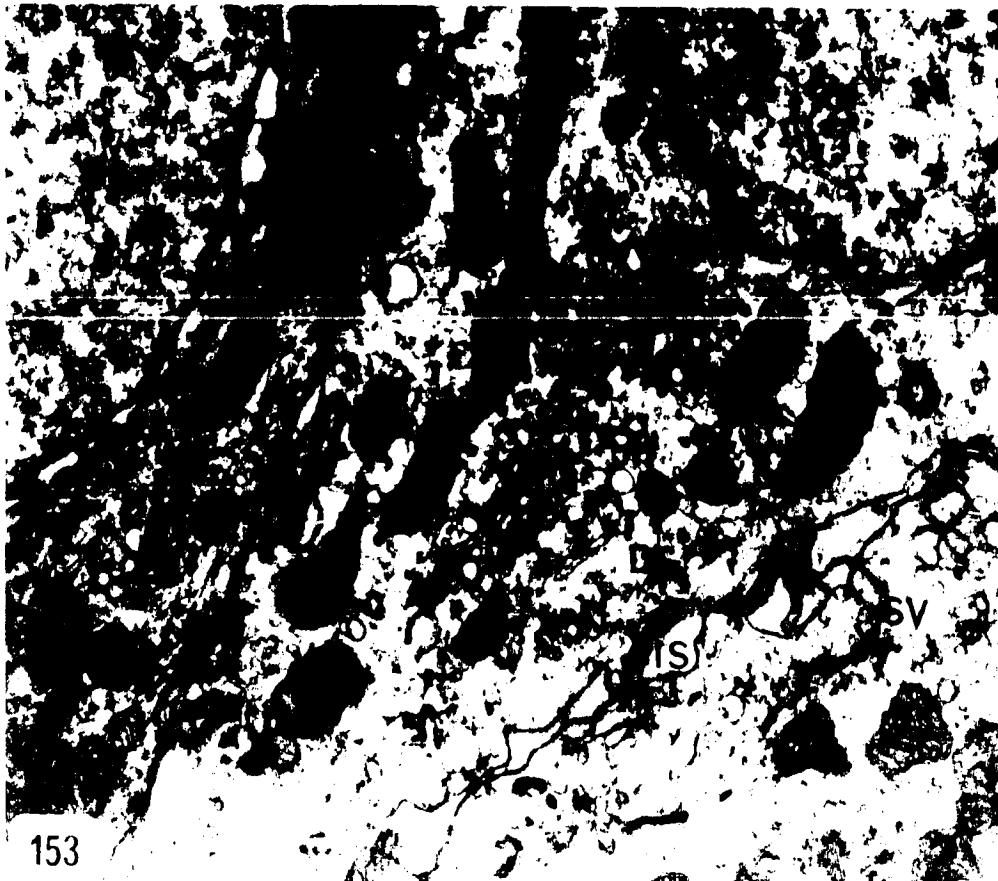
Figure 153: Electron micrograph of portions of three adjacent cells from a collecting segment; parasitic adult. A double-layered nuclear envelope is interrupted by pores (arrow). In the cytoplasm are found a Golgi apparatus (GA), mitochondria (M) dense granules (DG), and smooth vesicles (SV). Intercellular spaces (IS) between adjacent cells.

Osmium, Epon, UA-LC

X 18,400



152



153

Figure 154: Electron micrograph of a portion of a cell from a collecting segment; parasitic adult. Adjacent plasma membranes are fused laterally by desmosomes (DS) and intercellular spaces (IS) are seen. A few strands of rough ER (RER) and a coarse network of fibrils (FI) are seen in the cytoplasm.

Osmium, Epon, UA-LC

X 14,000



Figure 155: Electron micrograph showing the junction of three adjacent cells from a collecting segment; parasitic adult.

This tangential section shows the fusion of adjacent plasma membranes by desmosomes (DS) and the coarse network of fibrils (FI) running throughout the cytoplasm. Ribosomes (R) are seen in the cytoplasm.

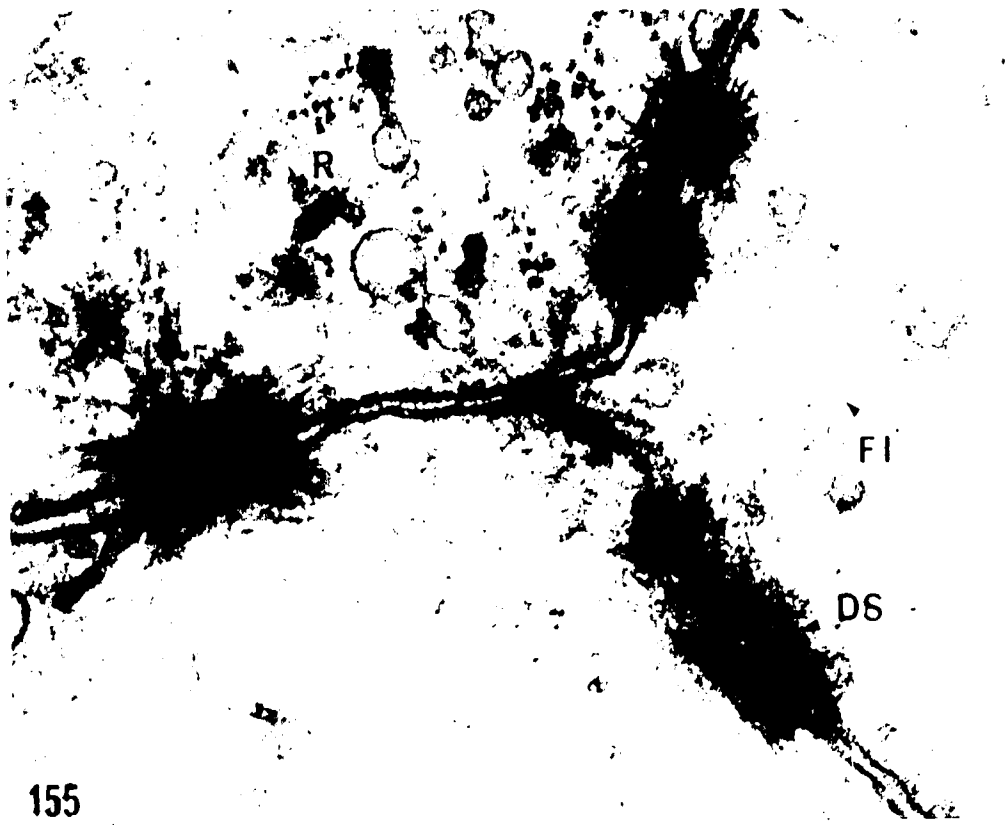
Osmium, Epon, UA-LC

X 69,000

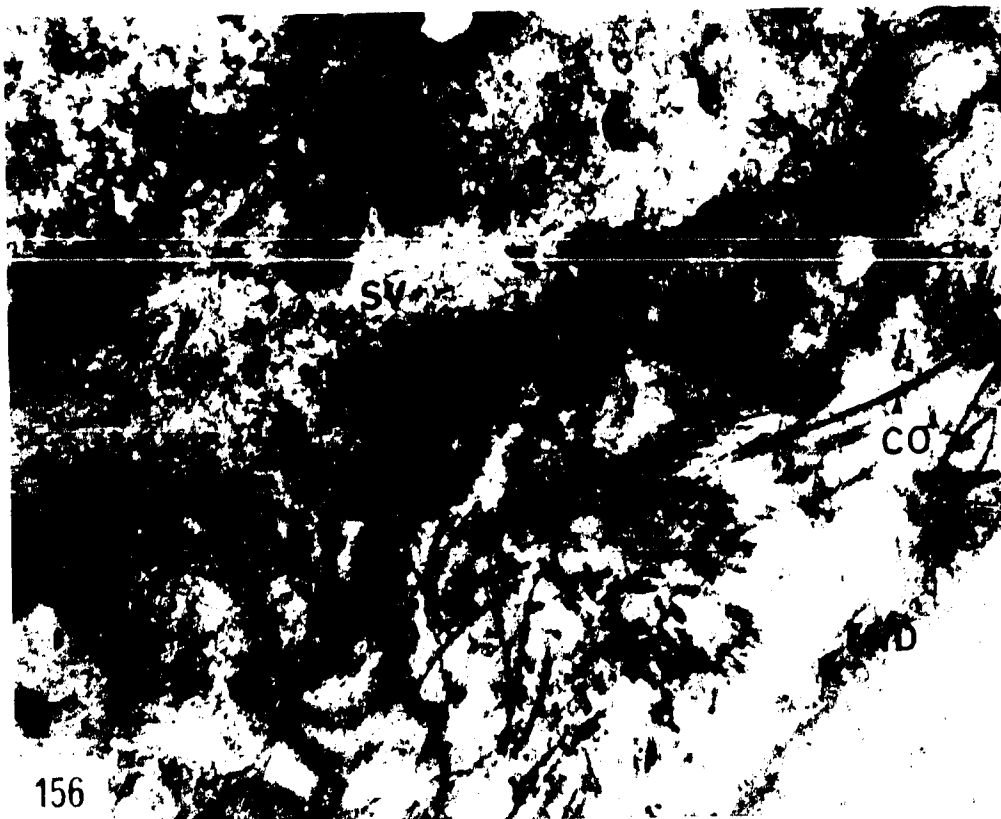
Figure 156: Electron micrograph of the base of a cell from a collecting segment; parasitic adult. Numerous smooth vesicles (SV) are seen at the base. Collagenous fibrils (CO) are found between the basement membrane (BM) and the endothelium (END) of sinusoids.

Osmium, Epon, UA-LC

X 18,500



155



156

Figure 157: Electron micrograph showing the apex of cells in the anterior portion of the archinephric duct; 98-mm ammocoetes.

The apical surface is covered by a fibrillar fuzz (FZ). The apical cytoplasm contains small dense granules (DG), ribosomes (R), mitochondria (M), smooth vesicles (SV), rough ER (RER) and a Golgi apparatus (GA). Intercellular spaces are found between the cells (arrows).

Osmium, Epon, UA-LC

X 14,000

Figure 158: Light micrograph of the archinephric duct; 125-mm ammocoetes.

This 0.5- μ section shows the stratified epithelium and the large sinusoids (S) surrounding the duct (AD).

Osmium, Epon, TB

X 1,100

Figure 159: Light micrograph of a portion of the archinephric duct; 55-mm ammocoetes.

This 0.5- μ section shows intercellular spaces (arrows) between cells.

Osmium, Epon, TB

X 4,200

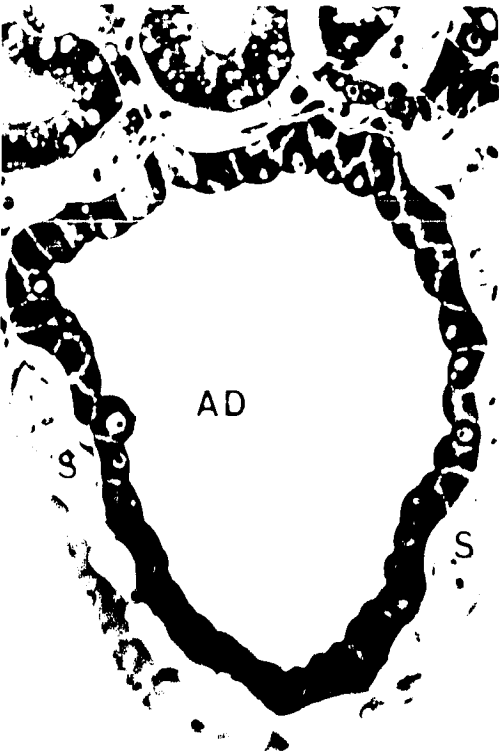
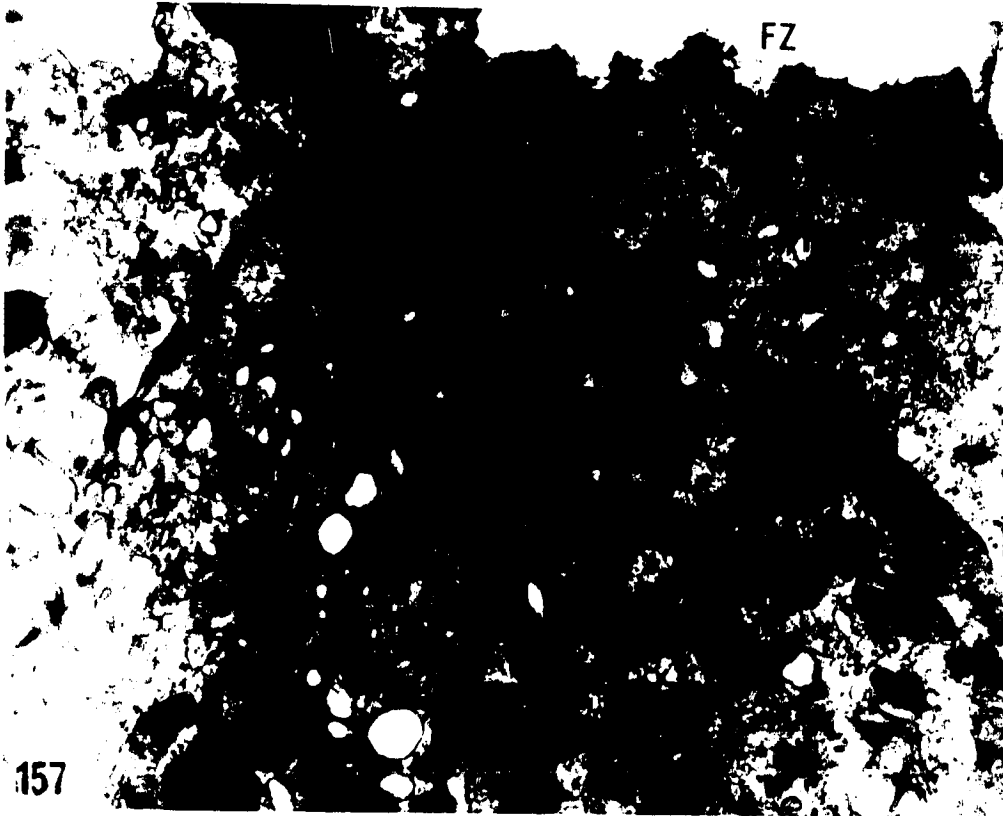


Figure 160: Electron micrograph of cells of the archinephric duct from the posterior part of the kidney; 125-mm ammocoetes.

The cells possess microvilli apically (arrows) and bridging the intercellular spaces (IS).

The nucleus contains peripheral chromatin (CH) and large nucleolus (n). Some cells (DC) appear more electron dense than others (LC).

Osmium, Epon, UA-LC

X 7,000



LC

IS

n



Figure 161:

Electron micrograph of the basal cells of the archinephric duct; 62-mm ammocoetes.

A dark cell (DC) can be distinguished from all other cells. Desmosomes (DS) are found at end of each intercellular space (IS). The cytoplasm of the lighter cells contains small amounts of glycogen (GLY), fibrils (FI), and smooth vesicles (SV). The epithelium rests on a basement membrane (BM) which is separated from a sinusoid (S) by collagenous fibrils (CO).

Osmium, Epon, UA-LC

X 9,000

Figure 162:

Electron micrograph of superficial cells of the archinephric duct; 62-mm ammocoetes.

The apex of the cell contains multivesicular bodies (MVB) and large numbers of mitochondria (M). Cells intermediate in location are attached only by their thin cytoplasmic projections (arrows).

Osmium, Epon, UA-LC

X 9,000

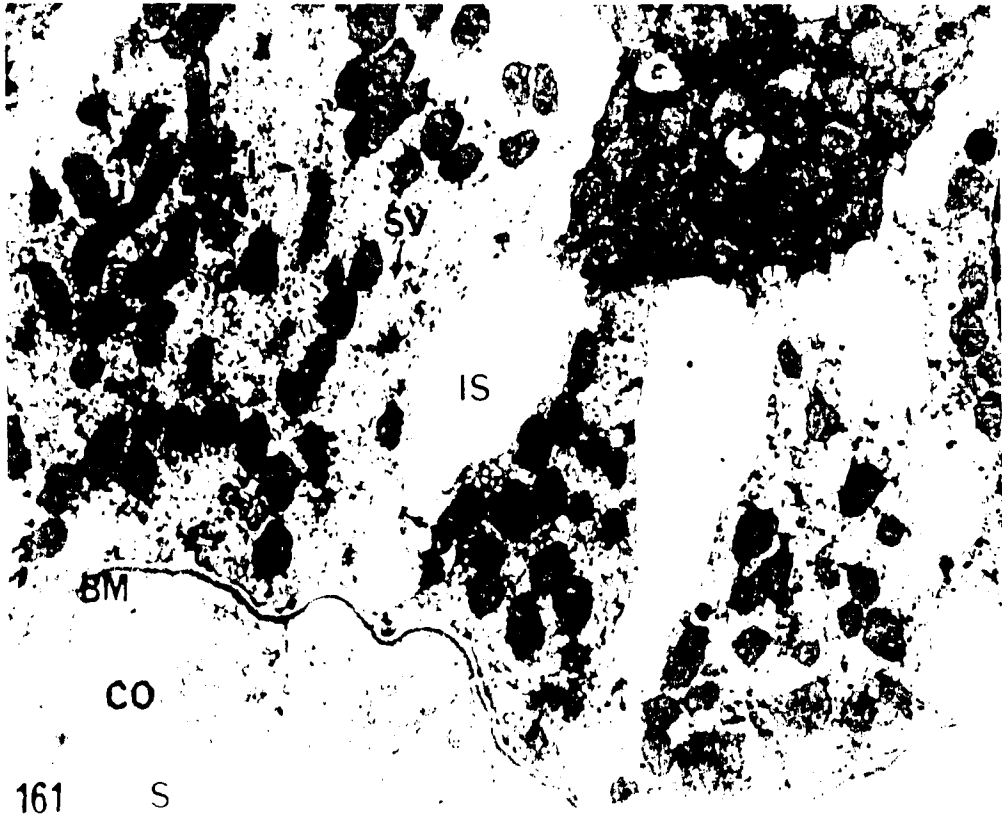


Figure 163: Electron micrograph of a portion of a dark cell from the archinephric duct; 125-mm ammocoetes. The cytoplasm contains myelin figures (arrow) and clumps of glycogen (GLY) surrounding mitochondria with angular cristae (CR). Smooth vesicles (SV) are located near the Golgi apparatus (GA).

Osmium, Epon, UA-LC

X 15,000

Figure 164: Electron micrograph of a portion of figure 162; 125-mm ammocoetes.

A myelin figure is composed of several membranous layers (MB) and contains dense deposits (DD).

Osmium, Epon, UA-LC

X 49,000

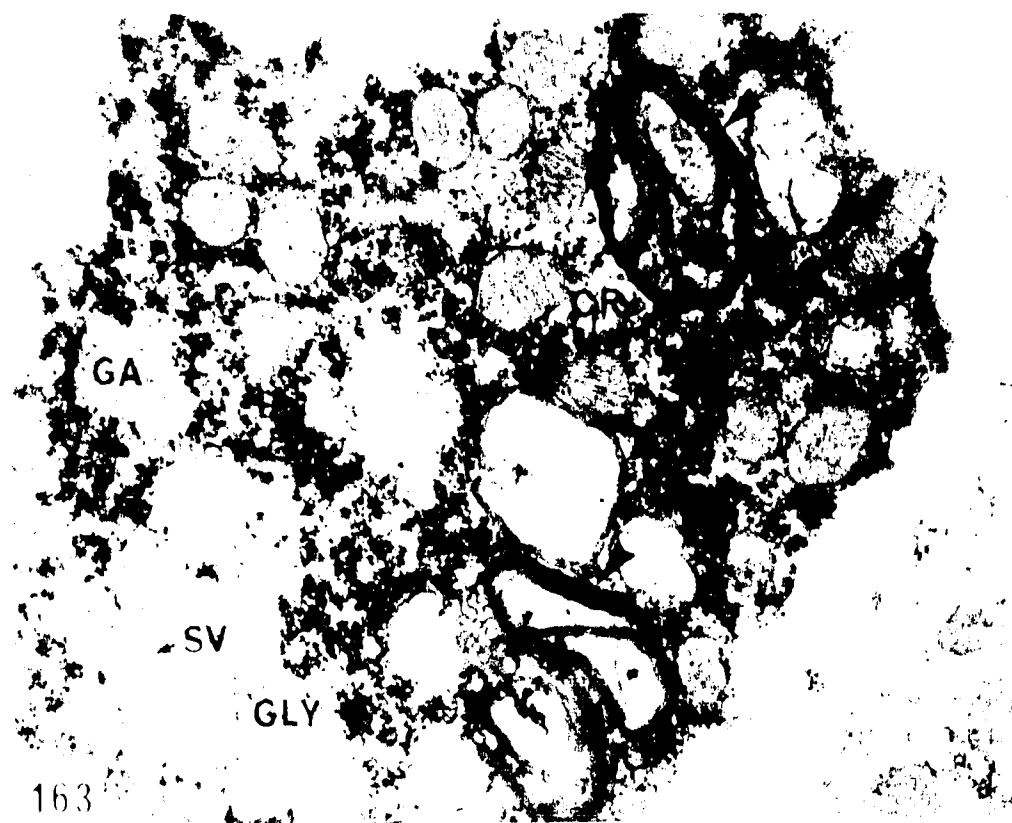


Figure 165A: Light micrograph of a portion of the wall of the archinephric duct; parasitic adult. The wall consists of four layers: an epithelium (a), connective tissue (b), smooth muscle (c), and dense connective tissue (d). Note the intensely staining superficial cells (arrows).

Bouin, Tissuemat, PAS-H-OG

X 3,000

Figure 165B: Light micrograph of a portion of the wall of the archinephric duct; parasitic adult. The superficial; cells are intensely stained with PAS in this 2.0- μ section. Intermediate (IN) and basal cells (BA) contain smaller numbers of PAS staining granules (arrows).

Osmium, Epon, PAS-H

X 3,000

Figure 166: Electron micrograph of the epithelium of the archinephric duct; parasitic adult. The superficial cells are type I (S_1). Inter-cellular spaces (IS) are found between intermediate (IN) and basal cells (BA).

Osmium, Epon, UA-LC

X 5,000

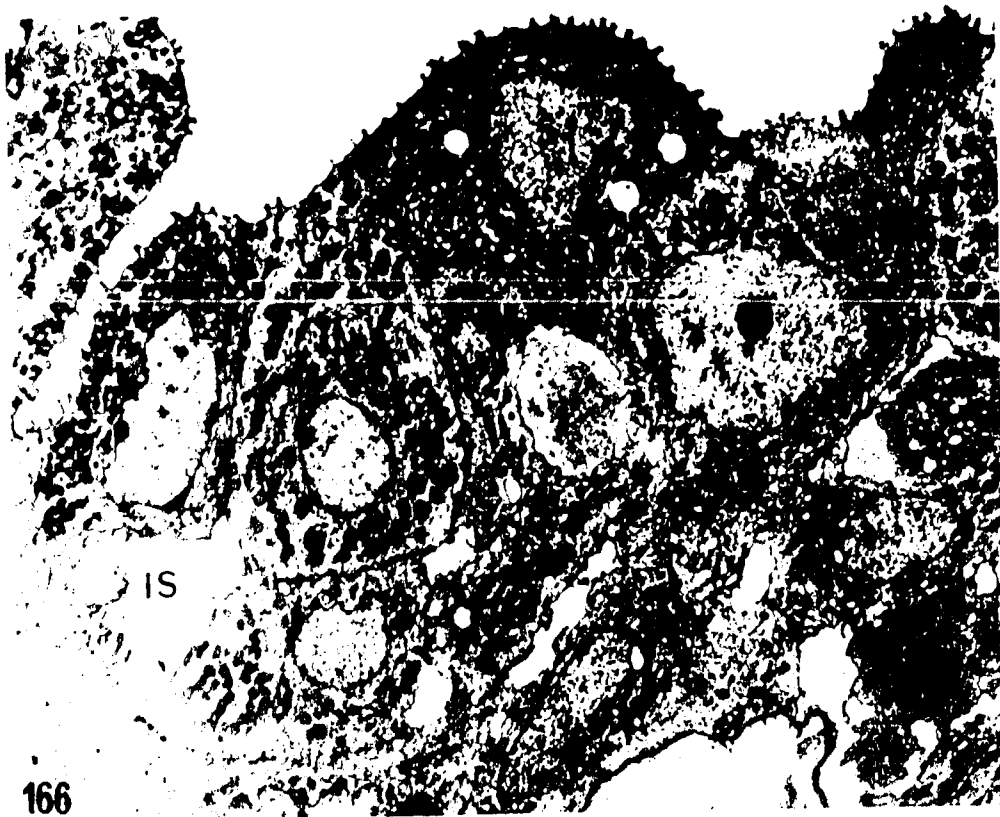


Figure 167: Electron micrograph of the base of archinephric duct epithelium; parasitic adult.

The base of the epithelium (EP) is irregular and is separated from the sinusoid endothelium (S) by a 2.5-to 4.0- μ space which contains collagenous fibrils (CO) and occasional blood cells (BC).

Osmium, Epon, UA-LC

X 5,000

Figure 168: Electron micrograph showing three layers of the archinephric duct; parasitic adult.

The basal cells are separated by intercellular spaces (IS). A collagenous layer (CO) separates the epithelium from a layer of smooth muscle (SM).

Osmium, Epon, UA-LC

X 6,500



Figure 169: Electron micrograph of the smooth muscle from the archinephric duct; parasitic adult.

The smooth muscle cells contain fibrils (FI), pinocytotic vesicles (PV), and mitochondria (M).

Osmium, Epon, UA-LC

X 14,000

Figure 170: Electron micrograph of basal epithelial cells of the archinephric duct; parasitic adult.

The cells are separated by interdigitating plasma membranes (arrow) which also enclose intercellular spaces (IS). The cytoplasm contains rough ER (RER), a Golgi apparatus (GA), smooth vesicles (SV), mitochondria (M) and free ribosomes (R).

Osmium, Epon, UA-LC

X 11,400

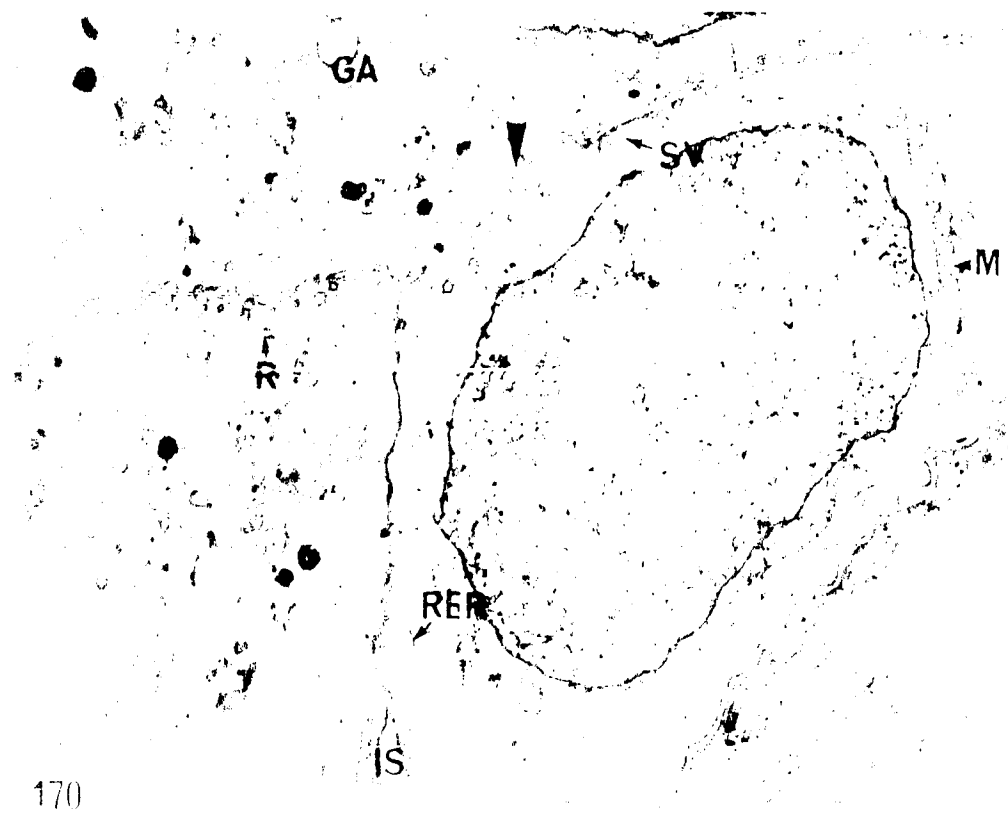
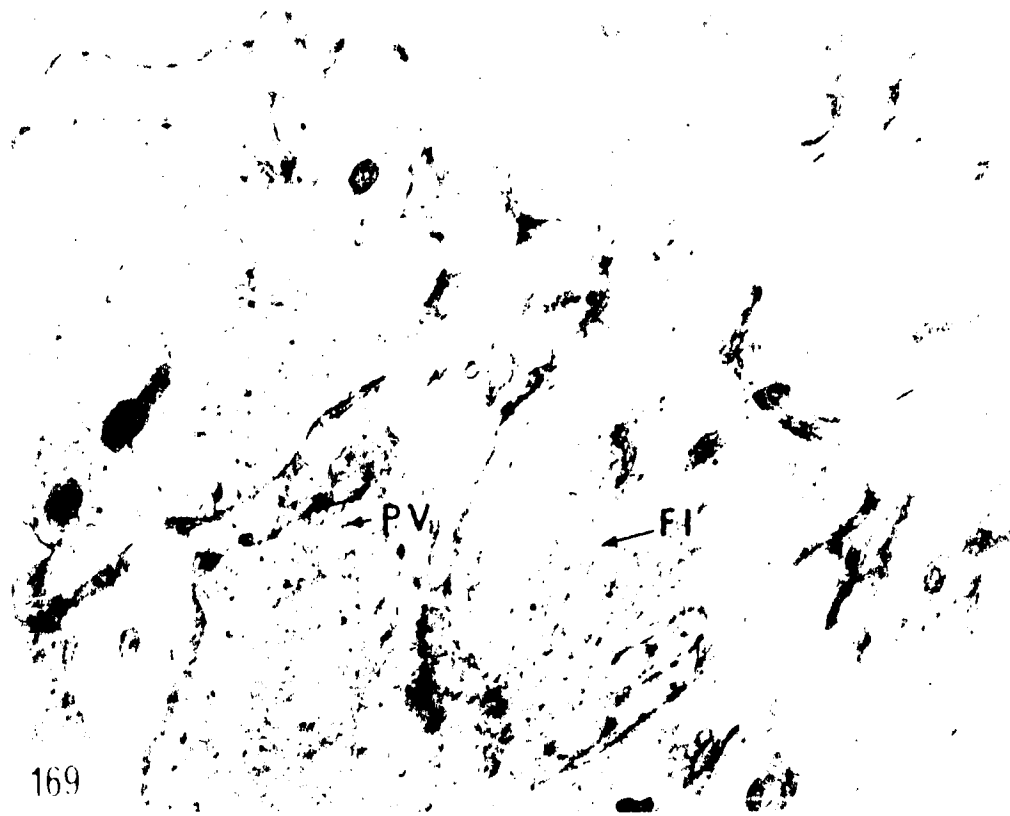


Figure 171: Electron micrograph of the apical surface of the epithelium of the archinephric duct; parasitic adult.

Type I cells (S₁) overlie intermediate cells which contain two or three Golgi apparatuses (GA), numerous mitochondria (M), and a nucleus with peripheral chromatin (CH) and a nucleolus (n).

Osmium, Epon, UA-LC

X 8,000

Figure 172: Electron micrograph of intermediate cells from the epithelium of the archinephric duct; parasitic adult.

The cells are limited by interdigitating plasma membranes (arrow). The cytoplasm contains several large Golgi apparatuses (GA), dense granules (DG), and numerous mitochondria (M). Microvilli (MV) are seen protruding into an intercellular space (IS) and smooth vesicles (SV) are found beneath the plasma membrane.

Osmium, Epon, UA-LC

X 9,000

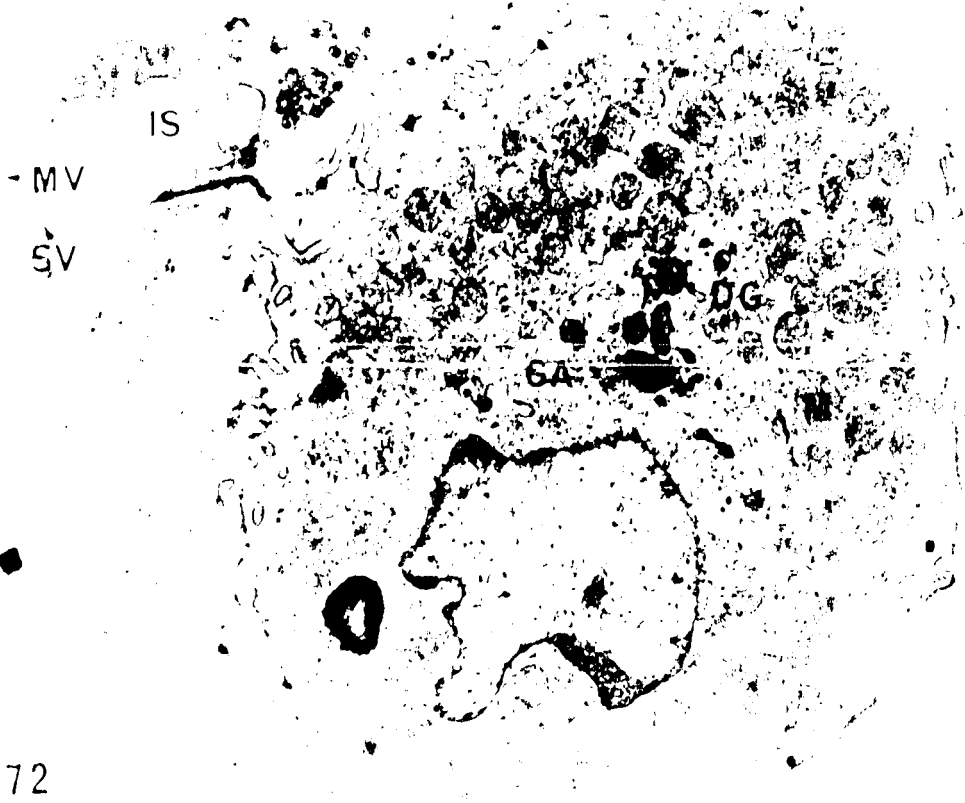
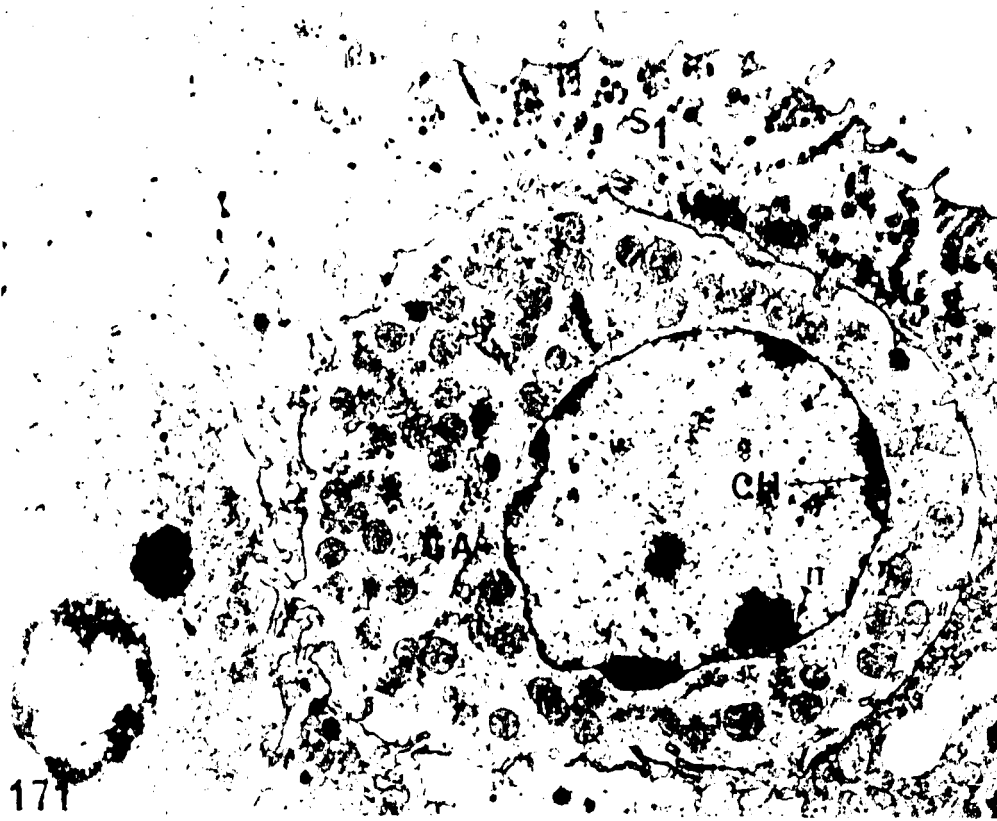


Figure 173: Two intermediate epithelial cells of the archinephric duct; parasitic adult.

Note the interdigitating plasma membrane (PM) and the porous nuclear envelope (arrows).

Osmium, Epon, UA-LC

X 17,600

Figure 174: Electron micrograph of a portion of Fig. 173; parasitic adult.

The plasma membranes (arrow) are highly interdigitated and the cytoplasm contains ribosomes (R), fibrils (FI), smooth vesicles (SV), and rough ER (RER).

Osmium, Epon, UA-LC

X 49,000



Figure 175: Electron micrograph of a superficial type I epithelial cell from the archinephric duct; parasitic adult.

The nucleus (N) is irregular and the cytoplasm contains numerous apical dense granules (DG), a large spherical body containing dense material and vacuoles (arrow), lipid droplets (LD), rough ER (RER), a laterally located Golgi apparatus (GA), and few mitochondria (M).

Osmium, Epon, UA-LC

X 10,800

Figure 176: Electron micrograph of the apical epithelium in a fold of the archinephric duct; parasitic adult.

Type I superficial cells with their irregular nucleus (N) and apical dense granules (DG) are contrasted with the intermediate cells (IN).

Osmium, Epon, UA-LC

X 8,600

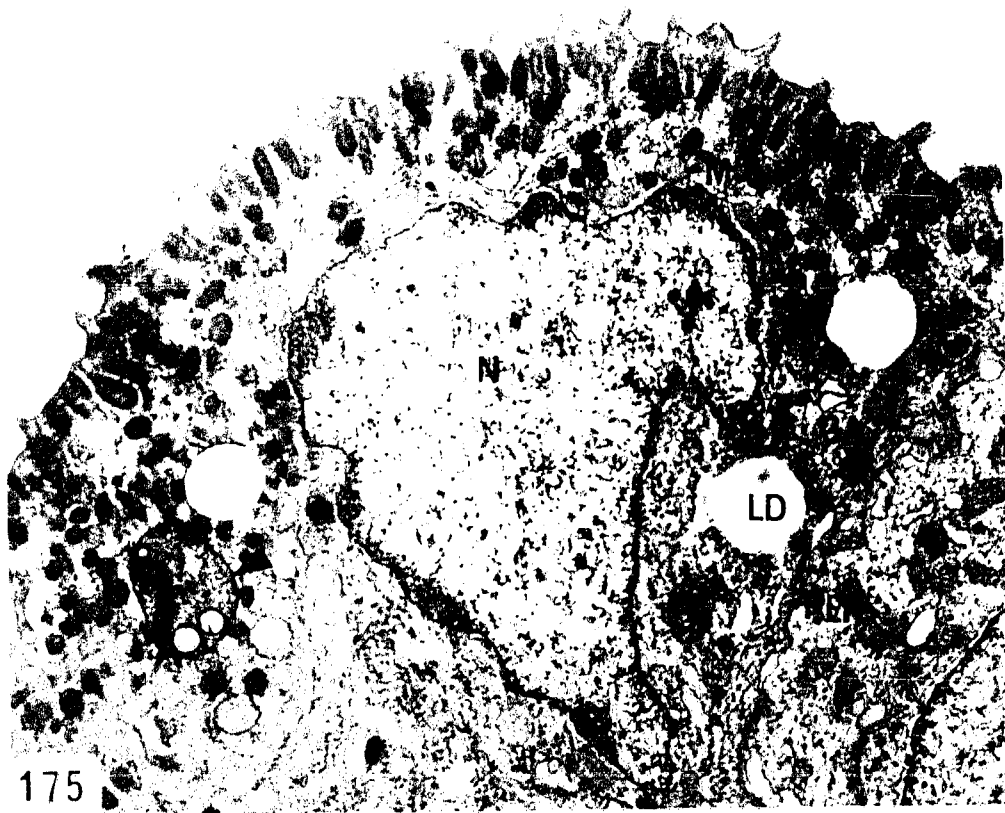


Figure 177:

Electron micrograph of the apex of a type I superficial epithelial cell from the archinephric duct; parasitic adult.

Microvilli are covered with an electron-dense fibrillar fuzz which often appears particulate (arrow). Dense granules (DG), 0.1 to 0.3- μ in diameter, and 0.25 to 0.6- μ in length are perpendicular to the surface. The apical cytoplasm also contains mitochondria (M) and rough ER (RER); nuclear chromatin (CH) is peripheral.

Osmium, Epon, UA-LC

X 34,500

Figure 178:

Electron micrograph of the apical surface of a superficial type I epithelial cell from the archinephric duct: parasitic adult.

The surface is coated by an electron-dense fuzz (FZ). The tri-laminar structure of the apical plasma membrane is apparent (SU). The apical granules are limited by a membrane (arrow).

Osmium, Epon, UA-LC

X 69,000

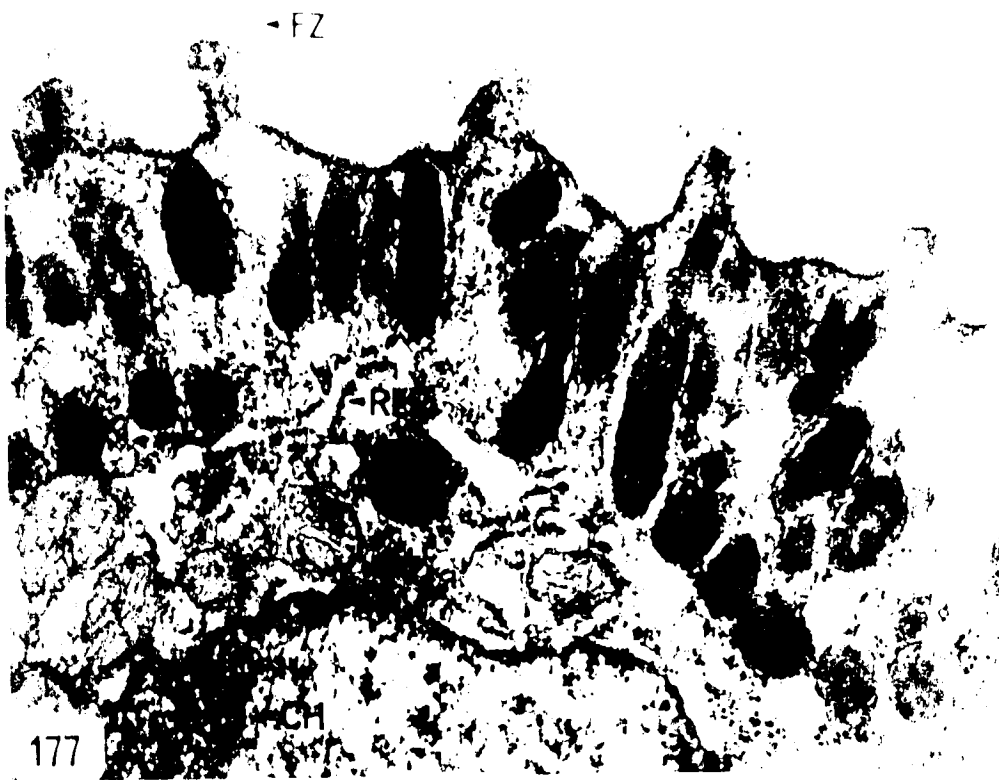


Figure 179: Electron micrograph of the apical surface of a type I superficial epithelial cell from the archinephric duct; parasitic adult. The membrane limited dense granules come in close contact with the apical plasma membrane (arrow). The cytoplasm also contains fibrils (FI) and ribosomes (R).
Osmium, Epon, UA-LC

X 69,000

Figure 180: Electron micrograph showing the junctional complex between two adjacent superficial type I epithelial cells from the archinephric duct; parasitic adult. The junctional complex composed of a zonula occludens (ZO) and a zonula adhaerens (ZA). A desmosome (DS) is located beneath the junctional complex and fibrils (FI) are seen emanating from it.
Osmium, Epon, UA-LC

X 65,000

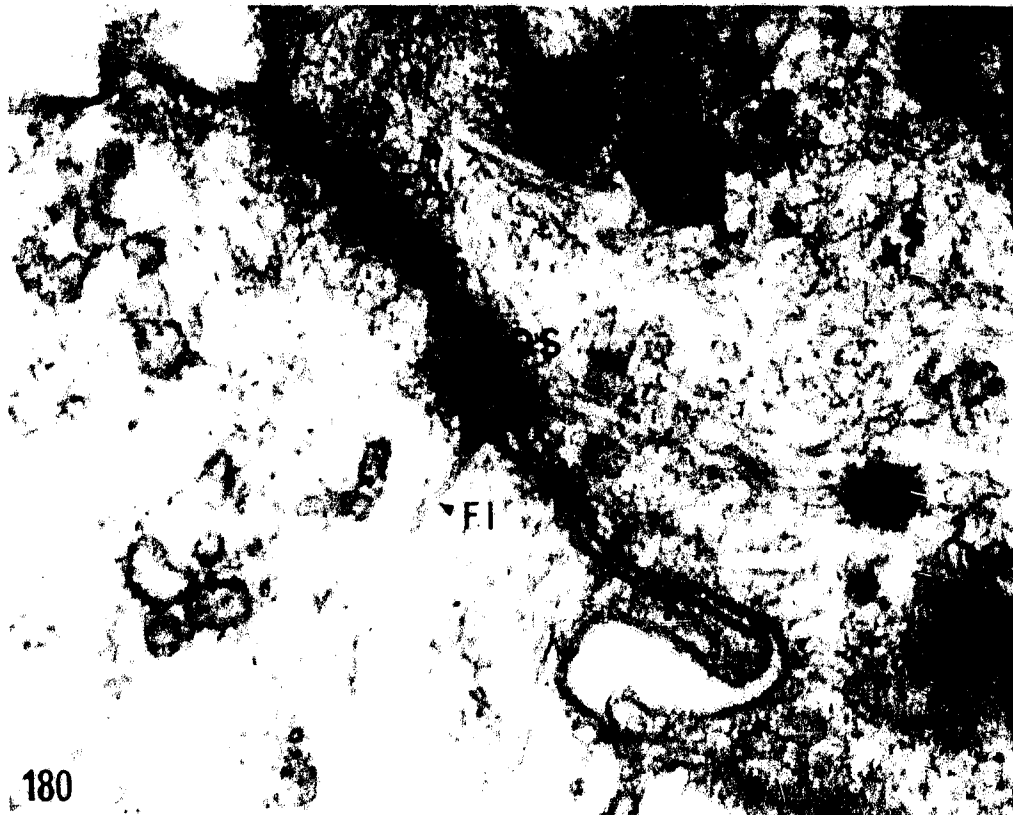
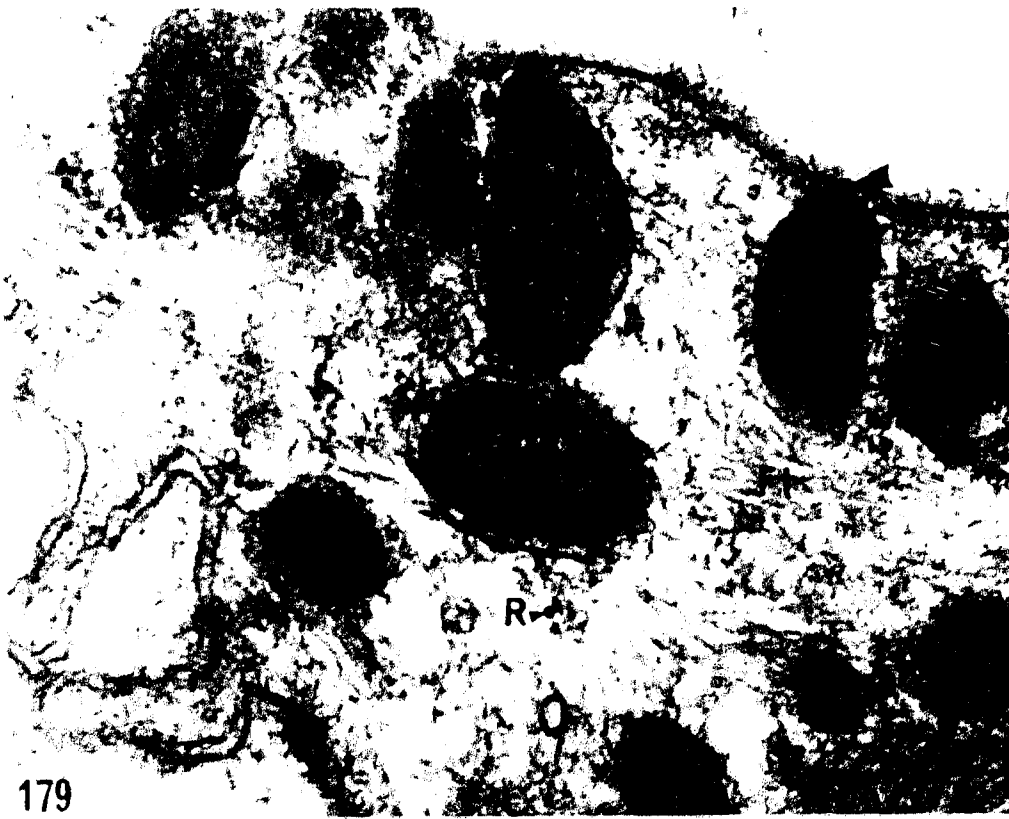


Figure 181: Electron micrograph of a type II superficial epithelial cell from the archinephric duct; parasitic adult.

The cell contains a flattened, basal nucleus (N) oriented parallel to the surface. The cytoplasm contains numerous mucous droplets (arrows) above the nucleus and a Golgi apparatus (GA) and rough ER (RER) at each end.

Osmium, Epon, UA-LC

X 11,300

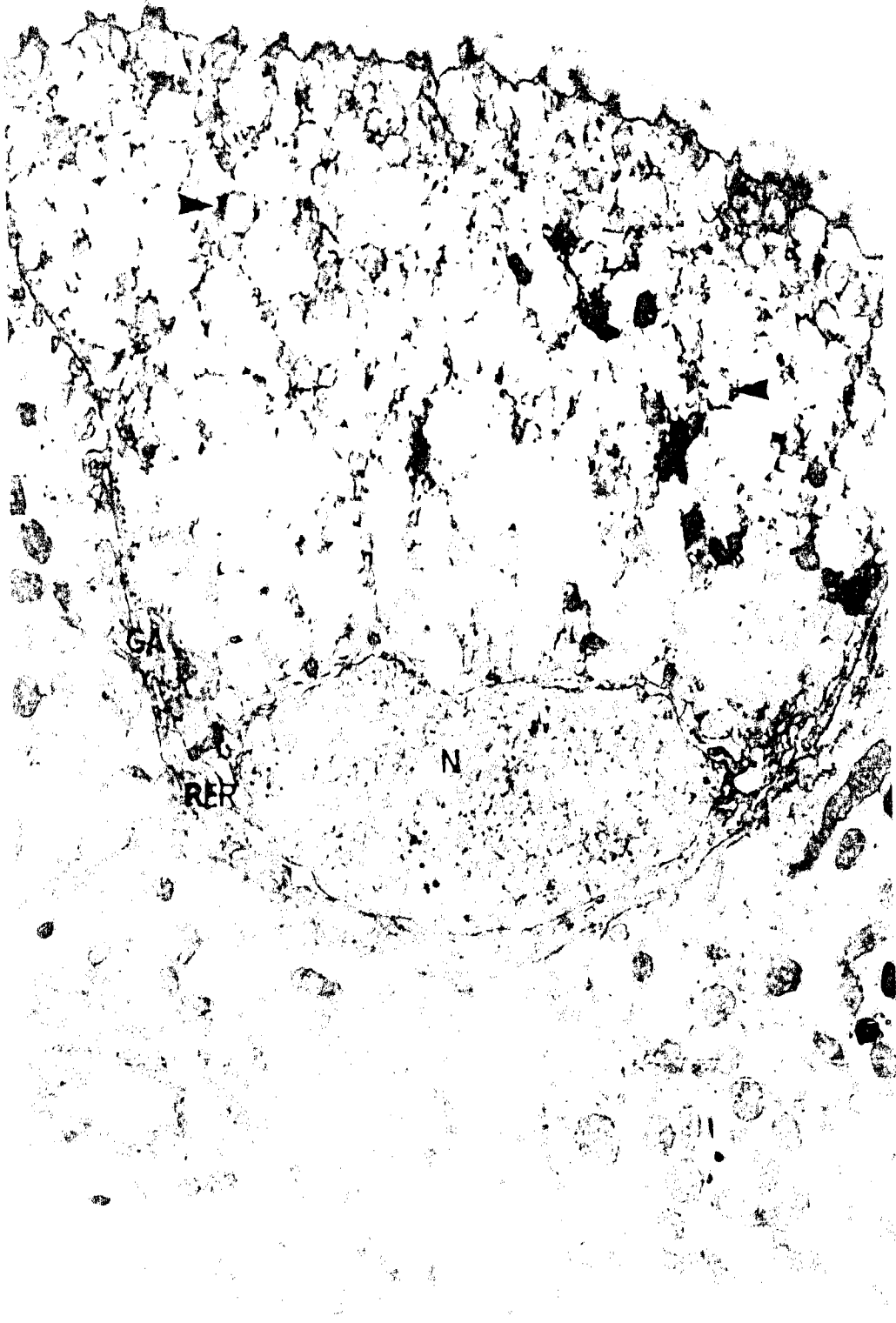


Figure 182:

Electron micrograph of the apical surface of a superficial type II epithelial cell from the archinephric duct; parasitic adult.

Short microvilli are coated with an electron-dense fuzz (FZ). The apical cytoplasm contains droplets which are not completely bound by a membrane (arrow), mitochondria (M) and ribosomes (R).

Osmium, Epon, UA-LC

X 43,500

Figure 183:

Electron micrograph of a portion of a superficial type II epithelial cell from the archinephric duct; parasitic adult.

The highly dilated rough ER appears to be continuous with the nuclear envelope (arrow) and is closely associated with the Golgi apparatus which consists of a flattened saccules (SA) and microvesicles (MI). Closely associated vesicles (V) resemble the dilated ends of the saccules. Mitochondria (M) are also seen.

Osmium, Epon, UA-LC

X 43,500



Figure 184:

Electron micrograph of a type III superficial epithelial cell from the archinephric duct; parasitic adult.

This club-shaped cell resembles the type II cell with mucous droplets (MD) but is more electron-dense and the nucleus (N) is pycnotic. It may represent an intermediate stage between types I and II.

Osmium, Epon, UA-LC

X 9,000

Figure 185:

Electron micrograph showing a portion of a superficial type III epithelial cell from the archinephric duct; parasitic adult.

The type III cell overlies an intermediate cell (IN) and is characterized by strong electron density. Its processes appear in the interdigitations between the cells (arrow). The apex contains microvilli and is covered by an electron-dense fuzz (FZ). The cytoplasm contains numerous dense granules (DG), a few mitochondria (M) and a Golgi apparatus (GA) all outlined by electron-dense material.

Osmium, Epon, UA-LC

X 18,500

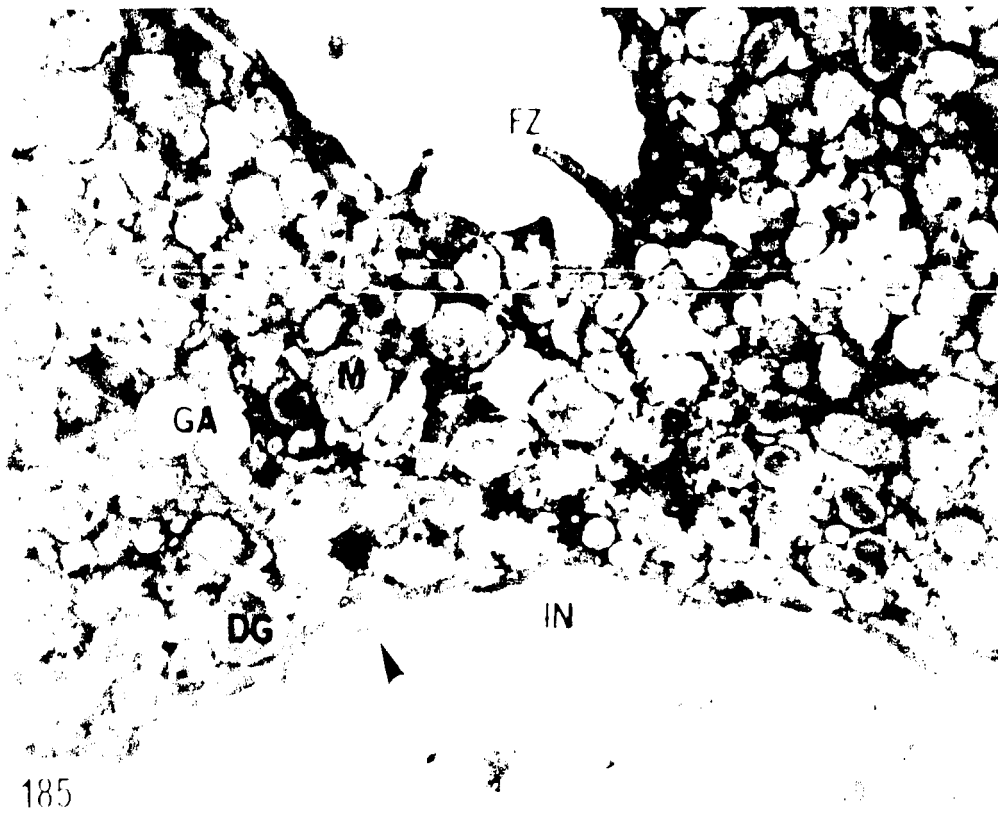
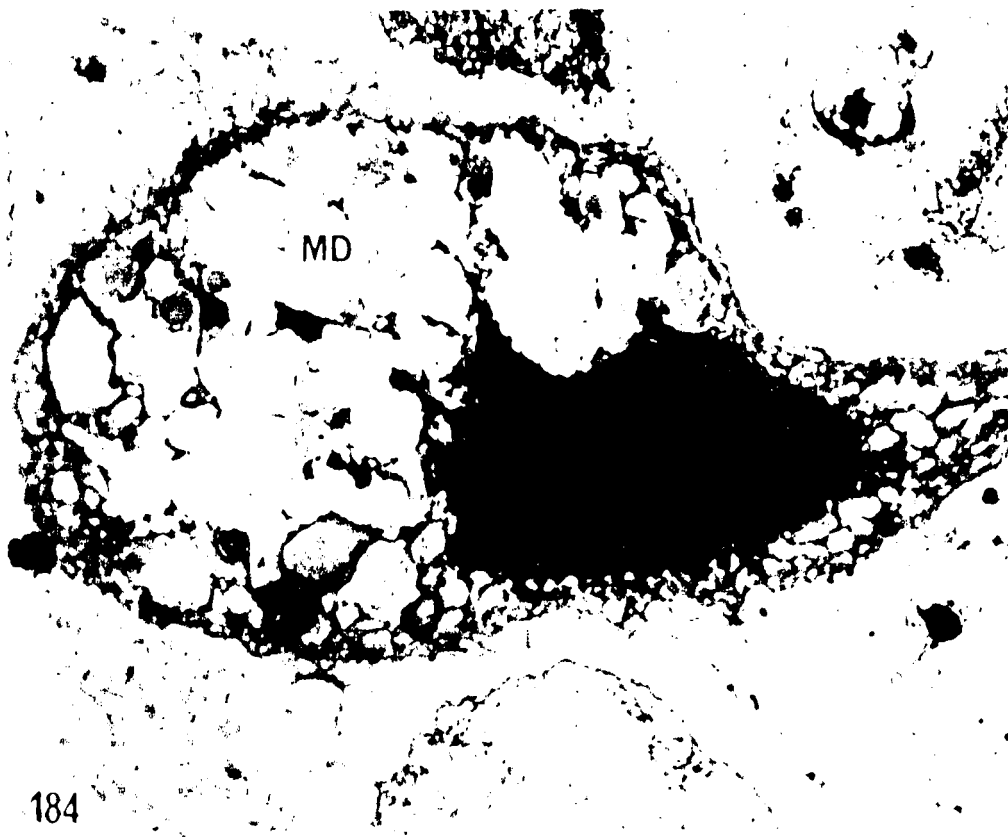


Figure 186: Light micrograph of the most posterior part of the kidney; 40-mm ammocoetes.
A group of cells (arrow) is seen between the kidney capsule (CA) and the archinephric duct (AD).
Bouin, Tissuemat, PAS-AH-OG

X 1,900

Figure 187: Light micrograph from the posterior part of the kidney; 40-mm ammocoetes.
Small tubules and the archinephric duct (AD) are seen. One tubule possesses a tiny lumen (L) and another contains cells undergoing mitosis (arrows).
Bouin, Tissuemat, PAS-AH-OG

X 2,200

Figure 188: Light micrograph from the posterior portion of the kidney; 16-mm ammocoetes.
This micrograph shows the formation of a renal corpuscle with its Bowman's capsule (BC) and invading vascular network (arrow).
Bouin, Tissuemat, PAS-AH-OG

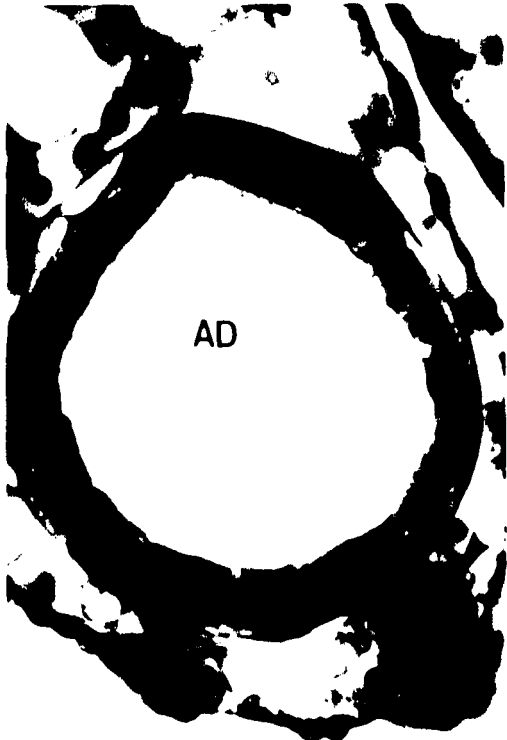
X 3,500

Figure 189: Light micrograph from the posterior portion of kidney; 125-mm ammocoetes.

This 0.5- μ section shows a tubule with intercellular spaces (arrow) and cytoplasmic lipid droplets (LD) similar to those seen in the intertubular cells.

Osmium, Epon, TB

X 4,700



186

CA



187



188



189

Figure 190: Electron micrograph of a portion of an undifferentiated tubule in the posterior part of the kidney; 125-mm ammocoetes.

The cells contain dense granules (DG), lipid droplets (LD), numerous mitochondria (M).

The nuclei usually contain a nucleolus (n).

Microvilli (MV) are seen on the apical surface of the cells.

Osmium, Epon, UA-LC

X 8,100



Figure 191: Electron micrograph of the apex of cell from an undifferentiated tubule; 125-mm ammocoetes. Microvilli (MV) are seen at the apical surface. The cytoplasm contains a multivesicular body (MVB) and mitochondria with rows of mitochondrial granules (arrows).
Osmium, Epon, UA-LC

X 15,000

Figure 192: Electron micrograph of the apex of a cell from an undifferentiated tubule; 125-mm ammocoetes. A cilium (CL) and an accompanying centriole (CT) are seen at the apical surface. Mitochondria contain hexagonally-arranged prismatic cristae (arrows). Autophagic vacuoles (AV) are seen.
Osmium, Epon, UA-LC

X 25,000



Figure 193: Electron micrograph of adjacent cells from an undifferentiated tubule; 125-mm ammocoetes. Cells are separated by large intercellular spaces (IS) but their plasma membranes are fused apically into a junctional complex (JC) and more basally by desmosomes (DS). The basement membrane (arrow) which separates the cells from sinusoids containing blood cells (BC). A lipid droplet (LD) is seen in the cytoplasm.

Osmium, Epon, UA-LC

X 13,500

Figure 194: Electron micrograph of the base of a cell from an undifferentiated tubule; 118-mm ammocoetes. The intercellular space appears to be continuous with the extracellular space (arrow). The basement membrane (BM) separates the cell from sinusoidal endothelium which possesses numerous pinocytotic vesicles (PV) and tiny invaginations which may be pores (PO). A large lipid droplet (LD) and glycogen (GLY) are seen in the cytoplasm of the tubule cell.

Osmium, Epon, UA-LC

X 53,000

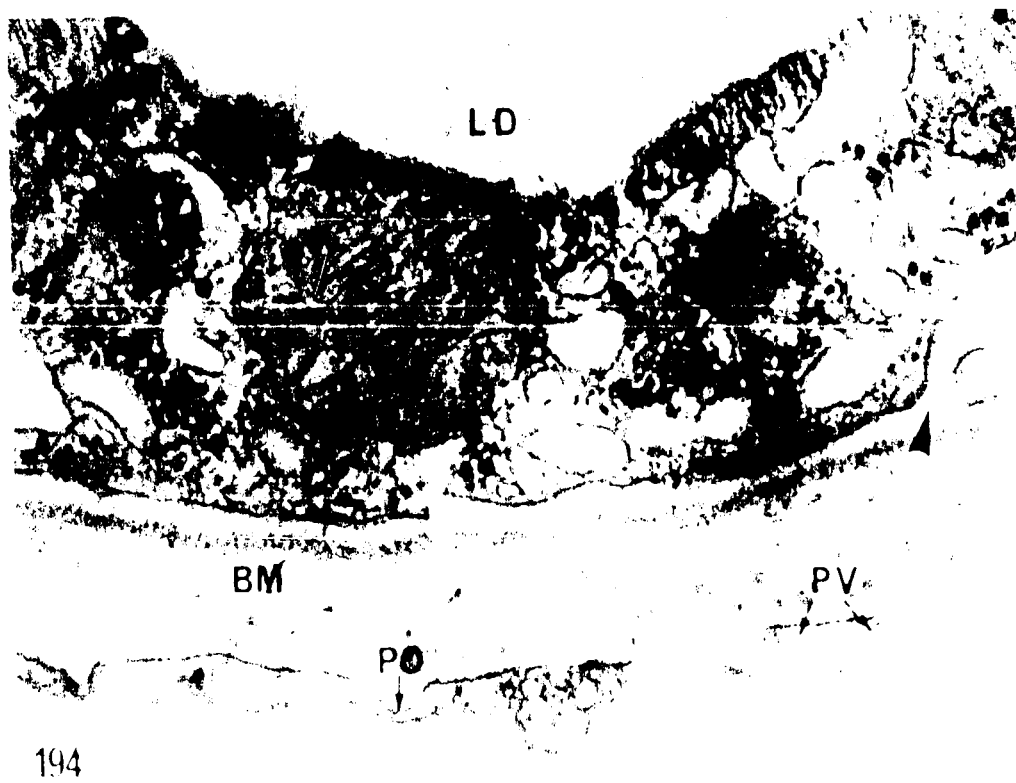
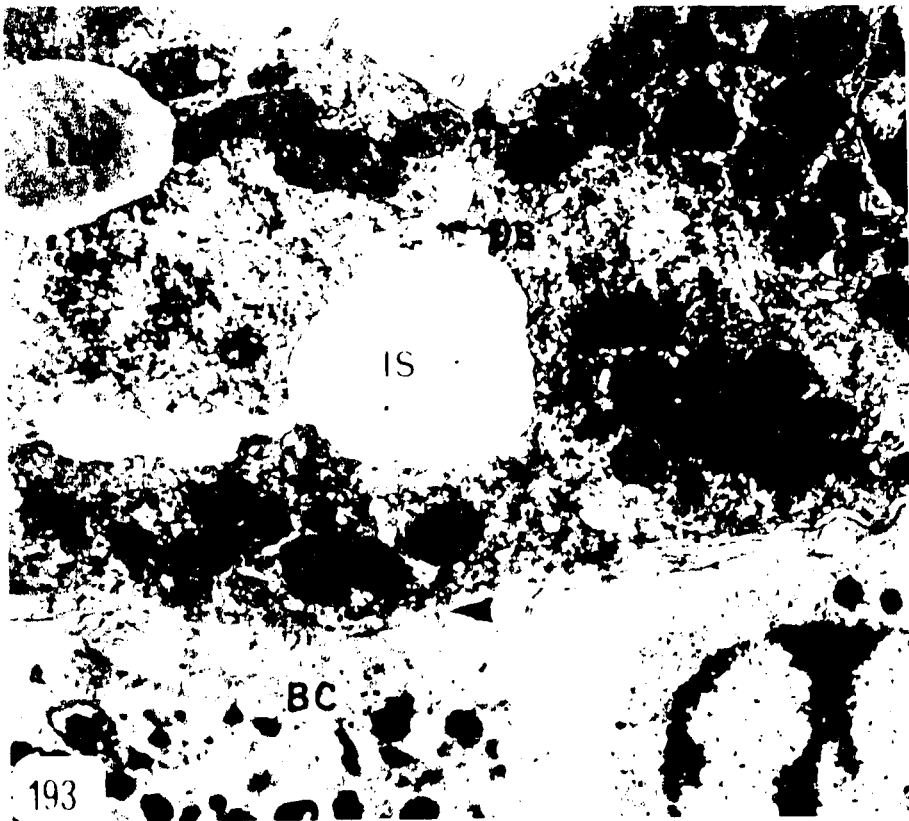


Figure 195: Electron micrograph of a portion of a cell from an undifferentiated tubule; 118-mm ammocoetes. A large Golgi apparatus is composed of a few saccules (SA) and numerous microvesicles (MI). The nucleus contains peripheral chromatin (CH). Fibrils (FI) are closely associated with the envelope. A multivesicular body (MVB) is seen near the apex and a mitochondrion possesses hexagonally arranged prismatic cristae forming a star (arrow). Free ribosomes and small strands of rough ER (RER) are seen.

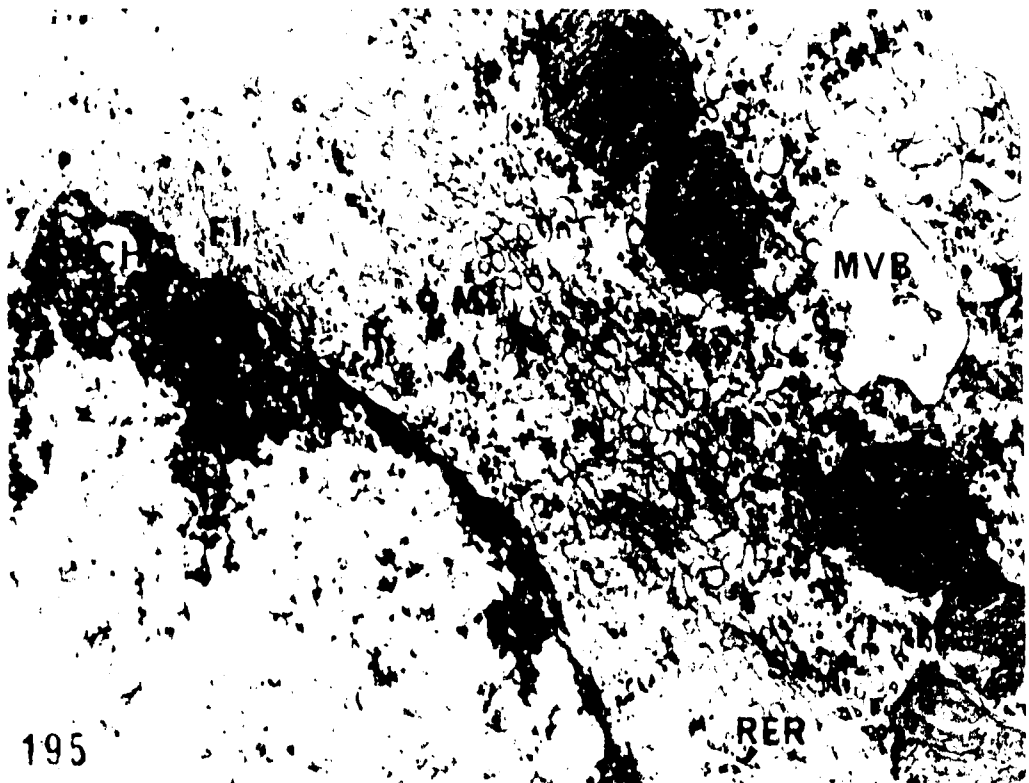
Osmium, Epon, UA-LC

X 31,300

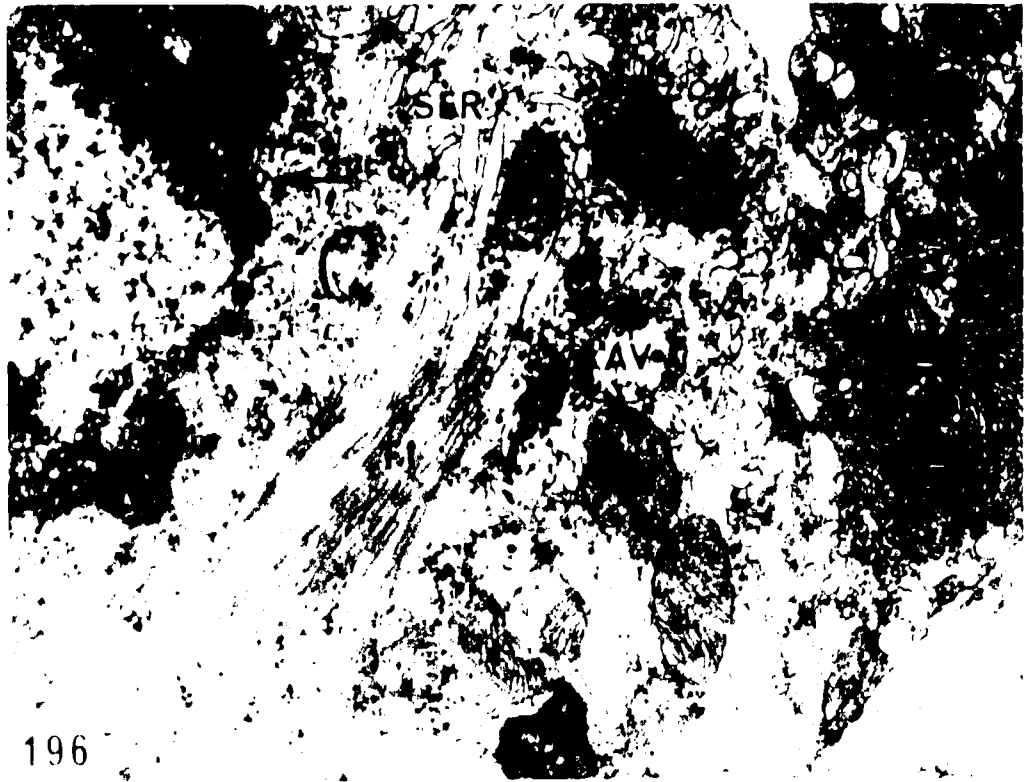
Figure 196: Electron micrograph of a portion of a cell from an undifferentiated tubule; 125-mm ammocoetes. The cytoplasm contains autophagic vacuoles (AV) and bundles of fibrils (FI) in close association to smooth ER (SER). Nuclear pores (arrows) in transverse section are seen.

Osmium, Epon, UA-LC

X 19,300



195



196

Figure 197:

Electron micrographs of mitochondria from cells
of an undifferentiated tubule; 125-mm ammocoetes.

- A. The cristae are cut in transverse section,
are hexagonally arranged, and surround a
mitochondrial granule (arrow).

Osmium, Epon, UA-LC

X 80,500

- B. 118-mm ammocoetes.

Numerous prismatic cristae are sectioned
transversely and their arrangement produces
several stars with a mitochondrial granule
(arrows) at the centre of each.

Osmium, Epon, UA-LC

X 80,100

- C. 125-mm ammocoetes.

The cristae are sectioned longitudinally so
that their limiting membranes are seen (MB).
Rows of mitochondrial granules appear to be
connected by thin dense strands (arrows) and
they are confined to spaces between the
cristal membranes.

Osmium, Epon, UA-LC

X 57,000

D. 125-mm ammocoetes.

Rows of mitochondrial granules are seen running in different planes and each row is separated by a cristalmembrane (arrows).

Osmium, Epon, UA-LC

X 54,400

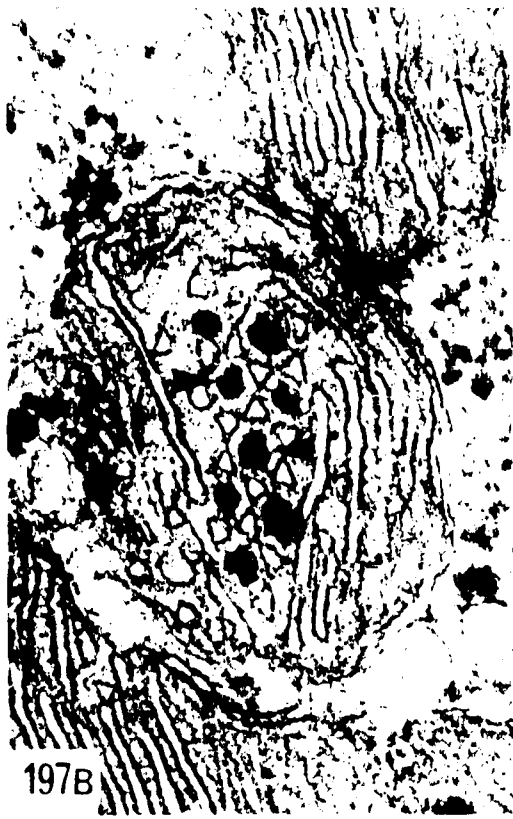


Figure 198: A schematic interpretation of the arrangement of prismatic cristae and mitochondrial granules in a mitochondrion from an undifferentiated tubule in the posterior part of the ammocoetes kidney.

Mitochondrial granules (MG) occur in rows within a hexagonal tube formed by the parallel arrangement of six prismatic cristae (CR). Each cristae of the original tube contributes to the formation of an adjacent tube which also enclosed mitochondrial granules.

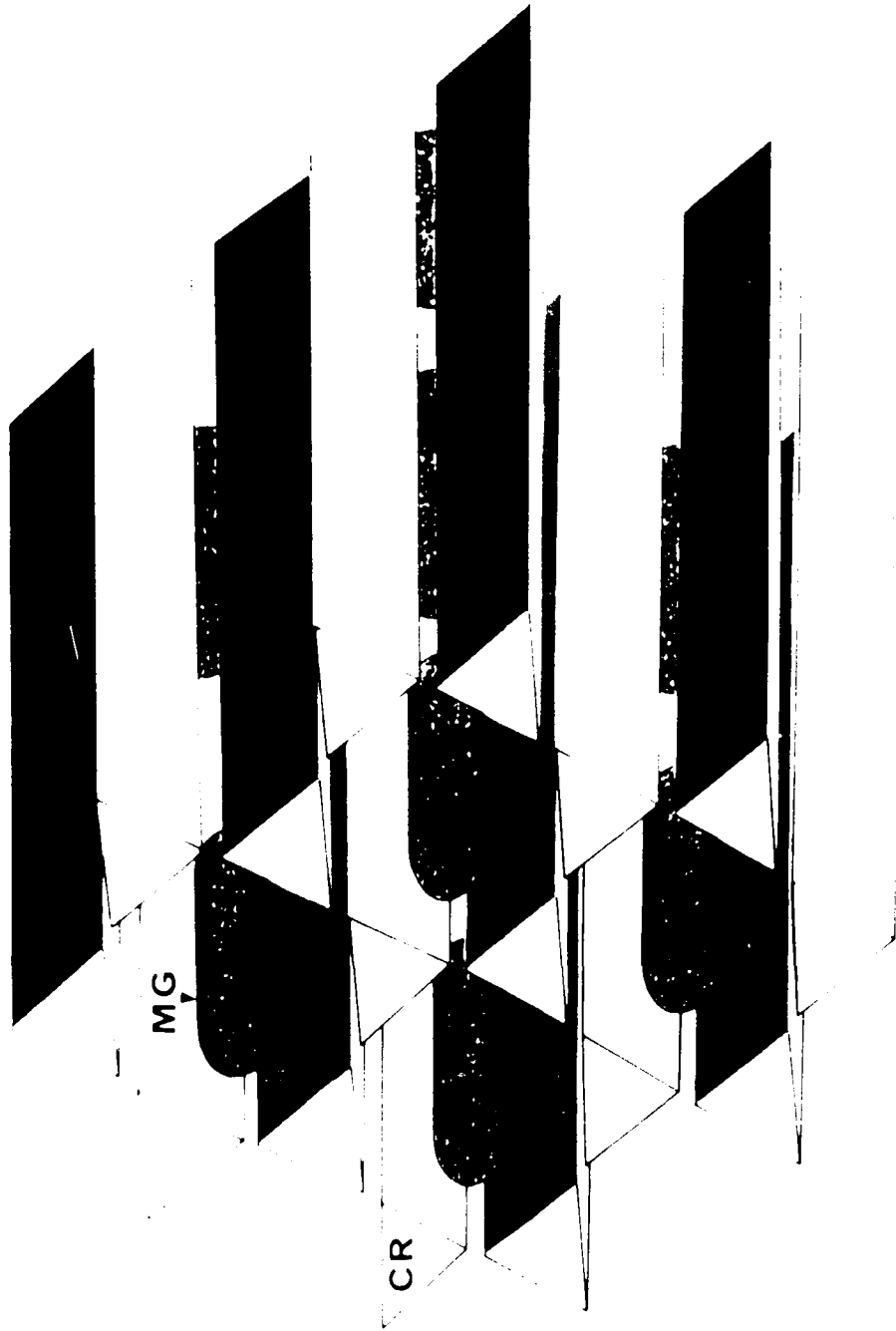


FIG. 198

Figure 199: Light micrographs of the degenerating anterior portion of the kidney; newly-transformed adult.
Bouin, Tissuemat, PAS-AH-OG

A. Degenerating tubules (T) are surrounded by phagocytitic tissue (PH).

X 230

B. An outline of an intensely PAS+ tubule is seen (arrow). Aggregations of phagocytes (PH) surround the tubules.

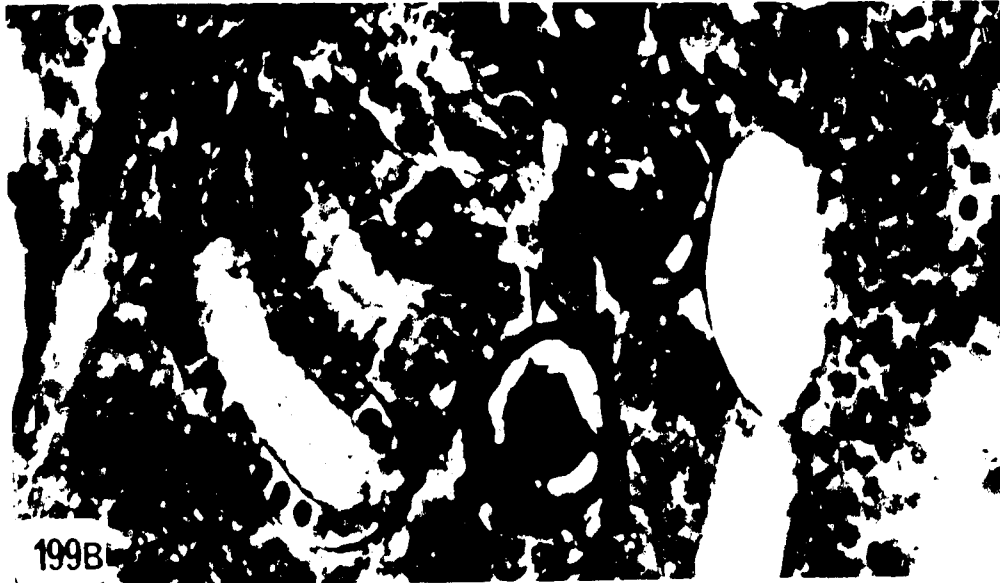
X 1,730

C. Here the kidney is reduced to an amorphous mass of PAS- material (arrow) and aggregations of phagocytes (PH).

X 1,730



199A



199B



199C

Figure 200: Light micrograph of the anterior tip of the kidney; parasitic adult.
Tubules contain PAS+ material in their lumina (arrow) and are surrounded by a thick basement membrane (BM). There is a thick layer of fibrous tissue (CO) surrounding the tubules.
Bouin, Tissuemat, PAS-AH-OG

X 570

Figure 201: Light micrograph of a portion of Figure 200; parasitic adult.

A shrunken tubule is surrounded by layers of fibrous tissue (arrow).

Bouin, Tissuemat, PAS-AH-OG

X 2,200

Figure 202: Light micrograph of the posterior portion of the kidney; migrating adult.

Tubules (T) are large and often contain phagocytic cells (PH).

Bouin, Tissuemat, PAS-AH-OG

X 140

Figure 203: Light micrograph of the posterior portion of the kidney; migrating adult.

This section shows a more advanced stage of phagocytic invasion in the kidney (arrow).

Bouin, Tissuemat, PAS-AH-OG

X 140

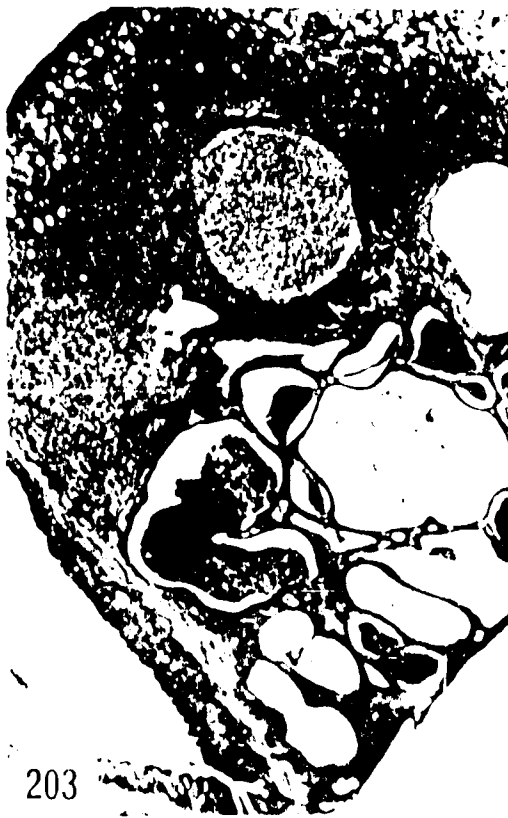
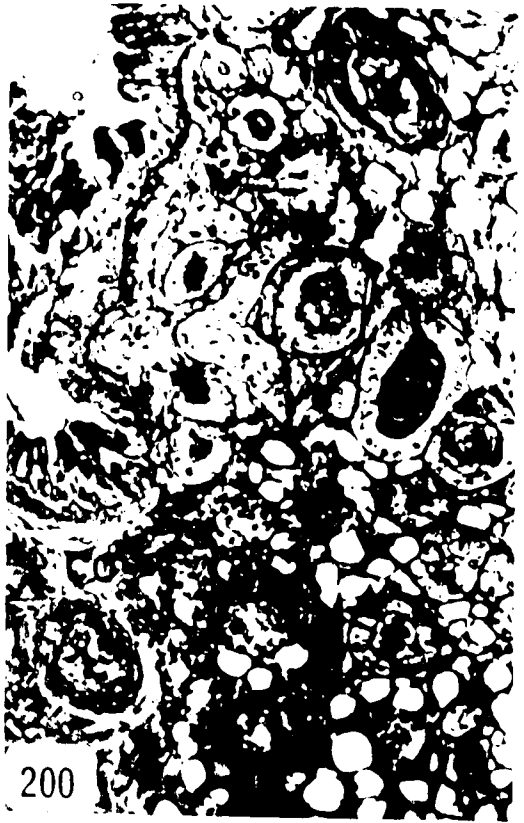


Figure 204: Electron micrograph of a portion of the glomerulus;
migrating adult.

Numerous mesangial cells (MS) and collagenous
fibrils (CO) are found between the endothelium
(END) and podocyte layer (PL). Note the presence
of a phagocyte (PH) in the lumen of a capillary.

Osmium, Epon, UA-LC

X 5,000

Figure 205: Electron micrograph of a portion of a cell
from the proximal pars convoluta; migrating
adult.

The cytoplasm contains large numbers of dense
granules (DG) of various shapes and sizes. A
sinusoidal endothelial cell possesses large
lipid droplets (LD).

Osmium, Epon, UA-LC

X 8,200

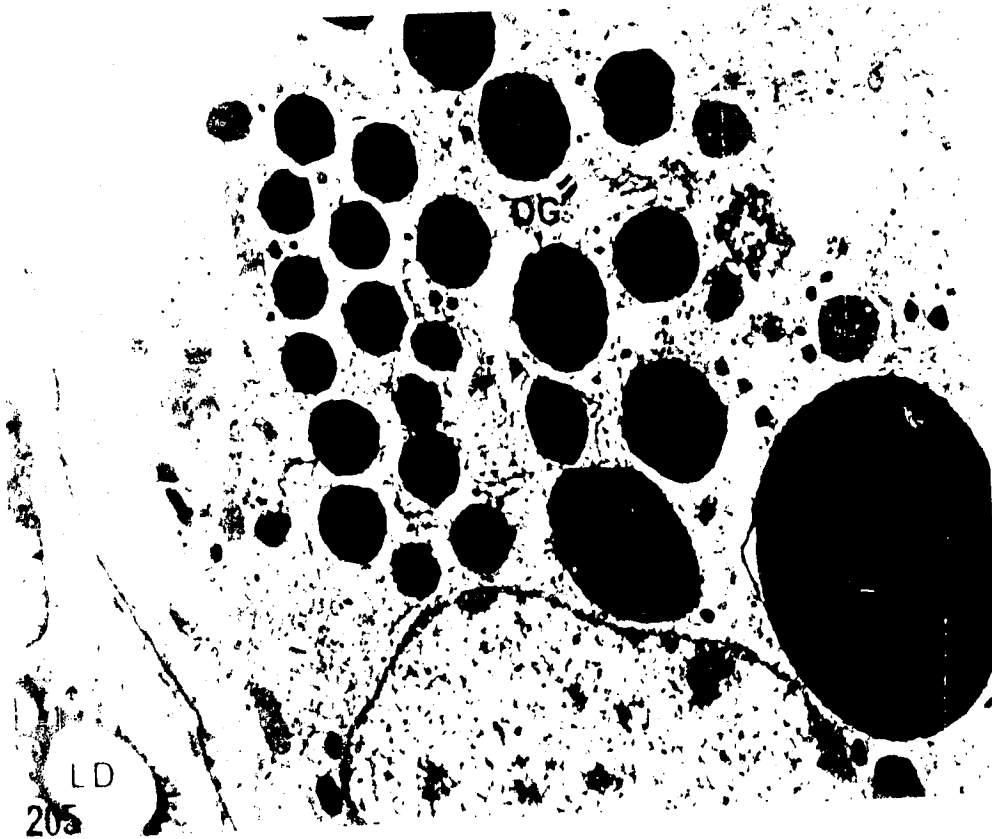
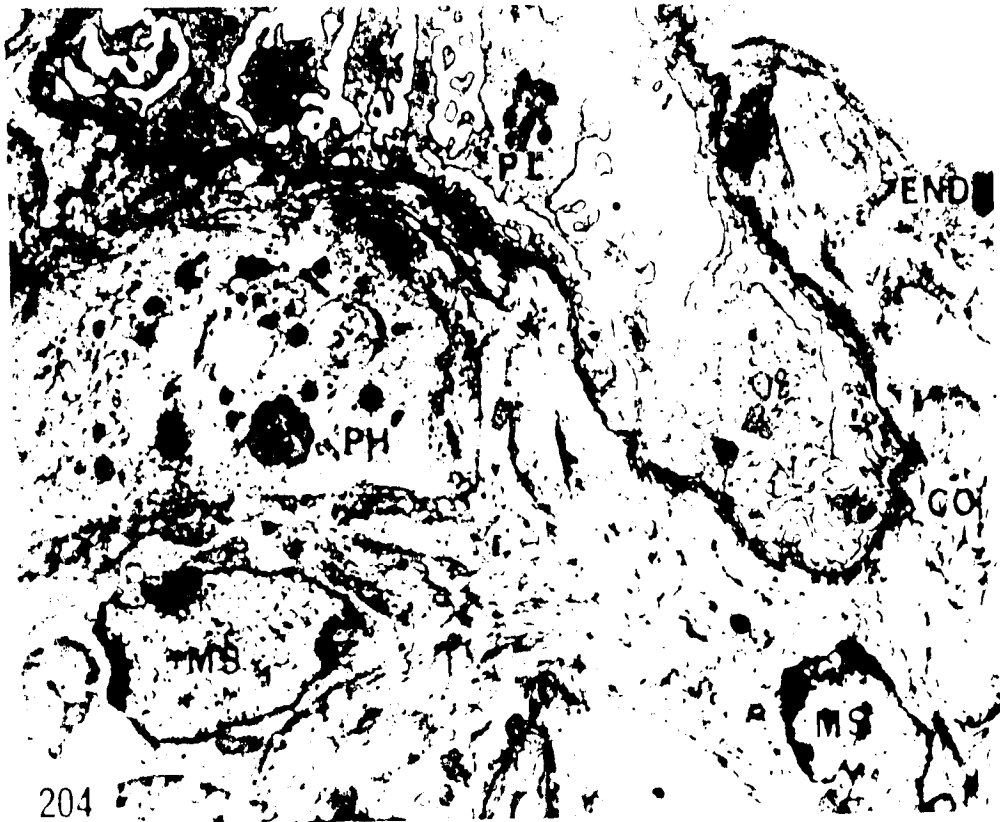
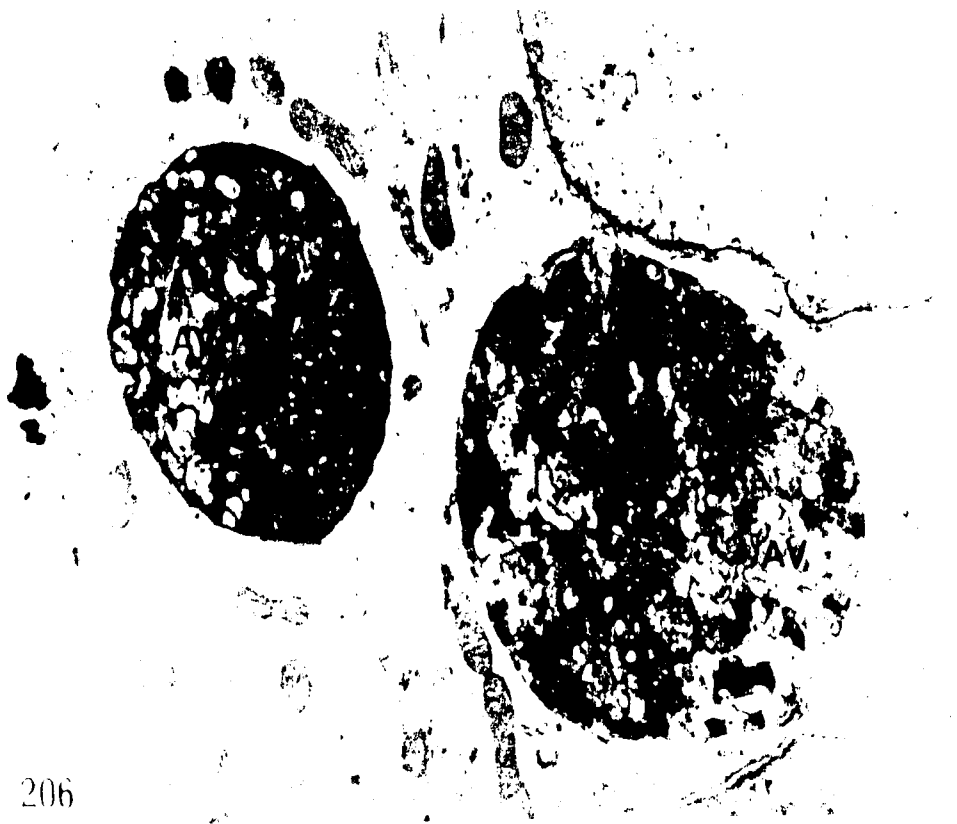


Figure 206: Electron micrograph of a portion of a cell from the distal pars recta; migrating adult. Two large autophagic vacuoles (AV) are seen in the basal cytoplasm. Osmium, Epon, UA-LC

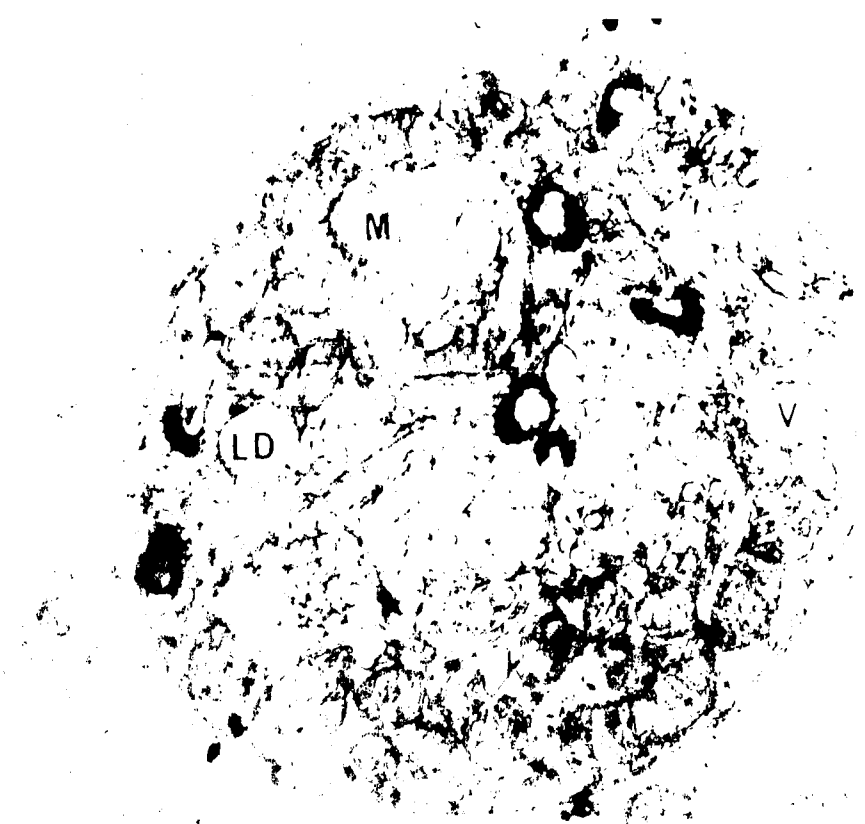
X 11,300

Figure 207: Electron micrograph of an autophagic vacuole in a cell of the distal pars recta; migrating adult. The autophagic vacuole contains mitochondria (M), vesicles (V), and a lipid droplet (LD). Osmium, Epon, UA-LC

X 21,400



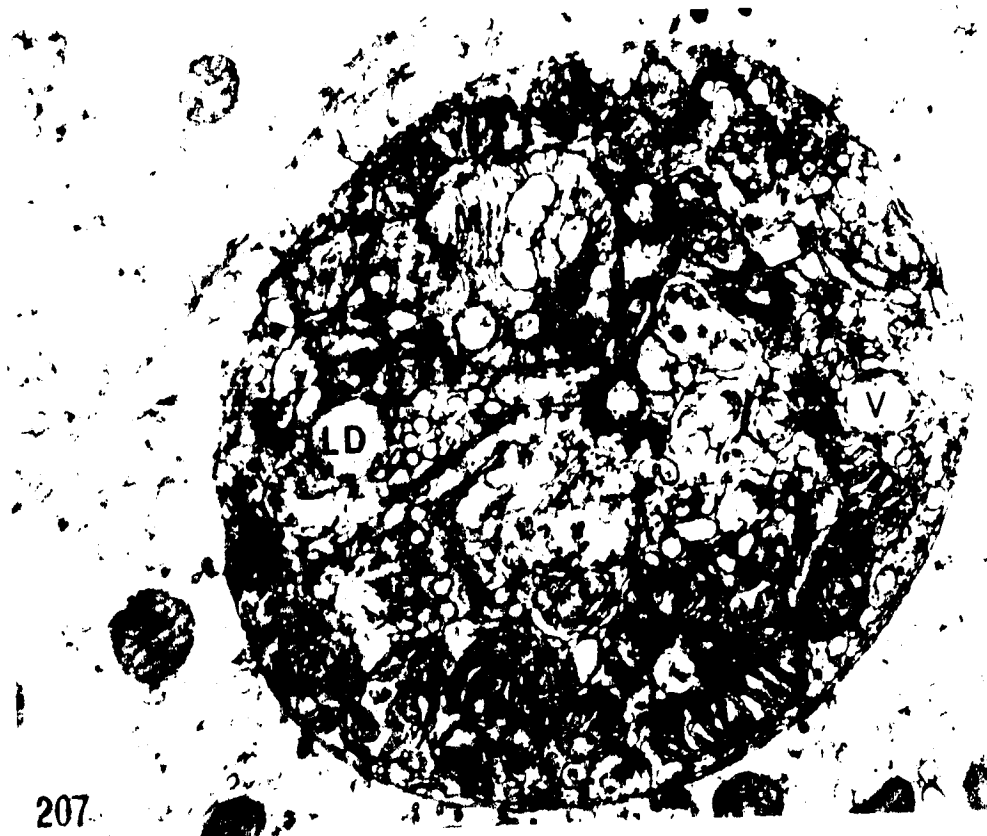
206



207



206



207

Figure 208: Electron micrograph of a crystalline body in a cell of the distal pars recta; migrating adult. At one end of the body parallel dense membranes are seen to run concentrically (A) while at the other end parallel membranes are seen to run in two directions and intersect at an angle of 60 to 65° (B).

Osmium, Epon, UA-LC

X 69,000

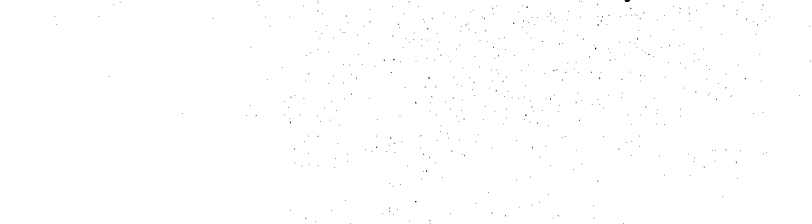
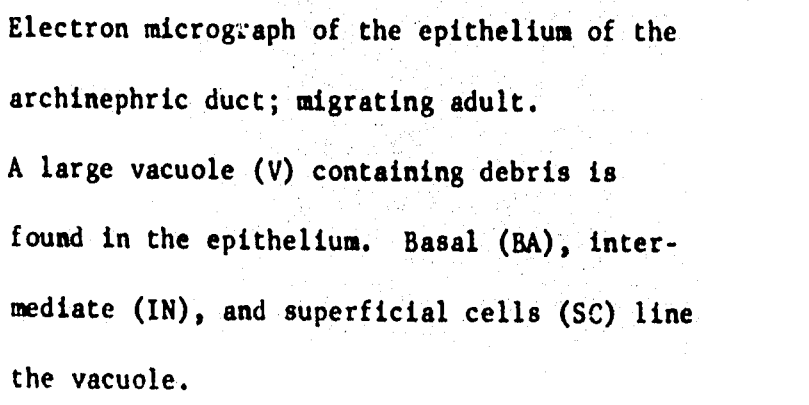


Figure 209: Electron micrograph of the epithelium of the archinephric duct; migrating adult. A large vacuole (V) containing debris is found in the epithelium. Basal (BA), intermediate (IN), and superficial cells (SC) line the vacuole.

Osmium, Epon, UA-LC

X 5,000



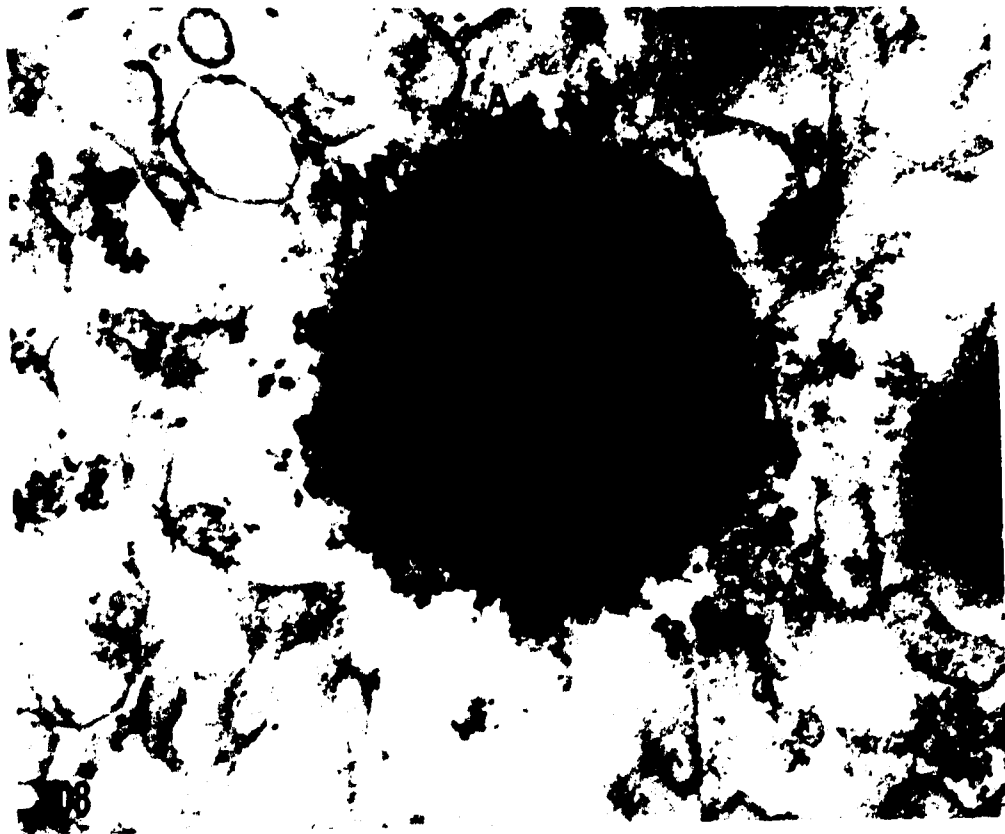


Figure 210: Electron micrograph of a superficial type I epithelial cell from the archinephric duct; migrating adult.

The cytoplasm contains a large number of lipid-like inclusions (arrows).

Osmium, Epon, UA-LC

X 11,900

Figure 211: Electron micrograph of the base of a cell from the distal pars recta; migrating adult. Small lipid-like droplets (arrows) are seen in the extracellular area between the basement membrane (BM) and the sinusoidal endothelium (END).

Osmium, Epon, UA-LC

X 21,400

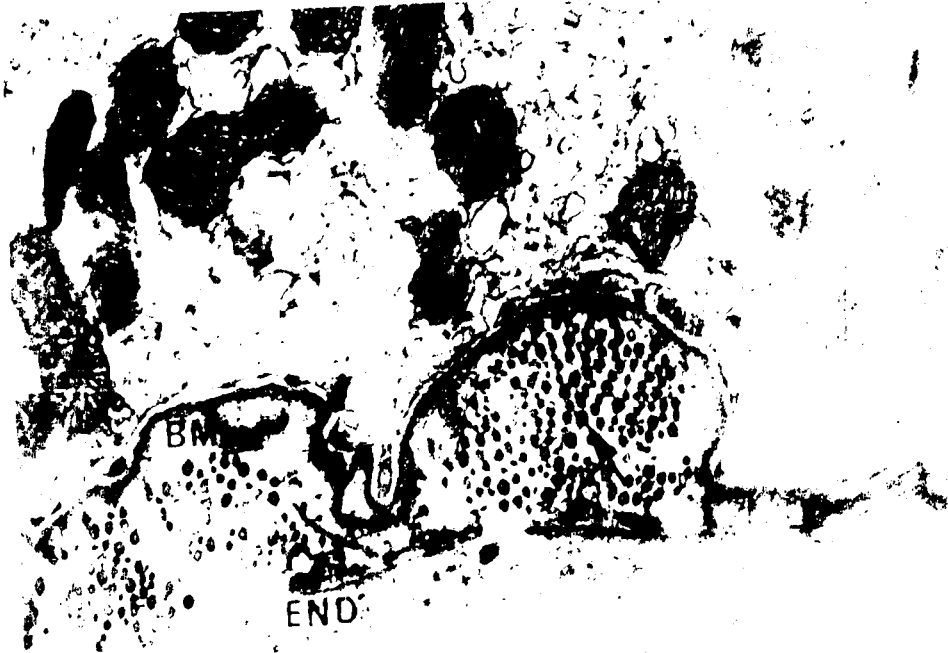
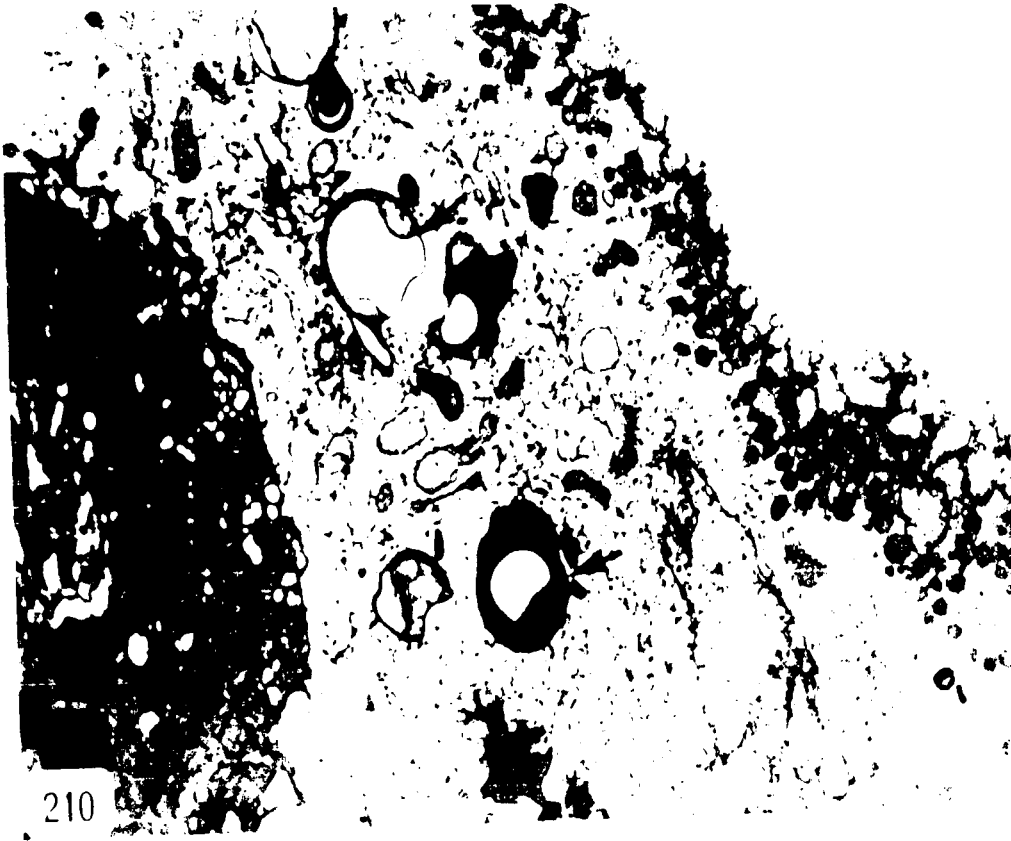


Figure 212: Electron micrograph showing cells in the inter-tubular area of the posterior part of the kidney; 125-mm ammocoetes.

Between the base of a tubule (T) and a sinusoid (S) are seen intertubular cells (IT), some of which contain large lipid droplets (LD), and processes of pigment cells containing granules (PG).

Osmium, Epon, UA-LC

X 7,500



Figure 213:

Electron micrograph of the intertubular area
in the dorso-anterior part of the kidney;
118-mm ammocoetes.

An intertubular cell (IT) and portions of
pigment cells (PC) are seen in this section
amongst various types of blood cells (BC).
Glutaraldehyde-Osmium, Epon, UA-LC.

X 6,100

Figure 214:

Electron micrograph of a pigment cell in the
intertubular area of the dorso-anterior part
of the kidney; 118-mm ammocoetes.

The pigment cell contains an irregular
nucleus with a prominent nucleolus (n) and
the cytoplasm is filled with pigment granules
(PG).

Glutaraldehyde-Osmium, Epon, UA-LC

X 5,000

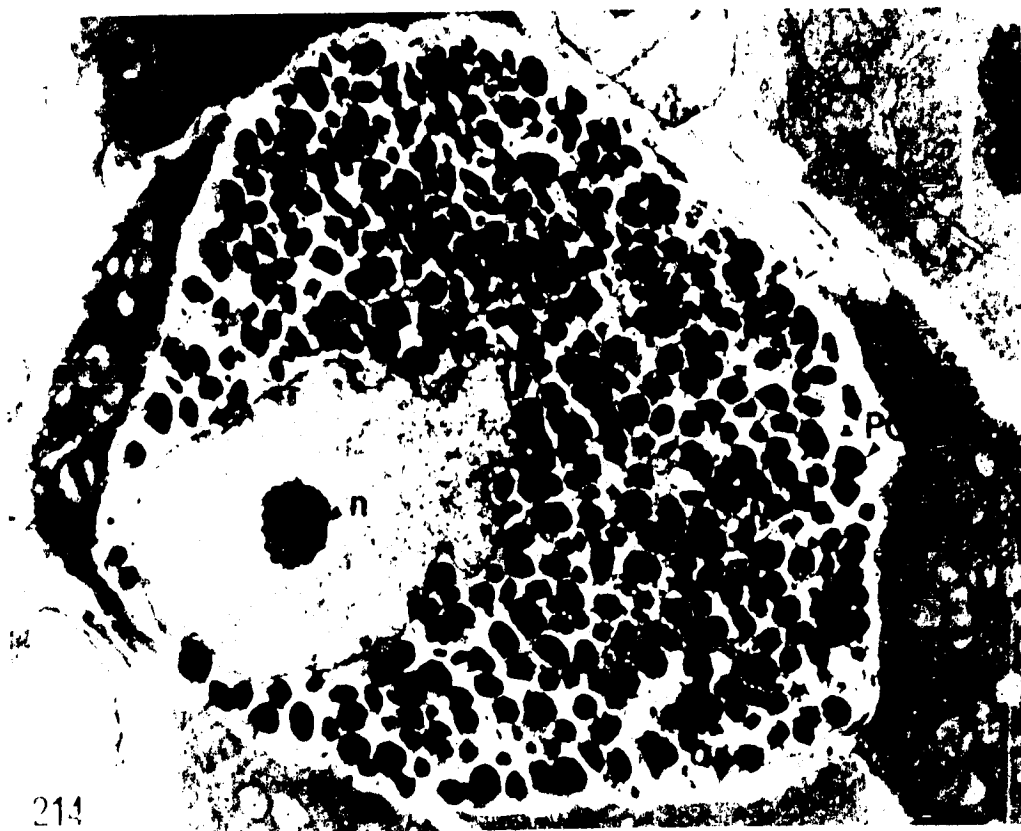
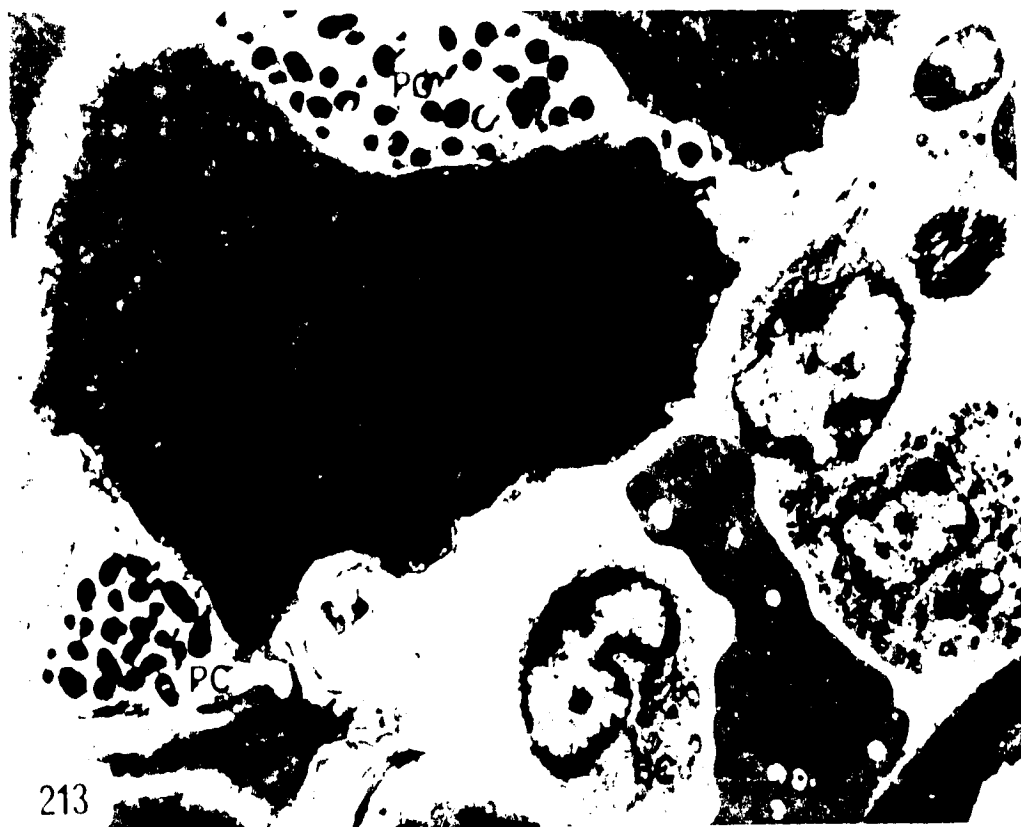


Figure 215: Electron micrograph of portions of an inter-tubular cell and a pigment cell from the dorso-anterior part of the kidney; 98-mm ammocoetes.

The intertubular cell possesses a large lipid droplet (LD) and large mitochondria (M).

In the pigment cell smooth vesicles (SV) are interspersed among pigment granules (PG).

Osmium, Epon, UA-LC

X 12,000

Figure 216: Electron micrograph of a portion of an inter-tubular cell in the posterior part of the kidney; 125-mm ammocoetes.

The cell is separated from the sinusoidal endothelium (S) and a fibroblast (FI) by an electron-dense coat (arrow). The cytoplasm contains rough ER (RER), clumps of glycogen (GLY), a small lipid droplet (LD), and an autophagic vacuole (AV).

Osmium, Epon, UA-LC

X 21,000

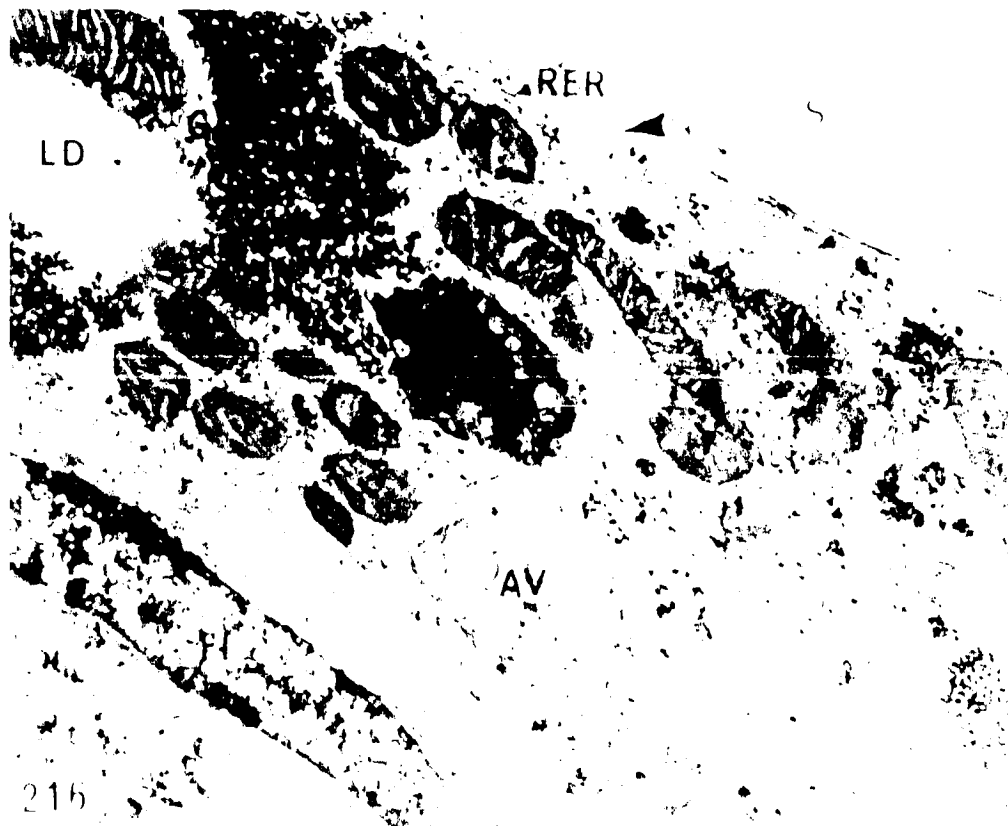
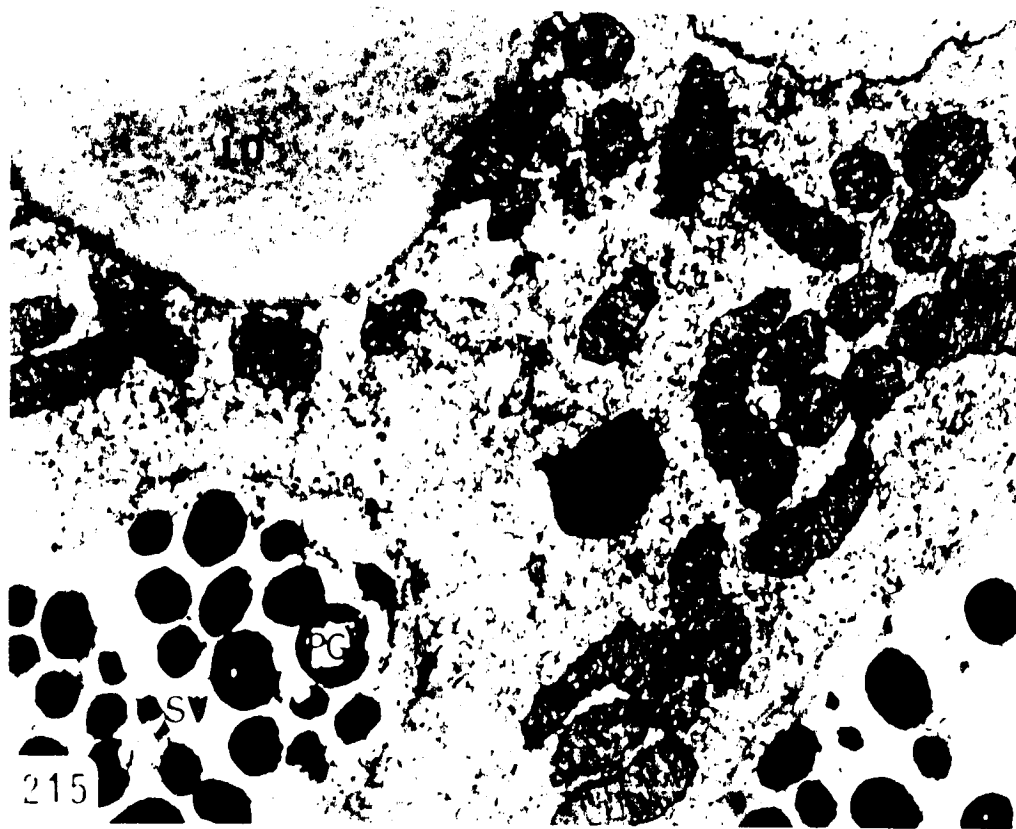


Figure 217: Electron micrograph of a portion of an inter-tubular cell in the posterior part of the kidney; 125-mm ammocoetes.

The cell possesses large mitochondria (M) and a Golgi apparatus (GA) at the ends of the elongate nucleus which contains a band of chromatin (CH).

Osmium, Epon, UA-LC

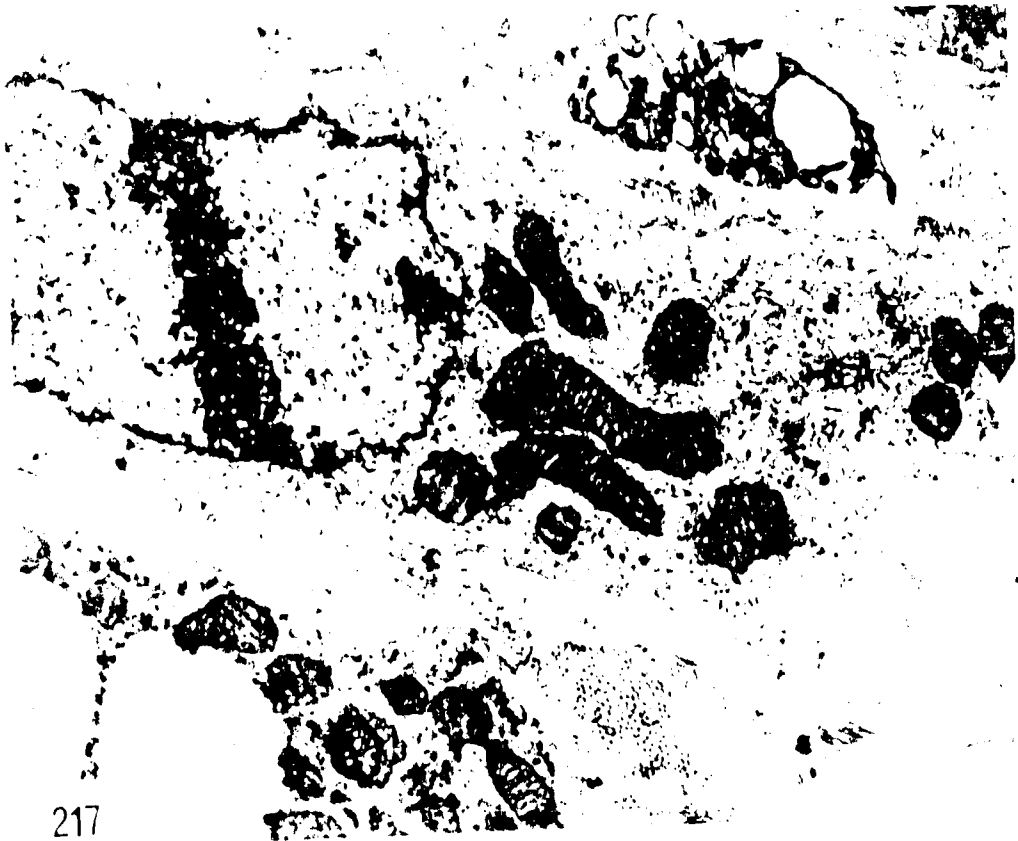
X 10,500

Figure 218: Electron micrograph of a portion of an inter-tubular cell from the posterior part of the kidney; 125-mm ammocoetes.

The cytoplasm contains clumps of glycogen (GLY), an autophagic vacuole (AV), ribosomes (R) and mitochondria with transverse cristae (CR) and mitochondrial granules (arrow).

Osmium, Epon, UA-LC

X 40,700



217



218

Figure 219: Electron micrograph of a portion of an inter-tubular cell from the dorso-anterior part of the kidney; 98-mm ammocoetes.

The cytoplasm contains ribosomes (R), smooth vesicles (SV), and chains of small vesicles near the plasma membrane (arrow).

Osmium, Epon, UA-LC

X 63,000

Figure 220: Electron micrograph of a portion of an inter-tubular cell from the dorso-anterior part of the kidney; 118-mm ammocoetes.

The cytoplasm contains glycogen (GLY) and a few strands of rough ER (RER).

Glutaraldehyde-Osmium, Epon, UA-LC

X 43,500



219



220